Supporting Information for the Assessment of the Health Risks from Radioactive Objects on Beaches in the Vicinity of the Sellafield Site

W Oatway, J Brown, G Etherington, T Anderson, T Fell, A Eslava-Gomez, A Hodgson, P G D Pellow and M Youngman

ABSTRACT

Since 2006 an intensive programme of monitoring for radioactive objects has been carried out on beaches in the vicinity of the Sellafield site in West Cumbria. By the end of the summer of 2009, over 650 radioactive objects were identified and removed. These comprised particles with sizes smaller or similar to grains of sand (less than 2 mm) and contaminated pebbles and stones. In 2007, the Environment Agency (EA) sought the formal advice of the Health Protection Agency (HPA) on the health implications of the findings of the enhanced beach monitoring near Sellafield and this advice has since been updated. In May 2008, EA asked HPA to undertake an assessment of the health risks to people using the beaches along the Cumbrian coast from contaminated objects on the beaches. This work has drawn on the considerable experience that was gained from the assessment of contaminated beaches around the Dounreay site in Scotland.

There are two main considerations when evaluating the risks to health from radioactive objects on the beaches. The first is an evaluation of the likelihood that people using these beaches for various activities will come into contact with radioactive objects that are on the beaches. The second is an evaluation of the health risks that would arise once an individual did come into contact with a radioactive object. Health risks are evaluated by assessing the radiation doses. These two strands considered together can be used to evaluate the overall risks to health for beach users from the discrete contaminated objects that are being found on the beaches.

The work undertaken in this study is presented in two reports. A main report (Brown and Etherington, 2011) is intended for a non-specialist audience, and presents the main results and conclusions of the study. This supporting report gives a detailed account of the risk assessment undertaken and includes the methodology and data used. It presents a detailed assessment of the probability of an individual encountering an object while using a beach and an assessment of the radiation doses and associated risks to an individual in the unlikely event that they come into contact with one of the

Centre for Radiation, Chemical and Environmental Hazards
Chilton, Didcot
Oxfordshire OX11 0RQ

Approval: April 2011
Publication: April 2011
£50.00
ISBN 978-0-85951-693-8

radioactive objects. The results of these two assessments provide the information needed to assess the overall health risks to people using the beaches in the vicinity of the Sellafield site.

This project was managed under the Environmental Assessment Department's Quality Management System, which has been approved by Lloyd's Register Quality Assurance to the Quality Management Standards ISO 9001:2008 and TickIT Guide Issue 5.5, Certificate No: LRQ 0956546.

Report version 1.0

CONTENTS

1 INTRODUCTION

Since 2006, an intensive programme of monitoring for radioactive objects has been carried out on beaches in the vicinity of the Sellafield site in West Cumbria. The main area that the monitoring programme has covered is from Allonby to Silecroft and this is the stretch of coastline that is considered in this study. During this programme over 650 radioactive objects were identified and removed up to the summer of 2009, comprising of particles with sizes smaller or similar to grains of sand (<2 mm) and also contaminated pebbles and stones which are objects with larger sizes (≥ 2 mm). These objects contain a range of radionuclides and associated levels of radioactivity. In this report the term 'object' is used to cover these contaminated particles, pebbles and stones found on the beaches. These discrete objects have a much higher activity content that can be distinguished from the ambient homogeneous levels of contamination on the beaches; information on these levels can be found in the Radioactivity in Food and the Environment (RIFE) series of reports (eg, Cefas, 2009a).

In July 2007, the Environment Agency (EA) sought the formal advice of the Health Protection Agency (HPA) on the health implications of the findings of the enhanced beach monitoring near Sellafield; this advice has been updated in September 2007 and January 2009. In May 2008, EA asked HPA to undertake an assessment of the health risks to people using the beaches along the Cumbrian coast from contaminated objects on the beaches. It was agreed with EA that the assessment should be based on the currently available knowledge at the time and monitoring data from the Groundhog Evolution2^{TM} detection system which was in use up to August 2009. This work was in support of the Environmnet Agency's programme of work set up to establish an overall understanding of the nature of the objects, their behaviour in the environment and the potential consequences of their presence to ensure that appropriate advice and information on public and environmental protection issues are provided to the relevant decision making authorities in a timely manner (EA, 2009). As part of this work, EA asked HPA to specifically address the following points.

- Whether a classification system can be defined for the contaminated objects based on their physical characteristics that would distinguish them from widely dispersed homogeneous contamination and enable the associated health effects to be evaluated;
- The production of an appropriate methodology for assessing the probability of encounter of objects on west Cumbrian beaches;
- Establishing suitable risk comparators so that perspective can be placed on the relative risks associated with objects on the beaches.

This work has drawn on the considerable experience that was gained from the assessment of contaminated beaches around the Dounreay site in Scotland. Where appropriate, a similar approach has been taken here. However, the nature of the contaminated objects found in the vicinity of the Sellafield site is very different to the fuel fragments found on beaches around Dounreay, as is the environment itself, and so any conclusions made by the Dounreay Particle Advisory Group (DPAG, 2006; 2008) cannot be directly applied to the situation under consideration in West Cumbria.

There are two main considerations when evaluating the risks to health from objects on the beaches. The first is an evaluation of the likelihood that people using these beaches for various activities will come into contact with radioactive objects that are on the beaches. The second is an evaluation of the health risks that may arise once an individual does come into contact with a radioactive object. Health risks are evaluated by assessing the radation doses. These two strands considered together can be used to evaluate the overall risks to health for a beach user from the discrete contaminated objects that are being found on the beaches. This approach is consistent with that recommended by HPA for the designation of contaminated land where the contamination is due to hot particles (HPA, 2006).

In order to evaluate the likelihood of an individual using the beach coming into contact with a contaminated object, a number of aspects need to be considered. Firstly, an estimate of the population of objects on the beaches is needed, obtained using information from the monitoring programme and information on the sensitivity of the detection system used for beach monitoring. Secondly, information is needed on the activities people carry out on the beaches and the time they spend on the beaches. Data on beach occupancy and beach activities have been compiled for west Cumbrian beaches from habit surveys undertaken in 2007 and 2009 by Cefas on behalf of EA. Lastly, the mechanisms by which an individual can become exposed to contaminated objects on the beaches need to be considered by taking into account the range of activities undertaken on the beaches.

The probability that an individual using the beaches could encounter a radioactive object has been estimated using a statistical approach in order to reflect the large variation in the habits of individuals using the beaches and the variability in the parameters used to describe their potential exposure to the objects. A statistical computer program has been used to estimate the range of the probability of encountering an object using these ranges in the input parameter values; the output is a probability distribution for the probability of encounter of an object which is described in terms of its 2.5 percentile, 50 percentile and 97.5 percentile. What these percentiles mean is that 2.5% of beach users have probabilities of encounter less than the 2.5 percentile, 2.5% of beach users have probabilities of encounter greater than the 97.5 percentile, and 95% of beach users have probabilities of encounter between those of the 2.5 and the 97.5 percentiles. Equal numbers of beach users have values above and below the 50 percentile (the median of the distribution).

In order to assess the risks to health in the unlikely event that an individual comes into contact with a contaminated object on a beach, radiation doses have been assessed based on the information available on the objects that have been retrieved from the beaches as a result of the monitoring and object retrieval programme. These radiation doses depend on the physical and chemical characteristics of the objects, their radionuclide content and the nature and duration of exposure.

The potential health risks to members of the public from contaminated objects that may be ingested via the consumption of seafood caught locally off the west Cumbrian coastline have also been taken into account, using the results of a scoping study carried out in consultation with the Food Standards Agency (FSA).

The work undertaken in this study is presented in two reports. This report is a supporting report that gives a detailed account of the risk assessment undertaken and includes the methodology and data used. It presents a detailed analysis of the probability of an individual encountering an object while using a beach and an assessment of the radiation doses and associated risks to an individual in the unlikely event that they come into contact with one of the radioactive objects. A short main report (Brown and Etherington, 2011) is intended for a non-specialist audience and presents the main results and conclusions of the study together with an assessment of the overall health risks to people using the beaches in the vicinity of the Sellafield site. This is referred to as the Main Report in the remainder of this report.

Throughout this report, information provided on the characteristics of the objects found on the beaches is used at the level of numerical accuracy provided. All intermediate steps in the assessment of health risks to beach users are presented to a high level of precision to avoid errors in rounding numerical values of the overall health risks. The level of precision presented does not necessarily imply a high level of confidence in the values.

2 OBJECTS RETRIEVED FROM BEACHES USING THE GROUNDHOG EVOLUTION2™ SYSTEM

The Environment Agency has placed a statutory requirement on Sellafield Ltd to carry out monitoring of beaches between Ravenglass and the Solway for small radioactive objects and particles using the best techniques available. In 2006 Sellafield Ltd tested a new, vehicle-mounted detector system (Groundhog Evolution2™) to monitor local beaches and this has been used routinely since then to survey beaches in the vicinity of the Sellafield site. The work is carried out by Nuvia Ltd on behalf of Sellafield Ltd.

Groundhog Evolution2™ uses an array of five sodium iodide (NaI(Tl) gamma-ray detectors mounted on the front of a low ground-pressure vehicle (Nuvia, 2008). Each of the five detectors is 0.4 m long, providing a continuous monitoring width of 2.0 m. The vehicle is driven over the survey area at a speed of approximately 1.0 m s^{-1}, with a GPS system providing information for a 'moving map' of the area surveyed. Count rates measured by the detectors are monitored continuously using an object detection algorithm. Evolution2™ is designed to detect objects containing caesium-137 (^{137}Cs), cobalt-60 (^{60}Co), americium-241 (^{241}Am) or strontium-90 (^{90}Sr). Caesium-137 and cobalt-60 are beta-gamma emitters and can be detected by measuring their high energy gamma-ray emissions, while ^{241}Am is an alpha emitter that can be detected by measuring its low energy (60 keV) gamma ray emission. Strontium-90 is present in equilibrium with its radioactive progeny radionuclide, ytrrium-90 (^{90}Y). Both are pure beta emitters whose radioactive decay does not directly result in emission of gamma-ray photons, but the deceleration of beta particles results in the emission of photons (Bremsstrahlung radiation) that can be detected by gamma ray detectors. Appendix A gives further information on the monitoring system, procedures and the detection algorithm.

If radioactive objects are detected they are retrieved manually and sent to Sellafield for analysis. Figure 1 shows the extent of the beach monitoring that has been undertaken in Cumbria since November 2006. For the purposes of this study, data from the monitoring period between November 2006 and August 2009 has been considered, this being the period that the Groundhog Evolution2™ detection system was in use. Beach monitoring has also been carried out on 2 beaches along the North Solway coast in Scotland; Goatwell Bay, Kirkudbrough and Southerness. No objects have been detected on these beaches.

Since September 2009 a new detection system, Groundhog 'Synergy', has been deployed with an improved detection capability for low energy photon emitters, particularly ^{241}Am and ^{90}Sr. Since the Synergy system had not collected a significant amount of data at the start of this assessment, and because Synergy has different characteristics from Groundhog Evolution2™, for example different detection efficiencies, it was agreed with EA and Sellafield Ltd that this assessment would only use monitoring data from the Groundhog Evolution2™ system.

Use of the Synergy system has resulted in the detection of increased numbers of alpha-rich objects. Some comments are made in Section 4.4 regarding the improved sensitivity of the Synergy system and the activity range of objects that would be expected to be detected with higher probabilities. Recommendations are given in Section 11 on the work needed to determine whether the increase in detected objects is completely attributable to improvements in sensitivity, or whether there is also an increase in the numbers of objects actually present on the beaches.

Monitoring conducted using the Groundhog Evolution2™ system between 2006 and 2009 found a total of 676 objects within a monitored area across all beaches of approximately 600 ha (6 10^6 m^2). Details of these finds are recorded in Sellafield Ltd's Beach Monitoring Summary Spreadsheet[*] (Dalton, 2010) and this information was reviewed by HPA as part of this work.

2.1 Classification of object finds

Objects found during monitoring have been classified by size and type by Sellafield Ltd. Any object with an average size of 2 mm or greater is defined as a stone and objects smaller than 2 mm are defined as particles. Once objects have been removed from the beach they are sent for further analysis which enables Sellafield Ltd to classify them based on their radionuclide content; this classification system is described in Table 1.

The object classification system used by Sellafield Ltd was also used for this assessment with one exception. The "excess beta" class of objects was intended to allow identification of objects with relatively high contents of ^{90}Sr/^{90}Y, but this classification has not been used in the assessment of object populations because no objects have been detected directly through measurement of their ^{90}Sr/^{90}Y content. Objects classified as "excess beta" in the Sellafield spreadsheet have therefore been

[*] Spreadsheet dated 18th January 2010

placed into the beta-rich category for the purposes of this assessment. Nevertheless, $^{90}Sr/^{90}Y$ has been measured in objects subsequently selected for radiochemical analysis (Section 2.2), and the contribution of $^{90}Sr/^{90}Y$ to doses is considered in the assessment of doses and risks to health (Section 9).

Table 1 Object classification

Object classification	Criteria for classification
Alpha-rich	Positive measurement of ^{241}Am activity that exceeds measured ^{137}Cs activity
Beta-rich	Positive measurement of ^{137}Cs activity that exceeds measured ^{241}Am activity
^{60}Co-rich	Positive measurement of ^{60}Co activity that exceeds measured ^{137}Cs activity
Excess beta[(a)]	Not alpha-rich or ^{60}Co-rich; contact beta/gamma dose rate in nSv h^{-1} exceeds 15 times ^{137}Cs activity in Bq

a) For this assessment, "excess beta" objects were placed in the beta-rich category rather than treated as a separate category

2.2 Information on objects retrieved from beaches

A summary of the object finds for each of the beaches monitored over the period when the Groundhog Evolution2™ detection system was used is given in Table 2. The maximum and minimum activity of the objects found on each beach for each object class is given in Table 3.

Table 2 Summary of objects found on each beach by Groundhog Evolution2™

Beach	Classification	Particles found[a,b]	Stones found[a]
Allonby	Beta-rich	1	0
Workington	Beta-rich	1	0
St Bees	Alpha-rich	4	0
	Beta-rich & excess beta	8	0
	^{60}Co-rich	1	0
Braystones	Alpha-rich	2	0
	Beta-rich & excess beta	8	0
	^{60}Co-rich	0	0
Sellafield	Alpha-rich	45	3
	Beta-rich & excess beta	181	364
	^{60}Co-rich	7	1
Seascale	Alpha-rich	4	0
	Beta-rich & excess beta	17	3
	^{60}Co-rich	1	0
Drigg	Alpha-rich	4	0
	Beta-rich	3	0

a) Taken from Sellafield Ltd's beach monitoring summary spreadsheet dated 18th January 2010 (Dalton, 2010)

Figure 1: Map showing the extent of the monitoring area (beaches monitored along the north Solway coast in Scotland are not shown)

Table 3: Minimum and maximum activities for each object class found on each beach using Groundhog Evolution2™ system

Class[a]	Beaches[b]	Particles		Stones	
		Min activity [a,c] (Bq)	Max activity [a,c] (Bq)	Min activity [a,c] (Bq)	Max activity [a,c] (Bq)
Alpha-rich	Braystones	$3.76\ 10^{4}$	$1.28\ 10^{5}$		
Alpha-rich	Drigg	$2.65\ 10^{4}$	$5.75\ 10^{4}$		
Alpha-rich	Seascale	$2.86\ 10^{4}$	$9.80\ 10^{4}$		
Alpha-rich	Sellafield	$3.23\ 10^{3}$	$6.34\ 10^{5}$	$7.60\ 10^{3}$	$3.54\ 10^{4}$
Alpha-rich	St Bees	$4.26\ 10^{3}$	$7.27\ 10^{4}$		
Overall alpha-rich		$3.23\ 10^{3}$	$6.34\ 10^{5}$	$7.60\ 10^{3}$	$3.54\ 10^{4}$
Beta-rich	Braystones	$5.72\ 10^{3}$	$3.50\ 10^{4}$		
Beta-rich	Drigg	$3.99\ 10^{3}$	$5.24\ 10^{4}$		
Beta-rich	Seascale	$4.75\ 10^{2}$	$6.02\ 10^{4}$	$1.81\ 10^{4}$	$3.73\ 10^{4}$
Beta-rich	Sellafield	$8.21\ 10^{2}$	$1.09\ 10^{5}$	$1.95\ 10^{3}$	$8.75\ 10^{5}$
Beta-rich	St Bees	$3.70\ 10^{3}$	$1.94\ 10^{4}$		
Overall beta-rich		$4.75\ 10^{2}$	$1.09\ 10^{5}$	$1.95\ 10^{3}$	$8.75\ 10^{5}$
^{60}Co-rich	Braystones				
^{60}Co-rich	Drigg	$8.65\ 10^{3}$	$8.65\ 10^{3}$		
^{60}Co-rich	Seascale	$6.46\ 10^{3}$	$6.46\ 10^{3}$		
^{60}Co-rich	Sellafield	$6.21\ 10^{3}$	$1.97\ 10^{4}$	$2.35\ 10^{4}$	$2.35\ 10^{4}$
^{60}Co-rich	St Bees	$8.43\ 10^{3}$	$8.43\ 10^{3}$		
Overall ^{60}Co-rich		$6.21\ 10^{3}$	$1.97\ 10^{4}$	$2.35\ 10^{4}$	$2.35\ 10^{4}$

a) Detected activity: ^{241}Am for alpha-rich objects; ^{137}Cs for beta-rich objects; ^{60}Co for ^{60}Co-rich objects.

b) On Allonby and Workington beaches, only one beta-rich particle has been found on each beach with ^{137}Cs content of 7.1 kBq and 18.2 kBq, respectively.

c) Values taken from Sellafield Ltd's beach monitoring summary spreadsheet dated 18th January 2010 (Dalton, 2010). The level of accuracy reflects that given in the monitoring summary spreadsheet.

The most active alpha-rich particle was found on Sellafield beach (Table 3) and is recorded in Sellafield Ltd's Beach Monitoring Summary spreadsheet (dated 18th January 2010) as containing 84 kBq of plutonium-238 (^{238}Pu), 309 kBq of the two plutonium isotopes ^{239}Pu + ^{240}Pu (commonly abbreviated to $^{239/240}$Pu) and 634 kBq ^{241}Am, with a total activity of these radionuclides of 1.03 MBq. It should be noted, however, that significant uncertainties may be associated with gamma spectrometric measurements of the activities of alpha-emitting Pu isotopes. The particle with the highest ^{137}Cs activity was also found on Sellafield beach and contained 110 kBq ^{137}Cs. Some stones had higher ^{137}Cs activities, up to 875 kBq. No measurements of ^{90}Sr are reported by Dalton (2010).

Sellafield Ltd. commissioned SERCO Technical & Assurance Services (SERCO) to carry out a comprehensive characterisation of 51 of these objects, which were delivered to SERCO (National Physical Laboratory (NPL)) in January 2008. Results have been reported by Cowper (2009). For each alpha-rich particle characterised, the sequence of analyses comprised initial high-resolution gamma-ray spectrometry (HRGS) on the sample as received, drying, separation of the particle from the accompanying residue, photography of the separated particle, HRGS on the particle and residue, and imaging

and chemical composition measurements using scanning electron microscopy (SEM) and energy-dispersive X-ray analysis (EDAX). Mass, volume and density of the particle were then determined non-destructively. At this stage, five particles were provided to HPA for the 1st *in vivo* study of gastro-intestinal absorption (see Section 8.2). (The particles that were subsequently provided to HPA for the 2nd *in vivo/in vitro* study were not part of the batch of 51 particles provided to SERCO in January 2008.) The remaining alpha-rich particles were subjected to destructive radiochemical analysis after sequential leaching of particles in synthetic seawater, a simulated stomach fluid and a simulated intestinal fluid, followed by total dissolution of remnant particles in strong acids (the NPL *in vitro* studies, Section 8.2.2). Radiochemical analysis gave results for gross α and β actvity, isotopes of uranium (U), isotopes of plutonium, ^{241}Am, ^{90}Sr and ^{99}Tc.

Analyses of beta-rich particles followed a similar sequence except that the SEM/EDAX measurements were followed by contact dose rate measurements. Radiochemical analysis gave results for gamma-emitting radionuclides, gross β activity, isotopes of U, ^{241}Am, ^{90}Sr and ^{99}Tc.

The sequence of analyses for pebbles and stones comprised initial HRGS on the sample as received, photography, non-destructive determination of mass, volume and density, and then destructive radiochemical analysis after sequential leaching of particles in concentrated acid solutions. Radiochemical analysis gave results for gamma-emitting radionuclides, gross β activity, isotopes of U, ^{241}Am, ^{90}Sr and ^{99}Tc.

The following summary of the results of the SERCO study is taken mainly from the Executive Summary of Cowper (2009). Thirteen alpha-rich particles, 26 beta-rich particles, and twelve stones were analysed. The majority of the activity of the alpha-rich particles was present as plutonium and americium, and results were reported for the contents of ^{238}Pu, $^{239/240}$Pu and ^{241}Am. For all but four of the beta-rich particles investigated in the SERCO study, the majority of the detectable activity was ^{137}Cs, with ^{137}Cs:^{90}Sr ratios in the range 1.21 – 3250. For the four remaining particles, the ^{90}Sr activity was in excess of that for ^{137}Cs, with ^{137}Cs:^{90}Sr ratios in the range 0.61 – 0.88. The highest ^{137}Cs activity in a particle was 61.9 kBq; the ^{90}Sr content of this particle was 18 Bq. The highest ^{90}Sr activity in a particle was 48.9 kBq; the ^{137}Cs content of this particle was 32.4 kBq. All of these activities and ratios were measured by radiochemical analysis.

The radioactive inventory of each of the 12 pebbles/stones measured by radiochemical analysis was dominated by ^{137}Cs, with measured values ranging from 1.9 kBq – ~100 kBq and ^{137}Cs:^{90}Sr ratios in the range 106 – 2350.

2.3 Use of data on objects found on the beaches in this study

Some objects recorded in the Sellafield spreadsheet (Dalton, 2010) have been excluded from use in this study. These are:

a 3 objects retrieved from Sellafield defined as silt and where no activity levels were measured;

b 14 objects for which no activity measurements were available;
c 1 object where only a maximum activity has been given and so it could not be classified using the system detailed in Table 1.

A total of 658 objects from the Groundhog Evolution2™ monitoring surveys were therefore considered in the determination of the population of objects on the beaches.

The majority of beach areas defined for monitoring matched well with those defined for the habit surveys (Cefas 2008a; 2010). One important exception was a 1 km long section of beach defined as part of Sellafield beach for the monitoring surveys and Braystones beach for the habit surveys. Forty objects were found in this area using Groundhog Evolution2™ up until August 2009. For the estimation of the object population on Sellafield and Braystones beaches, these objects were assigned to Braystones beach to be conservative when estimating the probability of encounter with an object, given that Braystones beach has the higher beach occupancy (see Section 5). The numbers of objects found on each beach as used in the study are shown in Table 4 and the corresponding minimum and maximum activities of the objects allocated to each beach are given in Table 5.

Table 4 Summary of objects found on each beach as used in the study

Beach[a]	Classification	Particles found[b,c]	Stones found[b,c]
Allonby	Beta-rich	1	0
Workington	Beta-rich	1	0
St Bees	Alpha-rich	4	0
	Beta-rich	7 (8)	0
	^{60}Co-rich	1	0
Braystones	Alpha-rich	10	0
	Beta-rich	31 (35)	2
	^{60}Co-rich	3	0
	Excess beta	4	0
Sellafield	Alpha-rich	37	3
	Beta-rich	140 (154)	362
	^{60}Co-rich	4	1
	Excess beta	14	0
Seascale	Alpha-rich	4	0
	Beta-rich	11 (17)	3
	^{60}Co-rich	1	0
	Excess beta	6	0
Drigg	Alpha-rich	4	0
	Beta-rich	3	0

a) The extent of each beach is as defined by Cefas for the beach habit surveys (Cefas, 2008a;2010)

b) Taken from Sellafield Ltd's beach monitoring summary spreadsheet dated 18th January 2010 (Dalton, 2010)

c) The value in brackets is the total beta object population, comprised of the sum of excess beta and beta-rich objects where this is different to the number of beta-rich objects. It is this population that is used within this study for estimating the total object population on each beach.

Table 5: Minimum and maximum activities for each object class found on each beach using Groundhog Evolution2™ system as used in the study

Class[a]	Beaches[b]	Particles		Stones	
		Min activity [a,c] (Bq)	Max activity [a,c] (Bq)	Min activity [a,c] (Bq)	Max activity [a,c] (Bq)
Alpha-rich	Braystones	$5.26\ 10^{3}$	$1.28\ 10^{5}$		
Alpha-rich	Drigg	$2.65\ 10^{4}$	$5.75\ 10^{4}$		
Alpha-rich	Seascale	$2.86\ 10^{4}$	$9.80\ 10^{4}$		
Alpha-rich	Sellafield	$3.23\ 10^{3}$	$6.34\ 10^{5}$	$7.60\ 10^{3}$	$3.54\ 10^{4}$
Alpha-rich	St Bees	$4.26\ 10^{3}$	$7.27\ 10^{4}$		
Overall alpha-rich		$3.23\ 10^{3}$	$6.34\ 10^{5}$	$7.60\ 10^{3}$	$3.54\ 10^{4}$
Beta-rich	Braystones	$1.85\ 10^{3}$	$3.50\ 10^{4}$	$5.87\ 10^{4}$	$7.49\ 10^{4}$
Beta-rich	Drigg	$3.99\ 10^{3}$	$5.24\ 10^{4}$		
Beta-rich	Seascale	$4.75\ 10^{2}$	$6.02\ 10^{4}$	$1.81\ 10^{4}$	$3.73\ 10^{4}$
Beta-rich	Sellafield	$8.21\ 10^{2}$	$1.09\ 10^{5}$	$1.95\ 10^{3}$	$8.75\ 10^{5}$
Beta-rich	St Bees	$3.70\ 10^{3}$	$1.94\ 10^{4}$		
Overall beta-rich		$4.75\ 10^{2}$	$1.09\ 10^{5}$	$1.95\ 10^{3}$	$8.75\ 10^{5}$
^{60}Co-rich	Braystones	$6.21\ 10^{3}$	$1.79\ 10^{4}$		
^{60}Co-rich	Drigg	$8.65\ 10^{3}$	$8.65\ 10^{3}$		
^{60}Co-rich	Seascale	$6.46\ 10^{3}$	$6.46\ 10^{3}$		
^{60}Co-rich	Sellafield	$7.17\ 10^{3}$	$1.97\ 10^{4}$	$2.35\ 10^{4}$	$2.35\ 10^{4}$
^{60}Co-rich	St Bees	$8.43\ 10^{3}$	$8.43\ 10^{3}$		
Overall Co60-rich		$6.21\ 10^{3}$	$1.97\ 10^{4}$	$2.35\ 10^{4}$	$2.35\ 10^{4}$

a) Detected activity: ^{241}Am for alpha-rich objects; ^{137}Cs for beta-rich objects; ^{60}Co for ^{60}Co-rich objects.

b) On Allonby and Workington beaches, only one beta-rich particle has been found on each beach with ^{137}Cs content of 7.1 kBq and 18.2 kBq, respectively.

c) Values taken from Sellafield Ltd's beach monitoring summary spreadsheet dated 18th January 2010 (Dalton, 2010). The level of accuracy reflects that given in the monitoring summary spreadsheet.

3 THE BEACHES CONSIDERED

In order to undertake a full evaluation of the health risks associated with people using the beaches along the west Cumbrian coastline, it is important to have sufficient data to be able to characterise both a realistic population of objects on each beach considered and the human activities undertaken on these beaches. To identify beaches for which a complete assessment could be made, a review was carried out of the currently available monitoring and habit survey data. This review showed that it is possible to undertake a quantitative evaluation of the health risks for five of the beaches between Allonby and Silecroft. These beaches are (in alphabetical order); Braystones, Drigg, Seascale, Sellafield and St Bees. Figure 2 shows the beach area that has been assigned to each of these five beaches. However, it should be noted that, even for these beaches, the information available is limited and robust assumptions have had to be made; the reliability of the assessment and the major areas of uncertainty are discussed in Section 11. For other beaches that have been monitored and areas that it has not been

Figure 2: Map showing the extent of the beaches included in this assessment

possible to monitor using the vehicle based detection system (Nethertown and Coulderton 'boulder fields'), there are insufficient monitoring data to enable a meaningful quantitative evaluation of health risks to be performed. Nevertheless, it is possible to provide some qualitative comments on the potential health risks to people using other beaches along the West Cumbian coast and this is done in Section 10.4.

Where possible, the spatial limits defining the length of coastline associated with each beach were those defined in the monitoring and habits survey reports as, in the majority of cases, these coincided. Any assumptions made in allocating data to these beaches are described in the relevant Sections of this report.

In Table 3, it is noted that one beta-rich object was found on both Allonby and Workington beaches. However, this did not constitute sufficient data to undertake a quantitative assessment; in particular, a realistic population of objects on the beach could not be predicted from only one object find. Allonby and Workington beaches were therefore not included in the main part of this assessment.

It should be noted that for beaches other than the five listed above, their omission from the quantitative evaluation of health risks does not mean that there are no radioactive objects present on them or that the likelihood of an individual using these beaches coming into contact with an object is zero. It merely means that there was insufficient data available to perform a meaningful quantitative estimate of the probability of encounter. Section 10.4 provides some comments on the potential health risks to people using other beaches along the West Cumbian coast.

3.1 Description of the beaches considered

The following descriptions for the five beaches considered in the quantitative evaluation of health risks have been taken from the reports on the habit surveys carried out in 2007 and 2009 (Cefas 2008a; 2010). These descriptions are intended to give an overview of each of the beaches and the use of the beaches at the time of the surveys.

3.1.1 St Bees

St Bees is a popular seaside resort with a 2 km long sandy beach, the southern end of which is locally known as Seamill. The beach is predominantly sand on the mid to lower foreshore and there are rock pools below the headland, midway along the beach and at the southern end. The upper foreshore along the high water mark is stones and is backed by soft glacial moraines. There is one access road at St Bees and one at Seamill, both with plenty of parking. There is a concrete slipway at the lifeboat station and the public uses the slipway to launch boats and jet-skis.

Activities undertaken regularly at St Bees throughout the year are dog walking, walking, beach combing, angling, and collecting winkles, razor shells and limpets. Activities undertaken by locals and tourists in the warmer weather are picnicking, playing ball games, building sandcastles and rock pooling.

During the surveys people were observed windsurfing and paddling. St Bees is also very popular with holidaymakers either staying at the caravan park or visiting the area. In periods of good weather it was observed that the beach often had large numbers of people on it. The main area of the beach used by families playing and picnicking is in front of the main St Bees car park to the north of the beach. Dog walkers use the beach daily and many walk the full length of the beach, often along the tide line. Rock pooling and winkle collecting take place near the headland, whilst bait digging takes place on the lower foreshore at low tide.

The beach is a popular location for visiting groups of school children. Two local schools were identified that arrange trips to St Bees beach. Activities undertaken during these trips include general beach studies and rock pooling.

3.1.2 Braystones

Moving south along Braystones beach the beach material changes from stones to predominantly sand with occasional small rocky scars. The lower foreshore is a large expanse of mud and sand at low tide and the strip of upper foreshore that backs onto the railway comprises stones and boulders. There are numerous beach chalets, which are a mixture of full-time residency, holiday lets and second homes. There is one access road to the beach and this is frequently washed away. The road is generally in a poor state and is more suitable for four-wheel drive vehicles or tractors which could deter tourists from visiting the area. There are two caravan parks situated just inland of the railway line.

Shore activities observed included winkle and mussel collection, angling and setting nets. Bait digging is a popular activity due to the large exposed areas of mud and sand at low tide. The beach is predominantly used by residents living at the beach chalets and people staying at the caravan sites. Local beach residents spend considerable amounts of time beach clearing, reinforcing sea defences, keeping the road clear of rubbish and filling potholes. Holidaymakers from the caravan parks undertake beach activities such as playing, building sandcastles, paddling, collecting shells, sunbathing and beachcombing. Beach leisure activities take place close to chalets or caravan sites either side of Braystones station. Dog walkers use the whole of the beach and anglers fish from the tide line and spread along the length of the beach. South of Braystones station, lower general beach occupancy was observed.

3.1.3 Sellafield

The River Ehen flows from the north-west and runs parallel with the beach, past High Sellafield, the Sellafield site, and into the sea at the Calder Viaduct. The dunes between the River Ehen and the beach are known as the Ehen Spit. The River Calder flows through the Sellafield site and feeds into the sea at the southern end of the Ehen Spit alongside the River Ehen. The beach at Sellafield is backed by sand dunes at the extreme high tide level, with a band of pebbles below this and mainly sand down to the extreme low water mark. There are areas of stones, rocks and honeycomb worm colonies, with two main colonies either side of the confluence of the rivers Ehen and Calder. The Sellafield nuclear site liquid discharge pipes enter the Irish Sea at the

northern end of the Ehen Spit with an on-site “sewer” pipe discharging at the confluence of the two rivers. There is an access road to Sellafield station but there is no public access on foot from Sellafield station to the beach. The only way for the public to access this section of beach is a 3 km walk from Braystones or a 2 km from Seascale. Local people walk from Seascale and from Braystones to access Sellafield beach. While being interviewed on other beaches, some individuals indicated that they did occasionally use Sellafield beach for beach combing, fishing and bait digging. No children were identified spending time on Sellafield beach.

3.1.4 Seascale

Seascale is a popular seaside town which has a large beach that is predominantly sand with a narrow stretch of stones and a small rocky scar (Whitriggs Scar) on the upper foreshore. There is one access road from Seascale and footpath access at Carl Crag. Seascale is a popular beach with locals and holidaymakers due to its easy access, ample car parking and local amenities. There is a secure boat compound in Seascale near the beach car park with a public slipway for launching boats.

Beach activities at Seascale include angling, playing, building sand castles, picnicking, rock pooling, paddling, body boarding and beach combing. At high tide the accessible beach is predominantly stone and the activities observed were mostly dog walking and walking.

The area in front of the main car park at Seascale is popular for beach leisure activities. Dog walkers and anglers use the whole length of the beach, often along the tide line and dog walkers frequently walk towards Sellafield.

3.1.5 Drigg

Drigg beach is predominantly sand and is backed by sand dunes. Below the sand dunes there is a narrow stretch of stones and areas of mud and sand on the lower foreshore. There are two rocky scars, one on the lower foreshore which is easily accessed from the beach and one situated below the low water mark which can only be accessed by foot during extreme spring tides. There is one access road at Drigg and there is footpath access to the north of the road.

The area of beach near the car park is popular with families undertaking beach leisure activities. The beach activities observed included dog walking, walking, angling, bait digging, playing on the beach, rock pooling, paddling, playing beach games, building sand castles, picnicking and kite buggying. The two rocky scars are popular areas for both mollusc and crustacean collection. Groups of local volunteers were observed collecting litter from the beaches during one of the surveys. Dog walkers and anglers were observed to use the full extent of the beach.

4 ESTIMATING THE POPULATION OF OBJECTS ON THE BEACHES

The first step in the evaluation of the likelihood that an individual using the beach could come into contact with a contaminated object is the determination of the population of objects. This is the best estimate of the number of objects present on a beach and is taken to be representative of the number present at any time that the beach is used. It is implicit in this definition that the population of objects has not been changing over time since the monitoring programme commenced. This pragmatic assumption is considered to be acceptable for the purpose of determining whether a significant risk to health is present. The population of objects per hectare may be determined using data on the area of the beach monitored. By making an appropriate assumption about the depth of sand to which particles may be detected, the population of objects per gram of sand may then be determined (ie, the population density of objects).

The beach monitoring systems in use are not capable of detecting all of the objects in the monitored area because the detection efficiency is typically less than 100%. In general, therefore, the detection of a single object within a particular depth range on a beach may indicate the presence of more than one object in that depth range within the area monitored. The number of objects present may be estimated by dividing the number of objects found (in this case, one) by the detection probability for that depth range. The detection probability is the fraction of the number of objects present that are expected to be detected under a specified set of conditions (ie, radionuclide, activity, depth, scan speed and background level). When the detection probability is close to 100%, the number of objects predicted to be actually present is close to the number found. However, when a particular object is found within a depth range where the probability of detection is low, the actual number of objects predicted is much larger than the number found.

Section 4.1 describes how HPA determined detection probabilities for the Groundhog Evolution2™ system, presents results for five areas of beach, and compares the results of this study with the results of recent *in situ* beach trials. Additional information is presented in Appendix A. Section 4.2 describes how these object detection probabilities were used in practice to determine object populations on each beach from the results of the beach monitoring programme.

It has not been possible to carry out a similar evaluation for the recently introduced Synergy system introduced in September 2009, because of the lack of available calibration and background data at the time the work reported here was carried out. Some comments on the expected performance of the Synergy system are presented in Section 4.4.

4.1 Efficiency of detection of objects

The primary aims of this study were to provide input data for estimating the population of objects as described in Section 4.2, and to provide an independent evaluation of the

performance of the Groundhog Evolution2™ system. Groundhog Evolution2™ (Nuvia, 2008) employs vehicle-mounted, trolley-mounted and portable detection systems to allow surveys of different types of terrain. This study evaluated only the performance of the vehicle-mounted system since the trolley-mounted system is not being used in Cumbria, while the portable system does not have alarms that respond to ^{241}Am, ^{90}Sr and ^{60}Co.

Work carried out to estimate probabilities of encounter at Dounreay focused on ^{137}Cs and, more recently, ^{60}Co. For Sellafield, ^{137}Cs and ^{60}Co bearing objects are also being detected, but other radionuclides of key interest are ^{241}Am and ^{90}Sr/^{90}Y. Americium-241 and ^{90}Sr/^{90}Y are more difficult to detect than ^{137}Cs and ^{60}Co, so the work previously carried out to determine particle detection efficiencies at Dounreay (Youngman and Etherington, 2003) cannot be applied directly to the situation at Sellafield.

4.1.1 Factors affecting object detection probability

Background counts

A radioactive object is said to be detected when the measured count is judged to be significantly in excess of the background count that would be measured in the absence of a radioactive object. Any counting measurement is subject to variability, so the measured value must be judged to be above the range of background counts that would usually be encountered. Variations in the background count arise from spatial and temporal variations in the true background level, as well as from the statistical variation that is inherent in any counting measurement. The range in background counts arising from statistical variation may be quantified by the standard deviation of the background count, which is itself proportional to the square root of the expected mean value of that background count. The well known formula given by Currie (1968) indicates that the minimum detectable amount (the amount that is expected to be detected by 95% of the count measurements on that object) is approximated by a constant multiplied by the standard deviation of the background count. Thus, the minimum detectable amount depends on the expected background count. Objects that give count measurements well in excess of the minimum detectable amount have detection probabilities that approach 100%. The detection probability for objects with an activity equal to the minimum detectable amount is by definition equal to 95%. As object activities decrease, detection probabilities decrease below 95%, and eventually approach zero. For any object activity, its detection probabilities decrease as background counts increase. Thus it is essential to have realistic assessments or measurements of background count rates if object detection probabilities are to be determined.

Calibration factors

The object activity corresponding to a count measurement that is judged to be significant is determined using conversion factors that give the activity corresponding to a particular net count rate (ie, the radioactive object measurement minus the background). These calibration factors are typically expressed in units of counts per second per kilobecquerel (c s^{-1} kBq^{-1}). Calibration factors depend on the position of the object with respect to the detector array, are generally lower for greater object depths, and differ for different radionuclides.

Scan speeds

The count measured from a particular object depends on the speed with which the detector array transits the object position. Higher scan speeds result in lower net counts and correspondingly lower detection probabilities, and vice versa.

4.1.2 Statistical analysis of object detection

A Monte Carlo technique was used to simulate the count rate measured by the detector system moving at a specified speed over an object of a specified radionuclide, activity and depth. Gross counts (object + background) were evaluated using real datasets of background counts for each of the beach areas of interest (identified in Table 6), and simulated count rates from the object were determined using calibration factors provided by Nuvia (Davies, 2009). The object detection algorithm specified by Nuvia was then applied to each 1-second count to determine whether the simulated object would have been detected. For each set of simulation conditions (ie, beach, scan speed, radionuclide, activity, object depth), the transits of large number of objects were simulated and the detection probability was obtained directly from the number of objects detected divided by the total number simulated. Full details of the simulation method, simulation geometry, the object detection algorithm and the software developed to implement the method are given in Appendix A.

4.1.3 Calculated object detection probabilities

Object detection probabilities for ^{137}Cs, ^{60}Co, ^{90}Sr and ^{241}Am were determined for each of the ten beach areas listed in Table 6; different areas were considered on each beach including sand and shingle areas and sand areas at low and high tide as detailed in the Table. Results for ^{137}Cs, ^{60}Co and ^{241}Am for the five beachs that were used in the assessment of the population of objects are given in Table 7 -Table 11. Results for all of the beach areas for which detection probabilities have been determined are given in Appendix A. The detection probabilities were calculated for object activities of 1 kBq, 10 kBq, 100 kBq and 1000 kBq, respectively. The object depths for which detection probabilities were calculated are listed in the Tables. The rounding that has been applied to the results in the Tables broadly reflects the level of precision for each reported value. It should be noted that uncertainties are large where calculated detection probabilities are low, particularly for values less than 1%. Calculations were performed for 1 kBq objects only for Barnscar (sand) and Braystones (sand) beach areas, because for objects of this activity differences between beaches are insignificant given the low detection probabilities and consequent lack of precision. The values for 1 kBq objects for Braystones beach (Table 7) were therefore used for all beaches.

Table 6: Background data sets provided by Nuvia (Davies, 2009)

Location	Description of beach	Date of measurements	No of records
Barnscar, Drigg	sand	Oct 2007	27898
Barnscar, Drigg	shingle	Oct 2007	19264
Braystones	sand	Sept 2008	144754
Braystones	shingle	Sept 2008	12195
Drigg	sand	Oct 2007	44749
Seascale	sand	Oct 2007	74618
Seascale	shingle	Oct 2007	15080
Sellafield	low sand	June 2008	29765
Sellafield	high sand	June 2008	33634
St Bees	sand	April 2008	123756

Table 7 Detection probabilities (%) on Braystones beach, sandy areas

Depth	^{60}Co activity (kBq)				^{137}Cs activity (kBq)				^{241}Am activity (kBq)			
(m)	1	10	100	1000	1	10	100	1000	1	10	100	1000
1 10^{-4}	1	100	100	100	0.1	94	100	100	0.3	5	100	100
0.05	0.4	95	100	100	0	25	100	100	0.2	0.3	6	100
0.1	0.2	52	100	100	0	2	100	100	0.2	0.2	0.3	7
0.15	0.1	15	100	100	0	0.2	83	100	0.2	0.2	0.2	0.3
0.2	0.1	3	100	100	0	0.1	20	100	-	-	-	-
0.3	0.1	0.2	39	100	0	0	0.4	85	-	-	-	-
0.4	-	-	-	-	0	0	0	5	-	-	-	-

Table 8 Detection probabilties (%) on Drigg beach, sandy areas

Depth	^{60}Co activity (kBq)				^{137}Cs activity (kBq)				^{241}Am activity (kBq)			
(m)	1	10	100	1000	1	10	100	1000	1	10	100	1000
1 10^{-4}	-	100	100	100	-	98	100	100	-	9	100	100
0.05	-	97	100	100	-	46	100	100	-	0.2	12	100
0.1	-	60	100	100	-	5	100	100	-	0.1	0.2	13
0.15	-	21	100	100	-	0.5	94	100	-	0.1	0.1	0.2
0.2	-	5	100	100	-	0.1	38	100	-	-	-	-
0.3	-	0.3	48	100	-	0	1	95	-	-	-	-
0.4	-	-	-	-	-	0	0.1	8	-	-	-	-

Table 9 Detection probabilities (%) on Seascale beach, sandy areas

Depth	^{60}Co activity (kBq)				^{137}Cs activity (kBq)				^{241}Am activity (kBq)			
(m)	1	10	100	1000	1	10	100	1000	1	10	100	1000
1 10^{-4}	-	100	100	100	-	98	100	100	-	6	100	100
0.05	-	93	100	100	-	41	100	100	-	0.2	9	100
0.1	-	47	100	100	-	4	100	100	-	0.1	0.1	10
0.15	-	14	100	100	-	0.4	93	100	-	0.1	0.1	0.2
0.2	-	3	99	100	-	0.1	35	100	-	-	-	-
0.3	-	0.2	35	100	-	0	0.8	94	-	-	-	-
0.4	-	-	-	-	-	0	0.1	8	-	-	-	-

Table 10 Detection probabilies (%) on Sellafield beach, "low sand" areas

Depth	^{60}Co activity (kBq)				^{137}Cs activity (kBq)				^{241}Am activity (kBq)			
(m)	1	10	100	1000	1	10	100	1000	1	10	100	1000
1 10^{-4}	-	100	100	100	-	96	100	100	-	5	100	100
0.05	-	91	100	100	-	31	100	100	-	0.3	7	100
0.1	-	42	100	100	-	2	100	100	-	0.2	0.2	8
0.15	-	12	100	100	-	0.4	88	100	-	0.2	0.2	0.2
0.2	-	3	99	100	-	0.1	26	100	-	-	-	-
0.3	-	0.1	32	100	-	0	0.6	89	-	-	-	-
0.4	-	-	-	-	-	0	0.1	6	-	-	-	-

Table 11 Detection probabilities (%) on St Bees beach, sandy areas

Depth	^{60}Co activity (kBq)				^{137}Cs activity (kBq)				^{241}Am activity (kBq)			
(m)	1	10	100	1000	1	10	100	1000	1	10	100	1000
1 10^{-4}	-	100	100	100	-	92	100	100	-	5	100	100
0.05	-	94	100	100	-	22	100	100	-	0.2	6	100
0.1	-	50	100	100	-	2	100	100	-	0.2	0.2	7
0.15	-	15	100	100	-	0.2	79	100	-	0.2	0.2	0.2
0.2	-	3	99	100	-	0	18	100	-	-	-	-
0.3	-	0.2	38	100	-	0	0.5	82	-	-	-	-
0.4	-	-	-	-	-	0	0	4	-	-	-	-

Although object detection probabilities were determined for both sand and shingle areas of the beaches where both are present, only the detection probabilities for sand areas were used in the subsequent estimation of the population of objects on each beach, even though differences between the two are significant in some cases. This was done because the habit surveys do not differentiate between the two types of area, although it is clear that occupancy times for sandy areas are greater than those for shingle areas.

4.1.4 Performance of the Groundhog Evolution2™ system

For objects on the surface of the beach, HPA's calculations indicate minimum detectable amounts (MDAs) of 11 kBq for ^{137}Cs, 5 kBq for ^{60}Co, 110 kBq for ^{90}Sr and 37 kBq for ^{241}Am. At greater depths (given in brackets), HPA's calculations indicate MDAs of 1.3 MBq for ^{137}Cs (0.3 m), 250 kBq for ^{60}Co (0.3 m), 620 kBq for ^{90}Sr (0.13 m) and 31 MBq for ^{241}Am (0.15 m).

A number of features may be observed in the data presented in Table 7 -Table 11 and given in more detail in Appendix A.

a) For buried objects within 0.1 m of the surface, the Groundhog Evolution2™ system is predicted to be most sensitive for objects containing ^{60}Co, followed in order of decreasing sensitivity by objects containing ^{137}Cs, ^{90}Sr and ^{241}Am.
b) For objects on the surface, the system is more sensitive to objects containing ^{241}Am than objects containing ^{90}Sr.
c) Table 12 lists the beaches in order of decreasing object detection probability for ^{137}Cs and ^{60}Co. While not identical, the two lists are broadly similar. The highest detection probability is predicted to be found on Drigg beach for both ^{137}Cs and ^{60}Co, while the lowest is found on the shingle areas of Braystones beach. Furthermore, all of the shingle areas are predicted to have lower detection probabilities than any of the sandy areas. This presumably arises because background levels on sandy beaches are generally lower than on shingle beaches, as shown by background data presented in Nuvia (2008). Similarly, background levels on Drigg beach are presumably lower than on other sandy beaches.
d) For all four radionuclides, an approximately exponential decrease in detection probability is found with increasing depth for those object activities where the detection probability varies over a significant part of the 0 – 100% range within the depth range investigated.

Table 12: Beaches listed in order of decreasing object detection probability

Ranking	Beach	
	^{137}Cs objects	^{60}Co objects
1	Drigg (sand)	Drigg (sand)
2	Barnscar, Drigg (sand)	Braystones (sand)
3	Seascale (sand)	Barnscar, Drigg (sand)
4	Sellafield (low sand)	St Bees (sand)
5	Braystones (sand)	Seascale (sand)
6	St Bees (sand)	Sellafield (low sand)
7	Sellafield (high sand)	Sellafield (high sand)
8	Barnscar, Drigg (shingle)	Barnscar, Drigg (shingle)
9	Seascale (shingle)	Seascale (shingle)
10	Braystones (shingle)	Braystones (shingle)

4.1.5 Comparison with the results of beach trials

In October 2009, Nuvia carried out *in situ* beach trials with the aim of quantifying the detection capability of the Groundhog Evolution2™ system. Radioactive sources of ^{137}Cs, ^{60}Co, ^{241}Am and ^{90}Sr/^{90}Y of varying levels of activity were buried at various specified depths within one of two test areas that were approximately 110 m long and 2 m wide. Test runs were carried out to examine "typical" and "worst case" performance, as described in detail in Appendix A. To ensure that the trials were carried out under exactly the same conditions as routine beach monitoring, a section of beach at Drigg below the spring high tide line and above the neap high tide line was used. The trials took place during low tides. Full details of the trials are given in Nuvia (2010a).

Comparison between HPA's calculated values and the results of the beach trials is informative, but it should be noted that a direct comparison is not possible. Although the beach trials were carried out at Drigg, the background data set for Drigg used in the HPA simulations was not from the same area. The best comparison that can be made is between Nuvia's typical case and HPA's results for sandy areas of Drigg beach, and between Nuvia's worst case and HPA's results for shingle areas of Braystones beach (effectively, HPA's worst case).

Table 13 - Table 16 show these comparisons for the object activities and depths used in the beach trials study, which had been chosen in order to avoid as far as possible conditions where objects would always be detected, or would be impossible to detect.

Although there are some discrepancies, agreement is broadly good for ^{137}Cs and ^{60}Co. For ^{241}Am, agreement is reasonable for conditions where detection probabilities are high, but for the conditions where the calculated values indicate detection probabilities below 10%, the beach trials found zero detection probabilities.

Agreement is rather poor for ^{90}Sr/^{90}Y. The only agreement is found for the highest object activity (1000 kBq) on the surface of the beach, where beach trials and calculations indicate 100% detection probability. For other conditions, the beach trials generally indicated zero detection probability where the calculations indicated detection probabilities significantly above zero. There is therefore some doubt as to whether the Groundhog Evolution2™ system is achieving the expected performance for detection of objects that contain only ^{90}Sr/^{90}Y. (Objects that contain both ^{90}Sr/^{90}Y and ^{137}Cs may of course be detected because of their ^{137}Cs content).

Table 13: Comparison of HPA's calculated object detection probabilities with the results of Nuvia's beach trials, for ^{137}Cs

Object activity (kBq)	Depth (m)	Probability (%)			
		Nuvia beach trials		HPA calculated values	
		Worst case	Best case	Braystones Shingle	Drigg Sand
10	0[(a)]	55	100	78	98
	0.05	0	25	9	46
100	0.1	100	95	100	100
	0.2	100	100	11	38
	0.3	0	5	0	1
1000	0.2	100	100	100	100
	0.3	100	100	71	95
	0.4	70	100	2	91

a) The calculations shown for 0 m were actually carried out for a depth of 0.0001 m.

Table 14: Comparison of HPA's calculated object detection probabilities with the results of Nuvia's beach trials, for ^{60}Co

Object activity (kBq)	Depth (m)	Probability (%)			
		Nuvia beach trials		HPA calculated values	
		Worst case	Best case	Braystones shingle	Drigg Sand
10	0[(a)]	95	100	100	100
	0.05	65	100	82	97
	0.1	20	70	21	60
100	0.1	100	100	100	100
	0.2	100	100	98	100
	0.3	35	100	16	48

a) The calculations shown for 0 m were actually carried out for a depth of 0.0001 m.

Table 15: Comparison of HPA's calculated object detection probabilities with the results of Nuvia's beach trials, for ^{90}Sr

Object activity (kBq)	Depth (m)	Probability (%)			
		Nuvia beach trials		HPA calculated values	
		Worst case	Best case	Braystones Shingle	Drigg Sand
10	0[(a)]	0	5	0.3	0.4
	0.05	0	0	0.3	0.3
100	0	0	0	46	95
	0.05	0	0	6	39
1000	0	100	100	100	100
	0.05	25	65	100	100

A) The calculations shown for 0 m were actually carried out for a depth of 0.0001 m.

Table 16: Comparison of HPA's calculated object detection probabilities with the results of Nuvia's beach trials, for ^{241}Am

Object activity (kBq)	Depth (m)	Probability (%)			
		Nuvia beach trials		HPA calculated values	
		Worst case	Best case	Braystones Shingle	Drigg Sand
10	0[(a)]	0	0	2	9
	0.05	0	0	0.3	0.2
100	0	60	100	100	100
	0.05	0	0	2	12
	0.1	0	0	0.3	0.2
1000	0.05	90	90	100	100
	0.1	0	0	2	13

a) The calculations shown for 0 m were actually carried out for a depth of 0.0001 m.

4.2 Estimating the population of objects on a beach

It is not expected that a lot more objects will have been found at depth compared to near the surface, and the evidence gathered from monitoring supports this assumption. Therefore any method used to estimate the population of objects (as defined at the beginning of Section 4) needs to comply with the following rules:

- Avoid, as far as possible, predicting very large numbers of objects at depth as a result of dividing numbers of actual finds at these depths by small detection probabilities when there is no evidence of large numbers of objects at shallower depths;
- Avoid, as far as possible, predicting no objects at shallow depths when they have been found at greater depths.

The population of objects has been estimated using two methods which aim to address these points, using the data available on the number of objects found, their depths and activities and the detection probabilities of the Groundhog Evolution2™ system. Both methods are discussed in this Section. The first method applies these rules directly and therefore needs to take account of the depth at which objects were detected on the beach. However, there is uncertainty on this depth because objects can become disturbed during retrieval and the method for estimating depth during the process of retrieval is imprecise. Furthermore, the data available for each object class (ie, alpha-rich, beta-rich or ^{60}Co-rich) and activity content are too sparse to develop a good picture of the distribution of objects with depth. A second method was therefore developed that does not make use of the information on the distribution of objects with depth on the beaches but instead assumes that all objects are uniformly distributed with depth. The disadvantage of using this method is that no account is taken of the information that is available on the depths of objects found on the beach.

The populations of objects per hectare estimated using these two methods are taken to be representative of the number of objects present per unit area at any time that the

beach is used. However, it should be recognised that during any single visit to a beach, the population of objects per hectare may be higher or lower than this value depending on a number of factors including movement of objects within and between beaches, beach sediment turnover and how recently the beach has been monitored and objects removed.

The predicted populations of objects on the beaches were based on information from monitoring which was carried out on sandy areas of the beaches. It has been assumed that these populations of objects are applicable for the entire beach, including both sandy and rocky areas. There are no compelling reasons to assume that the population of objects in rocky areas is significantly different to that in the monitored sandy areas. However, the application of these values to the unmonitored areas introduces an additional level of uncertainty. It may be noted that no objects have yet been found in the boulder fields at Nethertown and Coulderton as a result of Sellafield Ltd's 2010 monitoring programme using held-held monitoring equipment.

The probability of detection for each of the object classes specified in Section 4.1 was evaluated for object activities of 1, 10, 100 and 1000 kBq for each of the detected radionuclides at a number of object depths (Section 4.1.3). To allow this information to be combined with data on the number of objects found on each beach, the objects found have been grouped into corresponding activity 'bands' whose geometric mean is approximately equal to the activity at which the probability of detection was determined, and depth 'bands' whose arithmetic mean is approximately equal to the depth at which the probability of detection was determined. The activity 'bands' are shown in Table 17 and the depth 'bands' are shown in Table 18.

Table 17: Activity bands used for estimating populations of objects containing ^{60}Co, ^{137}Cs and ^{241}Am

Representative activity (kBq)[(a)]	Range of activity levels in each band (kBq)	
	Minimum	Maximum
10	3 [(b)]	30
100	30	300
1000	300	3000

(a) Probabilities of detection were evaluated at these activities

(b) Object populations have not been estimated for objects with activities less than 3 kBq, as discussed in Section 4.3.

Table 18: Depth bands used for estimating populations of objects containing ^{60}Co, ^{137}Cs and ^{241}Am

Representative depth (m)[(a)]	Range of depths in each band (m)	
	Minimum	Maximum
0	0	0.025
0.05	0.025	0.075
0.1	0.075	0.125
0.15	0.125	0.175
0.2	0.175	0.25
0.3	0.25	0.35
0.4	0.35	0.45

(a) Probabilities of detection were evaluated at these depths

The estimated population of objects on the beaches for use in a dose assessment should be representative of the number of objects on the beach at any time that the beach is used. This is not the same as the total number of object finds that have been detected and retrieved during the monitoring programme. For beaches that are monitored frequently and where the whole beach is monitored, the number of objects found during a complete, single scan of the beach, adjusted to take account of detection probability, may be taken to provide an estimate of the population of objects. However, the current situation with the monitoring of beaches in the vicinity of the Sellafield site is that it has not been possible to monitor the whole area of each beach

Table 19 shows the monitored area and the beach area for each of the beaches considered. Except for Drigg beach, all the beaches considered have been monitored to the extent that the total area monitored is greater than the area of the beach.

Table 19: Area of beach monitored in relation to the beach area

Areas	Braystones beach	Drigg beach	Seascale beach	Sellafield beach	St Bees beach
Area of beach (ha)	18.9	196.7	80.7	54.1	28.5
Total area monitored (ha)	80.6	60.2	146.8	246.8	108.5

Where the area monitored exceeds the area of the beach, the area monitored over the whole monitoring programme therefore has to be taken into account when estimating the population of objects from the total number of objects detected. The cumulative number of objects found in each activity and depth band from all scans of a particular beach may be denoted by $N_{C,a,d}$, where *a* and *d* are indices indicating the activity and depth band. The corresponding number of objects expected to be found by a single, complete scan of the beach may be denoted by $N_{S,a,d}$. $N_{S,a,d}$ may be determined from $N_{C,a,d}$ and the ratio of the area of the beach to the area monitored, as follows:

$$N_{S,a,d} = N_{C,a,d} \times A_{beach}/A_{monitored}$$

4.2.1 Estimating the population of objects – method 1

This Section describes the steps used in the first method to estimate the object population on each beach. A worked example of this method is given in Appendix B.

The initial estimate

The general relationship between the population of objects, P, the number of objects found at a particular depth by a single, complete scan of a beach, N, and the detection probability at a particular depth expressed as a percentage, E, is:

$$P = N \times 100/E$$

For example, if 16 objects were found and the detection efficiency was 80%, then the population of objects present would be estimated as 20.

The initial estimate of the population of objects in each activity and depth band, $P_{E1,a,d}$, is given by:

$$P_{E1,a,d} = N_{S,a,d} \times 100/E_{a,d}$$

where *a* and *d* are indices indicating the activity and depth band.

The second estimate

As noted in Section 4.1.3, the uncertainties on the detection probabilities are very large where the probabilities are small. Applying such small detection probabilities to the number of objects found on the beaches may therefore lead to over- or under-estimation of the object population. The initial estimate was therefore adjusted to give a second estimate, P_{E2}, using the following rules (illustrated in Figure 3).

- For depth layers and activity bands in which at least one object has been found and detection probability is 10% or greater, the initial estimate was accepted.
- For depth layers where the first estimate was zero, if the estimates for deeper layers were non-zero then the detected number of objects in the next lower non-zero layer was substituted. The detected rather than the estimated number of objects were used since the number of detected objects is a true, minimum value for the number of objects present, whereas the number of estimated objects could be subject to significant uncertainties. Allowance was made for the different thicknesses of each layer when substituting the number of detected objects, that is:

  $$P_{E2,a,d} = P_{E2,a,d+1} \times D_d / D_{d+1}$$

  where *d* is the index of a depth band, *d*+1 is the index for the next layer down and D_d is the thickness of layer d.
- For depth layers where the detection probability was less than 10%, if the first estimate was greater than the mean plus 2 standard deviations ($\bar{x} + 2\sigma$) of the first estimate for depth layers where the detection probability was greater than 10%, a substitution was made of the first estimate with the mean value of these

layers. The calculation of mean and standard deviation took account of the differences in layer thickness, as described above.

- Where there were fewer than two depth layers with detection probabilities greater than 10%, then the two depth layers with the highest detection probabilities were used with the same algorithm to allow an estimate of standard deviation to be made.

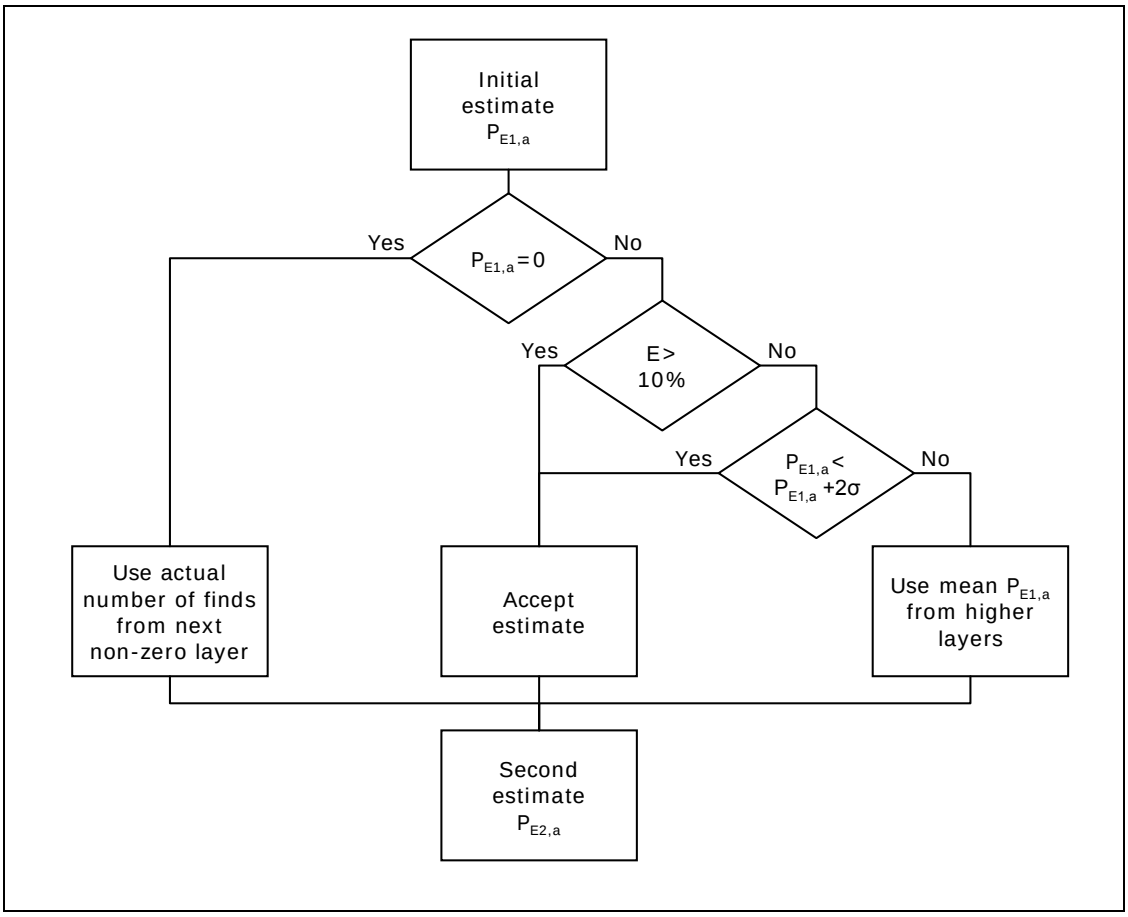

Figure 3: Method 1, algorithm for second estimate of object population

4.2.2 Estimating the population of objects - method 2

If the number of objects present per unit depth in a particular activity band, $n_{0,a}$, is assumed to be constant with depth, and the variation of detection probability with depth is described by a function *f*(x), then the number of objects in that activity band expected to be found by a single, complete scan of the beach is described by:

$$N_{S,a} = n_{0,a} \int_{x=0}^{x=md} f(x)dx$$

where

$N_{S,a}$ = Number of objects in the activity band found in the depth range 0 → md

$n_{0,a}$ = Number of objects present per unit depth in that activity band (m^{-1})

x = Depth: surface = 0 and md = maximum depth (m)

f(x) = Probability of detection as a function of depth for each activity band

$n_{0,a}$ is determined by dividing $N_{S,a}$ by the value of the integral:

$$n_{0,a} = \frac{N_{S,a}}{\int_{x=0}^{x-md} f(x)dx}$$

The population of objects in each depth band, $P_{a,d}$, may then be determined by multiplying $n_{0,a}$ by the thickness of the depth band, D_d:

$$P_{a,d} = n_{0,a} \times D_d$$

The detection probability is known at particular depth values, rather than being described by a known function, so the integral was evaluated using a numerical method (Simpsons rule). This method provides formulae for integrating a function whose value is known at equally spaced steps. For alpha-rich objects with four data points, Simpson's 3/8 rule was used:

$$\int_{X=1}^{X=4} f(x)dx = h\left[\frac{3}{8}f1 + \frac{9}{8}f2 + \frac{9}{8}f3 + \frac{3}{8}f4\right] + O(h^5 f^{(4)})$$

where

h = Interval range, 0.05 m

x = Depth (m)

f = Detection probability at depth x

$O(h^5 f^{(4)})$ = Error associated with the evaluated integral

The detection probability was calculated for values of x from 0.001 to 0.15. However, the formula requires evenly spaced intervals so 0.001 was replaced by 0.

For beta-rich and cobalt-rich objects, the extended Simpson's rule formula for pairs of intervals, given below, was used.

$$\int_{x1}^{x=n} f(x)dx = h\left[\frac{1}{3}f1 + \frac{4}{3}f2 + \frac{2}{3}f3 + \frac{4}{3}f4 + \ldots + \frac{2}{3}f_{n-2} + \frac{4}{3}f_{n-1} + \frac{1}{3}f_n\right] + O\left(\frac{1}{n^4}\right)$$

Where:

h = Interval range, 0.05 m

x = Depth (m)

f = Detection probability at depth x

n = Number of points, 6 for cobalt-rich objects and 9 for beta-rich objects

$O(1/N^4)$ = Error associated with the evaluated integral

4.2.3 Number of objects per gram of sand

The population of objects per unit area on each beach is determined by dividing the population of objects in each activity and depth band, $P_{a,d,}$ by the area of the beach, in hectares. When considering the exposure of individuals to radioactive objects, the likelihood of encountering an object depends on the mass of sand that an individual comes into contact with while carrying our various beach activities, for example, the amount of sand they get on their skin. The population density of objects (that is, the number of objects per gram of sand) was obtained by dividing the population of objects per hectare by the mass of sand contained in an area of one hectare with a depth equal to that for which the detection probability was greater than 0.1%. The density of sand was taken to be $2\ 10^6$ g m^{-3}.The depths used were 0.15 m for alpha-rich objects, 0.40 m for beta-rich objects and 0.30 m for cobalt-60-rich objects. This ensured that the total volume of sand used in the calculation of the population density of objects was the same as that in which the population of objects was estimated. In the absence of information to the contrary, it was assumed that the actual depth of sand in all of the monitored areas was greater than these values. Were this not to be the case for a particular area of beach, then the number of objects per gram of sand would be underestimated for that area of beach.

4.2.4 Estimated values for the population of objects on the beaches

The populations of objects for the five beaches, estimated using methods 1 and 2, are given in Table 20 and Table 21 for particles and stones, respectively. The populations of objects estimated using method 1, expressed in terms of numbers of objects per hectare of beach, are given in Table 22.

The maximum difference between the populations of objects estimated using the two methods is about a factor of five although most estimated populations are within a factor of two. A number of observations may be made on the populations of particles and stones shown in Table 20 and Table 21.

- Populations of lower activity objects are greater than for higher activity objects for all the beaches and for all categories of objects (alpha-rich, beta-rich or cobalt-rich).
- The population of alpha-rich particles is highest for Drigg beach, while Sellafield beach has the highest population of beta-rich particles.

- The populations of alpha-rich particles are higher than those of beta-rich particles; at Braystones, Seascale and Sellafield beaches by a factor in the approximate range 1.1 to 3, and at Drigg and St Bees beaches by a factor in the approximate range 10 to 200.
- The population of alpha-rich stones at Sellafield beach is somewhat less than that of alpha-rich particles, whereas the total population of beta-rich stones is somewhat greater than that of beta-rich particles. Alpha-rich stones have only been found on Sellafield beach.On Braystones and Seascale beaches, the only 2 beaches where beta-rich stones have been found, the total populations of beta-rich stones are less than those of beta-rich particles by factors of between 5 and 50.

The two methods for estimating the populations of objects were intended to reduce uncertainties as far as possible. Neither method resulted in consistently higher populations of objects and so neither is considered to be more cautious than the other. Based on these results, the two methods are considered to be in good agreement and show no significant differences when considering all the uncertainties in the data. Developing two independent methods has provided confidence in the estimated populations of objects.

Both methods have strengths and weaknesses. Method 1 attempts to take account of the depth at which the objects have been detected (which is in itself uncertain) and uses a complex algorithm that attempts to take account of numbers of objects at other depths. This approach has limitations where very few objects have been found below the beach surface as sufficient data are not available to make robust adjustments. Method 2 assumes a uniform distribution of objects with depth which does not take into account the depth distributions found while monitoring and retrieving objects from the beaches.

It was decided that method 1 would be used in the assessment of the population of objects on the five beaches considered because it takes account of the available information on object depths. Method 2 could be used if preferred, with any probability of encounter estimated being directly proportional to the difference in the estimated object populations. The ratios of the populations of objects for the two methods are given in Table 20 and Table 21 for reference.

In some circumstances, uncertainties in the estimate of the population of objects can be quite large. When the detection probability is close to 100%, uncertainties are low, but when a particular object is found at a depth where the probability of detection is low, uncertainties are greater. When only a few objects have been found at depth in a particular monitored area, the uncertainty in the estimate of the actual number of objects in that area can be large.

4.3 Inclusion of objects with low radioactivity content

Objects containing radionuclides with activities around 1 kBq or lower have not been included in the estimate of the population of objects on each beach. Only 22 beta-rich objects have been detected with the Groundhog Evolution2™ system on the beaches with activities at this level (of which 20 were on Sellafield beach). The evaluated detection probabilities for objects at this activity level are very low (less than 1%) even on the beach surface and their use to estimate the population of objects on a beach would represent a source of unreasonable uncertainty. Use of such data would therefore not provide reliable estimates of overall risks to beach users. On the basis of the monitoring results and information on the capability of the Groundhog Evolution2™ system to detect objects with this activity content, no predictions of the population of objects in this activity range can be made. It is not possible to conclude from the monitoring data whether there are very few objects on the beaches with low radioactivity content or whether they are present in higher numbers but cannot be detected with the available detection systems. Radiation doses and health risks from encountering objects with low radioactivity content are very low as discussed in Section 7.5. If a lot of very small, low activity objects are present on the beaches, they will become part of the ambient levels of contamination on the beach which are routinely monitored (see RIFE reports, eg, Cefas, 2009a).

Table 20: Estimated population of particles calculated using methods 1 and 2

Representative activity	Alpha-rich particles (particles g^{-1} sand)[a]			Beta-rich particles (particles g^{-1} sand)[a]			Cobalt-rich particles (particles g^{-1} sand)[a]		
	Method 1	Method 2	Method1/Method2	Method 1	Method 2	Method1/Method2	Method 1	Method 2	Method1/Method2
Braystones									
10 kBq	$3.2\ 10^{-10}$	$1.2\ 10^{-10}$	**2.67**	$1.1\ 10^{-10}$	$1.4\ 10^{-10}$	**0.79**	$2.4\ 10^{-12}$	$4.0\ 10^{-12}$	**0.60**
100 kBq	$3.9\ 10^{-11}$	$5.9\ 10^{-11}$	**0.66**	$1.5\ 10^{-12}$	$1.6\ 10^{-12}$	**0.94**	-	-	**-**
1000 kBq	-	-	**-**	-	-	**-**	-	-	**-**
Total	$3.6\ 10^{-10}$	$1.7\ 10^{-10}$	**2.12**	$1.1\ 10^{-10}$	$1.4\ 10^{-10}$	**0.79**	$2.4\ 10^{-12}$	$4.0\ 10^{-12}$	**0.60**
Drigg									
10 kBq	$2.8\ 10^{-09}$	$4.4\ 10^{-10}$	**6.36**	$6.2\ 10^{-12}$	$1.7\ 10^{-11}$	**0.36**	$8.8\ 10^{-12}$	$7.0\ 10^{-12}$	**1.26**
100 kBq	$5.2\ 10^{-11}$	$6.5\ 10^{-11}$	**0.80**	$6.2\ 10^{-12}$	$8.1\ 10^{-12}$	**0.77**	-	-	**-**
1000 kBq	-	-	**-**	-	-	**-**	-	-	**-**
Total	$2.8\ 10^{-09}$	$5.1\ 10^{-10}$	**5.49**	$1.2\ 10^{-11}$	$2.5\ 10^{-11}$	**0.48**	$8.8\ 10^{-12}$	$7.0\ 10^{-12}$	**1.26**
Seascale									
10 kBq	$2.1\ 10^{-11}$	$1.4\ 10^{-10}$	**0.15**	$3.2\ 10^{-11}$	$5.8\ 10^{-11}$	**0.55**	$6.2\ 10^{-13}$	$1.8\ 10^{-12}$	**0.34**
100 kBq	$1.6\ 10^{-11}$	$2.4\ 10^{-11}$	**0.67**	$2.2\ 10^{-12}$	$1.9\ 10^{-12}$	**1.16**	-	-	**-**
1000 kBq	-	-	**-**	-	-	**-**	-	-	**-**
Total	$3.7\ 10^{-11}$	$1.7\ 10^{-10}$	**0.22**	$3.4\ 10^{-11}$	$6.0\ 10^{-11}$	**0.57**	$6.2\ 10^{-13}$	$1.8\ 10^{-12}$	**0.34**
Sellafield									
10 kBq	$1.5\ 10^{-10}$	$3.2\ 10^{-10}$	**0.47**	$1.6\ 10^{-10}$	$1.5\ 10^{-10}$	**1.07**	$8.1\ 10^{-13}$	$1.8\ 10^{-12}$	**0.45**
100 kBq	$9.0\ 10^{-11}$	$5.1\ 10^{-11}$	**1.76**	$5.1\ 10^{-12}$	$5.3\ 10^{-12}$	**0.96**	-	-	**-**
1000 kBq	$8.9\ 10^{-13}$	$1.1\ 10^{-12}$	**0.81**	-	-	**-**	-	-	**-**
Total	$2.4\ 10^{-10}$	$3.7\ 10^{-10}$	**0.65**	$1.6\ 10^{-10}$	$1.5\ 10^{-10}$	**1.07**	$8.1\ 10^{-13}$	$1.8\ 10^{-12}$	**0.45**
St Bees									
10 kBq	$4.2\ 10^{-10}$	$2.0\ 10^{-10}$	**2.10**	$2.7\ 10^{-11}$	$3.2\ 10^{-11}$	**0.84**	$6.3\ 10^{-13}$	$1.1\ 10^{-12}$	**0.57**
100 kBq	$1.4\ 10^{-11}$	$1.1\ 10^{-11}$	**1.27**	-	-	**-**	-	-	**-**
1000 kBq	-	-	**-**	-	-	**-**	-	-	**-**
Total	$4.3\ 10^{-10}$	$2.1\ 10^{-10}$	**2.05**	$2.7\ 10^{-11}$	$3.2\ 10^{-11}$	**0.84**	$6.3\ 10^{-13}$	$1.1\ 10^{-12}$	**0.57**

- indicates that no particles have been estimated for this activity or beach.

a) Particles assumed to be within a depth range of 0.15 m for alpha-rich particles, 0.4 m for beta-rich particles and 0.3 m for ^{60}cobalt-rich particles (see Section 4.2.3).

Table 21: Estimated population of stones calculated with methods 1 and 2

Representative activity	Alpha-rich stones (stones g^{-1} sand)[a]			Beta-rich stones (stones g^{-1} sand)[a]			Cobalt-rich stones (stones g^{-1} sand)[a]		
	Method 1	Method 2	Method 1/Method2	Method 1	Method 2	Method 1/Method2	Method 1	Method 2	Method 1/Method2
Braystones									
10 kBq	-	-	**-**	-	-	**-**	-	-	**-**
100 kBq	-	-	**-**	$1.8\ 10^{-12}$	$1.6\ 10^{-12}$	**1.13**	-	-	**-**
1000 kBq	-	-	**-**	-	-	**-**	-	-	**-**
Total	-	-	**-**	$1.8\ 10^{-12}$	$1.6\ 10^{-12}$	**1.13**	-	-	**-**
Drigg									
10 kBq	-	-	**-**	-	-	**-**	-	-	**-**
100 kBq	-	-	**-**	-	-	**-**	-	-	**-**
1000 kBq	-	-	**-**	-	-	**-**	-	-	**-**
Total	-	-	**-**	-	-	**-**	-	-	**-**
Seascale									
10 kBq	-	-	**-**	$5.7\ 10^{-12}$	$8.3\ 10^{-12}$	**0.69**	-	-	**-**
100 kBq	-	-	**-**	$7.0\ 10^{-13}$	$9.2\ 10^{-13}$	**0.76**	-	-	**-**
1000 kBq	-	-	**-**	-	-	**-**	-	-	**-**
Total	-	-	**-**	$6.4\ 10^{-12}$	$9.2\ 10^{-12}$	**0.70**	-	-	**-**
Sellafield									
10 kBq	$2.0\ 10^{-10}$	$7.1\ 10^{-11}$	**2.82**	$2.8\ 10^{-10}$	$2.7\ 10^{-10}$	**1.04**	$5.7\ 10^{-13}$	$4.4\ 10^{-13}$	**1.30**
100 kBq	$3.0\ 10^{-13}$	$1.9\ 10^{-12}$	**0.16**	$2.4\ 10^{-11}$	$2.7\ 10^{-11}$	**0.89**	-	-	**-**
1000 kBq	-	-	**-**	$2.0\ 10^{-12}$	$6.5\ 10^{-13}$	**3.08**	-	-	**-**
Total	$2.0\ 10^{-10}$	$7.3\ 10^{-11}$	**2.74**	$3.0\ 10^{-10}$	$3.0\ 10^{-10}$	**1.00**	$5.7\ 10^{-13}$	$4.4\ 10^{-13}$	**1.30**
St Bees									
10 kBq	-	-	**-**	-	-	**-**	-	-	**-**
100 kBq	-	-	**-**	-	-	**-**	-	-	**-**
1000 kBq	-	-	**-**	-	-	**-**	-	-	**-**
Total	-	-	**-**	-	-	**-**	-	-	**-**

- indicates that no stones have been estimated for this activity or beach.

a) Particles assumed to be within a depth range of 0.15 m for alpha-rich particles, 0.4 m for beta-rich particles and 0.3 m for ^{60}cobalt-rich particles (see Section 4.2.3).

Table 22: The estimated population of objects on each beach

Beach	Object class	Number of objects per hectare of beach[a,b,c]			
		10 kBq (3 kBq–30 kBq)	100 kBq (30 kBq–300 kBq)	1000 kBq (>300 kBq)	Average find rate by Groundhog Evolution2™ [d]
Braystones	Alpha-rich	1	0.1	0	0.04
	Beta-rich	0.4	0.02	0	0.09
Drigg	Alpha-rich	8	0.2	0	0.06
	Beta-rich	0.03	0.05	0	0.06
Seascale	Alpha-rich	0.06	0.05	0	0.01
	Beta-rich	0.2	0.02	0	0.14
Sellafield	Alpha-rich	1	0.3	0.003	0.37
	Beta-rich	2	0.2	0.02	1.16
St_Bees	Alpha-rich	1	0.04	0	0.03
	Beta- rich	0.08	0	0	0.08

a) Objects includes particles and stones

b) The number of objects with activities of about 1 kBq or lower has not been calculated, as discussed in the text.

c) Objects assumed to be within a depth range of 0.15 m for alpha-rich particles, 0.4 m for beta-rich particles and 0.3 m for ^{60}cobalt-rich particles (see Section 4.2.3).

d) Data taken from Dalton, 2010

4.4 Detection of objects using the Groundhog Synergy system

The Groundhog Evolution2™ system was used for beach monitoring up until August 2009. In September 2009 a new system, Groundhog Synergy, was introduced which includes an additional array of detectors. These “FIDLER” detectors (Field Instrument for the Detection of Low-Energy Radiation) employ a thin crystal, 127 mm in diameter and 1.6 mm thick, and are designed to enhance the detection of low-energy photon radiation, particularly the 60 keV emission of ^{241}Am and the Bremsstrahlung radiation resulting from ^{90}Sr/^{90}Y decays.

It has not been possible to carry out an evaluation of the performance of the Groundhog Synergy system of the type presented here for the Groundhog Evolution2™ system because of the lack of availability of calibration and background data. Some brief comments are presented here on the improvements in detection probability expected from the deployment of Groundhog Synergy.

Table 23 compares minimum detectable activities for the Evolution2™ and Synergy systems for ^{241}Am. These data are taken from a Nuvia report to the Committee on Medical Aspects of Radiation in the Environment (COMARE) (Nuvia, 2010b).

Table 23: Typical minimum detectable activities (MDA) (95% confidence level) for the Evolution2™ and Synergy systems for ^{241}Am

Depth (m)	Activity (kBq)	
	Evolution2	Synergy
0	39	14
0.05	373	180
0.1	3700	1600
0.15	32600	
0.2	310000	130000

As can be seen, the MDAs for the Synergy system are a factor of about two less than those for the Evolution2™ system. Figure 4 illustrates what this means in terms of object detection probabilities for the example of objects detected at zero depth (ie, on the surface of the beach), where Synergy and Evolution2™ provide ^{241}Am MDAs of 14 kBq and 39 kBq, respectively. Use of Synergy should provide significant increases in object detection probabilities for particle activities in the range 5 kBq to 30 kBq. Below 5 kBq, both systems provide relatively low detection probabilities, while above 30 kBq, almost all objects would be detected by either system. The greatest improvement would be expected to occur for objects of about 10 kBq, with an increase in detection probability from ~ 10% to ~ 85%.

It is understood that the use of the Synergy system is currently resulting in significant increases in the number of objects being found. This increased find rate does not necessarily mean that there is an increase in the number of objects actually present on the beaches, since the increase could be completely attributable to improvements in sensitivity. Further work is needed to understand the reasons for the increased find rate. Firstly, a comparison should be made of the numbers of objects found and their activities, before and after the introduction of Synergy. The comparison should be made for measurements made over the same areas of beach. Since detection probability for ^{241}Am decreases rapidly with increasing object depth, the comparison is best made for objects detected on or very close to the surface, although comparisons at greater depths will also be useful. Comparison with predicted detection probabilities such as those shown in Figure 4 should provide a good indication of the reason for the increased find rate. Secondly, the detection probabilities for Synergy should be quantified by carrying out an investigation analogous to that carried out for Groundhog Evolution (Section 4.1).

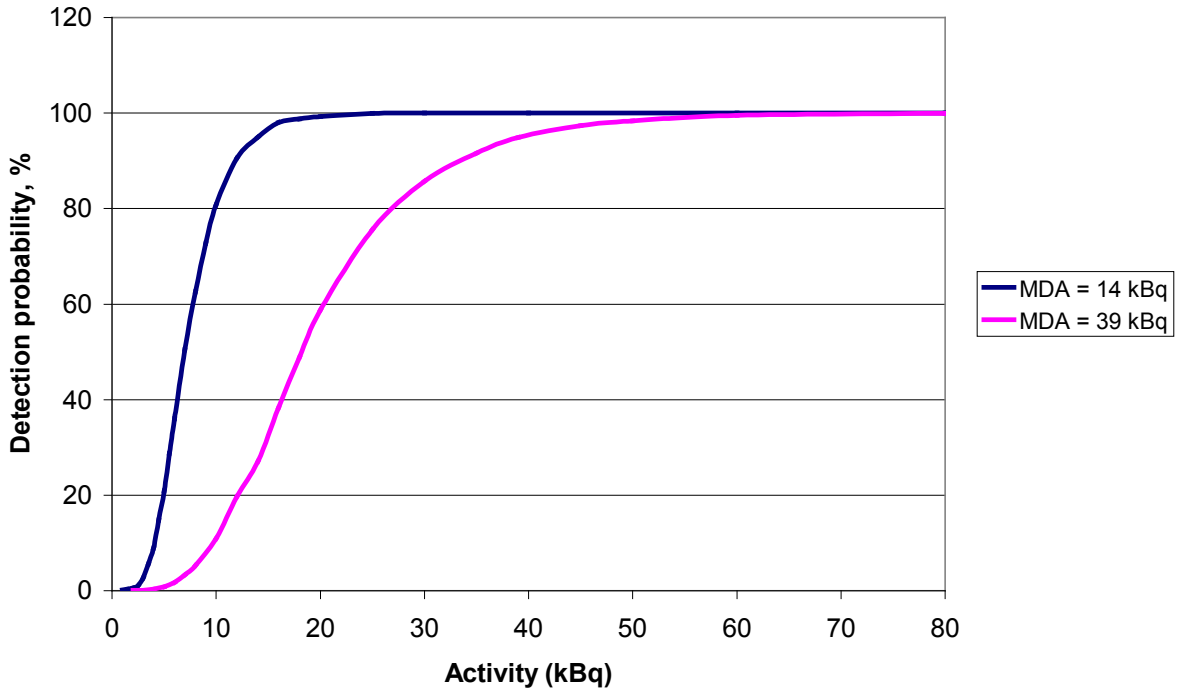

Figure 4: Detection probabilities corresponding to MDAs of 14 kBq and 39 kBq (illustrative)

5 INFORMATION ON THE USE OF THE BEACHES

In order to evaluate the likelihood of an individual being exposed to a contaminated object, information is needed on the activities people engage in and the time they spend on the beaches. Beach use defines how individuals can come into contact with sand and hence be exposed to radioactive objects on the beaches. The Environment Agency commissioned two detailed habits surveys along the coast around the Sellafield site to identify individuals who, through their activites on beaches in the vicinity of Selalfield, may increase their potential exposure to radioactive objects. The aim of the surveys was to identify the locations where different beach activities took place, where people spend their time on the beaches and how long they spend on the beaches. The surveys were conducted using both observation and interviews with individuals and were carried out in 2007 and 2009 (Cefas, 2008a; 2010).

The surveys were carried out mostly during the summer months and so there are some uncertainties regarding beach occupancy at other times of the year, particularly during the winter. It is recognised that the surveys can only provide a snap shot of what happens on a beach at the time of the survey and, even during the summer months, it is likely that some beach users could have been missed. However, it is considered that sufficient data have been collected such that the assessment of the probability of encountering an object on a beach for any beach user missed by the surveys will not be

higher than that estimated for those beach users included. This is because the individuals with the highest beach occupancy will have been identified during the two surveys.

Due to the wide range of beach users and activities undertaken on the beaches, beach users have been allocated to different groups for calculating the probability of encountering a radioactive object. These groups are based on age and activities undertaken on the beaches. The chosen groupings are described in Sections 5.1and 5.2.

5.1 Age groups considered

The people recorded by the habit surveys were divided into three age groups; “young children”, “children” and “adults”. The ages associated with these age groups has been based on guidance from ICRP (ICRP, 2006). The ages assumed to be associated with each of these age groups is as follows:

- **young children**: any individual between 0 and 5 years of age;
- **children**: any individual between 6 and 15 years of age, inclusive;
- **adults**: any individual over 16 years old. In addition, some entries reported within the habit surveys were noted as “unknown” age. It was confirmed by Cefas that these individuals were all adults who had declined to give their ages and hence all such individuals were placed within the adult age group.

Different age groups have been considered because both the probability that an individual using the beaches could encounter an object and the risks to health if an individual does encounter an object on a beach depend on the age of the beach user. Three age groups were considered: young children (aged 0-5 years); children (aged 6-15 years) and adults (over 16 years). For the assessment of health risks, these ages have been represented by a 1 year old for young children and a 20 year old for individuals over 16. The choice of a 1 year old child for the 0-5 years age group ensures that the highest health risks for young children who are active and mobile on the beach are assessed. Health risks have not been explicitly been evaluated for the 6-15 year old age group but will be lie between the values for a 1 year old child and a 20 year old adult.

It is important to note that because a distribution has been assigned to the input parameters used to describe mechanisms of exposure to the contaminated objects on the beaches and beach occupancy, there is expected to be considerable overlap in the estimated probability of encounter for these three age groups. Therefore, selecting slightly different age range brackets would not have affected the conclusions drawn from this study.

5.2 Beach activities considered

The habit surveys identified a wide range of activities that people undertook whilst using beaches in the vicinity of the Sellafield site. Beach activities with similar mechanisms for coming into contact with sand can be grouped as the probabilities of encountering a radioactive object while undertaking these activities will be similar. The grouping of beach activities provides a robust classification which can then be used for other beach activities, which were not identified during the habit surveys. Individuals were assigned to one of three beach activity groups which are described below.

- **Leisure**: includes playing in sand, paddling, rock pooling and general activities on sandy beaches where sand is likely to come into contact with a large fraction of the body. Many observations recorded people spending a large amount of time playing in the sand. The habit surveys showed that all age groups were involved in activities that could be taken to be leisure.

- **Angling/Bait digging**: includes all forms of activities involving digging for bait on the beach and angling. People carrying out these activities are likely to come into contact with a large amount of sand on the hands and be engaged in energetic digging, but would generally be fully clothed. Although adults were the main age group identified with this activity, on several beaches children were also reported to be angling/bait digging.

- **Walking**: includes dog walkers, general walking and those activities where the individual is likely to occasionally pick up objects from the beach but not actively dig into the sand. This group were considered to get their hands covered in sand and, in warmer weather, some other parts of their bodies such as the lower legs. However, in general they were considered to be wearing a reasonable amount of clothing. In most cases the observed age group participating in this activity was adults; however, some children and young children were also observed and these age groups were included for the relevant beaches.

5.2.1 Assumptions made on allocating individuals to beach activity groups

Some individuals were reported as undertaking activities on beaches that could fall within more than one of the above groups. For example, an individual might have been described as spending time “digging in sand and walking the dog”. An assumption therefore had to be made about which group would be appropriate for such an individual as there was not enough information available in the habit surveys to allow a breakdown of the total beach occupancy reported for such an individual into the separate beach activities.

Very few people undertook activities that would fall within both the angling and leisure groups and so people could be divided between these beach use groups relatively easily.

Walking is the activity which is likely to lead to the lowest direct contact with sand and therefore represents the activity which is likely to have the lowest probability of encountering an object. On this basis, where individuals were noted as undertaking

activities on a beach that could fall within more than one of the three activity groups, then that individuals' occupancy was assigned first to either leisure or angling. Only when the description of what the individual does on the beach did not fit into either the leisure or angling groups was the occupancy assigned to walking. For those few individuals where beach use could result in them being assigned to either the leisure or angling groups then the assignment of their occupancy was based on a review of all the information in the habit survey reports and a decision made on a case by case basis.

During the habit surveys, only the total amount of time spent angling and bait digging was collected, rather than the fraction of time undertaking these separate activities. As the probability of encountering an object was expected to be dominated by the time spent collecting bait, it was important to consider the fraction of the total time spent that is specifically bait digging. The habit surveys provide information on the time spent handling sediment and it has been assumed that this largely reflects the time spent digging for bait. The fraction of time spent bait digging was identified as being up to and including 100% of the total time spent on angling activities, and so some individuals were identified as bait diggers rather than anglers. Where the fraction of the time spent bait digging was high, it was noted that the time the individual spent on the beach was generally lower than the total for those individuals described as anglers. A representative fraction of the total time spent angling which was specifically bait digging was therefore used. This value used was 13%, the same fraction used previously for the assessment of health implications from fuel fragments on beaches around the Dounreay nuclear site (Smith and Bedwell, 2005).

5.3 Annual beach occupancy

The habit survey data for 2007 and 2009 (Cefas, 2008a; 2010) have been used to determine the time beach users spend on the beaches along the west Cumbrian coast. The range of occupancy times across all beach users has been considered for each beach, and individuals with the highest beach occupancy have been identified. Annual occupancy has been derived for each of the beach activity and age groups discussed in Sections 5.1 and 5.2.

From the available information within the habit surveys it was possible to determine either the length of time each individual spent on a particular beach or on a particular beach material, for example, sandy areas or rocky areas, but not both. In Section 4.2, it was explained that the population of objects was based on the total beach area and that it has not been possible to estimate the populations on different areas of the beaches. The occupancy data for the total time spent on each beach was therefore used to be consistent with the estimated population of objects for calculating the probability of encountering an object. It should be noted that, as discussed in Section 4.2, there is no information available to indicate that the population of objects is higher in rocky areas of the beaches and, as most beach activities were identified as taking place on sandy areas of the beaches, this assumption is reasonable.

5.3.1 Typical beach users

Although a considerable amount of data was collected during the habit surveys, it was found that, once these data had been divided between age groups and beach activities, for some groups there were insufficient or no data to allow a good statistical analysis to be made (that is, to define the 2.5%, 97.5% and median values of the distribution in beach occupancy). For example, some beaches were observed as only being used by a few individuals, such as a family group, with all family members having the same occupancy. It is not possible to derive a suitable distribution on beach occupancy using such data and so an alternative approach was used.

It was agreed, in consultation with the Environment Agency and Sellafield Ltd., that to establish the range in annual beach occupancy for general beach users, information from the two habit surveys would be pooled together and suitable distributions on beach occupancy derived. The data on beach occupancy would therefore be representative of that on beaches along the West Cumbrian coast rather than on specific beaches. This approach has the advantage that any statistical information derived from this dataset is from a suitably large number of individuals which gives more confidence in the values used. The pooled occupancy data were then assigned to all beaches where it was known, or thought feasible, that the identified groups of people spent time.

For general beach users, for each age group and beach use, the minimum beach occupancy recorded for any of the beaches was assumed to be the 2.5^{th} percentile of the distribution of beach occupancy times, although a lower cut-off of 30 minutes was used within the distribution to prevent any negative times being produced within the statistical programme. The maximum recorded occupancy time was assumed to be the 97.5^{th} percentile of the distribution and the median time was the 50^{th} percentile.

A summary of beach occupancy data used for assessing the probability of encountering an object for general beach users is given in Table 24. It is seen that in most cases the values for the pooled beach occupancy differ from the beach-specific occupancy by no more than a factor of between 3 and 5 (differences greater than a factor of 3 are shown in red in the table), with the pooled data in most cases being the more cautious for the median and 97.5% values. Although some of the beach-specific median occupancies are significantly higher than for the pooled data, this is considered unlikely to result in a significant underestimate of the estimated median probability of encounter. In addition it is also noted that any variation in the estimated probability of encounter because of this difference in the median occupancy would still fall within the range bounded by the 2.5^{th} and the 97.5^{th} percentiles. Although there are a few cases where beach specific values of the 2.5^{th} and 97.5^{th} percentiles of annual beach occupancy are more than a factor of 3 different to the pooled occupancy data, in all cases the distribution in annual beach occupancy using the pooled data encompasses the values for the individual beaches and the beach occupancy of individuals with the highest annual beach occupancy will not be underestimated.

Although the general assumption was that all age groups may use all of the beaches considered and all beach activities undertaken on them, there were several exceptions which are listed below. These were based on the information supplied from the habit surveys and judgement regarding the nature of each beach and the amenities available.

- It was assumed that no young children (0 – 5 year olds) spend time bait digging or angling as young children were not observed doing this in either of the habit surveys.
- Only adults were observed using Sellafield beach during the surveys, possibly due to the difficulties in reaching the beach on foot. Therefore, it was assumed that only the adult age group spend any time on Sellafield beach. However, the possibility that young children and children may use the beach now or in the future has been considered and additional information is provided in Section 7.
- Only walking and angling were observed to occur on Sellafield beach and therefore, in this assessment, no probability of encountering an object during leisure activities was considered.

5.3.2 Beach users with high beach occupancy

In addition to considering the range of beach occupancy across all beach users, people that spend the most time on each of the beaches considered were identified. These people were defined as 'high occupancy beach users' for the purposes of this study. For these individuals, a single value for occupancy was used which is the maximum value observed on each beach for people undertaking each beach activity in each age group (97.5^{th} percentile value in Table 24). The annual occupancy values used are reproduced in Table 25 for convenience. This approach is different to that used in Smith and Bedwell (2005) due to the lack, on most beaches, of suitable numbers of individuals with beach occupancy towards the upper end of the range. The range of beach occupancies within this high occupancy group was not considered and it can be seen from Table 24 that the annual beach occupancy for this group lie between the 50^{th} and 97.5^{th} percentiles of the distribution of the pooled occupancy data.

Table 24: Beach occupancy data used in the study (taken from Cefas, 2008a and 2010)[a]

Beach	Adult leisure	Adult Walking	Adult angling	Child leisure	Child Walking	Child angling	Young child leisure	Young child walking	Young child angling
Pooled beach occupancy data[b]									
2.5% (h y^{-1})	2	1	3	2	1	8	3	3	-
50% (h y^{-1})	53	120	88	36	35	62	52	65	-
97.5% (h y^{-1})	818	1095	900	300	200	276	365	280	-
Number of people observed	137	261	151	82	31	24	69	7	0
Braystones[c]									
2.5% (h y^{-1})	100	9	8	24	24	8	60	-	-
50% (h y^{-1})	169	65	160	100	24	276	120	-	-
97.5% (h y^{-1})	818	730	900	300	24	276	258	-	-
Number of people observed	8	29	27	8	2	6	5	0	0
Drigg[c]									
2.5% (h y^{-1})	2	2	16	2	45	39	5	-	-
50% (h y^{-1})	32	93	130	37	123	62	37	-	-
97.5% (h y^{-1})	210	1095	624	210	200	62	170	-	-
Number of people observed	10	24	24	5	2	5	9	0	0
Seascale[c]									
2.5% (h y^{-1})	4	20	14	4	24	-	4	-	-
50% (h y^{-1})	57	263	101	70	35		60	-	-
97.5% (h y^{-1})	150	910	571	120	200	-	150	-	-
Number of people observed	14	36	21	7	1	0	14	0	0
Sellafield[c]									
2.5% (h y^{-1})	-	2	15	-	-	-	-	-	-
50% (h y^{-1})		65	50					-	-
97.5% (h y^{-1})	-	143	195	-	-	-	-	-	-
Number of people observed	0	5	9	0	0	0	0	0	0
St Bees[c]									
2.5% (h y^{-1})	3	3	9	14	12	62	3	3	-
50% (h y^{-1})	32	126	104	29	24	62	45	65	-
97.5% (h y^{-1})	365	730	400	53	65	62	150	280	-
Number of people observed	25	66	21	14	7	4	16	7	0

- no people observed in this group during the habit surveys.

a) All differences greater than a factor of 3 between the beach specific data and the pooled beach occupancy data are marked in red.

b) Pooled beach occupancy data were derived using data from all beach users reported within the two habit surveys (Cefas, 2008a; 2010). These data were used to define the distributions associated with general beach users and were used for all beaches considered.

c) The highest beach occupancy was taken to be the 97.5%ile of the distributon.

Table 25: Annual beach occupancy for users with high beach occupancy as used in the study (taken from Cefas, 2008a and 2010)

Beach /occupancy, h y^{-1}	Adult leisure	Adult Walking	Adult angling	Child leisure	Child Walking	Child angling	Young child leisure	Young child walking	Young child angling
Braystones[(c)]									
	818	730	900	300	24	276	258	-	-
Drigg[(c)]									
	210	1095	624	210	200	62	170	-	-
Seascale[(c)]									
	150	910	571	120	200	-	150	-	-
Sellafield[(c)]									
	-	143	195	-	-	-	-	-	-
St Bees[(c)]									
	365	730	400	53	65	62	150	280	-

- no people observed in this group during the habit surveys.

5.4 Time spent on a beach per visit

The time spent on a beach during a single visit has not been used when determining the annual probability of encountering an object. However, it is important to consider the length of time that an individual object could be in close contact with the skin, either directly on trapped next to the skin in clothing or shoes, when considering the radiation dose that could be received. In many cases, when a person leaves the beach, any objects present will be removed quickly. For example, it can be assumed that clothes are removed and washed, shoes emptied of sand, sand is brushed off the skin and the skin is washed within a few hours of leaving the beach. In most cases, a realistic length of time for an object to remain in close close contact with the same are of skin is therefore the length of time of the beach visit.

The habit surveys (Cefas, 2008a; 2010) included information on the number of visits each individual made to a beach over a year as well as the time that the individual spent on a beach in a year. Based on this information, values for the time spent during a beach visit have been estimated and these times can be used as a guide when considering radiation doses arising from exposure to a radioactive object being in close contact with the skin. A common length of time spent per visit for all beach activities was between 1 and 3 hours; a time of 2 hours was taken to represent a typical visit. As a minimum, a person could spend only a short time on a beach, for example, while taking a quick walk; 30 minutes was taken to be a representative minimum beach occupancy time for a single visit. When considering the maximum length of a beach visit, it was assumed that someone could spend an entire day on the beach; a representative time of 8 hours was assumed. It is feasible that an object might remain in close contact with the same area of skin once an individual has left the beach and until they next change clothing or wash. A value of 12 hours is deemed a conservative maximum time for an object to remain in close contact with the same area of skin.

In the assessment of health implications from fuel fragments on the beaches around Dounreay (Smith et al, 2006), it was recognised that particles could also become lodged in the ears which may potentially result in longer skin contact when compared to an object located on other areas of skin. This is considered further in Section 9.1.1.1. It is also acknowledged that someone could carry an object attached to an item collected from the beach (eg, a shell) for some time after they leave the beach. This is discussed in Section 6.5.

The same length of a beach visit was considered to be applicable for each beach activity group (walking, leisure and angling). Although it could be expected that some beach activities are more likely to be associated with longer beach visits than others, the beach activity groups used are amalgams of several related activities and, as such, represent a range of beach uses. So, although an individual may not use the beach for walking for the whole visit, they may spend a few hours walking, a few hours picking up pebbles etc within a single visit and all of these activities are included within the "walking" activity.

A comparison between beaches covered in the habit surveys, where this is possible, has identified that there is no significant difference between beaches in terms of the length of a beach visit. The typical times for beach visits were therefore considered to be applicable to any of the beaches being considered.

6 METHODOLOGY FOR DETERMINING THE LIKELIHOOD OF BEACH USERS ENCOUNTERING OBJECTS

The potential for people to be exposed to objects (ie, both particles and stones) as a result of exposure to sand containing an object while using the beaches has been considered. The mechanisms by which individuals can come into contact with sand while using the beach and therefore be exposed to an object have been identified. The mechanisms involve either an object entering the body or direct contact with it on the skin. Exposure to an object can occur from inhalation of air in which sand is resuspended, from inadvertent ingestion of sand and from sand being in stationary contact with a small area of skin and the skin becoming externally irradiated. The term 'probability of encounter' is used in the remainder of the report to refer to the likelihood of a person being exposed to an object from these three exposure mechanisms. External exposures considered were from: an object directly on the skin (including in the ear or eye); an object located under fingernails or toenails; an object located within clothes and an object located within shoes. It is important to note that in order for an object in contact with the skin to lead to a deterministic effect on health, the object has to remain in stationary contact with the same small area of skin for a period of time. This is discussed in more detail in Sections 8 and 9. It is expected that external gamma exposure from objects distant from the body would be very small and this has been investigated. Appendix C provides details of estimated external gamma doses from objects on the beaches; the results confirm that the radiation exposures from this pathway are very small, even for the ^{60}Co-rich and beta-rich objects which have high

energy gamma-ray emissions, and this exposure pathway has not, therefore, been treated in detail in the determination of the probability of encountering an object.

The probability of getting an object in the eye and ear has also been investigated and the scoping calculations carried out are described in Appendix D. It is also possible that an individual could be exposed as a result of an object entering a wound either if an individual is injured while on the beach or has an open wound when visiting a beach. This is extremely unlikely; however an estimate has been made of the likelihood that an object could enter a wound. This takes into account both the likelihood of an individual on the beach having an open wound and the likelihood that an object could enter a wound during a beach visit. The scoping calculation made is described in Appendix E. Table 26 presents a summary of the exposure pathways considered for each of the beach activity groups.

For all parameters used to describe the mechanisms by which individuals can be exposed to objects on the beaches, ranges have been estimated that reflect the variation across the population. These ranges have been combined with the distribution of beach occupancies to calculate a distribution of the probability of encountering an object for the general population of beach users. For the high occupancy beach user, best estimate values have been adopted for the exposure pathway parameters used in the determination of the probability of encountering an object. This has been done so that the probabilities estimated are not overly conservative and are representative of a typical high occupancy beach user and not an extreme case where the exposure from each pathway is maximised.

The statistical calculations were undertaken using an Excel spreadsheet with the Crystal Ball^{TM} statistical tool add-on. Crystal Ball^{TM} uses Monte Carlo simulation to calculate a range of possible outcomes and the likelihood of achieving them. Crystal Ball^{TM} generates a value for each individual input variable where a range has been defined, bounded by parameters describing the distribution of the input variable.

The probabilities of encountering an object on a beach estimated in this study are for the range of typical individuals who spend time on the beaches. As a consequence, the estimated probabilities will not necessarily include those members of the population who have extreme habits. One such group are young children described as having the rare medical condition known as pica who persistently ingest non-nutritive substances for a period of time. The probability of ingesting an object by this group may be higher that the estimated 97.5% value for the general population because they ingest non-nutritional material deliberately rather than accidentally and, as a consequence, they may ingest more sand than other children. It is not possible to quantify the time that children with pica may spend on the beaches and so their probability of ingesting an object has not been explicitly calculated. It is unlikely, however, that thir probability of encountering an object will be significantly higher than the 97.5th percentile of the distribution for the general population.

The mouthing of a wide variety of non-food substances which can also be ingested has also been considered. This is most common in people with developmental disabilities, including autism and mental retardation, and in children between the ages of 2 and 3 and can include large objects (see Appendix F). The impact of including the deliberate

ingestion of large objects (defined as stones in this report) on the probability of encountering an object has been calculated and is discussed in Sections 7 and 10.

Table 26: Summary of the pathways associated with the exposed groups that are considered in detail[a]

Exposed group	Exposure pathway included
Angling	Inhalation
	Ingestion
	Trapped under fingernails
	Trapped in clothes
	Trapped in shoes
	Skin contact while bait digging[b]
Leisure	Inhalation
	Ingestion
	General skin contact
	Trapped under fingernails and toenails
	Trapped in clothes
	Trapped in shoes
Walking	Inhalation
	Ingestion
	General skin contact
	Trapped under fingernails
	Trapped in clothes
	Trapped in shoes

a) External irradiation from being in close proximity to an object and uptake from an object embedded in a wound have also been considered (see Appendices D and F, respectively)

b) This pathway replaces the general skin exposure pathway considered for leisure and walking activities

6.1 Impact of object size on exposure

The size of the objects found on the beaches covers a wide range, from fractions of a millimetre to around 20 cm. It is important to consider the size of the objects when identifying whether individuals can encounter them via the various exposure pathways being considered. A full discussion of exposure via the different pathways depending on object size is given in Appendices G - I for ingestion, inhalation and skin contact, respectively. For all exposure pathways it was assumed that there is no lower limit on the size of an object that can lead to exposure. Likely upper limits on object size have been established based on a review of the available information and the values are presented in Table 27. It is recognised that there will be some variation in this value between individuals. Except for deliberate ingestion, the upper size for objects that could result in exposure corresponds to that defined previously as the upper end of the size range of a particle, ie, about 1-2 mm. In order not to potentially underestimate the probability of encountering an object, it has been assumed that any particle could cause

an exposure through any of the pathways shown in Table 26, recognising this is a very cautious assumption for inhalation.

As the upper size limits for inadvertent ingestion and skin contact are approximately the same as the size used to classify objects as particles or stones (particles are less than 2 mm in size whilst stones are 2 mm and above), and many of the objects that have been classified as stones are not significantly larger in diameter than 2 mm, the probability of encountering stones has also been considered so that a cautious evaluation of the total probability of encountering an object can be made. The probability of encountering particles and stones are presented separately so that the overall health risks to both can be considered separately or together. The impact of including stones on the probability of encountering an object on the beaches is considered in Section 7.5.

Table 27: Summary of the upper size limits for objects to be ingested, inhaled and to adhere to the skin (see Appendices G – I for sources of values)

Route of exposure	Upper size limit (mm)
Inadvertent ingestion without detection in the mouth[(a)]	0.1
Inadvertent ingestion with detection in the mouth[(a)]	1
Deliberate ingestion, adult[b]	70
Deliberate ingestion, child[b]	40
Deliberate ingestion, young child[b]	20
Respirable size for inhalation (alveolar-interstitial region of the lungs)[(a)]	0.01
Respirable size for inhalation (extra-thoracic airways)[(a)]	0.1
Lodging under fingernail[(a)]	1
Adhesion to skin[(a)]	1

(a) These object sizes were not found to be significantly dependent on the individual's age.

(b) Not considered for the general population of beach users (see Section 6.2).

6.2 Inadvertent ingestion

Inadvertent ingestion of discrete objects might occur via the consumption of sand, for example, on food eaten on the beach. For the general population, it is only appropriate to consider inadvertent ingestion of the objects classified as particles (see Table 27). However, in order to be cautious and prevent the potential underestimation of the probability of encountering an object, both the probability of ingesting particles and stones is assessed because, as described earlier in Section 6, some people may deliberately ingest large objects. The impact of ingesting stones in terms of radiation doses and health risks is discussed in Section 8 and the probability of encountering a stone via deliberate ingestion is discussed in Section 7.

Appendix F contains a detailed account of the derivation of the distribution of values of the inadvertent ingestion rate of material that was used. The inadvertent ingestion rates used are shown in Table 28.

Table 28: Inadvertent ingestion rates (g h^{-1})

Activity	Age group	2.5% [(a)]	Mean [(a)]	97.5% [(a)]	Best estimate [(b)]	Distribution type
All	Young child	0.03	0.045	0.175	0.045	Lognormal
All	Children	0.006	0.009	0.035	0.009	Lognormal
All	Adult	0.003	0.0045	0.0175	0.0045	Lognormal

(a) Values from Smith and Bedwell (2005).

(b) Value used for high occupancy beach users.

6.2.1 Calculating the probability of inadvertent ingestion of an object

The following equation was used to estimate the probability of inadvertently ingesting an object.

P_{ing} = N * ING * T

P_{ing} = Probability of ingesting a radioactive object on the beach

N = Number of radioactive objects per gram of sand, g^{-1}, see Table 20 (Method 1 values)

ING = Ingestion rate of sand, g h^{-1}, see Table 28

T = Duration of time spent on the beach (hours). For an annual probability this is the time given in Table 24. The pooled beach occupancy data are used for a general beach user and the 97.5% value (maximum value) for each specific beach is used for the high occupancy beach users.

6.3 Inhalation

If an object is small enough, and the sand dry enough, then it could become airborne either through the action of the wind or by the activity of a person, for example when sand is thrown in the air while digging. If the object does become airborne then inhalation could occur.

In the case of the inhalation exposure pathway, the concept of probability of encounter equates to the probability that an object is present in the volume of air that a person is breathing from at any time during the period of beach occupancy. Whether an object can be inhaled (that is, whether it can enter the nose or mouth) depends on particle size, breathing conditions, and ambient air velocity and direction. Inhalability, also know as the intake efficiency or aspiration efficiency, is defined as that fraction of particles in an aerosol that can enter the mouth or nose when the air in which it is suspended is

inhaled. For a single particle, this fraction equates to a probability of inhalation. Recent studies suggest that, in very low wind speeds, inhalability drops off above about 120 µm aerodynamic diameter[2] and that a cut-off exists at about 140 µm aerodynamic diameter (see Appendix G). Unfortunately, comparable data are not available for higher wind speeds, and the inhalability of objects under these conditions remains uncertain.

After an object is inhaled, the location of deposition within the respiratory tract depends mainly on aerodynamic diameter, although factors such as breathing rate also have an influence. Particles larger than about 30 µm aerodynamic diameter deposit almost exclusively in the extrathoracic region, which comprises the anterior nose and the posterior nasal passages, larynx, pharynx and mouth. In ICRP's Human Respiratory Tract Model (HRTM) (CRP, 1994a), a cut-off of 100 µm aerodynamic diameter is suggested as an upper limit. Particles with aerodynamic diameters less than about 30 µm aerodynamic diameter may deposit in the airways of the lung (ie, the trachea, bronchi and bronchioles), but only particles smaller than 10 µm aerodynamic diameter are likely to reach the alveolar region of the lungs.

The inhalability of airborne objects, and the deposition of particles in the respiratory tract following inhalation, is discussed further in Section 8.5 and Appendix G.

To determine the probability of encounter by inhalation, data are needed on sand loadings in air above the beach and on the inhalation rate when undertaking various activities on the beach. Appendix G presents a review of the data on sand loadings in air above a beach and the values chosen to describe the range in values for use in this study are given in Table 29.

Table 29: Sand loading in air (g m^{-3})

Activity	Age group	2.5%[(a)]	Mean[(a)]	97.5%[(a)]	Best estimate[(b)]	Distribution type
All	Young child /Child	$1\ 10^{-5}$	$1\ 10^{-4}$	$1\ 10^{-3}$	$1\ 10^{-4}$	Lognormal
All	Adult	$1\ 10^{-5}$	$5\ 10^{-4}$	$1\ 10^{-3}$	$5\ 10^{-4}$	Lognormal

(a) Values from Smith and Bedwell (2005).

(b) Value used for high occupancy beach users.

Inhalation rates are recommended for people outdoors in ICRP Publication 66 (ICRP, 1994a) and are presented in Table 30 along with the assumptions made for each age group. Beals et al (1994) indicated that distributions on inhalation rates are approximately lognormal and that it would be reasonable to assume that the standard deviation of the lognormal distribution is approximately 15% of the mean. Using this information, distributions for inhalation rates for each age group and beach activity have been derived and are given in Table 31.

[2] The aerodynamic diameter of a particle is the diameter of the unit density spherical particle that has the same settling velocity in air.

Table 30: ICRP recommended inhalation rates for individuals outdoors (ICRP, 1994a)

Age group	Inhalation rate $m^3\ h^{-1}$	Assumptions
1 year old infant	0.31	1/3 sitting + 2/3 light exercise
5 year old child	0.49	1/3 sitting + 2/3 light exercise
10 year old child	0.87	1/3 sitting + 2/3 light exercise
15 year old child (male)	1.87	2/3 light exercise + 1/3 heavy exercise
Adult (sedentary male worker)	1.21	½ sitting + 3/8 light exercise + 1/8 heavy exercise
Adult (outdoor worker)	1.69	7/8 light exercise + 1/8 heavy exercise

Table 31: Inhalation rates used in this assessment ($m^3\ h^{-1}$)

Activity	Age group	2.5%[(a)]	Mean[(b)]	Standard deviation[(c)]	Best estimate[(d)]	Distribution type
Angling	Children	0.38	0.87	0.1305	0.87	Lognormal
	Adults	0.54	1.69	0.2535	1.69	Lognormal
Leisure	Young child	0.15[(d)]	0.49[(d)]	0.0735	0.49	Lognormal
	Children	0.31	0.87	0.1305	0.87	Lognormal
	Adults	0.45	1.21	0.1815	1.21	Lognormal
Walking	Young child	0.22[(e)]	0.49[(e)]	0.0735	0.49	Lognormal
	Children[(f)]	0.38	0.87	0.1305	0.87	Lognormal
	Adults	0.54	1.21	0.1815	1.21	Lognormal

(a) The 2.5% value represents the inhalation rate whilst sitting (for angling and walking) and sleeping (for leisure) given in ICRP Publication 66 (ICRP, 1994a).

(b) Values from Smith and Bedwell (2005).

(c) The standard deviation was taken to be equal to 15% of the mean. The mean of the inhalation rate and its standard deviation were used in Crystal Ball to describe the distribution of the inhalation rate.

(d) Value used for high occupancy beach users.

(e) For young children the 2.5% value for inhalation rate was based on data for a 1 year old, representing the minimum age within the age range of this group for which a rate is given in (ICRP, 1994a). The mean rate was based on data for a 5 year old as that represents the upper end of the age range for this group. The use of a higher inhalation rate represents a more cautious approach.

(f) For children, value for a 10 year old is used.

6.3.1 Calculating the probability of encountering an object via inhalation

The following equation was used to estimate the probability of inhaling an object whilst on a beach.

$P_{inh,h}$ = N * SI * INH * T

$P_{inh,h}$ = Probability that a radioactive object is present in the volume of air breathed during one hour spent on a beach

N = Number of radioactive objects per gram of sand, g^{-1}, see Table 20 (Method 1 values)

SI = Sand loading in air, g m^{-3}, see Table 29

INH = Inhalation rate, $m^3\ h^{-1}$, see Table 31

T = Duration of time spent on the beach (hours). For an annual probability this is the time given in Table 24. The pooled beach occupancy data are used for a general beach user and the 97.5% value (maximum value) for each specific beach is used for the high occupancy beach users.

6.4 Skin contact with discrete objects

The exposure pathways considered where there could be skin contact with an object are: an object directly on the skin, an object located under fingernails or toenails, an object located within clothes and an object located within shoes. For these exposure pathways an assumption has been made that the mass of sand on the skin would be continuously refreshed for the duration of the time spent on the beach. It is unknown what this refresh rate could be, as it is likely to be dependent on a number of factors such as beach activity, object size, the location on the body where the object is, the material of the clothing, etc. Therefore, the robust assumption has been made that the mass of sand present on the body or in clothing at any time represents the average mass accumulated over an hour spent on the beach. After an hour, any sand present is assumed to be replaced with an equal mass of sand from the beach. This is likely to be cautious as not every hour spent on the beach will result in attachment of sand to the skin or clothing and some sand is likely to be on parts of the body that will not result in a rapid exchange with new beach material. Any objects associated with the mass of sand being encountered were assumed to be attached at the same rate.

6.4.1 Direct contact with the skin

It is expected that sand will get onto the skin during any visit to a beach. The mass of sand that becomes stuck on the skin, and by implication the probability that an object will also be on the skin, is dependent on a number of factors. These include the area of skin that is exposed to the sand, which in itself will depend to some extent on the weather because of the amount of clothing worn, whether the sand is wet or dry, and the size of the individual as larger individuals will have a larger skin area. A discussion of how each of these factors affects the area of skin that could come into contact with sand for beach users throughout the year and any differences between the different beach activities is given in Appendix H.

Different approaches for estimating the probability of encountering an object on the skin were used depending on the beach activity. These largely follow the method used in the assessment of the health implications of fuel fragments on beaches around Dounreay (Smith and Bedwell, 2005).

Skin exposure from leisure and walking activities

The following equation was used to estimate the probability of encountering an object on the skin whilst walking or using a beach for leisure activities. A description of the derivation of this equation is given in Appendix H.

$$P_{skin} = T * N * (F_w * M_{sand,w} + F_c * M_{sand,c})$$

Where

P_{skin} = Probability of encountering a radioactive object on the skin

T = Duration of time spent on the beach (hours). For an annual probability this is the time given Table 24. The pooled beach occupancy data are used for a general beach user and the 97.5% value (maximum value) for each specific beach is used for the high occupancy beach users.

N = Number of radioactive objects per gram of sand, g^{-1}, see Table 20 (method 1 values)

F_w = Fraction of time spent on the beach in warm weather conditions over a year, dimensionless, see Table 32

$M_{sand,w}$ = Average mass of sand adhering to the skin per hour spent on the beach during warm weather, g h^{-1}

F_c = Fraction of time spent on the beach in cold weather conditions over a year, dimensionless, see Table 33

$M_{sand,c}$ = Average mass of sand adhering to the skin per hour spent on the beach during cold weather, g h^{-1}

The values used to define the mass of sand on the skin (M_{sand}) are discussed and presented in Appendix H.

6.4.1.1 Fraction of the time spent on the beach in warm and cold weather conditions

When assessing the probability of encountering an object on the skin, account has to be taken of the amount of skin exposed to the sand. This is likely to be weather-dependent for most people. Appendix H presents a discussion of the fraction of time that an individual is typically likely to spend on a beach in different types of weather conditions over a year. A summary of the fractions that are used in this study, is given in Table 32 and Table 33 for warm and cold weather conditions, respectively.

Table 32: Fraction of time spent on the beach in warm weather conditions over a year

Activity	Age group	2.5%	Mean	97.5%	Best estimate[(a)]	Distribution type
All	Young child	0.75	1	1	1	Triangular
All	Children	0.5	0.75	1	0.75	Triangular
Leisure	Adult	0.5	0.75	1	0.75	Triangular
Walking	Adult	0.25	0.25	0.5	0.25	Triangular

(a) Value used for the high occupancy beach users.

Table 33: Fraction of time spent on the beach in cold weather conditions over a year

Activity	Age group	2.5%	Mean	97.5%	Best estimate[(a)]	Distribution type
All	Young child	0	0	0.25	0	Triangular
All	Children	0	0.25	0.5	0.25	Triangular
Leisure	Adult	0	0.25	0.5	0.25	Triangular
Walking	Adult	0.5	0.75	0.75	0.75	Triangular

(a) Value used for the high occupancy beach users.

Skin exposure during angling activities

For anglers, it was assumed that sand will mostly get on the skin during bait digging when the individual is digging in the sand and mud on a beach looking for bait to use when fishing. Once the angler has collected bait it is assumed that hands would be washed before fishing to remove most of the sand on them. Therefore, exposure to material on the skin has only been considered for the time spent bait digging rather than the whole time spent on the beach angling.

Skin exposure during bait digging was considered to result from wet sand coming into contact with the hands as a result of handling bait that has been dug up, regardless of the weather, and so the effect of weather conditions has not been included.

The methodology used in this assessment is the same as that used in the study on the health impact of fuel fragments on the beaches around the Dounreay site (Smith and Bedwell, 2005).

The following equation was used to estimate the probability of encountering an object on the skin whilst bait digging.

$P_{dig} = N * T * F_b * M_b * N_b * F_b$

P_{dig} = Probability of encountering a radioactive object per hour of bait digging

N = Number of radioactive objects per gram of sand, g^{-1}, see Table 20 (method 1 values)

T = Duration of time spent on the beach (hours). For an annual probability this is the time given Table 24. The pooled beach occupancy data are used for a general beach user and the 97.5% value (maximum value) for each specific beach is used for the high occupancy beach users.

F_b = Fraction of the total time angling that was spent bait digging, see Table 34

M_b = Mass of sand adhering to each item picked up during bait digging, g, see Table 34

N_b = Number of items picked up per hour whilst bait digging, see Table 34

F_b = Fraction of sediment on an item that will come into contact with skin, see Table 34

The best estimate values and ranges for M_b, N_b, F_b are summarised in Table 34.

Table 34: Parameters used for estimating the probability of encounter during bait digging

	2.5%	Mean	97.5%	Best estimate[a]	Distribution type
Fraction of time spent digging [b] (F_a)	0.07	0.13	1.00[c]	0.13	Triangular
Amount of sand per bait item (g) [b] (M_b)	10	30	50	30	Triangular
Number of items picked per hour [b] (N_h)	30	60	100	60	Triangular
Fraction of sand contacting skin [b] (F_h)	0.01	0.05	0.1	0.05	Triangular

(a) Value used for the high occupancy beach users.

(b) Values from Smith and Bedwell (2005).

6.4.2 Objects trapped under a fingernail or toenail

When the hands and feet are exposed to sand, then sand particles and any associated radioactive objects may become trapped under finger nails or toenails. The term 'nails' is used in the following text to represent both fingernails and toenails. The following equation was used to estimate the probability of encountering an object under a nail.

$P_{nail} = T * N * (M_f + M_T * F_w)$

P_{nail} = Annual probability of a particle becoming trapped under a nail

T = Duration of time spent on the beach (hours). See Table 24. The pooled beach occupancy data are used for a general beach user and the 97.5% value (maximum value) for each specific beach is used for the high occupancy beach users.

N = Number of radioactive objects per gram of sand, g^{-1}, see Table 20 (method 1 values)

M_f = Average mass of sand under a fingernail per hour on a beach, see Table 35

M_T = Average mass of sand under a toenail per hour on a beach, see Table 36

F_w = Fraction of time spent on the beach in warm weather conditions, dimensionless, see Table 32

It was assumed that fingernails were exposed to sand during any beach visit, whether that visit occurred during cold or warm weather. However, for toenails, it assumed that feet would only be exposed during warm weather.

Information is not available on the mass of sand likely to be present under a nail when on a beach, so a subjective evaluation was made where the mass of sand, and hence the potential probability of an object being present under a nail, was related to the volume of the space under a nail and the number of nails which will be exposed to sand. In order to do this, a number of assumptions have been made which are described below.

Figure 5 shows a schematic of a nail used for determining the volume of sand that could become trapped under a nail. Fingernails of adults are typically 9 – 14 mm in breadth (ICRP, 2002) and a breadth of 12 mm was assumed to be typical. The length of the white tip of the nail, extending away from the finger is variable depending on the individual concerned. The full range can be assumed to extend from 0 mm to in excess of 10 mm. However, the length of nail under which sand could get trapped was assumed to be between 0.5 mm and 4 mm, as only the part of the nail would form a "wedge" with the adjacent skin. A typical length of 2 mm was assumed. The maximum height between the nail, where sand could be trapped, and the skin of the finger was assumed to have a range of 1mm to 2 mm, with a typical value of 1 mm.

No equivalent information could be found on the dimensions of toenails. ICRP 89 (ICRP, 2002) gives the mass of toenails and fingernails and it has been assumed for this study that the mass of material that could be trapped under a toenail is directly related to the mass of a nail, the mass being an approximate surrogate for nail size. The mass of the toenails is approximately 3 times smaller than the mass of the fingernails (ICRP, 2002). The mass of sand trapped under a toenail was therefore assumed to be a factor of 3 lower than that of a fingernail

No data were found on typical nail sizes for children. It was therefore assumed that the distance between the nail and the skin would not differ from that for an adult but that the breadth of the nail would be smaller by a factor equal to the ratio of the hand area for children and adults. The ratio used was 0.3 for young children and 0.6 for children.

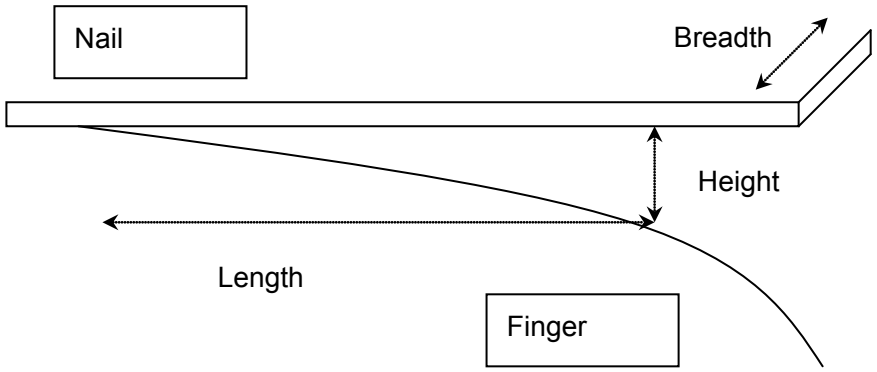

Figure 5: Schematic of the parameters used to define the amount of sand that could be trapped under a nail

The dimensions assumed indicate that there is enough space under a nail for an object of up to a few millimeters in diameter to become trapped. Practical experience suggests that single objects up to around 1 mm in diameter can lodge under the nail without detection; above that size the object causes discomfort and so is likely to be removed after a very short time. This is consistent with a grain of sand becoming lodged under

the nail (<2 mm). This size of object corresponds to those objects labeled as “particles” within the classification system used by Sellafield (see Section 2.1) and it is cautiously assumed that all such particles could become trapped under a nail.

The estimates of the mass of sand that could become trapped under fingernails and toenails are given in Table 35 and Table 36, respectively. Table 37 summarises those activities for which it was assumed that sand could become trapped under nails when individuals are on a beach.

Table 35: Mass of sand trapped under a fingernail per hour on a beach (g) [a,b]

Age group	2.5% [c]	Mean [d]	97.5% [e]	Best estimate[(f)]	Distribution type
Young child	0.0014	0.0360	0.3360	0.0360	Triangular
Children	0.0027	0.0720	0.6720	0.0720	Triangular
Adult	0.0045	0.1200	1.1200	0.1200	Triangular

(a) Assumes the density of sand is 2 10^6 g m^{-3} (Kowe et al, 2007).

(b) These masses were calculated and the number of decimal places does not imply detailed knowledge of the potential mass of material that could be trapped under a fingernail.

(c) This assumes sand is located under 1 fingernail which has the minimum dimensions for the space between the nail and skin.

(d) Representing sand trapped under 5 fingernails which have the average dimensions for the space between the nail and skin.

(e) Representing sand trapped under 10 fingernails which have the maximum dimensions for the space between the nail and skin.

(f) Value used for the high occupancy beach users.

Table 36: Mass of sand trapped under a toenail per hour on a beach (g) [a,b,c]

Age group	2.5% [d]	Mean [e]	97.5% [f]	Best estimate [g]	Distribution type
Young child	0.0005	0.0120	0.1120	0.0120	Triangular
Children	0.0009	0.0240	0.2240	0.0240	Triangular
Adult[(e)]	0.0015	0.0400	0.3733	0.0400	Triangular

(a) Assumes the density of sand is 2 10^6 g m^{-3} (Kowe et al, 2007).

(b) For an angler no sand was assumed to be trapped under a toenail so these masses refer to leisure and walking activities only. For anglers the parameter M_T is therefore zero.

(c) These masses were calculated and the number of decimal places does not imply detailed knowledge of the potential mass of material that could be trapped under a fingernail.

(d) This assumes sand is located under1 toenail which has the minimum dimensions for the space between the nail and skin.

(e) Representing sand trapped under 5 toenails which have the average dimensions for the space between the nail and skin.

(f) Representing sand trapped under 10 toenails which have the maximum dimensions for the space between the nail and skin.

(g) Value used for the high occupancy beach users.

Table 37: Summary of when the sand was assumed to be present under a fingernail or toenail

Activity	Age group	Warm weather conditions		Cold weather conditions	
		Fingernail	Toenail	Fingernail	Toenail
Leisure	Young child	Yes	Yes	Yes	No
	Child	Yes	Yes	Yes	No
	Adult	Yes	Yes	Yes	No
Walking	Young child	Yes	Yes	Yes	No
	Child	Yes	Yes	Yes	No
	Adult	Yes	Yes	Yes	No
Angling	Adult	Yes	No	Yes	No
	Child	Yes	No	Yes	No

6.4.3 Objects adhering to clothes

While an individual is on a beach, sand can adhere to clothes and sand could become trapped next to the skin. The mass of sand that adheres to clothing will depend on both the type of clothing worn, as some fabrics are able to trap more sand than others, and the amount of clothing worn. Information could not be found that gave a definitive value for the amount of sand that could adhere to clothing when on a beach. A conservative approach has therefore been adopted for estimating the probability of encountering an object on the skin from it adhering to clothing, which makes a number of assumptions.

The following equation was used to estimate the probability of encountering an object adhering on clothing.

$P_{cl} = T * N * A_c * M_c$

P_{cl} = Annual probability of a radioactive object adhering to clothing becoming trapped next to the skin when on a beach

T = Duration of time spent on the beach (hours). See Table 24. The pooled beach occupancy data are used for a general beach user and the 97.5% value (maximum value) for each specific beach is used for the high occupancy beach users.

N = Number of radioactive objects per gram of sand, g^{-1}, see Table 20 (method 1 values)

A_c = Area of clothing that is exposed to sand, cm^2, see Table 38

M_c = Average mass of sand per unit area of clothing, g cm^{-2} per hour on the beach, see Table 39

It was cautiously assumed that, for the time spent on a beach, the same clothes were worn and that the clothes had sand adhering to them for the whole time. In the absence of any specific data, it was assumed that the loading of sand on clothing would be the same as that for dry sand on skin other than on hands or feet. This is likely to be a conservative assumption for most clothing materials which will provide a less adherent

surface than skin. The areas of clothing which could have sand adhering to them are given in Table 38 and the mass of adhered sand is given in Table 39. Between visits it is assumed that clothes are removed and washed and any particles present are removed. It should be noted that the assumption is implicitly made that any particle adhering to clothing that is in contact with the skin remains in stationary contact with a small area of skin (see Section 6.4).

Table 38: Area of clothing which sand could adhere to (cm^2)

Activity	Age group	2.5%	Mean	97.5% [(d)]	Best estimate[(e)]	Distribution type
Leisure	Young child	100 [(a)]	2650 [(b)]	5300	2650 [(b)]	Triangular
	Child	500 [(a)]	5600 [(b)]	11200	5600 [(b)]	Triangular
	Adult	1000 [(a)]	9500 [(b)]	19000	9500 [(b)]	Triangular
Walking	Young child	2650 [(b)]	4240 [(c)]	5300	4240 [(c)]	Triangular
	Child	5600 [(b)]	8960 [(c)]	11200	8960 [(c)]	Triangular
	Adult	9500 [(b)]	15200 [(c)]	19000	15200 [(c)]	Triangular
Angling	Child	5600 [(b)]	8960 [(c)]	11200	8960 [(c)]	Triangular
	Adult	9500 [(b)]	15200 [(c)]	19000	15200 [(c)]	Triangular

(a) Representative values for a swimming costume.

(b) 50% of the total body surface area, representing someone wearing a t-shirt and shorts.

(c) 80% of the total body surface area, representing someone wearing a t-shirt and trousers.

(d) 100% of the total body surface area, representing someone wearing clothes that cover the entire body.

(e) Value used for the high occupancy beach users.

Table 39: Mass of sand trapped in clothing (g cm^{-2})

	Age group	2.5%	Mean	97.5%	Best estimate[(a)]	Distribution type
Mass of sand per unit clothing area [(b)]	All	10^{-5}	10^{-4}	10^{-3}	10^{-4}	Triangular

(a) Value used for the high occupancy beach users.

(b) Values from Smith and Bedwell (2005).

6.4.4 Objects trapped in shoes

While an individual is on a beach, it was assumed that sand and any associated radioactive objects could get into shoes or sandals. The following equation was used to estimate the probability of encountering an object in shoes.

$P_{shoe} = T * N * M_s$

P_{shoe} = Annual probability of having a radioactive object trapped in shoes that is in contact with the skin

T = Duration of time spent on the beach (hours). See Table 24. The pooled beach occupancy data are used for a general beach user and the 97.5% value

(maximum value) for each specific beach is used for the high occupancy beach users.

N = Number of radioactive objects per gram of sand, g^{-1}, see Table 20 (method 1 values)

M_s = Average mass of sand in shoes per hour spent on the beach, g h^{-1}, see Table 40

There is no information available for the amount of sand that could become trapped in a shoe when on a beach. A previous study, which assessed the exposure to fuel fragments on beaches around the Dounreay site, assumed that the amount of sand that can be trapped in shoes ranged between 8 and 50 grammes (Smith and Bedwell, 2005) and this mass was also used here. Table 40 presents the best estimate and distribution on the mass of sand trapped in shoes per hour spent on the beach that has been assumed in this study. In the absence of data specifically for different ages and beach activity the values in Table 40 have been applied to all age and beach activity groups. It should be noted that the assumption is implicitly made that any particle trapped in shoes remains in stationary contact with a small area of skin.

Table 40: Mass of sand that can become trapped in shoes per hour on a beach, g [(a)]

Beach activity	Age group	2.5%	Mean	97.5%	Best estimate[(b)]	Distribution type
All	All	1	10	50	10	Triangular

(a) From Smith and Bedwell (2005).

(b) Value used for the high occupancy beach users.

6.5 Removing an object from a beach

During the habit surveys (Cefas, 2008a; 2010), no observations were made of anyone removing large volumes of sand from the beach, for example to fill a play area at home. However, it was noted that children removed shells for use in decorating projects at local schools and that some individuals removed seaweed for use as a garden conditioner. For these situations it was deemed appropriate to assume that the probability of encountering an object would be similar to that for individuals in the 'walking' beach activity group, as this group covers activities such as picking material up from the beach that could lead to the exposure of hands to sand. It was assumed that the probability of encountering an object is effectively the same for someone picking an object up off the beach and subsequently discarding it as for someone picking an object up and then taking it away from the beach. This is because the probability of encounter is dependent on the amount of sand coming into contact with the body and, once an item has been picked up, the amount of sand coming into contact with the body will not increase. The difference in the case of removing items from the beach is that the length of time an object could be in stationary contact with the body could be longer. For example, if a shell is removed from the beach, the amount of sand associated with the shell will not increase with time so the probability of encountering an object on the shell

will not increase. However, if a contaminated object is on the shell, then the contact time may increase if the shell is held during the journey home compared to a shell that is picked up and later discarded before leaving the beach. The radiation doses arising from the contact of objects with the skin and the length of time these need to be in contact with the skin to give rise to discernable health effects are discussed in Sections 8 and 9.

6.6 Likelihood of encountering an object from consuming locally caught seafood

No direct monitoring of offshore sediments has been carried out that can be used to clarify the likelihood and nature of radioactive particles that could become incorporated in seafood along the west Cumbrian coastline. A programme of work is underway to develop a suitable approach for seabed monitoring in the future. In the meantime, it is important to scope the likelihood of members of the public ingesting a radioactive particle from the consumption of seafood and the associated health risks.

The Food Standards Agency (FSA) with support from HPA, EA and Sellafield Ltd via the Sellafied Sea-bed Monitoring Working Group, has undertaken a scoping assessment of the risks to seafood consumers from ingestion of radioactive particles. The methodology adopted is that developed for the assessment of the risks to seafood consumers from radioactive fuel fragments in the vicinity of the Dounreay nuclear site (Smith and Bedwell, 2005 and Wilkins et al, 1998). The FSA assessment is included within this report on the HPA study on health risks from radioactive objects on beaches in the vicinity of the Sellafield site so that the health risks can be considered along side those for people using the beaches. The scoping assessment is described in Appendix I.

7 ANNUAL PROBABILITY OF ENCOUNTERING AN OBJECT ON THE BEACHES

Detailed results are presented in this report for both the probability of an individual encountering an object while using a beach and the radiation doses and associated risks to an individual in the unlikely event that they come into contact with one of the radioactive objects. The calculated radiation doses and risks for alpha-rich and beta-rich contaminated objects are given in Sections 8 and 9, respectively. This Section presents the results for the probability of encountering a radioactive object for individuals using the five beaches considered quantitatively in this study.

Sufficient information was available to undertake a quantitative evaluation of the probability of encountering an object on five beaches along the Cumbrian coast; St Bees, Braystones, Sellafield, Seascale and Drigg, as discussed in Section 3. Two groups of beach users were considered; the first is representative of typical beach users and for this group a statistical approach was used to estimate the 2.5%, 50% and 97.5% probabilities of encountering a radioactive object to cover the variation between beach

users. For this group the beach occupancy data used were typical for the Cumbrian coast, comprising pooled habit data for all the beaches included in the habit surveys. This means that the same beach occupancy is assumed for each of the beaches for the activities undertaken on that beach. The only difference between the probabilities of encounter for the five beaches is therefore due to the estimated population of objects on each beach. The second group are people who spend the most time on each of the beaches considered. These people are defined as 'high occupancy beach users' for the purposes of this study and the probability that they encounter a radioactive object was estimated using the maximum beach occupancy found for each beach. Therefore, for this group, the probability of encountering an object on a beach is dependent on both beach specific occupancy and the population of objects on the beach.

The annual probability of encountering a radioactive object has been estimated using the methodology described in Section 6 and these results are presented in this Section. The probability of encountering an object per hour spent on each beach has also been calculated. These supplementary results and how they can be interpreted are discussed in Appendix J.

The size of the objects found on the beaches is important when considering whether people can be exposed to them via the different exposure pathways considered, as discussed in Section 6.1. The majority of the objects classified as stones (≥ 2 mm) are too large to give rise to exposure via any of the pathways considered for the majority of beach users. Such objects could not be inadvertently ingested but could be deliberately ingested by adults and older children. Results have therefore been presented in this Section for particles and stones separately so the impact of including exposure to stones when evaluating the probability of encountering objects on the beaches can be taken into account. It is recommended that the probability of encountering a particle is used as a realistic estimate of the overall probability for the general beach user; including the probability of encountering a stone is considered to be very cautious.

Information on the annual probability of encountering either a particle or stone is presented in a series of tables. In order to avoid presenting many similar tables of results for the different beaches, object types, beach uses and age groups, summary tables are provided along with the information needed to calculate the probability of encounter for any combination of beach, object type, object activity, beach use and age group. The following information is provided:

a Section 7.1 presents the highest annual probabilities of encountering either a particle or a stone for a general beach user summed over all exposure pathways (based on the median value of the distribution) and for a high occupancy beach user. Results are presented for alpha-rich, beta-rich and ^{60}Co-rich objects for each beach.

b Section 7.1.1 presents information on the probability of encounter for each age group and beach activity (defined in Sections 5.1 and 5.2) relative to the group with the highest probability of encounter (adult anglers or adult walkers). The relative probabilities are the same for particles and stones.

c Section 7.1.2 presents information on the relative contributions of each exposure pathway to the total probability of encounter for each age group and beach activity. The relative contributions are the same for particles and stones.

d Section 7.1.3 presents guidance on how to use the information in (a) – (c) above to estimate the annual probability of encounter for any age group and beach activity group combination and the annual probability of encountering an object via the different exposure pathways considered.

e Section 7.2 presents the distribution of annual probabilities of encountering a particle across all beach users for each beach for general beach user and the annual probabilities for a high occupancy beach user. Results are presented for alpha-rich, beta-rich and ^{60}Co-rich objects for each activity band. The beach activity giving the highest probability is identified in each table.

f Section 7.3 presents the information described in (d) above for stones.

7.1 Highest annual probabilities of encountering radioactive particles and stones on the beaches

This Section presents results of the highest annual probability of encounter for each beach for both general beach users summed over all exposure pathways (based on the median value of the distribution across all beach users) and for beach users with high annual occupancy. Results are presented for the age group and beach activity group with the highest probability of encounter, which is either the adult angler group or the adult walking group The annual probability is given for alpha-rich, beta-rich and ^{60}Co-rich particles and stones.

Table 41 presents the total annual probability of encountering any radioactive particle for a general beach user (summed over the activity bands 3-30 kBq, 30-300 kBq and >300 kBq). Table 42 presents the same information for high occupancy beach users for each beach.

Table 43 presents the total annual probability of encountering any radioactive stone for a general beach user (summed over the activity bands 3-30 kBq, 30-300 kBq and >300 kBq). Table 44 presents the annual probability for high occupancy beach users for each beach. No radioactive stones have been found on Drigg or St Bees beaches using the Groundhog Evolution2^{TM} system and therefore no estimate of the probability of encounter was possible for these beaches.

Table 41: Highest annual probability of encountering a radioactive particle for a general beach user summed over all exposure pathways [(a)(b)]

		Braystones beach	Drigg beach	Seascale beach	Sellafield beach	St Bees beach
Alpha-rich	2.5%	$1.2\ 10^{-7}$	$9.5\ 10^{-7}$	$1.3\ 10^{-8}$	$8.1\ 10^{-8}$	$1.5\ 10^{-7}$
	50%	$1.7\ 10^{-6}$	$1.3\ 10^{-5}$	$1.7\ 10^{-7}$	$1.1\ 10^{-6}$	$2.0\ 10^{-6}$
	97.5%	$2.5\ 10^{-5}$	$1.9\ 10^{-4}$	$2.5\ 10^{-6}$	$1.6\ 10^{-5}$	$3.0\ 10^{-5}$
Beta-rich	2.5%	$3.9\ 10^{-8}$	$4.3\ 10^{-9}$	$1.2\ 10^{-8}$	$5.7\ 10^{-8}$	$9.7\ 10^{-9}$
	50%	$5.3\ 10^{-7}$	$5.8\ 10^{-8}$	$1.6\ 10^{-7}$	$7.7\ 10^{-7}$	$1.3\ 10^{-7}$
	97.5%	$7.7\ 10^{-6}$	$8.4\ 10^{-7}$	$2.4\ 10^{-6}$	$1.1\ 10^{-5}$	$1.9\ 10^{-6}$
Cobalt-rich	2.5%	$8.5\ 10^{-10}$	$3.1\ 10^{-9}$	$2.2\ 10^{-10}$	$2.9\ 10^{-10}$	$2.2\ 10^{-10}$
	50%	$1.1\ 10^{-8}$	$4.1\ 10^{-8}$	$2.9\ 10^{-9}$	$3.8\ 10^{-9}$	$2.9\ 10^{-9}$
	97.5%	$1.6\ 10^{-7}$	$6.0\ 10^{-7}$	$4.2\ 10^{-8}$	$5.5\ 10^{-8}$	$4.3\ 10^{-8}$

(a) Highest value based on the 50%ile of the distribution across all beach users.

(b) These probabilities of encounter are for the adult angler. Table 45 shows how the results for other beach uses and age groups are related to these results.

Table 42: Highest total annual probability of encountering a radioactive particle for a high occupancy beach user summed over all exposure pathways

	Alpha-rich	Beta-rich	Cobalt-rich
Braystones[a]	7.6E-06	2.3E-06	5.0E-08
Drigg[b]	4.5E-05	1.9E-07	1.4E-07
Seascale[b]	5.0E-07	4.6E-07	8.3E-09
Sellafield[a]	1.1E-06	7.3E-07	3.7E-09
St Bees[b]	4.6E-06	2.9E-07	6.8E-09

(a) The highest probabilities of encounter for Braystones and Sellafield beaches are for the adult angler. Table 46 shows how the results for other beach uses and age groups are related to these results.

(b) The highest probabilities of encounte for Drigg, Seascale and St Bees beaches are for the adult walker. Table 46 shows how the results for other beach uses and age groups are related to these results.

Table 43: Highest total annual probability of encountering a radioactive stone for a general beach user summed over all exposure pathways [a,b]

		Braystones beach	Drigg beach	Seascale beach	Sellafield beach	St Bees beach
Alpha-rich	2.5%	-	-	-	$6.9\ 10^{-8}$	-
	50%	-	-	-	$9.6\ 10^{-7}$	-
	97.5%	-	-	-	$1.3\ 10^{-5}$	-
Beta-rich	2.5%	$6.4\ 10^{-10}$	-	$2.3\ 10^{-9}$	$1.1\ 10^{-7}$	-
	50%	$8.6\ 10^{-9}$	-	$3.0\ 10^{-8}$	$1.4\ 10^{-6}$	-
	97.5%	$1.3\ 10^{-7}$	-	$4.6\ 10^{-7}$	$2.2\ 10^{-5}$	-
Cobalt-rich	2.5%	-	-	-	$1.9\ 10^{-10}$	-
	50%	-	-	-	$2.7\ 10^{-9}$	-
	97.5%	-	-	-	$3.9\ 10^{-8}$	-

(a) Highest value is based on the 50%ile of the distribution across all beach users. The highest probabilities of encounter are for adult anglers.

(b) - indicates that no estimate could be made of the probability of encountering a radioactive stone as no such stones have been found using the Groundhog Evolution2™ system.

Table 44: Highest total annual probability of encountering a radioactive stone for a high occupancy beach user summed over all exposure pathways [a,b]

	Alpha-rich stone	Beta-rich stone	Cobalt-rich stone
Braystones	-	$3.8\ 10^{-8}$	-
Drigg	-	-	-
Seascale	-	$8.6\ 10^{-8}$	-
Sellafield	$9.1\ 10^{-7}$	$1.4\ 10^{-6}$	$2.6\ 10^{-9}$
St Bees	-	-	-

a) - indicates that no estimate could be made of the probability of encountering a radioactive stone as no such stones have been found using the Groundhog Evolution2™ system.

b) The highest probabilities of encounter are for adult anglers. For Seascale beach, the probability of encounter is the same for adult walkers.

7.1.1 Dependence of the annual probability of encountering a radioactive object on beach use

Table 45 shows the relative probabilities of encountering a radioactive object on a beach for each of the age groups and beach activities compared with the group with the highest probability of encounter for general beach users. Table 46 gives the same information for the high beach occupancy group. For the high beach occupancy group the information is given for each of the 5 beaches considered. These relative values are independent of the population of objects on the beaches and hence they are applicable for each of the object types (alpha-rich, beta-rich and cobalt-rich) and activity content of the objects. Results are given for the median value (50^{th} percentile) of the distribution. There is some variation in the relative probabilities if other points on the distribution are used, although this variation is small.

As an example, Table 45 shows that a child angler has around two thirds of the probability of encountering a radioactive object compared to an adult angler. However, when considering high occupancy beach users (see Table 46) on Braystones beach, the child angler has around a third of the probability of encountering a radioactive object compared to an adult angler on the same beach. The differences between these two scenarios is due to the use of pooled habit data for the general beach user and beach specific habit data for the high occupancy beach user.

Table 45: Probabilities of encountering a radioactive object on a beach for each age group and beach activity relative to the probability of encounter for the highest age/beach activity group[a] for a general beach user

Adult			Child			Young child	
Angling	Walking	Leisure	Angling	Walking	Leisure	Walking	Leisure
1.00	0.82	0.48	0.69	0.22	0.26	0.33	0.29

(a) Adult angler was the age group and beach activity that was estimated to have the highest probability of encounter for a general beach user.

(b) The relative probabilities of encounter are subject to variation as they are based on statistical results. The values in this table are for the 50% (median) results.

Table 46: Probabilities of encountering a radioactive object on a beach for each age group and beach activity relative to the highest probability of encounter for high occupancy beach users[a]

	Adult			Child			Young child	
	Angling	Walking	Leisure	Angling	Walking	Leisure	Walking	Leisure
Braystones	1.00	0.51	0.80	0.30	0.02	0.24	-	0.17
Drigg	0.90	1.00	0.27	0.09	0.17	0.21	-	0.14
Seascale	0.99	1.00	0.23	-	0.20	0.15	-	0.15
Sellafield	1.00	0.46	-	-	-	-	-	-
St Bees	0.87	1.00	0.69	0.13	0.08	0.08	0.31	0.19

(a) - indicates that this age group was not observed on the beach doing the indicated beach activity and has not been included in calculating annual probabilities of encounter. Appendix J gives values for hourly probabilities of encounter for these groups for completeness.

7.1.2 Contribution of different exposure pathways to annual probability of encounter

Table 47 presents the estimated contribution of each exposure pathway to the total probability of encountering a radioactive object for a general beach user. It should be noted that these contributions are not dependent on the beach because the relative importance of each exposure pathway is not dependent on beach occupancy or the population of objects on the beach. Results are given for the median value (50th percentile) of the distribution. There is some variation in the relative probabilities if other points on the distribution are used although this variation is small.

For all beach activities, the probability of encountering a radioactive object via ingestion or inhalation is not significant compared to having a radioactive particle close to the skin, with contributions to the total probability being less than 1%.

Based on the observations made on the activities people undertake on the beach and the assumptions made about exposure to sand (and hence potentially to objects), Table 47 indicates that for walking activities, encountering an object via sand becoming trapped in shoes is likely to give the highest contribution to the total probability of encounter. For leisure activities, the relative contributions from objects trapped in shoes and objects in direct contact with the skin are broadly similar for adults and children. However, for young children, objects trapped in shoes contribute significantly more to the overall probability of encounter than objects in direct contact with the skin. This is because the assessment assumed that the amount of sand (and hence objects) that can be trapped in shoes is not age dependent and the relative importance of thes two pathways is therefore dependent on the mass of sand encountered in shoes compared to on the skin. For adults, the mass of sand assumed to be on the skin relative to that in shoes is small compared to that assumed for young children.

For angling, Table 47 shows that the most significant exposure pathway contributing to the probability of encountering a radioactive object is from an object on the skin, with objects trapped in shoes contributing around a third of the total and objects adhering to clothing contributing less than 10% of the total.

Table 47: Percentage contribution of each exposure pathway to the median probability of encountering a radioactive particle on a beach for a generic beach user [(a)]

	Particle inadvertently ingested	Particle inhaled	Particle trapped under a nail	Particle trapped in shoes	Particle on the skin	Particle trapped in clothes
Adult - leisure	0.0072	0.0014	1.1	41	52	6.3
Adult - fishing	0.0059	0.0016	0.63	33	59	8.2
Adult - walking	0.0094	0.0018	1.2	55	31	13
Child - leisure	0.018	0.00028	0.82	53	41	4.9
Child - fishing	0.012	0.00018	0.4	35	59	5.3
Child - walking	0.021	0.0003	0.93	62	28	9.2
Young child - leisure	0.12	0.00019	0.57	69	28	2.9
Young child - walking	0.13	0.00021	0.62	76	17	5.5

(a) Due to the use of statistics in the derivation of these values there will be some variation in the contribution when other percentiles of the distribution are considered.

Table 48 shows the same information for high occupancy beach users. The Table shows that the exposure pathways that dominate the probability of encountering a radioactive object by a high occupancy beach user are the same as for a general beach user, although the relative contributions of pathways are slightly different.

Appendix D discusses the probability of an object becoming trapped in the ear and eye. It is expected that material in the eye would irritate the eye and be removed quickly and so it would be extremely unlikely to remain in constant contact with the eye for long periods of time. In addition, the scoping calculation in Appendix D shows that the probability of an object getting into the eye is very low when compared with the probability of an object coming into contact with other parts of the body. For an object in the ear the scoping calculation in Appendix D shows that the probability of encounter is less than that of an object coming into contact with the skin on other parts of the body. Therefore, in terms of the probability of encountering an object on the skin, the probability of an object being located in the ear would not significantly increase the overall probability of encounter. There is therefore no reason to consider material trapped in the ear as a separate exposure pathway except in discussing the potential length of time an object could remain in stationary contact with an area of skin. Health effects of particles trapped in the ear or eye are discussed in Section 9.1.4.

Table 48: Percentage contribution of each exposure pathway to the probability of encountering a radioactive particle on a beach for a high occupancy beach user [(a)]

	Particle inadvertently ingested	Particle inhaled	Particle trapped under a nail	Particle trapped in shoes	Particle on the skin	Particle trapped in clothes
Adult - leisure	0.022	0.003	0.73	49	46	4.6
Adult - fishing	0.019	0.0036	0.51	43	50	6.5
Adult - walking	0.03	0.0041	0.88	68	21	10
Child - leisure	0.055	0.00053	0.55	61	35	3.4
Child - fishing	0.04	0.00038	0.32	44	52	4.0
Child - walking	0.066	0.00064	0.66	74	19	6.6
Young child - leisure	0.33	0.00036	0.35	73	24	1.9
Young child - walking	0.38	0.00041	0.4	84	12	3.6

(a) Due to the use of statistics in the derivation of these values there will be some variation in the contribution when other percentiles of the distribution are considered.

7.1.3 Use of information presented to calculate the annual probability of encounter for any age group and beach activity combination and from any exposure pathway

If the probability of encountering an object is required for a different beach activity and age group combination than given in Section 7.1, or if the probability of encountering an object is required for a specific exposure pathway, then the information in Table 41 - Table 48 can be combined. As an example, Table 41 shows that the beach activity and age group which always has the highest probability of encountering an object for a general beach user is the adult angler. If the probability of encountering an object is required for a different beach use or age group, for example for a general child beach user undertaking leisure activities, then the probabilities in Table 41 can be scaled with the values for 'child leisure' in Table 45 (Section 7.1.1).

If the probability of encounter is required for a specific exposure pathway, then the total probabilities given in Section 7.1 can be scaled using the appropriate factors in Sections 7.1.1 and 7.1.2. As an example, if the probability of encountering an object from exposure due to objects trapped within clothing for a child walking on a beach is required, then the highest probability of encounter from Section 7.1 is firstly scaled with the values for 'child walking' in Table 45 (Section 7.1.1) for a general beach user or with the values in Table 46 (Section 7.1.1) for a high occupancy beach user on a specific beach. To determine the probability from objects trapped in clothing, a second scaling is needed using the information presented on the relative pathway contributions (an object in clothing) for a 'child walking' in Table 47 (Section 7.1.2), for a general beach user or with the values in Table 48 (Section 7.1.2) for a high occupancy beach user on a specific beach.

The probability of encountering a particle can be summed with the probability of encountering a stone to give an overall probability of encountering any object on a beach. However, it should also be noted, that, as discussed above, this is overly cautious for a general beach user. To do this, the probabilities must be summed for the same group of individuals using the information given in Sections 7.2 and 7.3.

7.2 Annual probability of encounter of particles on each beach

The Tables in this Section give the annual probability of encountering particles on each of the beaches considered for each age group and beach activity. The annual probabilities are given for each activity band for alpha-rich, beta-rich and ^{60}Co-rich particles. The probabilities of encounter for each activity band take account of the number of objects estimated in each activity band, as described in Section 4.2. The total probability of encounter for each particle type can be obtained by summing the probabilities across the different activity bands represented by the midpoints of 10 kBq, 100 kBq and 1000 kBq.

7.2.1 Annual probability of encountering a radioactive particle on Braystones beach

Table 49 presents the annual probability of encountering a particle by a general beach user on Braystones beach for each activity band. Table 50 presents similar information for a high occupancy beach user.

Table 49: Annual probability of encountering a radioactive particle on Braystones beach for a general beach user summed over all exposure pathways[a]

		Alpha-rich particles		Beta-rich particles		Cobalt-rich particles
		10 kBq	100 kBq	10 kBq	100 kBq	10 kBq
Adult[b]	2.50%	$1.1\ 10^{-7}$	$1.3\ 10^{-8}$	$3.7\ 10^{-8}$	$5.3\ 10^{-10}$	8.9E-10
	50%	$1.5\ 10^{-6}$	$1.8\ 10^{-7}$	$5.0\ 10^{-7}$	$7.1\ 10^{-9}$	1.1E-08
	97.50%	$2.1\ 10^{-5}$	$2.7\ 10^{-6}$	$7.1\ 10^{-6}$	$1.0\ 10^{-7}$	1.6E-07
Child[c]	2.50%	$1.5\ 10^{-7}$	$1.7\ 10^{-8}$	$5.0\ 10^{-8}$	$6.6\ 10^{-10}$	1.1E-09
	50%	$1.0\ 10^{-6}$	$1.3\ 10^{-7}$	$3.6\ 10^{-7}$	$4.9\ 10^{-9}$	7.8E-09
	97.50%	$7.4\ 10^{-6}$	$8.8\ 10^{-7}$	$2.5\ 10^{-6}$	$3.3\ 10^{-8}$	5.5E-08
Young child[d]	2.50%	6.6E-08	8.3E-09	2.2E-08	2.9E-10	4.5E-10
	50%	4.8E-07	6.1E-08	1.7E-07	2.3E-09	3.6E-09
	97.50%	3.0E-06	3.8E-07	1.1E-06	1.4E-08	2.3E-08

(a) The estimated population of particles does not contain any particles with a radioactivity content of 1000 kBq.

(b) Highest probabilities of encounter are for adult angler.

(c) Highest probabilities of encounter are for child angler.

(d) Highest probabilities of encounter are for young child walking.

Table 50: Annual probability of encountering a radioactive particle on Braystones beach for a high occupancy beach usersummed over all exposure pathways [a]

	Alpha-rich particles		Beta-rich particles		Cobalt-rich particles
	10 kBq	100 kBq	10 kBq	100 kBq	10 kBq
Adult[b]	$6.7\ 10^{-6}$	$8.2\ 10^{-7}$	$2.3\ 10^{-6}$	$3.2\ 10^{-8}$	$5.0\ 10^{-8}$
Child[c]	$2.0\ 10^{-6}$	$2.4\ 10^{-7}$	$6.9\ 10^{-7}$	$9.4\ 10^{-9}$	$1.5\ 10^{-8}$
Young child[d]	$1.1\ 10^{-6}$	$1.4\ 10^{-7}$	$3.9\ 10^{-7}$	$5.3\ 10^{-9}$	$8.4\ 10^{-9}$

(a) The estimated population of particles does not contain any particles with a radioactivity content of 1000 kBq.

(b) These probabilities of encounter are for the adult angler.

(c) Highest probabilities of encounter are for child angler.

(d) Highest probabilities of encounter are for young child leisure.

7.2.2 Annual probability of encountering a radioactive particle on Drigg beach

Table 51 presents the annual probability of encountering a particle by a general beach user on Drigg beach for each activity band. Table 52 presents similar information for a high occupancy beach user.

Table 51: Annual probability of encountering a radioactive particle on Drigg beach for a general beach usersummed over all exposure pathways[a]

		Alpha-rich particles		Beta-rich particles		Cobalt-rich particles
		10 kBq	100 kBq	10 kBq	100 kBq	10 kBq
Adult[b]	2.50%	$9.6\ 10^{-7}$	$1.8\ 10^{-8}$	$2.1\ 10^{-9}$	$2.2\ 10^{-9}$	$3.3\ 10^{-9}$
	50%	$1.3\ 10^{-5}$	$2.5\ 10^{-7}$	$2.8\ 10^{-8}$	$2.9\ 10^{-8}$	$4.2\ 10^{-8}$
	97.50%	$1.8\ 10^{-4}$	$3.6\ 10^{-6}$	$4.0\ 10^{-7}$	$4.1\ 10^{-7}$	$5.9\ 10^{-7}$
Child[c]	2.50%	$1.3\ 10^{-6}$	$2.3\ 10^{-8}$	$2.8\ 10^{-9}$	$2.7\ 10^{-9}$	$4.0\ 10^{-9}$
	50%	$9.0\ 10^{-6}$	$1.7\ 10^{-7}$	$2.0\ 10^{-8}$	$2.0\ 10^{-8}$	$2.9\ 10^{-8}$
	97.50%	$6.5\ 10^{-5}$	$1.2\ 10^{-6}$	$1.4\ 10^{-7}$	$1.4\ 10^{-7}$	$2.0\ 10^{-7}$
Young child[d]	2.50%	5.7E-07	1.1E-08	1.3E-09	1.2E-09	1.7E-09
	50%	4.2E-06	8.1E-08	9.3E-09	9.3E-09	1.3E-08
	97.50%	2.6E-05	5.1E-07	5.9E-08	5.7E-08	8.3E-08

(a) The estimated population of particles does not contain any particles with a radioactivity content of 1000 kBq.

(b) Highest probabilities of encounter are for adult angler.

(c) Highest probabilities of encounter are for child angler.

(d) Highest probabilities of encounter are for young child walking.

Table 52: Annual probability of encountering a radioactive particle on Drigg beach for a high occupancy beach user summed over all exposure pathways[a]

	Alpha-rich particles		Beta-rich particles		Cobalt-rich particles
	10 kBq	100 kBq	10 kBq	100 kBq	10 kBq
Adult[b]	$4.5\ 10^{-5}$	$8.4\ 10^{-7}$	$1.0\ 10^{-7}$	$1.0\ 10^{-7}$	$1.4\ 10^{-7}$
Child[c]	$9.7\ 10^{-6}$	$1.8\ 10^{-7}$	$2.1\ 10^{-8}$	$2.1\ 10^{-8}$	$3.1\ 10^{-8}$
Young child[d]	$6.5\ 10^{-6}$	$1.2\ 10^{-7}$	$1.4\ 10^{-8}$	$1.4\ 10^{-8}$	$2.0\ 10^{-8}$

(a) The estimated population of particles does not contain any particles with a radioactivity content of 1000 kBq.

(b) These probabilities of encounter are for the adult walker. Table 46 shows how the relationship of other beach uses and age groups are related to these results.

(c) Highest probabilities of encounter are for child leisure.

(d) Highest probabilities of encounter are for young child leisure.

7.2.3 Annual probability of encountering a radioactive particle on Seascale beach

Table 53 presents the annual probability of encountering a particle by a general beach user on Seascale beach for each activity band. Table 54 presents similar information for a high occupancy beach user.

Table 53: Annual probability of encountering a radioactive particle on Seascale beach for a general beach usersummed over all exposure pathways[a]

		Alpha-rich particles		Beta-rich particles		Cobalt-rich particles
		10 kBq	100 kBq	10 kBq	100 kBq	10 kBq
Adult[b]	2.50%	$7.2\ 10^{-9}$	$5.4\ 10^{-9}$	$1.1\ 10^{-8}$	$7.7\ 10^{-10}$	$2.3\ 10^{-10}$
	50%	$9.9\ 10^{-8}$	$7.6\ 10^{-8}$	$1.5\ 10^{-7}$	$1.0\ 10^{-8}$	$3.0\ 10^{-9}$
	97.50%	$1.4\ 10^{-6}$	$1.1\ 10^{-6}$	$2.1\ 10^{-6}$	$1.5\ 10^{-7}$	$4.2\ 10^{-8}$
Child[c]	2.50%	$9.7\ 10^{-9}$	$7.2\ 10^{-9}$	$1.5\ 10^{-8}$	$9.7\ 10^{-10}$	$2.8\ 10^{-10}$
	50%	$6.7\ 10^{-8}$	$5.3\ 10^{-8}$	$1.0\ 10^{-7}$	$7.2\ 10^{-9}$	$2.0\ 10^{-9}$
	97.50%	$4.9\ 10^{-7}$	$3.6\ 10^{-7}$	$7.2\ 10^{-7}$	$4.9\ 10^{-8}$	$1.4\ 10^{-8}$
Young child[d]	2.50%	4.3E-09	3.4E-09	6.5E-09	4.3E-10	1.2E-10
	50%	3.2E-08	2.5E-08	4.8E-08	3.3E-09	9.4E-10
	97.50%	2.0E-07	1.6E-07	3.1E-07	2.0E-08	5.8E-09

(a) The estimated population of particles does not contain any particles with a radioactivity content of 1000 kBq.

(b) Highest probabilities of encounter are for adult angler.

(c) Highest probabilities of encounter are for child angler.

(d) Highest probabilities of encounter are for young child walking.

Table 54: Annual probability of encountering a radioactive particle on Seascale beach for a high occupancy beach user summed over all exposure pathways[a]

	Alpha-rich particles		Beta-rich particles		Cobalt-rich particles
	10 kBq	100 kBq	10 kBq	100 kBq	10 kBq
Adult[b]	$2.8\ 10^{-7}$	$2.2\ 10^{-7}$	$4.3\ 10^{-7}$	$3.0\ 10^{-8}$	$8.3\ 10^{-9}$
Child[c]	$5.7\ 10^{-8}$	$4.4\ 10^{-8}$	$8.7\ 10^{-8}$	$6.0\ 10^{-9}$	$1.7\ 10^{-9}$
Young child[d]	$4.3\ 10^{-8}$	$3.3\ 10^{-8}$	$6.5\ 10^{-8}$	$4.5\ 10^{-9}$	$1.3\ 10^{-9}$

(a) The estimated actual population of particles does not contain any particles with a radioactivity content of 1000 kBq.

(b) Highest probabilities of encounter are for adult walking.

(c) Highest probabilities of encounter are for child walking.

(d) Highest probabilities of encounter are for young child leisure.

7.2.4 Annual probability of encountering a radioactive particle on Sellafield beach

Table 55 presents the annual probability of encountering a particle by a general beach user on Sellafield beach for each activity band. Table 56 presents similar information for a high occupancy beach user.

Table 55: Annual probability of encountering a radioactive particle on Sellafield beach for a general beach user summed over all exposure pathways[a]

		Alpha-rich particles			Beta-rich particles		Cobalt-rich particles
		10 kBq	100 kBq	1000 kBq[(b)]	10 kBq	100 kBq	10 kBq
Adult[(c)]	2.5%	$5.1\ 10^{-8}$	$3.1\ 10^{-8}$	$3.2\ 10^{-10}$	$5.4\ 10^{-8}$	$1.8\ 10^{-9}$	$3.0\ 10^{-10}$
	50%	$7.1\ 10^{-7}$	$4.3\ 10^{-7}$	$4.1\ 10^{-9}$	$7.3\ 10^{-7}$	$2.4\ 10^{-8}$	$3.9\ 10^{-9}$
	97.5%	$9.9\ 10^{-6}$	$6.2\ 10^{-6}$	$6.1\ 10^{-8}$	$1.0\ 10^{-5}$	$3.4\ 10^{-7}$	$5.4\ 10^{-8}$

(a) Highest probabilities of encounter are for the adult angler.

(b) Maximum activity for an alpha-rich particle found on the beach is 634 kBq ^{241}Am.

(c) Only adults considered as beach users for Sellafield beach.

Table 56: Annual probability of encountering a radioactive particle on Sellafield beach for a high occupancy beach user summed over all exposure pathways [a]

	Alpha-rich particles			Beta-rich particles		Cobalt-rich particles
	10 kBq	100 kBq	1000 kBq[(b)]	10 kBq	100 kBq	10 kBq
Adult[(c)]	$6.8\ 10^{-7}$	$4.1\ 10^{-7}$	$4.1\ 10^{-9}$	$7.3\ 10^{-7}$	$2.3\ 10^{-8}$	$3.7\ 10^{-9}$

(a) Highest probabilities of encounter are for the adult angler.

(b) Maximum activity for an alpha-rich particle found on the beach is 634 kBq ^{241}Am.

(c) Only adults considered as beach users for Sellafield beach.

7.2.5 Annual probability of encountering a radioactive particle on St Bees beach

Table 57 presents the annual probability of encountering a particle by a general beach user on St Bees beach for each activity band. Table 58 presents similar information for a high occupancy beach user.

Table 57: Annual probability of encountering a radioactive particle on St Bees beach for a general beach user summed over all exposure pathways[a]

		Alpha-rich particles		Beta-rich particles	Cobalt-rich particles
		10 kBq	100 kBq	10 kBq	10 kBq
Adult[b]	2.50%	$1.4\ 10^{-7}$	$4.8\ 10^{-9}$	$9.1\ 10^{-9}$	$2.3\ 10^{-10}$
	50%	$2.0\ 10^{-6}$	$6.6\ 10^{-8}$	$1.2\ 10^{-7}$	$3.0\ 10^{-9}$
	97.50%	$2.8\ 10^{-5}$	$9.6\ 10^{-7}$	$1.7\ 10^{-6}$	$4.2\ 10^{-8}$
Child[c]	2.50%	$1.9\ 10^{-7}$	$6.3\ 10^{-9}$	$1.2\ 10^{-8}$	$2.8\ 10^{-10}$
	50%	$1.3\ 10^{-6}$	$4.6\ 10^{-8}$	$8.8\ 10^{-8}$	$2.0\ 10^{-9}$
	97.50%	$9.7\ 10^{-6}$	$3.2\ 10^{-7}$	$6.1\ 10^{-7}$	$1.4\ 10^{-8}$
Young child[d]	2.50%	8.6E-08	3.0E-09	5.5E-09	1.2E-10
	50%	6.4E-07	2.2E-08	4.1E-08	9.5E-10
	97.50%	4.0E-06	1.4E-07	2.6E-07	5.9E-09

(a) The estimated actual particle population does not contain any particles with a radioactivity content of 1000 kBq.

(b) Highest probabilities of encounter are for adult angler.

(c) Highest probabilities of encounter are for child angler.

(d) Highest probabilities of encounter are for young child walking.

Table 58: Annual probability of encountering a radioactive particle on St Bees beach for a high occupancy beach usersummed over all exposure pathways[a]

	Alpha-rich particles		Beta-rich particles	Cobalt-rich particles
	10 kBq	100 kBq	10 kBq	10 kBq
Adult[b]	$4.5\ 10^{-6}$	$1.5\ 10^{-7}$	$2.9\ 10^{-7}$	$6.8\ 10^{-9}$
Child[c]	$5.9\ 10^{-7}$	$2.0\ 10^{-8}$	$3.8\ 10^{-8}$	$8.9\ 10^{-10}$
Young child[d]	$1.4\ 10^{-6}$	$4.7\ 10^{-8}$	$9.0\ 10^{-8}$	$2.1\ 10^{-9}$

(a) The estimated actual particle population does not contain any particles with a radioactivity content of 1000 kBq.

(b) Highest probabilities of encounter are for adult walking.

(c) Highest probabilities of encounter are for child angler.

(d) Highest probabilities of encounter are for young child walking.

7.3 Annual probability of encounter of stones on each beach

The Tables in this Section give the same information as is presented in Section 7.2, for stones.

7.3.1 Probability of encountering a radioactive stone on Braystones beach

Table 59 presents the annual probability of encountering a stone by a general beach user on Braystones beach for each activity band. Table 60 presents similar information for a high occupancy beach user.

Table 59: Annual probability of encountering a radioactive stone on Braystones beach for a general beach user summed over all exposure pathways

		Beta-rich stone 100 kBq
Adult[a]	2.50%	$6.3\ 10^{-10}$
	50%	$8.5\ 10^{-9}$
	97.50%	$1.2\ 10^{-7}$
Child[b]	2.50%	$8.0\ 10^{-10}$
	50%	$5.9\ 10^{-9}$
	97.50%	$4.1\ 10^{-8}$
Young child[c]	2.50%	3.5E-10
	50%	2.7E-09
	97.50%	1.7E-08

(a) Highest probabilities of encounter are for adult angler.

(b) Highest probabilities of encounter are for child angler.

(c) Highest probabilities of encounter are for young child walking.

Table 60: Annual probability of encountering a radioactive stone on Braystones beach for a high occupancy beach user summed over all exposure pathways

	Beta-rich stone 100 kBq
Adult[a]	$3.8\ 10^{-8}$
Child[b]	$1.1\ 10^{-8}$
Young child[c]	$6.3\ 10^{-9}$

(a) Highest probabilities of encounter are for adult angler.

(b) Highest probabilities of encounter are for child angler.

(c) Highest probabilities of encounter are for young child leisure.

7.3.2 Probability of encountering a radioactive stone on Seascale beach

Table 61 presents the annual probability of encountering a stone by a general beach user on Seascale beach for each activity band. Table 62 presents similar information for a high occupancy beach user.

Table 61: Annual probability of encountering a radioactive stone on Seascale beach for a general beach user summed over all exposure pathways

		Beta-rich stone	
		10 kBq	100 kBq
Adult[a]	2.50%	$2.1\ 10^{-9}$	$2.5\ 10^{-10}$
	50%	$2.7\ 10^{-8}$	$3.3\ 10^{-9}$
	97.50%	$3.8\ 10^{-7}$	$4.8\ 10^{-8}$
Child[b]	2.50%	$2.5\ 10^{-9}$	$3.1\ 10^{-10}$
	50%	$1.9\ 10^{-8}$	$2.3\ 10^{-9}$
	97.50%	$1.3\ 10^{-7}$	$1.6\ 10^{-8}$
Young child[c]	2.50%	1.2E-09	1.4E-10
	50%	8.8E-09	1.1E-09
	97.50%	5.4E-08	6.8E-09

(a) Highest probabilities of encounter are for adult angler.

(b) Highest probabilities of encounter are for child angler.

(c) Highest probabilities of encounter are for young child walking.

Table 62: Annual probability of encountering a radioactive stone on Seascale beach for a high occupancy beach user summed over all exposure pathways

	Beta-rich stone	
	10 kBq	100 kBq
Adult[a]	$7.7\ 10^{-8}$	$9.4\ 10^{-9}$
Child[b]	$1.6\ 10^{-8}$	$1.9\ 10^{-9}$
Young child[c]	$1.2\ 10^{-8}$	$1.4\ 10^{-9}$

(a) Highest probabilities of encounter are for the adult angler.

(b) Highest probabilities of encounter are for child walking.

(c) Highest probabilities of encounter are for young child leisure.

7.3.3 Probability of encountering a radioactive stone on Sellafield beach

Table 63 presents the annual probability of encountering a stone by a general beach user on Sellafield beach for each activity band. Table 64 presents similar information for a high occupancy beach user.

Table 63: Annual probability of encountering a radioactive stone on Sellafield beach for a general beach user summed over all exposure pathways

		Alpha-rich stone		Beta-rich stone			Cobalt-rich stone
		10 kBq	100 kBq	10 kBq	100 kBq	1000 kBq[c]	10 kBq
Adult[a,b]	2.5%	$7.0\ 10^{-8}$	$1.0\ 10^{-10}$	$1.0\ 10^{-7}$	$8.4\ 10^{-9}$	$7.0\ 10^{-10}$	$2.0\ 10^{-10}$
	50%	$9.4\ 10^{-7}$	$1.4\ 10^{-9}$	$1.3\ 10^{-6}$	$1.1\ 10^{-7}$	$9.2\ 10^{-9}$	$2.6\ 10^{-9}$
	97.5%	$1.4\ 10^{-5}$	$2.1\ 10^{-8}$	$1.9\ 10^{-5}$	$1.6\ 10^{-6}$	$1.4\ 10^{-7}$	$3.8\ 10^{-8}$

(a) Highest probabilities of encounter are for the adult angler.

(b) Only adults considered as beach users for Sellafield beach.

(c) Maximum activity for a beta-rich stone found on the beach is 875 kBq.

Table 64: Annual probability of encountering a radioactive stone on Sellafield beach for a high occupancy beach usersummed over all exposure pathways[a]

	Alpha-rich stone		Beta-rich stone			Cobalt-rich stone
	10 kBq	100 kBq	10 kBq	100 kBq	1000 kBq[(b)]	10 kBq
Adult[(c)]	$9.1\ 10^{-7}$	$1.4\ 10^{-9}$	$1.3\ 10^{-6}$	$1.1\ 10^{-7}$	$9.1\ 10^{-9}$	$2.6\ 10^{-9}$

(a) These probabilities of encounter are for the adult angler. Table 46 shows how the relationship of other beach uses and age groups are related to these results.

(b) Maximum activity for a beta-rich particle found on the beach is 875 kBq.

(c) Only adults considered as beach users for Sellafield beach.

7.4 Annual probability of encounter of a particle via consumption of seafood

The estimated annual probabilities of ingesting an object for an adult consuming shellfish are given in Table 65. A description of the methodology adopted is given in Appendix I. The consumption of molluscs gives rise to the highest probability of ingesting a particle. The findings of a study in which the Cefas monitoring database for mollusc samples sourced from the Sellafield area was investigated to identify if there were incidences of high activities that could be due to contaminated particles are helpful to put the estimated probabilities of encounter into perspective (Cefas, 2008b). The study concluded that, under the search criteria adopted, Cefas' monitoring and analysis database was not found to contain any samples that would conclusively indicate the ingestion of a contaminated particle. Although a number of samples did contain activity concentrations that exceeded the arbitrary secondary screening level set, they did not approach the activity levels recorded in analyses of particles found on the beaches (Cefas, 2008b). It is likely, therefore, that given this finding and the conservative approach taken in estimating the probability of a seafood consumer ingesting a particle, that the values given in Table 65 are very conservative. The annual probabilities of encounter for children consuming shellfish will be significantly lower due to their low consumption rate of seafood.

Table 65: Probability of an adult encountering a radioactive particle from the consumption of shellfish

Particle type	Probability per year			
	Crabs	Lobsters	Molluscs	Total[a]
Alpha-rich	$1.7\ 10^{-6}$	$9.6\ 10^{-9}$	$5.2\ 10^{-6}$	$6.9\ 10^{-6}$
Beta-rich	$9.8\ 10^{-7}$	$5.6\ 10^{-9}$	$3.0\ 10^{-6}$	$4.0\ 10^{-6}$

a) The total value is only applicable if it is assumed that an individual is a high-rate consumer of all species of shellfish.

7.5 Summary of the estimated total annual probabilities of encountering objects on the beaches

The estimated annual probability of encounter varies between beaches and is dependent on the estimated number of objects that could be on each beach, the activities undertaken on the beaches and the time members of the public spend on each beach. Across the five beaches considered, the median value of the probability of a typical beach user encountering any particle (ie, 50% of beach users will have a higher probability of encounter and 50% a lower probability) range from $1\ 10^{-7}$ (chance of 1 in 10 million per year) to $1\ 10^{-5}$ (chance of 1 in 100 thousand per year). Five percent of beach users are estimated to have a probability of encountering a particle of about a factor of 10 higher than this. Based on the information available, the probability of encounter is highest for adult beach users, with values for children typically being about a factor of 2 – 3 lower. The majority of the particles are in the activity range of 3 – 30 kBq and the total annual probability is dominated by the probability of encountering such particles. The probability of encountering particles with activities greater than 300 kBq (the highest activity range considered) is several orders of magnitude lower and it should be noted that particles with activities in this range have only been detected on Sellafield beach.

The estimated annual probability of encountering an object for individual adult beach users with high annual beach occupancy ranges from $1\ 10^{-6}$ (chance of 1 in a million per year) to $4\ 10^{-5}$ (chance of 1 in 25 thousand per year). This is higher than the median value for typical beach users but within the range of values across all beach users.

On some of the beaches, contaminated stones (diameter >2 mm) have been found (see Table 2); these are predominantly beta-rich stones found on Sellafield beach. As discussed in Section 6.1, it is highly unlikely that general beach users will be exposed to these stones as they are generally too large to adhere to the skin (directly or in clothing and shoes) or to be taken into the body. However, if it is assumed that general beach users could be exposed to these stones, the total probability of encountering an object (ie, both particles and stones) would be effectively the same as that from encountering a particle for all beaches except for Sellafield beach, due to the very small estimated number of stones on these beaches. For Sellafield beach, the total probability of encountering an object would be higher than that for particles by about a factor of 2.

When considering the likelihood that individuals will encounter an object on one of the beaches, there are some general observations that can be made on how the probability is likely to vary depending on beach use and which routes of exposure are more likely to lead to an individual being exposed to an object. The most likely way this can occur is from the object adhering to the skin or becoming trapped in clothing or shoes so that it is in stationary contact with a small area of skin. The probability of inadvertently ingesting an object is very small and much lower than 1% of the total probability of encountering an object. The probability of inhaling an object is even smaller.

Figures 6 and 7 show the relative importance of the different ways an object can be encountered for a beach user walking or spending leisure time on a beach and for anglers, assuming that they also dig for bait.

Figure 6 shows that the probability of encounter is dominated by exposure from contact with the skin and, for walkers, this is dominated by objects becoming trapped in shoes whereas for people carrying out leisure activities, although this pathway is still important, direct contact on the skin is likely to be relatively more important because of the higher likelihood of individuals having more contact with sand (and objects). For anglers (Figure 7), the most important exposure pathway is direct contact with significant amounts of sand during bait digging which could lead to particles adhering to the skin.

For the adult groups considered, it is estimated that anglers or walkers will have the highest annual probability of encountering an object. For walking and leisure activities, differences observed in the probabilities of encounter across the five beaches considered depend on the observed main use of the beach; for St Bees, for example, it is mainly walking while for Braystones, leisure activities are more important. For children, angling is typically less important, although on Braystones beach the habit surveys indicated a number of children who regularly fish. Young children are observed as predominantly playing on the beaches.

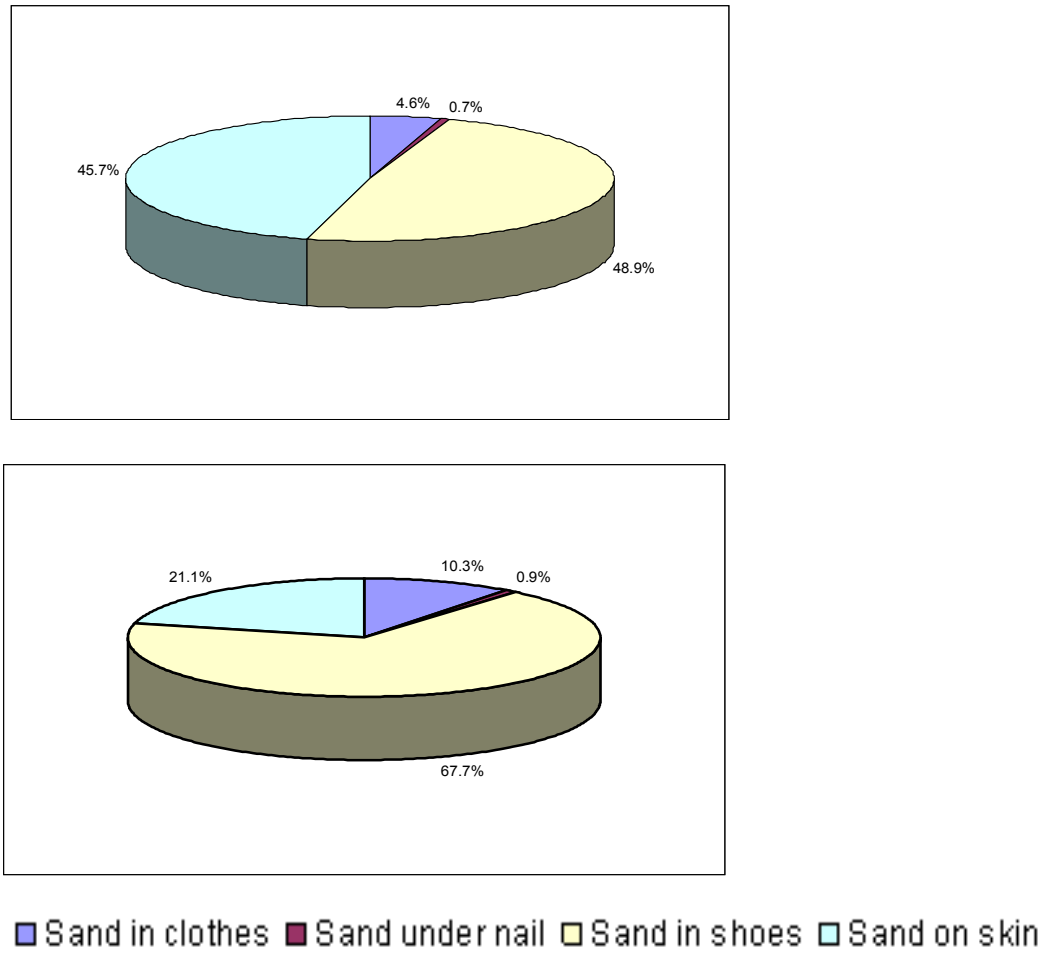

Figure 6: The relative contributions of exposure pathways to the total probability of encountering a radioactive particle for walking (above) and leisure activities (below)

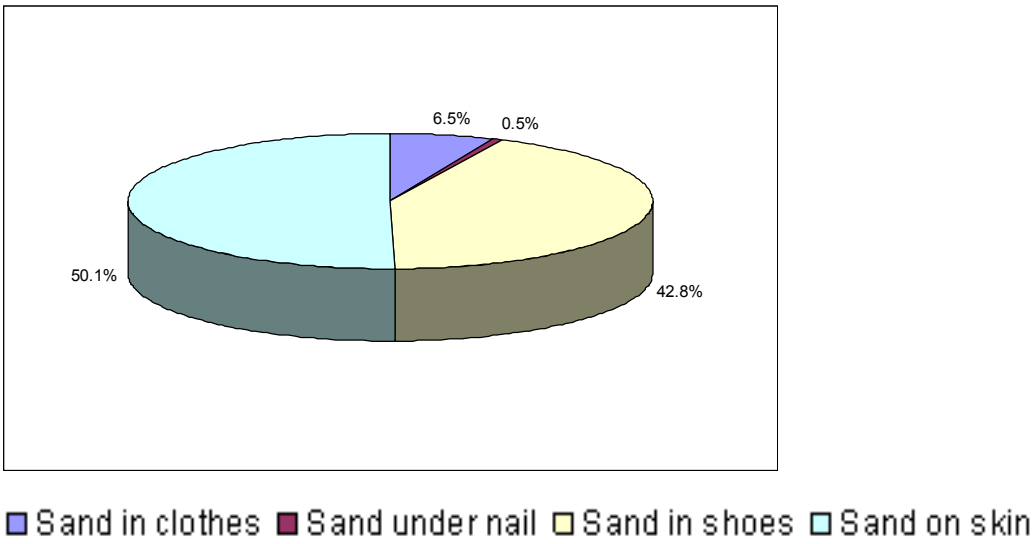

Figure 7: The relative contributions of exposure pathways to the total probability of encountering a radioactive particle for angling activities

8 DOSES AND RISKS TO HEALTH ARISING FROM EXPOSURES TO ALPHA-RICH OBJECTS

Health effects can generally be categorised as:

- *Stochastic effects*, which include cancers and heritable effects. The *probability* of occurrence of the effect increases with increasing radiation dose without a threshold, but the *severity* of the effect is independent of dose (ICRP, 2007b). Stochastic effects may take many years to develop. Examples include cancers such as colon cancer and leukaemia.
- *Deterministic effects*, which occur only for high radiation doses above a certain *threshold*. Once the threshold is exceeded, the *severity* increases with increasing dose. Deterministic effects often occur within hours or days of the radiation exposure. Examples include skin ulceration, or depletion of red bone marrow cells.

Where the aim is to assess the likelihood and severity of deterministic effects, the absorbed dose to organs, for example the skin, is the dosimetric quantity that should be used. The unit of absorbed dose is the gray, abbreviated to Gy. To ensure an adequate level of radiological protection, the probability of stochastic effects also needs to be considered and equivalent doses to organs and effective dose are the dosimetric quantities that can be used. The unit of both equivalent dose and effective dose is the sievert, abbreviated to Sv. Equivalent dose is determined from absorbed dose by

multiplying by a radiation weighting factor for each radiation type (ICRP, 2007). The radiation weighting factor broadly reflects the differences in the effectiveness of each radiation type in causing stochastic effects. For photons and beta radiation, the radiation weighting factor is equal to 1; for alpha radiation, it is 20. (Since the radiation weighting factor is defined in terms of the probability of stochastic effects, it is clear that equivalent dose should not be used for the assessment of deterministic effects.) Effective dose is a weighted average of the equivalent doses to the organs of the body. It provides a single quantity that broadly reflects the risk of stochastic effects across a population, summed over all organs and tissues.

This Section describes the assessments of radiation doses that have been carried out to determine risks to health in the unlikely event that an individual encounters an alpha-rich object on the beaches in the vicinity of the Sellafield site. In this Section, the highest activity content of each object type has been used in order to estimate the maximum doses that could result from exposure to alpha-rich objects and the highest risks to health if an alpha-rich object is encountered. In general, ingestion and inhalation are the most important exposure pathways for alpha-emitting radionuclides. Stochastic risks to health are the most important consideration following ingestion or inhalation because absorbed doses to the gastro-intestinal tract, lungs and red bone marrow would have to approach very high values, in excess of threshold values for acute exposure of 23, 5.5 and 2.2 Gy, respectively (NRPB, 1996), before deterministic effects would occur. As will be shown later in this section, the highest absorbed doses that could be received are orders of magnitude less than these thresholds.

With respect to the ingestion pathway, absorption from the gastro-intestinal (GI) tract is the main factor determining effective dose. Section 8.1 / Appendix K present a review of published data on absorption of ingested plutonium (Pu) and americium (Am). Section 8.2 presents the results of experimental studies on the ingestion of alpha-rich particles retrieved from beaches in the vicinity of the Sellafield site carried out recently at HPA. Sections 8.3 and 8.4 discuss the conclusions of these studies and the implications of the results for doses and stochastic risks. Section 8.5 considers the inhalation pathway while the topic of skin doses from alpha-rich objects is addressed in Sections 8.6 and 8.7. Significant doses to the skin are not expected to arise from alpha irradiation of the skin by alpha-rich objects, although skin doses resulting from the 60 keV gamma-ray emission of ^{241}Am do need to be considered.

Doses and risks to health associated with uptake from wounds in which a particle is embedded are considered in Appendix E.

8.1 Review of published data on the absorption of ingested plutonium and americium in adults

In the absence of human data, data from other mammalian species are considered the most important because the absorption processes are expected to operate in a similar way and comparisons generally show similar results in different mammalian species. The results of a literature review of the absorption of ingested Pu and Am are described in Appendix K.

8.2 Doses and stochastic risks for ingestion of alpha-rich particles

The most important factor determining the dose per unit intake for ingestion of an alpha-rich particle is the fractional uptake of the alpha-emitting radionuclides as the particle passes through the GI tract. For very low uptake fractions (typically 10^{-8} or less), equivalent doses to organs resulting from systemic uptake are relatively low, and effective dose is dominated by the dose to the regions of the GI tract exposed as the particle passes through it. For higher uptake fractions (above about 10^{-4}), the contribution from systemic organ doses dominates and the relationship between the committed effective dose per unit intake, e(50), and uptake fraction is almost linear.

If a particle dissolves completely in the GI tract, then the uptake is characterised by the fractional absorption value (f_1), which is the fraction of an ingested element that is directly absorbed from the GI tract to the body fluids (ICRP, 1997) when it is in a biologically available form. However, if a particle does not undergo complete dissolution in the GI tract, only the elements in dissolved form are available for uptake. Pellow et al (2009) defines the particle uptake fraction, F_U^P, as the fraction of the element contained in the particle that is absorbed into the body. This is determined from the product of the particle dissolution fraction, F_D^P, and the f_1 value for the element, ie,

$$F_U^P = F_D^P \; x \; f_1$$

An *in vivo* study was carried out at HPA to determine uptake fractions for five alpha-rich particles (Pellow et al, 2009), and complementary *in vitro* studies were carried out at the National Physics Laboratory (NPL) as part of SERCO's particle characterisation study to determine particle dissolution fractions for another set of alpha-rich particles (Cowper, 2009). In an attempt to resolve discrepancies between the results of the HPA *in vivo* study and NPL's *in vitro* study, a second, combined *in vivo/in vitro* study was carried out at HPA. These studies are described in Sections 8.2.1, 8.2.2 and 8.2.3.

8.2.1 1st *in vivo* study at HPA

Pellow et al (2009) carried out an *in* vivo study using laboratory rats to determine F_U^P for ^{238}Pu, $^{239/240}$Pu and ^{241}Am for each of five alpha-rich particles.

The five particles were selected using the following criteria:

- particles should be small enough to pass down a plastic cannula with internal diameter of 1 mm, so that each particle could be administered to a rat
- particles should have sufficient activity that absorption into the rat of mBq levels could be measured, so that particle uptake fractions as low as 1 x 10^{-6} and preferably 1 x 10^{-7} could be measured
- a range of particle types should be included, to cover the range of likely particle dissolution fractions and uptake fractions. This criterion was applied by selecting the most visually diverse set of particles from their electron micrographs.

A full description of the experimental methods and the data analysis methodology is given by Pellow et al (2009). In summary, each particle was dispensed *via* a plastic cannula into the stomach of a rat. Urine and faeces were collected separately. On the fifth day after administration of the particles, the animals were killed and various tissues dissected. The Pu and Am content of all tissue and excreta samples were determined by radiochemical analysis. The particle uptake fraction for each radionuclide was determined by summing the activities in those tissues that contribute to the total systemic uptake (ie, the carcass, liver and pelt) and then adding the activity excreted in urine. This was then divided by the activity of the administered particle, determined by summing the activities measured in all tissues and in urine and faeces. The particle uptake fractions ranged from approximately 10^{-7} to 10^{-5} for ^{238}Pu, 10^{-7} to 10^{-5} for $^{239/240}$Pu and approximately 10^{-8} to 10^{-5} for ^{241}Am.

8.2.2 *In vitro* studies at NPL

A concurrent study was undertaken at NPL on a further eight alpha-rich particles to determine particle dissolution *in vitro* in simulated gut fluids (Cowper, 2009). This study showed particle dissolution fractions for Pu and Am ranging from 0.04 to 0.97, with the dissolution fraction in five of the eight particles exceeding 0.75 and of these, three exceeding 0.9. The corresponding particle uptake fractions may be estimated by multiplying the dissolution fraction by the f_1 value for the element. The choice of f_1 is a matter of scientific judgement; choosing the ICRP default value for unknown compounds of Pu and Am of 5 10^{-4} results in particle uptake fractions of the order of 10^{-4} or greater. Thus, while the *in vivo* study yielded relatively low particle uptake fractions, the particle dissolution fractions measured *in vitro* suggest that particle uptake fractions are significantly higher.

8.2.3 2nd *in vivo/in vitro* study at HPA

To resolve the discrepancy, a second study was carried out at HPA on a further batch of five alpha-rich particles. This included both *in vivo* and *in vitro* work, aiming to:

g determine whether the particles used in the first *in vi vo* study are representative of the solubility of the particles being recovered from Cumbrian beaches, rather than a relatively insoluble subset

h provide more data and a better understanding of the bioavailability and *in vivo* gastrointestinal absorption of Pu and Am from the range of alpha-rich particles that are being recovered

i determine whether the *in vitro* methodology can be validated, by comparing *in vivo* and *in vitro* absorption measurements obtained for the same particle (by undertaking in vitro dissolution measurements at HPA on particles recovered from the faecal material after they had passed through the rats)

The choice of particles for *in vivo* study was limited as only ten particles were available and of these three were unsuitable because they had fragmented. Particle appearance was excluded from the selection criteria (Section 8.2.1) because the first study had shown no discernible link between appearance and GI tract absorption of Pu and Am

(Pellow et al, 2009). For the *in vitro* intercomparison, portions of a particle that had fragmented into a number of pieces were provided to NPL and HPA.

Methods used were similar to those described in Section 8.2.1, except that an additional stage was added to permit the collection of intact particles from faeces. Faeces were collected in 24 hour lots, and at the end of each 24 hour period, the animal and the faeces collected during that period were monitored to determine whether the particle had been eliminated. An attempt was then made to recover the active particle from the faeces. Four out of five particles were successfully recovered.

In vitro dissolution measurements were then performed on the four recovered particles and on the intercomparison sample. The *in vitro* procedure used by HPA and NPL was agreed in advance and was a modified version of that used in the first NPL study (Cowper, 2009). A full description of the *in vitro* methodology is given by Pellow et al (2010).

8.2.4 Activities of particles administered to rats in the two HPA studies

The activities of the particles investigated in the two studies are shown in Table 66. For each particle and radionuclide, the activity was calculated by summing the activity measured in the tissues and excreta, and where necessary the activity contained in samples resulting from the *in vitro* experiment. In the first study, the particle remained in the faeces and so the measured faecal activity included the activity of the excreted particle. For those particles in the second study that were recovered from faeces for further *in vitro* measurements, the activities of the particles were measured separately. Total particle alpha activities ranged from 56 kBq to 1.14 MBq.

Table 66: Total ^{238}Pu, $^{239/240}$Pu and ^{241}Am activity administered to each rat

Sellafield particle reference number (LSN ID)	Activity, Bq (± 2 sigma uncertainty)			Total activity, Bq
	^{238}Pu	$^{239/240}$Pu	^{241}Am	
1st study (Pellow et al, 2009)				
1101226	10600 (1000)	13400 (1200)	32100 (4700)	56100
1102166	9570 (960)	145000 (12000)	94300 (13000)	248870
1121836	116000 (11000)	669000 (64000)	354000 (53000)	1139000
1122564	4510 (1500)	58500 (20000)	70200 (30000)	133210
1122757	4090 (390)	26500 (2600)	25900 (4000)	56490
2nd study (Pellow et al, 2010)				
1137844	7190 (1040)	31100 (3090)	31500 (4600)	69790
1137858	5160 (770)	59400 (6230)	49000 (7770)	113560
1172767	13100 (1520)	77600 (7830)	69500 (10800)	160200
1188608	39800 (4520)	51200 (5620)	104000 (12800)	195000
1195129	31500 (3290)	35400 (3600)	76400 (11700)	143300

For some of the particles, not all of the material was administered to the rat due to break-up of the particle during administration

The measured ^{238}Pu:$^{239/240}$Pu:^{241}Am isotopic ratios are shown in Table 67. The $^{239/240}$Pu:^{241}Am ratio lies in the range 0.4:1 – 2:1 and for a number of particles is close to 1:1. The ^{238}Pu:$^{239/240}$Pu ratio is more broadly distributed in the range 1:1 to 1:16.

Table 67: Ratios of ^{238}Pu, $^{239/240}$Pu and ^{241}Am activity for each particle

Sellafield LSN ID	Isotopic ratio relative to ^{238}Pu		
	^{238}Pu	$^{239/240}$Pu	^{241}Am
1st study			
1101226	1.00	1.26	3.03
1102166	1.00	15.2	9.85
1121836	1.00	5.76	3.05
1122564	1.00	13.0	15.6
1122757	1.00	6.49	6.34
2nd study			
1137844	1.00	4.32	4.39
1137858	1.00	11.5	9.50
1172767	1.00	5.94	5.32
1188608	1.00	1.29	2.61
1195129	1.00	1.12	2.42
1145282B	1.00	1.06	1.84

8.2.5 *In vitro* results from the 2nd HPA study

For each particle, the particle dissolution fraction for each isotope was calculated by dividing the dissolved activity by the activity of the particle used. The results are shown in Figure 8.

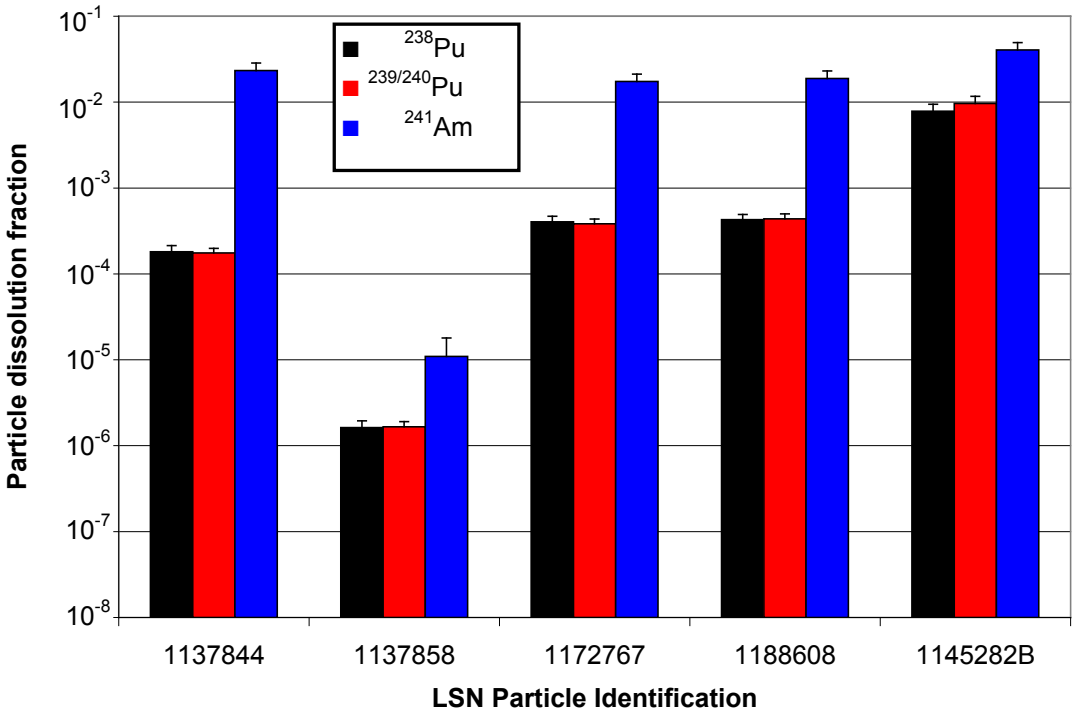

Figure 8: Particle dissolution fraction, F_D^P, for each particle measured *in vitro*. LSN 1145282B is the *in vitro* intercomparison particle

The results show that:

- the F_D^P for ^{238}Pu and $^{239/240}$Pu are very similar for each particle, implying that the Pu isotopes are available in the same chemical form
- the F_D^P for ^{241}Am were greater than those for Pu for each particle
- the F_D^P for ^{alpha}Pu for three of the *in vivo/in vitro* particles are similar (in the approximate range 10^{-4} to 10^{-3}). The dissolution fraction for the remaining *in vivo/in vitro* particle, is approximately 100 fold less (approximately 10^{-6})
- the F_D^P for ^{241}Am for three of the *in vivo/in vitro* particles are similar (between 1 and 4 x 10^{-2}). The remaining *in vivo/in vitro* particle is about 2000 fold less (approximately 10^{-5}).

8.2.6 Comparison of *in vivo* and *in vitro* results from the 2nd HPA study

To allow comparison of the *in vitro* and *in vivo* results, the *in vitro* particle dissolution fractions for ^{238}Pu, $^{239/240}$Pu and ^{241}Am for each particle were converted to a particle uptake fraction by multiplying by an f_1 value of 5 10^{-4}, the ICRP Publication 67 default value for unknown chemical forms of Pu and Am (ICRP, 1993). The comparison is shown in Figure 9.

For ^{241}Am, the *in vitro* results for two particles overestimate the particle uptake fractions determined *in vivo* by a factor of about 50, the fraction is underestimated by a factor of about 30 for one particle, while agreement is reasonable for a fourth particle. For the Pu isotopes, the *in vitro* results underestimate the particle uptake fractions determined *in vivo* by factors of between 2 and 1000. Use of a different default f_1 value would not improve the overall agreement between *in vitro* and *in vivo* results; agreement of the results for some particles would be improved but it would be worse for others.

It should be noted, however, that the four particles in the second study were exposed to the harsh environment of the GI tract before being exposed to the simulated stomach and intestinal fluids. It is possible that the dissolution fractions determined for these particles were not representative of the results that would be obtained if the original particles had been studied *in vitro* only. Therefore this study cannot invalidate the *in vitro* procedure.

8.2.7 *In vivo* results from the 2nd HPA study

Figure 10 shows the *in v ivo* uptake fractions and the fraction range (2 sigma uncertainty) of ^{238}Pu, $^{239/240}$Pu and ^{241}Am for each particle, for all of the ten particles investigated in the two studies (Pellow et al, 2009; 2010). The values are arranged by particle so that the uptake fraction for the different isotopes in each particle can be compared. The five sets of results below the dotted line are from the first study (Pellow et al, 2009) and those above are from the second study (Pellow et al, 2010).

Results from the first and second studies are consistent. Results for all ten particles show that the particle uptake fractions ranged from 1.7 10^{-7} to 1.7 10^{-5} (approximately 10^{-7} to 10^{-5}) for ^{238}Pu, 1.5 10^{-7} to 2.4 10^{-5} (approximately 10^{-7} to 10^{-5}) for $^{239/240}$Pu and 4.0 10^{-8} to 1.8 x 10^{-5} (approximately 10^{-8} to 10^{-5}) for ^{241}Am. The results from the second study showed a slight increase in the maximum value found for ^{238}Pu, $^{239/240}$Pu and ^{241}Am compared with the first study, but did not extend the lower value of the range. For the majority of particles the uptake fractions are in the range 10^{-7} to 10^{-6}, but for two particles (LSN 1102166 and LSN 1188608), the uptake fractions are higher. For LSN 1102166 (from the first study), the particle uptake fractions are approximately 10^{-5}, while for LSN 1188608 (from the second study) they are in the region of 2 10^{-5}. The maximum particle uptake fractions are approximately 1.7 10^{-5} for ^{238}Pu, 2.4 10^{-5} for $^{239/240}$Pu and 1.8 10^{-5} for ^{241}Am.

The uptake fractions for ^{238}Pu, $^{239/240}$Pu and ^{241}Am for all of the particles were low in comparison to the value for fractional absorption (f_1) of 5 10^{-4} recommended by ICRP for unknown compounds of Pu and Am. The reason for this is likely to be that the materials making up the particles are rather insoluble and it is the low particle dissolution fraction for these materials that determines the particle uptake fraction for Pu and Am, which are minor constituents of the particle matrix.

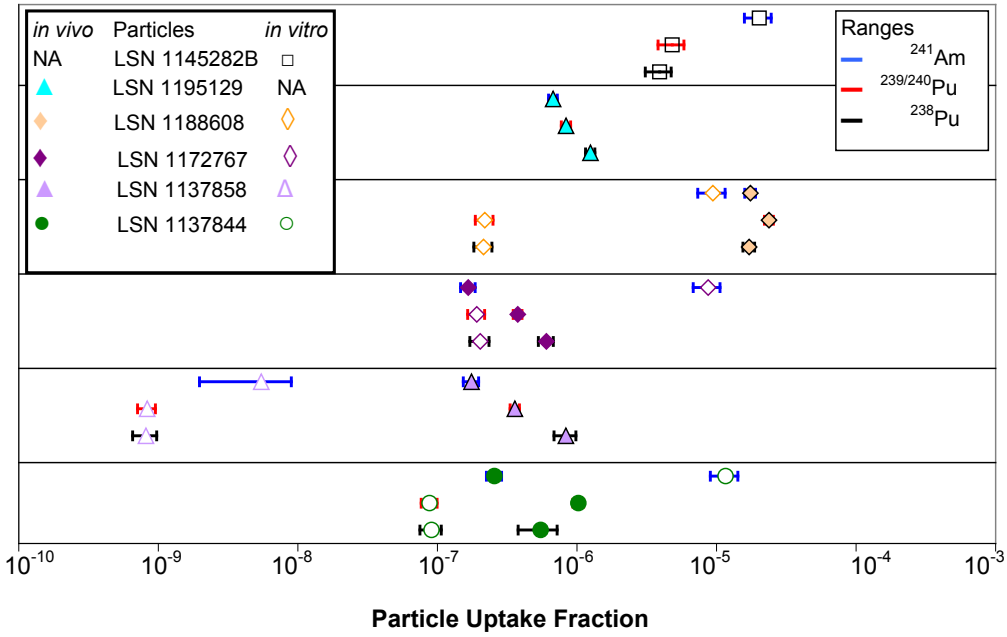

Figure 9: Particle uptake fraction, F_U^P , for each particle either measured *in vivo* or estimated from the *in vitro* results assuming f_1= 5 x 10^{-4}. (NA – data not available). For each particle the upper, middle and lower symbols represent uptake fractions for ^{241}Am, $^{239/240}$Pu and ^{238}Pu, respectively

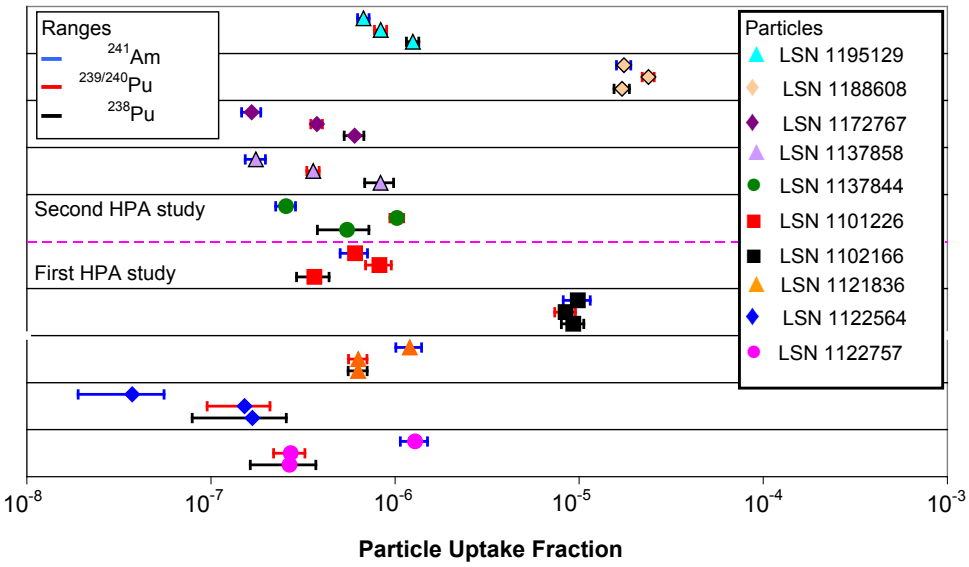

Figure 10: Particle uptake fraction and fraction range (2 sigma uncertainty) for each particle from the first and second *in vivo* studies at HPA. For each particle the upper, middle and lower symbols represent particle uptake fractions for ^{241}Am, $^{239/240}$Pu and ^{238}Pu, respectively

8.3 Dependence of equivalent doses and effective dose on absorption

The relationship between particle uptake fraction, equivalent doses to the colon and bone surfaces, and the committed effective dose per unit intake, e(50), calculated using both the ICRP Publication 30 model of the GI tract (ICRP, 1979) and the ICRP Publication 100 Human Alimentary Tract (HAT) model (ICRP, 2006b) are shown in Table 68 and Table 69, respectively. Equivalent dose to bone surfaces is included in order to give an indication of doses to organs resulting from systemic uptake. Figure 11 shows the dependence of e(50) for ^{239}Pu on particle uptake fraction for the two models.

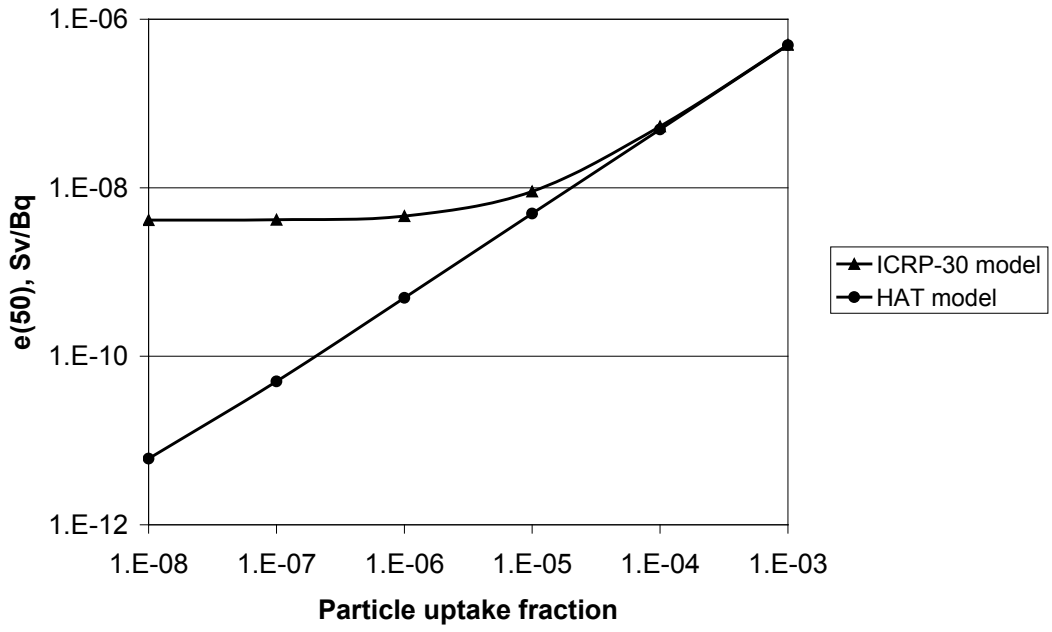

Figure 11: The dependence of e(50) for ^{239}Pu on particle uptake fraction, calculated using the ICRP Publication 30 GI tract model and the ICRP Publication 100 Human Alimentary Tract (HAT) model

In the ICRP Publication 30 model (Figure 11 and Table 68), the dose to the contents of the GI tract is taken as the surrogate dose to the GI tract wall. For very low particle uptake fractions (below $1\ 10^{-7}$), the contribution from systemic organ doses is negligible, GI tract doses dominate and e(50) is almost independent of uptake fraction. For higher particle uptake fractions ($> 1\ 10^{-4}$), the contribution from systemic organ doses dominates and the relationship between e(50) and uptake fraction is almost linear. Between $1\ 10^{-7}$ and $1\ 10^{-4}$, systemic organ doses and GI tract doses both contribute to e(50). It can be seen from Table 68 that for f_1 values $<1\ 10^{-4}$, a 10,000 fold reduction of the f_1 value only decreases the dose coefficient by a factor of about 10.

The dose to the GI tract from alpha irradiation calculated using the HAT model (Figure 11 and Table 69) is negligible because alpha radiation does not penetrate to the radiosensitive cells. The contribution to e(50) from the colon is therefore much lower than that calculated using the ICRP Publication 30 model. As a result the contribution to e(50) from the bone surface increases considerably whilst the value of e(50) calculated using the HAT model is significantly lower than predicted by the ICRP Publication 30 model for uptake fractions less than about $1\ 10^{-5}$. For the HAT model, the linear relationship between uptake fraction and e(50) extends down to $1\ 10^{-6}$ for ^{241}Am and $1\ 10^{-7}$ for ^{238}Pu and $^{239/240}$Pu.

The results calculated using the ICRP Publication 100 HAT model are presented here to illustrate the more realistic treatment of alpha irradiation of the GI Tract by this model. The Publication 100 HAT model is being used to compute new ingestion dose coefficients that will be presented in forthcoming ICRP publications. Until these data are published, it is recommended that the ICRP Publication 30 model should be used for ingestion dose calculations for Sellafield particles. For the uptake fraction at the upper limit of the range found by the *in vivo* studies (ie, $3\ 10^{-5}$), the difference between the dose coefficients predicted by the two models is small, as shown by Figure 11.

8.4 Conclusions of the HPA *in vivo* and *in vitro* studies of ingested alpha-rich particles

The results presented and discussed in Section 8.2.6 show that it has not been possible to validate the *in vitro* method. As discussed by Pellow et al (2010), there is no consistent relationship between the *in vivo* uptake fraction and *in vitro* dissolution fraction determined for the four particles studied using the two techniques. Thus, it is not possible to apply a single correction factor to the *in vitro* dissolution fractions to obtain reliable estimates of uptake fractions. It is therefore recommended that results obtained using the *in vitro* procedure should not be used to determine intestinal absorption of alpha-rich Sellafield particles, and that the results of the *in vivo* studies should be taken as the definitive assessment of intestinal absorption of the ten particles studied.

On the other hand, it cannot be said that the *in vitro* method has been invalidated by the results of the *in vivo* study. For instance, the physico-chemical characteristics of the particles collected from faeces may not have been the same as when they were administered to the rats, since they had been exposed to the harsh environment of the GI tract before being exposed to the simulated stomach and intestinal fluids in the *in vitro* study.

Particles were selected for the first HPA *in vivo* study based on their visual diversity and their suitability for instillation into the GI tract of a rat, with the intention that they would encompass the range of absorption that could be encountered. There is no guarantee that this was achieved. Nevertheless, the fact that the range of particle uptake fractions for the second batch of particles was consistent with the range found for the first batch provides support for the assumption that the results are representative of the population of alpha-rich particle finds.

Table 68: Relationship between dose coefficient and particle uptake fraction for ^{238}Pu, ^{239}Pu and ^{241}Am at values below 1 10^{-3} calculated using the ICRP Publication 30 model of the GI tract (ICRP 1979)

Nuclide	Particle uptake fraction, F_U^P	Dose Coefficient, e(50) (Sv/Bq)	Dose coefficient for F_U^P of 1 x 10^{-3} divided by dose coefficients for lower F_U^P values	Equivalent dose to Bone Surface (Sv/Bq)	% Contribution to dose coefficient from weighted dose to Bone Surface	Equivalent dose to Colon (Sv/Bq)	% Contribution to dose coefficient from weighted dose to Colon
^{241}Am	1 x 10^{-3}	4.03 x 10^{-7}	1.0	1.80 x 10^{-5}	44.8	7.75 x 10^{-8}	2.0
	1 x 10^{-4}	4.45 x 10^{-8}	9.1	1.80 x 10^{-6}	40.6	4.00 x 10^{-8}	10.8
	1 x 10^{-5}	8.59 x 10^{-9}	46.9	1.80 x 10^{-7}	21	3.72 x 10^{-8}	52
	1 x 10^{-6}	5.01 x 10^{-9}	80.4	1.81 x 10^{-8}	3.6	3.69 x 10^{-8}	88.6
	1 x 10^{-7}	4.65 x 10^{-9}	86.7	1.81 x 10^{-9}	0.4	3.69 x 10^{-8}	95.3
	1 x 10^{-8}	4.61 x 10^{-9}	87.4	1.89 x 10^{-10}	0	3.69 x 10^{-8}	96.1
^{239}Pu	1 x 10^{-3}	4.97 x 10^{-7}	1.0	1.64 x 10^{-5}	33.1	6.21 x 10^{-8}	1.5
	1 x 10^{-4}	5.34 x 10^{-8}	9.3	1.64 x 10^{-6}	30.8	3.61 x 10^{-8}	8.1
	1 x 10^{-5}	9.06 x 10^{-9}	54.9	1.64 x 10^{-7}	18.1	3.35 x 10^{-8}	44.3
	1 x 10^{-6}	4.62 x 10^{-9}	107.6	1.64 x 10^{-8}	3.6	3.32 x 10^{-8}	86.2
	1 x 10^{-7}	4.18 x 10^{-9}	118.9	1.64 x 10^{-9}	0.4	3.32 x 10^{-8}	95.3
	1 x 10^{-8}	4.13 x 10^{-9}	120.3	1.65 x 10^{-10}	0	3.32 x 10^{-8}	96.3
^{238}Pu	1 x 10^{-3}	4.52 x 10^{-7}	1.0	1.48 x 10^{-5}	32.7	6.12 x 10^{-8}	1.6
	1 x 10^{-4}	4.91 x 10^{-8}	9.2	1.48 x 10^{-6}	30.1	3.80 x 10^{-8}	9.3
	1 x 10^{-5}	8.88 x 10^{-9}	50.9	1.48 x 10^{-7}	16.6	3.57 x 10^{-8}	48.3
	1 x 10^{-6}	4.86 x 10^{-9}	93.0	1.48 x 10^{-8}	3	3.55 x 10^{-8}	87.6
	1 x 10^{-7}	4.46 x 10^{-9}	101.3	1.48 x 10^{-9}	0.3	3.55 x 10^{-8}	95.5
	1 x 10^{-8}	4.42 x 10^{-9}	102.3	1.48 x 10^{-10}	0	3.55 x 10^{-8}	96.3

Dose are calculated for adults

These dose calculations were performed using the computer program PLEIADES (Program for LinEar Internal Age-dependent DosES) (Fell et al, 2007).

Table 69: Relationship between dose coefficient and particle uptake fraction for ^{238}Pu, ^{239}Pu and ^{241}Am at values below 1 10^{-3} calculated using the ICRP Publication 100 Human Alimentary Tract (HAT) model (ICRP, 2006)

Nuclide	Particle uptake fraction, F_U^P	Dose Coefficient, e(50) (Sv/Bq)	Dose coefficient for F_U^P of 1 x 10^{-3} divided by dose coefficients for lower F_U^P values	Equivalent dose to Bone Surface (Sv/Bq)	% Contribution to dose coefficient from weighted dose to Bone Surface	Equivalent dose to Colon (Sv/Bq)	% Contribution to dose coefficient from weighted dose to Colon
^{241}Am	1 x 10^{-3}	3.99 x 10^{-7}	1	1.81 x 10^{-5}	45.3	3.08 x 10^{-8}	0.9
	1 x 10^{-4}	3.99 x 10^{-8}	10	1.81 x 10^{-6}	45.3	3.25 x 10^{-9}	1.0
	1 x 10^{-5}	4.03 x 10^{-9}	99	1.81 x 10^{-7}	44.9	4.94 x 10^{-10}	1.5
	1 x 10^{-6}	4.36 x 10^{-10}	915	1.81 x 10^{-8}	41.5	2.18 x 10^{-10}	6.0
	1 x 10^{-7}	7.71 x 10^{-11}	5175	1.82 x 10^{-9}	23.5	1.91 x 10^{-10}	29.7
	1 x 10^{-8}	4.12 x 10^{-11}	9684	1.89 x 10^{-10}	4.6	1.88 x 10^{-10}	54.7
^{239}Pu	1 x 10^{-3}	4.93 x 10^{-7}	1	1.65 x 10^{-5}	33.4	2.90 x 10^{-8}	0.7
	1 x 10^{-4}	4.93 x 10^{-8}	10	1.65 x 10^{-6}	33.4	2.91 x 10^{-9}	0.7
	1 x 10^{-5}	4.93 x 10^{-9}	100	1.65 x 10^{-7}	33.4	2.98 x 10^{-10}	0.7
	1 x 10^{-6}	4.94 x 10^{-10}	998	1.65 x 10^{-8}	33.3	3.66 x 10^{-11}	0.9
	1 x 10^{-7}	5.04 x 10^{-11}	9782	1.65 x 10^{-9}	32.7	1.05 x 10^{-11}	2.5
	1 x 10^{-8}	6.09 x 10^{-12}	80952	1.65 x 10^{-10}	27.0	7.89 x 10^{-12}	15.5
^{238}Pu	1 x 10^{-3}	4.47 x 10^{-7}	1	1.48 x 10^{-5}	33.1	2.58 x 10^{-8}	0.7
	1 x 10^{-4}	4.47 x 10^{-8}	10	1.48 x 10^{-6}	33.1	2.60 x 10^{-9}	0.7
	1 x 10^{-5}	4.47 x 10^{-9}	100	1.48 x 10^{-7}	33.1	2.78 x 10^{-10}	0.7
	1 x 10^{-6}	4.50 x 10^{-10}	993	1.48 x 10^{-8}	33.9	4.55 x 10^{-11}	1.2
	1 x 10^{-7}	4.77 x 10^{-11}	9371	1.48 x 10^{-9}	31.0	2.233 x 10^{-11}	5.6
	1 x 10^{-8}	7.47 x 10^{-12}	59839	1.48 x 10^{-10}	19.8	2.00 x 10^{-11}	32.1

Dose are calculated for adults

These dose calculations were performed using the computer program PLEIADES (Program for LinEar Internal Age-dependent DosES) (Fell et al, 2007). Values are provisional

All three isotopes have approximately the same dose coefficients. Therefore the e(50) for an alpha-rich particle containing all three isotopes is largely dependent on the total activity present and only to a small extent on the proportion of each isotope present.

Prior to the experimental work undertaken on the Sellafield particles, HPA advised that a particle uptake fraction of $1\ 10^{-4}$ should be adopted and that this value was sufficiently precautionary (Tandy, 2007). In the report on the first *in vivo* study (Pellow et al, 2009), taking into account the NPL *in vitro* results, it was recommended that a particle uptake fraction of $1\ 10^{-4}$ should be retained for Pu and Am until more *in vivo* data became available. This would provide conservative dose estimates for ingestion of these particles.

Most of the *in vivo* measurements for Pu and Am particle uptake fractions lay in the range $1\ 10^{-7}$ to $1\ 10^{-6}$, with $2.4\ 10^{-5}$ being the highest found out of thirty *in vivo* measurements. It is recommended that a particle uptake fraction corresponding to the largest value measured should be used, rounded up to one significant figure to provide an additional degree of conservatism. Therefore a particle uptake fraction of $3\ 10^{-5}$ is recommended for all ages accept a 3 month old infant. ICRP recommends that for absorption values in the adult of 0.001 or less, an increase by a factor of 10 should be assumed for infants (ICRP, 1996), and so a particle uptake fraction of $3\ 10^{-4}$ is assumed for a 3 month old infant. As a direct result, dose coefficients for a 3 month old infant are about a factor of 20 higher than the adult values.

The corresponding e(50) values derived using both ICRP Publication 30 and HAT models are shown in Table 70, Table 71 and Table 72 for an adult, a 1 year old child and a 3 month old infant, respectively. As can be seen, the values predicted by the two models using the recommended particle uptake fraction are generally quite similar. As explained in Section 8.3, it is recommended that, for the present, the values predicted using the ICRP Publication 30 model should be used for ingestion dose calculations for Sellafield particles.

Table 70: Dose Coefficient, e(50), calculated for ingestion by an adult, for ^{238}Pu, $^{239/240}$Pu and ^{241}Am, using both ICRP 30 and HAT models assuming a particle uptake fraction of $3\ 10^{-5}$

Model	Dose Coefficient, e(50) (Sv Bq^{-1})		
	^{238}Pu	$^{239/240}$Pu	^{241}Am
ICRP 30	$1.8\ 10^{-8}$	$1.9\ 10^{-8}$	$1.7\ 10^{-8}$
HAT	$1.3\ 10^{-8}$	$1.5\ 10^{-8}$	$1.2\ 10^{-8}$

Table 71: Dose Coefficient, e(70), calculated for ingestion by an 1 year old child, for ^{238}Pu, $^{239/240}$Pu and ^{241}Am, using both ICRP 30 and HAT models assuming a particle uptake fraction of $3\ 10^{-5}$

Model	Dose Coefficient, e(70) (Sv Bq^{-1})		
	^{238}Pu	$^{239/240}$Pu	^{241}Am
ICRP 30	$5.5\ 10^{-8}$	$5.4\ 10^{-8}$	$5.4\ 10^{-8}$
HAT	$2.2\ 10^{-8}$	$2.3\ 10^{-8}$	$2.0\ 10^{-8}$

Table 72: Dose Coefficient, e(70), calculated for ingestion by a 3-month old infant, for ^{238}Pu, $^{239/240}$Pu and ^{241}Am, using both ICRP 30 and HAT models assuming a particle uptake fraction of 3 10^{-4}

Model	Dose Coefficient, e(70) (Sv Bq^{-1})		
	^{238}Pu	$^{239/240}$Pu	^{241}Am
ICRP 30	2.9 10^{-7}	3.0 10^{-7}	2.7 10^{-7}
HAT	2.4 10^{-7}	2.5 10^{-7}	2.2 10^{-7}

Object populations of alpha-rich particles and the corresponding probabilities of encounter were estimated within specified ^{241}Am activity bands (Table 17). To obtain an upper estimate of the overall risk to a beach user for each activity band, estimates of committed effective dose have been made for the most active object within each band.

The most active alpha-rich particle recorded in Sellafield Ltd's Beach Monitoring Summary spreadsheet contains 634 kBq ^{241}Am and so is allocated to the 300 – 3000 kBq band, while the particles with the highest ^{241}Am content in the 30 – 300 kBq and 3 – 30 kBq bands contain 200 kBq and 30 kBq ^{241}Am, respectively.

Table 73 summarises the committed effective doses that would result from the ingestion of particles with these activities by a 3-month old infant, a 1 year old child and an adult, using the highest value of e(50) in Table 70 – 40 calculated using the ICRP Publication 30 model (ie, the e(50) value for $^{239/240}$Pu). Ingestion of the most active particle would result in doses of 340 mSv, 62 mSv and 22 mSv for a 3-month old infant, a 1 year old child and an adult, respectively.

Table 73: Activities and committed effective doses for the alpha-rich particles with the highest ^{241}Am content in each activity band

	Particle activity (kBq)				Committed effective dose (Sv)		
^{241}Am activity band (kBq)	^{241}Am	^{238}Pu	$^{239/240}$Pu	Total alpha	3-m old	1-y old	Adult
300 - 3000	634 [a]	84	309	1027	3.1 10^{-1}	5.5 10^{-2}	2.0 10^{-2}
30 – 300	200 [b]	74	49	323	9.7 10^{-2}	1.7 10^{-2}	6.1 10^{-3}
3 – 30	30 [c]	6.0	4.7	40.7	1.2 10^{-2}	2.2 10^{-3}	7.7 10^{-4}

(a) Particle LSN 1121836

(b) Particle LSN 1148999

(c) Particle LSN 1254472

As discussed in Section 6, people with the medical condition called pica can deliberately ingest non-food materials such as sand and possibly large objects. In order to address this, committed effective doses that would result from the ingestion of alpha-rich stones have been calculated. The most active alpha-rich stone found up until August 2009 contains 35.4 kBq ^{241}Am and so is allocated to the 30 – 300 kBq range, while the stone with the highest ^{241}Am content in the in the 3 – 30 kBq range contains 9.3 kBq ^{241}Am.

Table 74 summarises the committed effective doses that would result from the ingestion of these two stones by a 1 year old child and an adult, using the highest value of e(50) in Table 70 – Table 72. Ingestion of the most active stone would result in doses of 4 mSv and 2 mSv for a 1 year old child and an adult, respectively.

Table 74: Activities and committed effective doses for the alpha-rich stones with the highest ^{241}Am content in each activity band[a]

	Particle activity (kBq)				Committed effective dose (Sv)	
^{241}Am activity band (kBq)	^{241}Am	^{238}Pu	$^{239/240}$Pu	Total alpha	1-y old	Adult
300 - 3000	-	-	-	-	-	-
30 – 300	35.4 [b]	8.1[d]	38.3	81.8	$4.4\ 10^{-3}$	$1.6\ 10^{-3}$
3 – 30	9.3 [c]	2.1[c]	9.3 [c]	20.7	$1.1\ 10^{-3}$	$3.9\ 10^{-4}$

(a) Ingestion of stones not considered for a 3 month old infant.

(b) LSN 1133640.

(c) LSN 1144421.

(d) Values estimated using the average Pu:Am isotopic ratios measured for the ten particles studied in vivo at HPA (Pellow et al, 2010).

The lifetime risks of fatal cancer following ingestion of the most active alpha-rich particle in each activity band are shown in Table 75, and for the most active alpha-rich stone in each activity band in Table 76. ICRP Publication 103 (ICRP, 2007) does not present risk coefficients for children, and so specific calculations were carried out for a 3 month old infant, a 1 year old child and a 20 year old adult (Haylock, 2010). The risks are for all cancers, calculated using the ICRP Publication 103 excess relative and additive risk models for all solid cancers and UNSCEAR relative and additive risk models for leukaemia (UNSCEAR, 2006). The calculations take account of protraction of the received dose over the lifetime of the individual, and the increase in age of the individual over the time of the exposure. Both doses and health risks given may be assumed to scale with the activity of the object.

The lifetime risks of radiation-induced fatal cancer that would result from an intake giving rise to a committed effective dose of 1 Sv are estimated to be 16% and 9% for the child and the adult, respectively. The calculations of the lifetime risk of radiation-induced fatal cancer took into account the fact that the dose is received over many years following the intake, as well as the increase in age of the individual over the period that the dose is received. It may be noted that the adult value differs from ICRP's nominal risk coefficient for lethality-adjusted cancer risk for adult workers of 4.1% Sv^{-1} (ICRP, 2007) mainly because ICRP's value is averaged over ages between 18 and 64 and risks decrease with age because of decreasing life expectancy. Uncertainties on these risk coefficients are likely to be large, particularly for infants and children.

Table 75: Lifetime risk of exposure-induced death from all cancers after ingestion of the most active alpha-rich particle in each activity band (Table 73)

Age group	Age at time of intake	^{241}Am activity band (kBq)	Committed effective dose (Sv)	Lifetime risk (%)
3-month old infant	100 days	300 - 3000	3.1×10^{-1}	4%
		30 – 300	9.7×10^{-2}	0.9%
		3 – 30	1.2×10^{-2}	0.2%
1-year old child	1 year	300 - 3000	5.5×10^{-2}	1%
		30 – 300	1.7×10^{-2}	0.3%
		3 – 30	2.2×10^{-3}	0.04%
Adult	20 years	300 - 3000	2.0×10^{-2}	0.2%
		30 – 300	6.1×10^{-3}	0.06%
		3 – 30	7.7×10^{-4}	0.007%

Table 76: Lifetime risk of exposure-induced death from all cancers after ingestion of the most active alpha-rich stone in each activity band (Table 74)

Age group[a]	Age at time of intake	^{241}Am activity band (kBq)	Committed effective dose (Sv)	Lifetime risk (%)
1-year old child	1 year	300 - 3000	-	-
		30 – 300	4.4×10^{-3}	0.07%
		3 – 30	1.1×10^{-3}	0.02%
Adult	20 years	300 - 3000	-	-
		30 – 300	1.6×10^{-3}	0.01%
		3 – 30	3.9×10^{-4}	0.004%

a) Ingestion of stones not considered for a 3 month old infant.

8.5 Inhalation of alpha-rich particles

Inhalability (also referred to as the inhalable fraction or aspiration efficiency) is the fraction of suspended material in ambient air that enters the nose or mouth with the volume of air inhaled. The inhalability of particles as a function of their aerodynamic size is discussed in Appendix G. Briefly, inhalability tends to decrease with increasing aerodynamic particle size at lower wind speeds (up to 4 m s^{-1}) but increases with aerodynamic particle sizes at higher wind speeds (up to 9 m s^{-1}). There is a paucity of data for particles larger than 100 µm aerodynamic diameter, because particle losses are high due to impaction and settling. However, recent studies suggest that, in very low wind speeds, inhalability drops off above about 120 µm aerodynamic diameter and that a cut-off exists at about 140 µm aerodynamic diameter. Unfortunately, comparable data are not available for higher wind speeds, and the inhalability of objects under these conditions remains uncertain. The only information on size of particles found on beaches in the vicinity of the Sellafield site is that provided by the SERCO beach finds characterisation study (Cowper, 2009). Approximate aerodynamic diameters were calculated for the 39 particles (14 alpha-rich and a further 25 beta-rich particles) reported in Cowper (2009) to ascertain if any of these particles could be considered inhalable, ie, were less than 140 µm aerodynamic diameter. For each particle the

geometric diameter was assumed to be the average of the width, depth and height measurements and the value provided for the density for each particle was applied to derive the aerodynamic diameter. Where more than one value for density was given then an averaged value was used, and for "less than" values ('<') the value provided was assumed. An average density of 4 g cm^{-3} was assumed when no value was provided. The calculated aerodynamic diameters for the particles for which information (eg, diameter and density measurements) was available in Cowper (2009) are shown in Table 77 and Table 78. The origin of the measurements used in the calculation is given in the caption for each table.

The data clearly show that all particles reported in Cowper (2009) considerably exceed 140 µm aerodynamic diameter with the aerodynamic diameter of the smallest particle calculated to be 329 µm. It is therefore concluded that the probability that one of the particles investigated in the SERCO study could be inhaled is likely to be small, at least at low wind speeds.

The particles investigated in the SERCO study are, however, only a small sub-set of the particles found (39 out of 447 found up to 29 March 2010) and the question therefore arises as to whether smaller particles could be present. Figure 12 shows that the relationship can be regarded as approximately linear between ^{241}Am particle activity and volume within the size range of 22 alpha-rich particles[3] for which data are available. This implies that the specific activity of the particles is similar, and that the activity is probably uniformly distributed throughout the particle. The figure also shows the relationship between particle activity and volume if this linear relationship extends to lower particle sizes. Parker (2010) has noted that there is a better correlation between activity and volume (correlation coefficient of about 0.85) than between activity and surface area (correlation coefficient in the range 0.4 – 0.7).

[3] These 22 particles were taken from the 14 alpha-rich particles that were provided to SERCO for their particle characterisation study (Cowper, 2009) and a further ten alpha-rich particles that were subsequently provided to SERCO.

Table 77: Mass, volume (estimated from SEM data) and density measurements for separated alpha-rich particles. (Cowper, 2009)

NPL Source number	Sellafield LSN	Mass (µg)	Width/mm	Depth/mm	Height/mm	Estimated Box volume /cm^3	'Box' Density g/cm^3	Estimated Ovoid Volume / cm^3	'Ovoid' Density g/cm^3	Aerodynamic Diameter (µm)
IM08010003	1083114	<50	0.5	0.41	0.31	$6.34\ 10^{-5}$	<0.8	$3.32\ 10^{-5}$	<1.5	436
IM08010003A	1083114	37 ± 16	0.37	0.58	0.85	$1.80\ 10^{-4}$	0.21	$9.44\ 10^{-5}$	0.39	329
IM08010004	1101226	<50	0.54	0.34	0.45	$8.25\ 10^{-5}$	<0.6	$4.32\ 10^{-5}$	<1.2	421
IM08010006	1101809	<50	0.88	0.63	0.41	$2.28\ 10^{-4}$	<0.22	$1.19\ 10^{-4}$	<0.4	356
IM08010010	1102166	<50	0.84	0.58	0.58	$2.82\ 10^{-4}$	<0.18	$1.47\ 10^{-4}$	<0.34	340
IM08010018	1103088	323 ± 4	0.98	0.58	0.55	$3.08\ 10^{-4}$	1.05	$1.61\ 10^{-4}$	2.01	870
IM08010030	1121836	575 ± 16	1.05	1.04	0.65	$5.57\ 10^{-4}$	1.03	$3.72\ 10^{-4}$	1.55	1037
IM08010034	1122429	62 ± 4	0.55	0.41	0.55	$1.23\ 10^{-4}$	0.5	$6.45\ 10^{-5}$	0.96	430
IM08010035	1122564	<50	0.29	0.33	0.21	$1.97\ 10^{-5}$	<2.54	$1.03\ 10^{-5}$	<4.85	532
IM08010036	1122565	<50	0.52	0.37	0.12	$2.30\ 10^{-5}$	<2.2	$1.21\ 10^{-5}$	<4.13	599
IM08010042	1122757	<50	0.55	0.29	0.32	$5.09\ 10^{-5}$	<1	$2.67\ 10^{-5}$	<1.9	466
IM08010048	1128922	<50	0.29	0.25	0.18	$1.32\ 10^{-5}$	<3.8	$6.89\ 10^{-5}$	<7.3	565
IM08010049	1128923	<50	0.35	0.33	0.25	$2.94\ 10^{-5}$	<1.7	$1.54\ 10^{-5}$	<3.3	490
IM08010050	1129241	8991 ± 4	2.68	1.38	2.19	$8.10\ 10^{-3}$	1.11	$4.24\ 10^{-3}$	2.12	2648

Table 78: Particle reference codes and dimensions (Cowper, 2009)

NPL Source number	Sellafield LSN	Width/ mm	Depth/m m	Height A/mm	Height B/mm	Height/ mm	Estimated maximum volume /cm^3	Density (kg/m^3)	Density (g/cm^3)	Aerodynamic diameter (µm)
IM08010001	LSN 1074635	*7.35*	*4.59*	29.35	32.6	*3.25*	$1.10\ 10^{-1}$	4480	4.48	10717
IM08010002	LSN 1074745	*7.46*	*4.45*	35.58	38.17	*2.59*	$8.60\ 10^{-2}$	4050	4.05	9727
IM08010009	LSN 1102165	*3.93*	*3.39*	27.14	28.52	*1.38*	$1.84\ 10^{-2}$	4920	4.92	6433
IM08010014	LSN 1102513	*0.639*	*0.41*	24.04	24.15	*0.11*	$2.88\ 10^{-5}$	6800	6.80	1007
IM08010015	LSN 1103080	*1.08*	*0.579*	20.27	21.43	*1.16*	$7.25\ 10^{-4}$	2300	2.30	1425
IM08010019	LSN 1103090	*5.34*	*3.71*	23.66	25.34	*1.68*	$3.33\ 10^{-2}$	4100	4.10	7242
IM08010020	LSN 1103096	*2.1*	*2.02*	21.92	23.15	*1.23*	$5.22\ 10^{-3}$	2230	2.23	2663
IM08010023	LSN 1103514	*3.84*	*0.1*	23.28	23.52	*0.24*	$9.29\ 10^{-5}$			2787
IM08010024	LSN 1103943	*0.846*	*0.816*	20.18	20.52	*0.34*	$2.35\ 10^{-4}$	2130	2.13	974
IM08010025	LSN 1104080	*0.402*	*0.417*	20.67	20.94	*0.27*	$4.53\ 10^{-5}$	<6400	6.40	918
IM08010026	LSN 1121563	*0.408*	*0.299*	42.37	42.27	*0.1*	$1.22\ 10^{-5}$	21000	21.00	1233
IM08010027	LSN 1121566	*1.1*	*0.822*	24.89	25.68	*0.79*	$7.14\ 10^{-4}$	2090	2.09	1307
IM08010029	LSN 1121806	*2.72*	*2.2*	21.98	22.91	*0.93*	$5.57\ 10^{-3}$	3060	3.06	3411
IM08010032	LSN 1122256	*1.23*	*0.976*	27.04	28.06	*1.02*	$1.22\ 10^{-3}$	1460	1.46	1299
IM08010033	LSN 1122259	*2.49*	*1.6*	25.05	26.16	*1.11*	$4.42\ 10^{-3}$	2390	2.39	2680
IM08010037	LSN 1122566	*0.458*	*0.41*	20.08	20.54	*0.46*	$8.64\ 10^{-5}$			885
IM08010038	LSN 1122744	*4.9*	*4.53*	22.97	25.12	*2.15*	$4.77\ 10^{-2}$	2540	2.54	6152
IM08010039	LSN 1122749	*0.386*	*0.317*	20.05	20.16	*0.11*	$1.35\ 10^{-5}$	<15000	15.00	1050
IM08010040	LSN 1122754	*2.56*	*2.52*	22.77	25.05	*2.28*	$1.47\ 10^{-2}$	2570	2.57	3933
IM08010044	LSN 1125132	*0.496*	*0.296*	21.85	22.28	*0.43*	$6.31\ 10^{-5}$	3720	3.72	786
IM08010045	LSN 1125708	*1.25*	*0.842*	23.82	24.45	*0.63*	$6.63\ 10^{-4}$	1870	1.87	1241
IM08010046	LSN 1125859	*0.233*	*0.159*	19.87	20.24	*0.37*	$1.37\ 10^{-5}$	<14000	14.00	950
IM08010047 A	LSN 1126325	*0.31*	*0.282*	25.09	25.41	*0.32*	$2.80\ 10^{-5}$	1510	1.51	374
IM08010047 B	LSN 1126325	*0.782*	*0.896*	24.42	25.38	*0.96*	$6.73\ 10^{-4}$	1510	1.51	1081
IM08010051	LSN 1129215	*1.94*	*1.13*	19.27	20.05	*0.78*	$1.71\ 10^{-3}$	4370	4.37	2683

Twenty out of 22 of the particles have activities that are above the 95% decision threshold of the Groundhog Evolution 2 beach monitoring system for particles on the surface. (The decision threshold is the minimum activity that, if measured, would indicate that an active particle had been detected. The minimum detectable activity at the 95% confidence level is approximately 37 kBq ^{241}Am for particles on the surface (see Appendix A), and the decision threshold is approximately half this value, ie, 19 kBq.) It is therefore highly likely that the lower limit of the activity range of the particles investigated by SERCO was determined by the detection capabilities of the Groundhog system, and that lower activity particles may well be present although undetected.

If it is assumed that the relationship between particle activity and volume within the range of particle sizes measured is linear, it is probable that these lower activity particles would have smaller physical and aerodynamic diameters. For instance, if the linear relationship shown in Figure 12 does extend below the lowest particle size measured, then particles with aerodynamic diameters of 100, 10, and 1 μm, would have ^{241}Am activities of 3.7 kBq, 3.7 Bq and 3.7 mBq respectively (assuming a density of 3 g cm^{-3}). While particle activities would decrease with particle size, the inhalability of these particles would increase, increasing deposition in the extrathoracic airways (the anterior nose and the posterior nasal passages, larynx, pharynx and mouth). Particles larger than about 30 μm aerodynamic diameter deposit almost exclusively in the extrathoracic region. Particles with aerodynamic diameters less than about 30 μm aerodynamic diameter may deposit in the airways of the lung (ie, the trachea, bronchi and bronchioles), but only particles smaller than 10 μm aerodynamic diameter are likely to reach the alveolar region of the lungs (Figure 13).

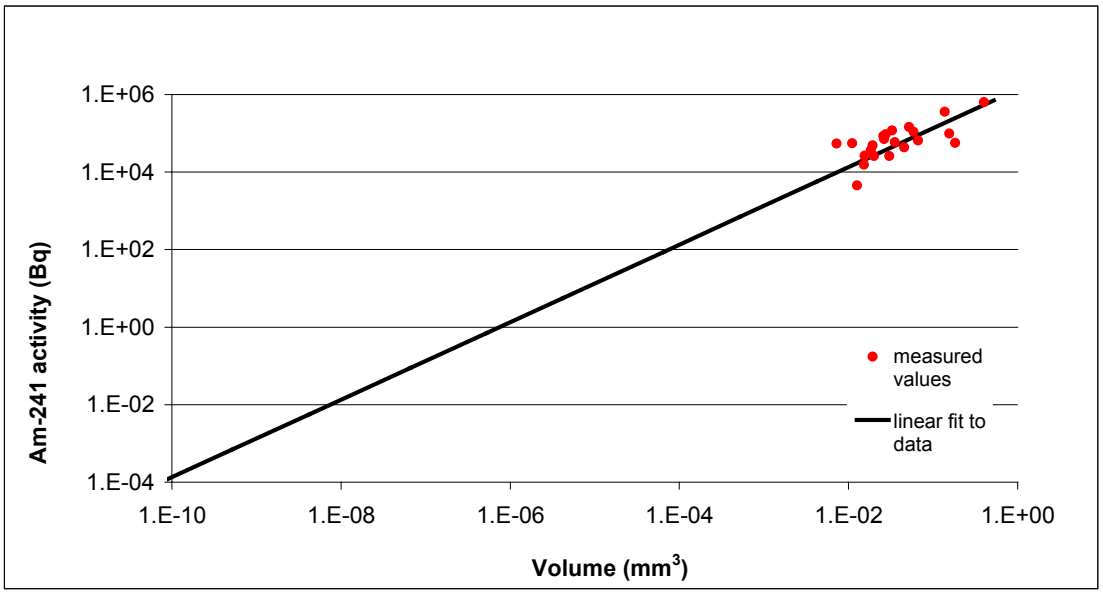

Figure 12: ^{241}Am activities and volumes measured by SERCO (Cowper, 2009) and a linear fit to the data with no intercept. Particles with physical diameters of 1 µm, 10 µm, 100 µm and 1 mm have volumes of 5 10^{-10} mm^3, 5 10^{-7} mm^3, 5 10^{-4} mm^3 and 0.5 mm^3, respectively.

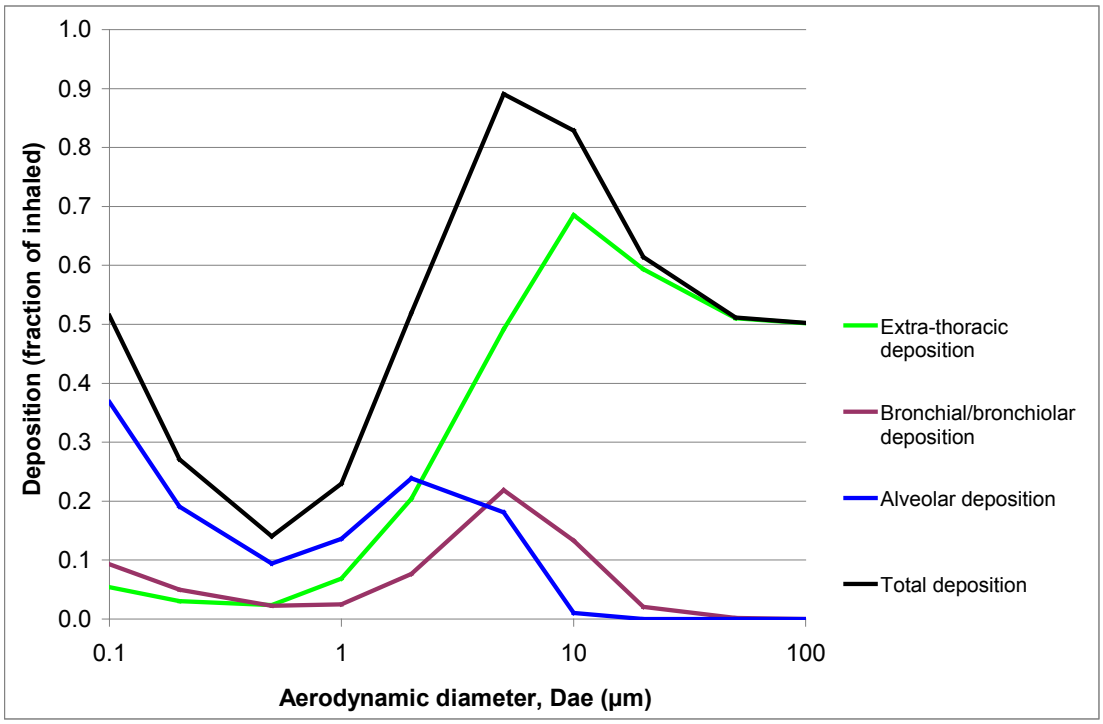

Figure 13: The dependence of deposition of monodisperse inhaled particles in the regions of the respiratory tract on aerodynamic diameter, as predicted by ICRP's Human Respiratory Tract Model (ICRP, 1994). Deposition is expressed as a fraction of the amount present in the volume of ambient air inhaled.

Depending on the balance between decreasing particle activity and increased respiratory tract deposition as particle size decreases, elevated lung and effective doses could result. Figure 14 shows the dependence on particle aerodynamic diameter of the equivalent dose to the extrathoracic region of the respiratory tract, the equivalent dose to the lungs and the effective dose corresponding to a single particle of the specified aerodynamic diameter, for adults. Effective doses for a 3-month old are approximately 2 – 3 times higher. Here it is assumed that the linear relationship between particle activity and volume (Figure 12) extends down to an aerodynamic diameter of 0.1 μm, so that there is a direct relationship between particle aerodynamic diameter and particle activity, with smaller particle diameters corresponding to lower particle activities.

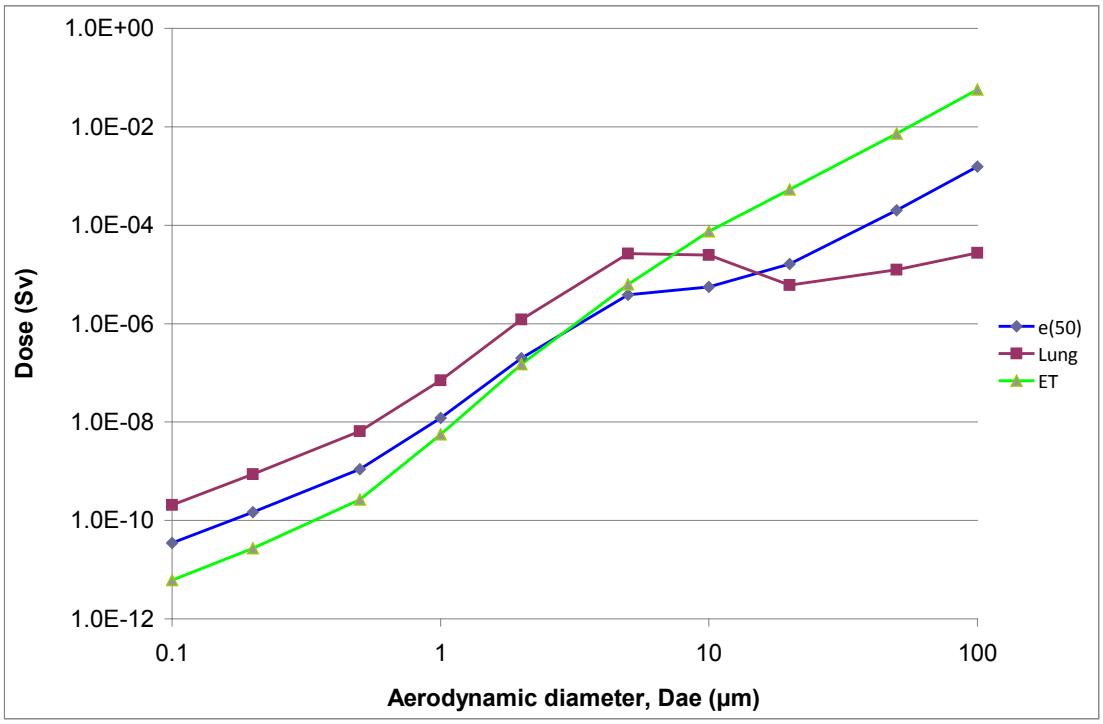

Figure 14: Effective dose and equivalent doses to the lungs and extrathoracic (ET) region, for a population potentially exposed to the inhalation of a single particle of the specified aerodynamic diameter containing ^{241}Am (Type S), as predicted by ICRP's Human Respiratory Tract Model (ICRP, 1994a)

Care needs to be taken in interpreting these results. Deposition fractions of the type shown in Figure 13 are intended to be applied to an aerosol containing a large number of particles; the deposition fraction is the fraction of the number of particles inhaled that are deposited in the specified respiratory tract region. When only a single particle is available for inhalation and subsequent deposition, these deposition fractions must be interpreted as deposition probabilities. Figure 14 presents the results of a prospective dose calculation assuming exposure to a single particle containing Type S ^{241}Am, and gives the average dose for a population potentially exposed to a particle of the specified aerodynamic diameter. (Similar results would be found for particles containing ^{238}Pu and $^{239/240}$Pu). For some members of this population the particle would deposit and a dose would be received, while for others, no deposition would occur and no dose would be received. Doses estimated retrospectively for an individual for whom a particle had

deposited in the respiratory tract would be larger. For instance, if a 100 μm aerodynamic diameter particle had deposited in the extrathoracic (ET) region, the dose to ET would be about twice that shown in Figure 14, because data in that figure takes account of the ET deposition probability of about 50% for such a particle.

Although the effect of increased lung deposition on lung and effective doses for aerodynamic diameters below about 20 μm can be seen, the highest effective dose is found for the largest particle sizes considered. (It should be noted that the Human Respiratory Tract Model does not predict doses for aerodynamic diameters in excess of 100 μm.) For aerodynamic diameters above about 20 μm, the ET dose is the major contributor to effective dose. At 100 μm, the equivalent dose to the ET region is about 60 mSv and the effective dose is approximately 1.5 mSv. The highest lung dose (30 μSv) is found at an aerodynamic diameter of 5 μm.

In conclusion, it may be observed that particles with the higher ^{241}Am activities (greater than about 10 kBq) are likely to have aerodynamic diameters in excess of 200 μm. Such particles are very unlikely to be inhaled in low wind speed conditions. Inhalability at higher wind speeds is uncertain, but any inhaled particles with aerodynamic diameters in excess of a few tens of μm would be deposited in the extra-thoracic airways rather than the lungs. Acute effects associated with high radiation doses to the deep lung (ie, the alveolar-interstitial (AI) region), specifically pneumonitis and fibrosis, are very unlikely to occur, because only particles of aerodynamic diameters less than about 10 μm can travel sufficiently deeply into the respiratory tract to be deposited in the AI region and such particles are unlikely to be active enough to produce the high doses associated with acute lung effects. For particle sizes that are likely to be inhaled, the effective dose resulting from inhalation of a single particle would be no greater than a few mSv, based on currently-available information. Since effective doses arising from inhalation of alpha-rich particles are expected to be low, absorbed doses to organs would also be well below thresholds for deterministic effects, and the probability of such effects arising from inhalation is therefore expected to be extremely low.

8.6 Skin doses and deterministic effects

The University of Birmingham (Dr MW Charles) was sub-contracted by HPA to carry out a study of the likelihood of induction of deterministic effects in the skin, eyes and ears from external exposures resulting from alpha-rich and beta-rich objects in contact with these tissues. This section describes the results of this work with respect to doses arising from contact with alpha-rich objects. Part of the University of Birmingham study involved an evaluation of the direct dose measurements on particles, pebbles and stones carried out by SERCO (Cowper, 2009) as part of their particle characterisation work (described in Section 2.2).

ICRP recommends that skin doses should be averaged over a 1 cm^2 skin area regardless of the area exposed (ICRP, 2007), and that for general radiological protection purposes, the dose should be evaluated at a skin depth of 70 μm (ICRP, 1991a;1991b; 2007). In this report, doses calculated for a skin area of 1 cm^2 at a depth of 70 μm are abbreviated as (1 cm^2, 70 μm).

8.6.1 Calculations and measurements of skin dose rates

The main components of the alpha-rich objects are americium (^{241}Am) and plutonium (^{238}Pu, ^{239}Pu, ^{240}Pu and ^{241}Pu), and the majority of the objects investigated by SERCO are particles with dimensions of about 1 mm (Cowper, 2009).

The three alpha emitters ^{238}Pu, ^{239}Pu and ^{240}Pu have alpha energies predominantly between 5.1 and 5.5 MeV, while ^{241}Am has alpha energies predominantly in the region of 5.5 MeV. The absorbed dose from thin extended plane sources of 5.1 - 5.5 MeV alpha radiation has been calculated as a function of tissue depth using ALDOSE (Turner and Huston, 1991). The results are shown in Figure 15. The equivalent dose can be obtained by applying a radiation weighting factor of 20. Figure 15 shows that the range of alpha particles is up to ~45 µm in tissue. This is less than the nominal depth of 70 µm recommended by ICRP (1991b; 2007), and it is clear from Figure 15 that the skin dose at this nominal depth is zero.

The alpha emitter ^{241}Am, the low energy beta emitter ^{241}Pu, and the alpha-emitting plutonium radionuclides emit very low energy electrons and photons, of which only the photons can contribute to skin dose at a depth of 70 µm or greater. No skin dose rate measurements for alpha-rich particles were reported by SERCO. Skin doses from photon emissions from point and disc sources of these radionuclides were calculated by Monte Carlo methods by Rohloff and Heinzelmann (1996), and values for standard 1 kBq point sources are given in Table 79. The University of Birmingham study applied these factors to estimate the skin dose rate for the particle with the highest ^{241}Am activity investigated in the SERCO study (Cowper, 2009). This particle (IM08010006; LSN 1101809) contained 147kBq ^{238}Pu, 185 kBq $^{239/240}$Pu, 2.8 MBq ^{241}Pu and 371 kBq ^{241}Am. The expected skin dose rate (1 cm^2, 70 µm) from this particle (Table 79) is about 5 mGy h^{-1} and arises predominantly from ^{241}Am 60 keV photons. A similar calculation can be performed for the alpha-rich particle with the highest ^{241}Am activity recorded in Sellafield Ltd's Beach Monitoring Summary spreadsheet. This particle (LSN 1121836) is also the highest activity alpha-rich object recorded by Sellafield Ltd, containing 84 kBq ^{238}Pu, 309 kBq $^{239/240}$Pu, 4.97 MBq ^{241}Pu and 634 kBq ^{241}Am. The expected dose rate (1 cm^2, 70 µm) for this particle is about 8 mGy h^{-1}.

Some alpha-rich particles contain measurable amounts of ^{137}Cs, but in all cases the levels measured are less than a few tens of Bq (Dalton, 2010). Even if the ^{137}Cs:^{90}Sr ratio is pessimistically assumed to be 0.61:1, the contribution to the skin dose rate from this source is negligible.

These dose rates are similar to the average skin dose rate for beta-rich particles measured in the SERCO study (as discussed later in Section 9.1.1). Similar calculations were made using the VARSKIN3 program (Durham, 2006), a semi-empirical code which calculates skin doses for beta/gamma emitters. Calculations were performed for the photon emissions from alpha-rich particles and indicate doses 25-50% higher than those given by Rohloff and Heinzelmann (1996) for these radionuclides. This difference is to be expected since VARSKIN uses specific gamma ray constants to calculate gamma doses and does not account for lack of electronic equilibrium near to point sources. This is a shortcoming which is being addressed in an update of VARSKIN by the US DoE.

The effects of self absorption of 60 keV photons for particles with dimensions of about 1mm and densities of a few g cm^{-3} are negligible.

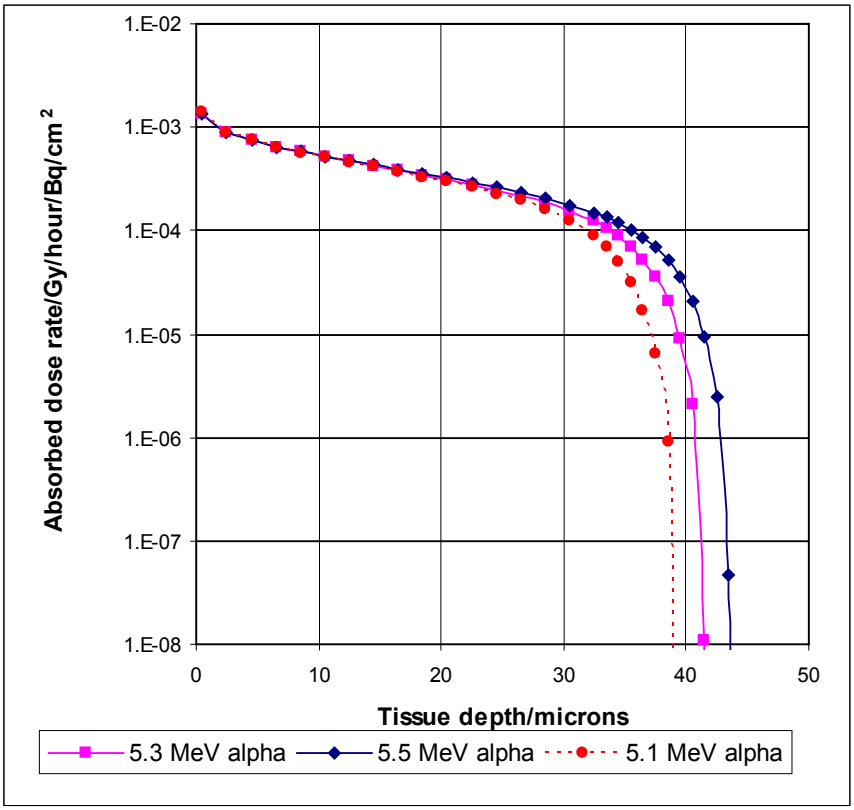

Figure 15: Absorbed dose rate from alpha irradiation as a function of tissue depth

Table 79: Calculated skin dose rates from photons for the major radionuclides in alpha-rich particles

Radionuclide	Skin dose rate over 1 cm^2 at 70 μm for a 1 kBq point source	Components of skin dose rate for the particle in the SERCO study with the highest ^{241}Am activity (IM08010006; LSN 1101809)	
	mGy h^{-1}	kBq (Cowper, 2009)	mGy h^{-1}
^{238}Pu	1.99 10^{-3}	147	0.29
^{239}Pu	7.45 10^{-4}	92.5	0.07
^{240}Pu	1.89 10^{-3}	92.5	0.17
^{241}Pu	1.17 10^{-6}	2800	0.003
^{241}Am	1.20 10^{-2}	371	4.45
Total		3500	4.98

8.6.2 Potential biological effects of alpha-rich Sellafield particles on skin

8.6.2.1 Alpha irradiation of the skin

As noted above, the standard ICRP approach to the calculation of skin dose is to calculate the average dose to the most exposed 1 cm^2 at a depth of 70 μm (ICRP, 1991a; 2007). ICRP refers to a range of epidermal thickness of 20 μm to 100 μm, including the majority of body sites, but uses the nominal average value of 70 μm for general dosimetric purposes, as does the ICRU (1997). However, ICRP (2002) has published reference values for the thickness of epidermis of 45 μm for the newborn, 1-year-old and 5-year-old children, 50 μm for 10-y-old children and 60 μm for 15-y-old children, as well as 70 μm for adults. The question presented is therefore whether skin dose should be calculated at shallower depths for the younger age groups. The assumed depth can be important in the calculation of doses from radionucldies with low energy beta or alpha particle emissions. ICRP has now agreed that doses should continue to be calculated as an average over 1 cm^2 at a depth of 70 μm for all ages (Harriosn, 2011). This is because:

a threshold and ED_{50} values for skin damage are calculated in relation to a depth of 70 μm; different values are obtained for calculations relating to other assumed depths. The conservative ICRP deterministic limit of 500 mSv is for dose calculated at 70 μm, as is the highly conservative value of 50 mSv for members of the public;

b the variations in skin thickness for different regions of the body substantially exceed the differences implied by the reference epidermal thickness values given in ICRP Publication 89 (ICRP, 2002);

c the ICRP Task Group on the biological basis for skin dose limitation considered that for normalising effects of different energy beta particle emissions from radioactive particles, the best measure was an average over 1 cm^2 at a depth of 150 μm (ICRP, 1991b).

On the basis of assessment of dose at a depth of 70 μm, dosimetry assessments for Sellafield objects leads to the conclusion that the alpha-sources found on beaches in the vicinity of the Sellafield site are not of adequate alpha particle energy (and therefore penetrating power) to irradiate the sensitive cells in the skon. They are not therefore expected to give rise to adverse effects on health.

8.6.2.2 Photon irradiation of the skin

In contrast to the Sellafield beta-rich particles, the Sellafield alpha-rich particles have no analogue in the study of health effects due to radioactive contamination at Dounreay (Harrison et al, 2005). Dounreay fuel fragments (DFFs) contain only small amounts of alpha-emitters. The Sellafield alpha-rich particles have little or no ^{137}Cs but contain relatively high levels of ^{241}Am as well as Pu radioisotopes. As explained in Section 8.6.2.1, alpha particles of the energies considered in this report will not deliver dose at a depth of 70 μm in the skin. However, doses due to the 60 keV gamma-ray emission from ^{241}Am do need to be considered. The majority of the objects studied to date are particles with dimensions less than 1 mm, and photon irradiation from such particles would be localised and highly non-uniform.

Although there are extensive data on skin effects following localised beta particle exposures (ICRP, 1991a), there is little information for localised photon sources. The gamma rays from ^{241}Am will irradiate the full depth of the skin but will produce a non-uniform spatial distribution of dose across the skin surface because of the point-source geometry of the exposure, similar to the situation for high energy beta emitters. The basis for limiting skin exposure given by the ICRP (1991a; 2007) should thus be appropriate in this case.

No skin dose measurements have been made for the Sellafield alpha-rich particles but doses should be relatively independent of particle size and density and should be adequately assessed by calculation. Table 79 gives a dose conversion factor (1 cm^2, 70 µm) of 1.2 x 10^{-2} mGy/h/kBq ^{241}Am. Assuming a reasonable residence time for a particle to remain stationary on the skin of 8 h (see Section 5.4), a particle would need to have an ^{241}Am activity of 21 MBq for the 2 Gy threshold dose (1 cm^2, 70 µm) (Section 9.1.4) for localised skin ulceration from small radioactive particles to be reached.

The alpha-rich particle with the highest ^{241}Am activity is recorded in Sellafield Ltd's Beach Monitoring Summary spreadsheet as containing 634 kBq ^{241}Am, 84 kBq ^{238}Pu, 309 kBq $^{239/240}$Pu and 4.97 MBq ^{241}Pu (Dalton, 2010). The expected skin dose rate (1 cm^2, 70 µm) for this particle is approximately 8 mGy h^{-1} (Section 7.6.1). An exposure time of about 250 h would be required to exceed the 2 Gy threshold for skin ulceration, well in excess of any time of exposure that could reasonably be expected. It should be noted that this threshold dose only applies for particles in *stationary* contact, and that if the particle moved by a distance equivalent to its own size, then the threshold value would be significantly higher.

It is worthy of note that the predicted dose rate of 8 mGy h^{-1} for this particle places it well within the DPAG "minor" category (^{137}Cs activity less than 10^5 Bq), which has an upper dose rate threshold of 0.3 Gy h^{-1} (DPAG, 2008). For objects in the DPAG minor category, it was concluded that … "*There would be no discernible health effects even if the (object) was kept in stationary contact with skin*" … for any time of exposure that could reasonably be expected. The DPAG hazard categorisation scheme is discussed in more detail in Section 9.1.4.

8.6.3 Health effects on the skin as a surrogate for other organs/tissues

8.6.3.1 Auditory canal, anterior nasal compartment, ear drum and cornea of eye

The most comprehensive consideration of the possibility of high activity particle damage to skin and other organs is that included in NCRP Report No 130 (NCRP, 1999). While concentrating on the most likely types of hot particle exposures of the skin, the NCRP review also considered possible effects of particle entry into the ear or eye. This has been summarised extensively in the context of the health effects of Dounreay fuel fragments (DFFs) (Harrison et al, 2005). In summary, NCRP concluded that the same limits should apply to the skin lining the auditory canal, the anterior nasal compartment and the ear drum as to other skin regions. They also concluded that the same limit should prevent damage to the cornea of the eye, the site at greatest risk if a particle were to lodge in the eye.

The Sellafield alpha-rich particles require special consideration since they give rise to non-uniform low energy photon exposures predominantly from ^{241}Am. As an illustration, Figure 16 gives calculated depth doses for point sources of ^{241}Am in comparison with point sources of (^{137}Cs/^{137m}Ba : ^{90}Sr/^{90}Y = 1:1), indicating that for equal activities the doses from ^{241}Am point sources (averaged over 1cm^2 or 1mm^2) are significantly less than for (^{137}Cs/^{137m}Ba + ^{90}Sr/^{90}Y) point sources. Thus, alpha-rich particles should give rise to significantly lower doses and risks per unit activity than DFFs. In the first instance, if alpha-rich particles are assessed on the basis that the ^{241}Am activity is actually ^{137}Cs/^{137m}Ba, an assessment of their health effects will be pessimistic.

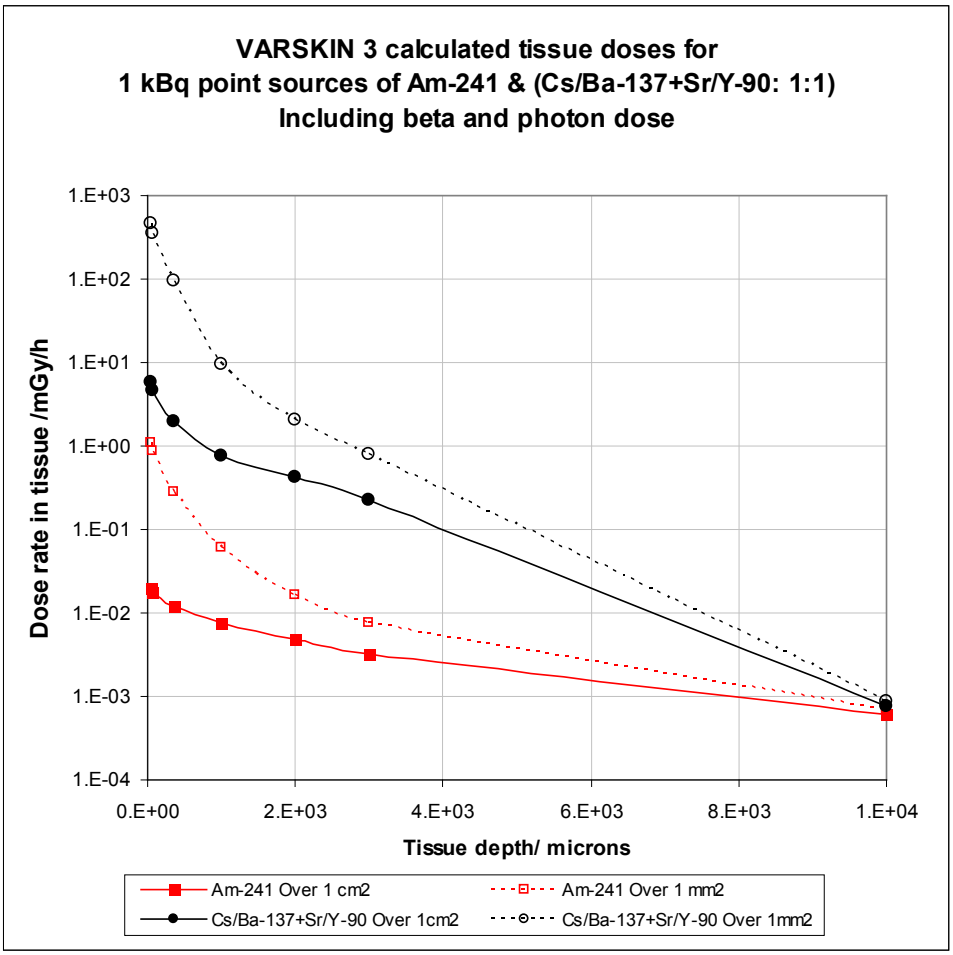

Figure 16: VARSKIN3 (Durham, 2006) calculations of depth doses for 1 kBq point sources of (^{137}Cs/^{137m}Ba : ^{90}Sr/^{90}Y = 1:1) and ^{241}Am (beta and photon doses included). Doses are calculated as averages over 1 cm^2 and 1 mm^2

8.6.3.2 Eye lens

The eye lens lies at a depth of at least 2 mm from the eye surface. In the consideration of cataract induction by Dounreay fuel fragments it was argued that the dose to the lens

due to beta radiation from fragments from the Materials Test Reactor (MTR) on the cornea would be significantly reduced by absorption in the anterior chamber of the eye. Since the mean dose to the equatorial cells of the lens is considered to be the appropriate measure of dose-related cataract induction the distance from a particle on any position of the cornea is likely to be on average several mm, in some cases more than 1 cm. The reduction in beta dose with depth from particles containing $^{137}Cs/^{137m}Ba$ and $^{90}Sr/^{90}Y$ is thus significant. Depth doses calculated using VARSKIN3 (Durham, 2006) and shown in Figure 16 indicate that for the same activity values the dose at any depth is less for small particles of ^{241}Am than for $^{137}Cs/^{137m}Ba$ + $^{90}Sr/^{90}Y$. Small alpha-rich particles should thus present a lower risk of cataract induction from a given level of activity of ^{241}Am due to photon exposure than from the same level of activity of $^{137}Cs/^{137m}Ba$ + $^{90}Sr/^{90}Y$ for Dounreay fuel fragments. In the first instance, if alpha-rich particles are assessed on the basis that the ^{241}Am activity is actually $^{137}Cs/^{137m}Ba$, an assessment of their health effects will be pessimistic.

8.7 Skin doses and stochastic effects

The risk of stochastic effects resulting from localised irradiation of the skin by the 60 keV gamma-ray emission from ^{241}Am needs to be considered. ICRP (1991a) relates the risk of skin cancer to the average dose to the total area of skin, 1.9 m^2 in adult man and 0.48 m^2 for a one year old child (ICRP, 2002). No value is presented for a 3 month old infant, so the value for a new-born infant (0.24 m^2) is taken to apply. A number of animal studies, mainly using skin exposures of mice and rats, have evaluated the carcinogenic risk of hot particles in comparison with spatially uniform radiation exposures. For the same average dose there is little evidence, within a factor of ± 3, of any dependence of cancer risk on spatial dose distribution (Charles et al, 2005). The overall finding is that the use of mean dose to predict carcinogenic risks, as advocated by the ICRP, is appropriate for hot particle exposures.

The threshold dose (1 cm^2, 70 μm) for observable skin ulceration from small radioactive particles is approximately 2 Gy (Section 9.1.4) for particles remaining in stationary contact. A dose of 2 Gy to 1 cm^2 of skin corresponds to an equivalent dose to the skin of 0.1 mSv in adults, 0.4 mSv in one year old children and 0.8 mSv in 3 month old infants. The effective dose is then the equivalent dose to skin multiplied by the tissue weighting factor, w_T, for the skin of 0.01: that is, 1 μSv for adults 4 μSv for one year old children and 8 μSv in 3 month old infants. There will be an additional contribution to the effective dose from objects located at the body surface due to a small whole body exposure from the gamma emissions of ^{241}Am, as described in Section 9.2. This additional contribution has been evaluated for ^{137}Cs (Walters et al, 1999) and the additional contribution to effective dose is expected to be less for ^{241}Am because of the lower yield and lower energy of its 60 keV gamma ray emission. Thus, the additional whole body exposure contribution to effective dose for ^{241}Am will be no greater than that for ^{137}Cs, which increases the estimated effective doses corresponding to 2 Gy to 1 cm^2 of skin to maximum values of about 4 μSv in adults, about 25 μSv in one year old children and no greater than 100 μSv in 3 month old infants.

As discussed in Section 9.1, none of the objects found up till August 2009 result in skin doses that approach the threshold for localised skin ulceration, and so it is clear that stochastic risks for resulting from alpha-rich particles in contact with the skin are negligible.

8.8 Summary of results for doses and risks to health from alpha-rich objects

8.8.1 Ingestion of alpha-rich particles: Stochastic risk

In vivo experimental studies of the intestinal absorption of alpha-rich particles have resulted in a recommendation that a particle uptake fraction of $3\ 10^{-5}$ should be used in calculations of effective dose and equivalent doses to organs, for both Pu and Am. This recommendation should result in conservative estimates of doses. The dose coefficients (ie, committed effective dose per unit intake) for adults, 1-y old children and 3-month old infants determined using this particle uptake fraction are $1.9\ 10^{-8}$ $SvBq^{-1}$, $5.4\ 10^{-8}$ $SvBq^{-1}$ and $3.0\ 10^{-7}$ $SvBq^{-1}$, respectively. These dose coefficients are almost independent of Pu:Am ratios for the main alpha-emitting radionuclides present (^{238}Pu, $^{239/240}Pu$, or ^{241}Am)

The highest activity alpha-rich particle found up until August 2009 is recorded in Sellafield Ltd's Beach Monitoring Summary spreadsheet as containing 84 kBq ^{238}Pu, 309 kBq $^{239/240}Pu$ and 634 kBq ^{241}Am, with a total activity of these radionuclides of 1.03 MBq. In the unlikely event that an alpha-rich particle with this activity was ingested, the committed effective dose would be 20 mSv for an adult, 55 mSv for a 1-y old child, and 310 mSv for a 3-month old infant. The corresponding lifetime risk of exposure-induced death from all cancers is estimated to be 0.2% for an adult, 0.9% for a 1-y old child and 4% for a 3-month old infant. Uncertainties on these risk estimates are likely to be large, particularly for infants and children.

8.8.2 Ingestion of alpha-rich particles: Likelihood of deterministic effects

Deterministic effects would not be expected to occur unless absorbed doses to the gastro-intestinal tract, lungs and red bone marrow approach very high values, in excess of threshold values for acute exposure of 23 Gy, 5.5 Gy and 2.2 Gy, respectively. Effective doses and equivalent doses to the gastrointestinal tract, lungs and other organs of the body have been calculated or estimated (Section 8.3); the results indicate that absorbed doses to organs arising from ingestion of an alpha-rich particle with the highest activity found are orders of magnitude less than these thresholds.

8.8.3 Inhalation of alpha-rich particles: Stochastic risk and deterministic effects

Particles with the higher ^{241}Am activities (greater than about 10 kBq) are likely to have aerodynamic diameters in excess of 200 μm. Such particles are very unlikely to be inhaled in low wind speed conditions. Inhalability at higher wind speeds is uncertain, but any inhaled particles with aerodynamic diameters in excess of a few tens of μm would be deposited in the extra-thoracic airways rather than the lungs. Acute effects

associated with high radiation doses to the deep lung (ie, the alveolar-interstitial (AI) region), specifically pneumonitis and fibrosis, are very unlikely to occur, because only particles of aerodynamic diameters less than about 10 μm can travel sufficiently deeply into the respiratory tract to be deposited in the AI region and such particles are unlikely to be active enough to produce the high doses associated with acute lung effects. For particle sizes that are likely to be inhaled, the effective dose resulting from inhalation of a single particle would be no greater than a few mSv, based on currently-available information. Since effective doses arising from inhalation of alpha-rich particles are expected to be low, absorbed doses to organs would also be well below thresholds for deterministic effects, and the probability of such effects arising from inhalation is therefore expected to be extremely low.

8.8.4 Skin doses from alpha-rich particles: deterministic effects

For alpha-rich particles, the main component of the absorbed dose to the skin arises from gamma irradiation by the 60 keV photon emission from ^{241}Am. The alpha-rich particle with the highest ^{241}Am activity is recorded in Sellafield Ltd's Beach Monitoring Summary spreadsheet as containing 634 kBq ^{241}Am, 84 kBq ^{238}Pu, 309 kBq $^{239/240}$Pu and 4.97 MBq ^{241}Pu (Dalton, 2010). The expected skin dose rate (1 cm^2, 70 μm) from this particle is approximately 8 mGy h^{-1}.

The (1 cm^2, 70 μm) threshold dose for localised skin ulceration from small radioactive particles in stationary contact with the skin is about 2 Gy, and so for a particle with these activities the exposure time required to exceed this threshold would be about 250 hours. It is extremely unlikely that particles could remain in contact with the skin for times as long this.

8.8.5 Skin doses from alpha-rich particles: stochastic effects

A (1 cm^2, 70 μm) skin dose of 2 Gy resulting from the presence of an alpha-rich particle on the skin would correspond to maximum values of effective dose of about 4 μSv in adults, about 25 μSv in one year old children and no greater than 100 μSv in 3 month old infants. Since none of the objects found result in skin doses that approach the 2 Gy threshold for localised skin ulceration, it is clear that stochastic risks resulting from alpha-rich particles in contact with the skin are negligible.

9 DOSES AND RISKS TO HEALTH ARISING FROM EXPOSURES TO BETA-RICH OBJECTS

This Section describes the assessments of radiation doses that have been carried out to determine risks to health in the unlikely event that an individual encounters a beta-rich object in the vicinity of the Sellafield site. The highest activity content of each object type has been used in order to estimate the maximum doses that could result from exposure to beta-rich objects and the highest risks to health if a beta-rich object is encountered. The potential for deterministic effects in tissues is the most important

issue when considering risks arising from exposure to beta-rich objects, because direct irradiation could result in high localised doses to tissues if activities are high enough. The University of Birmingham (Dr M W Charles) was sub-contracted by HPA to carry out a study of the likelihood of induction of deterministic effects in the skin, eyes and ears from external exposures resulting from alpha-rich and beta-rich objects in contact with these tissues. Section 8.6 described the results of this work with respect to doses arising from contact with alpha-rich objects. This section describes the results of the University of Birmingham work with respect to doses arising from contact with beta-rich objects, and for convenience also includes the results for ^{60}Co-rich objects.

In addition, this Section describes the results of work carried out at HPA-CRCE to investigate the likelihood of induction of deterministic effects in the gastro-intestinal (GI) tract resulting from ingestion of beta-rich objects. Although of lesser concern, the probability of stochastic effects resulting from irradiation of the skin by beta-rich objects in contact with the skin, and from ingestion of beta-rich objects and subsequent uptake to the body, are also addressed. Lastly, stochastic risks and the potential for deterministic effects resulting from inhalation of beta-rich particles are considered.

It may be noted that absorbed doses, equivalent doses and effective doses per unit activity are higher for an object containing only ^{90}Sr as compared to a similar object containing only ^{137}Cs, mainly because of the high energy beta emissions from the ^{90}Y daughter. Thus, for particles with similar activities, those with lower ^{137}Cs/^{90}Sr ratios are associated with higher absorbed dose rates to the skin, higher absorbed doses to the gastro-intestinal tract, higher equivalent doses resulting from ingestion or inhalation and higher effective doses.

9.1 Skin doses and deterministic effects

As part of their particle characterisation work (described in Section 2.2, SERCO carried out direct dose rate measurements on a small selection of the beta-rich particles and stones that have been retrieved from beaches as part of the monitoring programme between November 2006 and August 2009, using a SmartIon (ion chamber) dose rate meter and TLD (thermo-luminescence dosimetry) dosemeters provided by the HPA dosimetry service (Gilvin et al, 2007).

Sellafield Ltd also commissioned AMEC Nuclear UK Ltd (AMEC) to characterise a small selection of radioactive particles found on Cumbrian beaches in the vicinity of the Sellafield plant (Delaney et al, 2009). AMEC carried out radiological assessments for 19 beta-rich particles, using particle characterisation data provided by SERCO, to calculate the skin equivalent doses and the effective doses potentially arising from contact, ingestion and inhalation. For the calculations of dose rates to the skin, the data used consisted of SERCO's results from high-resolution gamma spectrometry measurements of ^{137}Cs and ^{60}Co particle content, analytical measurements of ^{90}Sr/^{90}Y particle content, and data on particle compositions, densities and diameters. Calculations were performed for skin depths of 40, 70 and 350 μm, showing the sensitivity of the calculated dose rates to the assumed depth of the sensitive tissues.

Calculations of skin dose rates arising from contact with stones were made as part of the University of Birmingham study. These calculations made use of SERCO's radionuclide measurements on leachates (Cowper, 2009) obtained by dissolving the surface layer of the stones (80 – 160 μm thick). The radionuclide content of these leachates was predominantly ^{137}Cs, and the ^{137}Cs content of the stones was largely removed (typically, 99% removal). Measurements of ^{137}Cs content were performed using high resolution gamma spectrometry, and ^{90}Sr/^{90}Y contents were measured by radiochemical analysis.

9.1.1 Review of the results of the AMEC and SERCO studies

The University of Birmingham study reviewed the AMEC and SERCO assessments of skin dose rates.

9.1.1.1 Beta-rich particles

Table 80 compares the skin dose rates for beta-rich particles measured by SERCO with the (1 cm^2, 70 μm) skin dose rates calculated by AMEC.

Measurements made with the SmartIon ion chamber dose rate meter must be multiplied by a correction factor to provide an estimate of the dose rate averaged over a 1 cm^2 area of skin. For the data presented in Table 80, SERCO used a SmartIon correction factor of 95 to provide an estimate of the (1 cm^2, 70 μm) skin dose rate. A correction factor also has to be applied to the TLD measurements. All of the beta-rich particles have sizes that are less than the TLD area (0.18 cm^2) and most of the beta-dose that would be deposited in the skin from a particle on the skin surface is deposited within the TLD area. The average dose over 1 cm^2 is therefore determined by multiplying the dose recorded on the TLD by a TLD correction factor of 0.18.

The skin dose rates calculated by AMEC and presented in Table 80 are derived from tabulated doses calculated using the VARSKIN3 program (Durham, 2006). Calculations were performed for spherical particles with densities of 1.6, 3.1 and 4.6 g cm^{-3} and particle diameters in the range 100 μm – 5 mm, for uniformly-distributed ^{137}Cs/^{137m}Ba and ^{90}Sr/^{90}Y[a]. Where necessary, skin dose rates for gamma and X-ray emitters were calculated using tabulations of Monte Carlo calculations (Rohloff and Heinzelmann, 1996). Dose rates for specific particle sizes/densities were evaluated by interpolation of the data in these tabulations.

Table 80 shows that the calculated skin dose rate values are a factor of about 3 and 4 times smaller than the corrected TLD and corrected SmartIon measurements, respectively, when averaged over the particles investigated. Dose rates measured using the SmartIon are generally greater than those measured using TLD. Averaged over the particles investigated, the SmartIon measurements are in reasonable agreement with the TLD measurements (TLD / SmartIon = 0.74), although individual values of the ratio

[a] Unless otherwise stated, subsequent references to ^{137}Cs may be taken to include its ^{137m}Ba daughter, and references to ^{90}Sr may be taken to include its ^{90}Y daughter, with both daughter radionuclides assumed to be in secular equilibrium with the parent.

vary widely, with values for three particles below less than 5% of the mean value. The highest measured (1 cm^2, 70 µm) dose rate in the SERCO study is 26.5 mGy h^{-1}, measured by TLD, while the largest calculated (1 cm^2, 70 µm) dose rate value in the AMEC study is 29.7 mGy h^{-1}. The latter value was calculated for a particle that weighed 540 µg, had a volume of 0.24 mm^3, contained 32.4 kBq ^{137}Cs and 48.9 kBq ^{90}Sr, and when dissolved was found to contain a piece of irradiated graphite (Cowper, 2009). It is noteworthy that this beta-rich particle had a $^{137}Cs/^{90}Sr$ ratio of about 0.66:1, close to the lowest value found (0.61:1). In comparison, the highest dose rate for a beta-rich particle dominated by ^{137}Cs was about 12 mGy h^{-1}, measured by TLD. This particle had a $^{137}Cs/^{90}Sr$ ratio of about 2.45. It has been generally found that the particles giving the higher dose rates have lower $^{137}Cs/^{90}Sr$ ratios, and this is to be expected since the contribution to the calculated dose rate per unit activity from ^{90}Sr is about 8 times higher than that from ^{137}Cs for the particles investigated by AMEC.

Table 81 presents dose rates calculated by AMEC for skin depths of 40 µm, 70 µm and 350 µm. Skin dose rates from beta-rich particles are not strongly dependent on skin depth; the dose rates calculated for a skin depth of 40 µm are about 16% higher that the 70 µm dose rates, while the 350 µm dose rates are about 55% lower.

Figure 17 shows SmartIon and TLD (1 cm^2, 70 µm) dose rate measurements plotted as a function of ^{137}Cs content, differentiating between particles with high and low ^{137}Cs:^{90}Sr ratios in order to show the relative contribution to dose rate from $^{90}Sr/^{90}Y$. These data are compared with the results of theoretical calculations for point sources and spherical particles containing either pure ^{137}Cs or mixed ^{137}Cs and ^{90}Sr. To illustrate the effect of the presence of ^{90}Sr in a particle, an activity ratio (^{137}Cs:^{90}Sr) of 1:1 was used. Calculations for point sources are appropriate to small sources where self absorption is small and effects of particle shape and density are not important. These calculations are broadly predictive of dose rates from the beta-rich particles with lower mass, lower activity and some $^{90}Sr/^{90}Y$ content. It may be noted that the beta-rich particles with high $^{90}Sr/^{90}Y$ contents are all small, with masses less than 0.4 mg. For the larger spherical particles, calculations show that self absorption results in a significant reduction in dose rate.

Table 80: Comparison of SERCO measured and AMEC calculated skin dose rates for beta-rich particles

NPL Source number	Sellafield LSN	SmartIon[(a)] skin dose rate /mSv h^{-1}	TLD x 0.18 skin dose rate /mSv h^{-1}	AMEC calculated skin dose rate (1cm^2, 70 μm) /mSv h^{-1}	SmartIon measured/AMEC calculated skin dose rate	TLD x 0.18 measured/ AMEC calculated skin dose rate	Cs-137/Bq
IM08010001	1074635	1.51	0.81	0.29	5.2	2.8	7690 ± 320
IM08010002	1074745	6.72	2.47	1.39	4.8	1.8	42100 ± 3200
IM08010009	1102165	0.88	0.31	0.37	2.4	0.8	11200 ± 2300
IM08010014	1102513	5.28	0.23	2.14	2.5	0.1	11800 ± 500
IM08010015	1103080	3.34	5.54	2.63	1.3	2.1	10400 ± 500
IM08010019	1103090	8.06	5.04	2.04	4.0	2.5	61900 ± 3300
IM08010020	1103096	11.30	5.92	1.87	6.0	3.2	43400 ± 2100
IM08010023*	1103514	1.53	2.00				72 ± 4
IM08010024	1103943	6.93	10.12	0.36	19	28	13800 ± 700
IM08010025	1104080	9.58	1.82	4.83	2.0	0.4	17300 ± 900
IM08010026	1121563	4.89	0.07				8400 ± 1900
IM08010027	1121566	6.64	0.90	1.95	3.4	0.5	4930 ± 210
IM08010029	1121806	0.82	0.40				3760 ± 820
IM08010032	1122256	17.65	26.53	13.1	1.3	2.0	10700 ± 500
IM08010033	1122259	7.10	1.32	1.35	5.3	1.0	31400 ± 1500
IM08010037	1122566	13.44	8.35	(b)			8400 ± 1700
IM08010038	1122744	0.77	0.44	0.19	4.1	2.3	7400 ± 320
IM08010039	1122749	7.74	0.22				4290 ± 190
IM08010040	1122754	0.53	0.43	0.12	4.4	3.6	2760 ± 130
IM08010044	1125132	5.87	4.45				5000 ± 1100
IM08010045	1125708	12.07	2.99	10.7	1.1	0.3	11000 ± 500
IM08010046	1125859	4.69	12.47	3.98	1.2	3.1	5900 ± 1300
IM08010047/48[(c)]	1126325	11.78	23.04	10.5	1.1	2.2	8100 ± 330
IM08010051#				29.7			32400 ± 1500
* Primarily Co-60				Average ratio	4.1	3.3	

(a) SmartIon measurements have been multiplied by a factor of 95

(b) density & size not provided

(c) ID numbers IM08010047 and IM08010048 used in AMEC and SERCO reports refer to the same sample.

Table 81: Skin dose rates calculated by AMEC for various skin depths for beta-rich particles. Based on Table 7 and Annex F of AMEC report (Delaney et al, 2009)

Particle[a]	Total skin dose rate (mGy h^{-1})		
	Skin thickness (µm)		
	40	70	350
IM08010001	$3.22\ 10^{-1}$	$2.86\ 10^{-1}$	$1.32\ 10^{-1}$
IM08010002	$1.57\ 10^{0}$	$1.39\ 10^{0}$	$5.87\ 10^{-1}$
IM08010009	$4.18\ 10^{-1}$	$3.69\ 10^{-1}$	$1.56\ 10^{-1}$
IM08010014	$2.75\ 10^{0}$	$2.14\ 10^{0}$	$5.41\ 10^{-1}$
IM08010015	$3.38\ 10^{0}$	$2.63\ 10^{0}$	$6.51\ 10^{-1}$
IM08010019	$2.31\ 10^{0}$	$2.04\ 10^{0}$	$8.64\ 10^{-1}$
IM08010020	$2.13\ 10^{0}$	$1.87\ 10^{0}$	$7.34\ 10^{-1}$
IM08010024	$3.97\ 10^{-1}$	$3.57\ 10^{-1}$	$1.73\ 10^{-1}$
IM08010025	$6.24\ 10^{0}$	$4.83\ 10^{0}$	$1.19\ 10^{0}$
IM08010027	$2.22\ 10^{0}$	$1.95\ 10^{0}$	$1.01\ 10^{0}$
IM08010032	$1.48\ 10^{1}$	$1.31\ 10^{1}$	$7.03\ 10^{0}$
IM08010033	$1.54\ 10^{0}$	$1.35\ 10^{0}$	$5.31\ 10^{-1}$
IM08010037 [b]			
IM08010038	$2.13\ 10^{-1}$	$1.92\ 10^{-1}$	$9.27\ 10^{-2}$
IM08010040	$1.35\ 10^{-1}$	$1.19\ 10^{-1}$	$4.67\ 10^{-2}$
IM08010045	$1.19\ 10^{1}$	$1.07\ 10^{1}$	$6.34\ 10^{0}$
IM08010046 [c]	$4.82\ 10^{0}$	$3.98\ 10^{0}$	$1.61\ 10^{0}$
IM08010048 [a]	$1.19\ 10^{1}$	$1.05\ 10^{1}$	$5.67\ 10^{0}$
IM08010051	$3.27\ 10^{1}$	$2.97\ 10^{1}$	$1.82\ 10^{1}$

(a) Due to an error in SERCO data tables, particle No 48 is also listed as No 47. Sellafield ID number matches for particle 47 & 48 so in all cases the particle is referred to as particle No 48.

(b) Density & size not provided

(c) density considered questionable

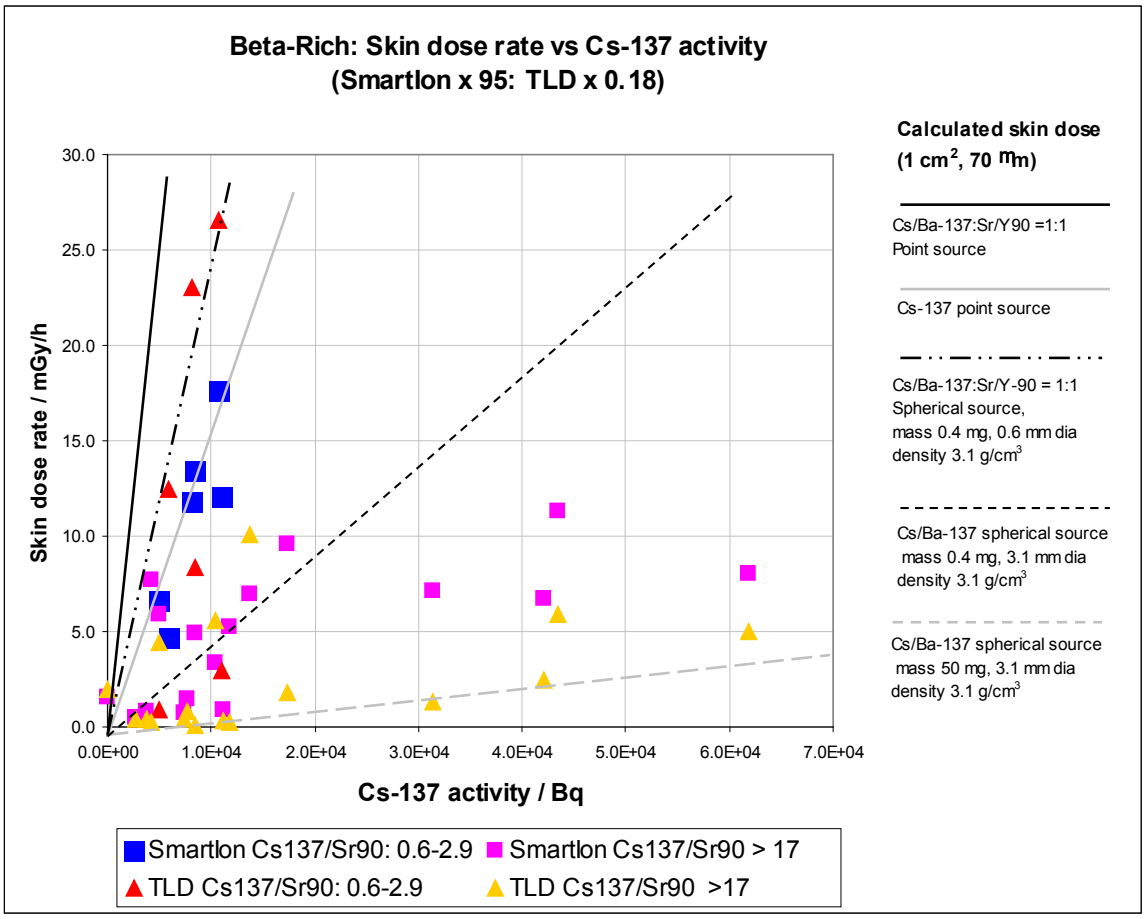

Figure 17: SmartIon (x 95) and TLD (x 0.18) skin dose rate vs. Cs-137 activity for beta-rich particles

9.1.1.2 Beta-rich stones

Table 82 presents the TLD and SmartIon dose rate measurements for the stones (Cowper, 2009). The highest dose rate was a TLD measurement of 19.8 mGy h^{-1}, for an object with a volume of 0.13 cm^3, a total a total ^{137}Cs activity of 86 kBq and a surface concentration of 70 kBq cm^{-2}.

As the size of objects increases, the (1 cm^2, 70 µm) skin dose rate is expected to become more closely related to the ^{137}Cs activity per unit surface area of the stone, rather than the total activity. Figure 18 shows an appropriate conversion factor based on TLD measurements of 0.86 mGy/h/kBq/cm^2 for the larger stones with surface areas greater than about 13 cm^2.

In the University of Birmingham study, the VARSKIN3 program (Durham, 2006) was used to calculate the skin dose rate (1 cm^2, 70 µm) from a 1 cm^2 plane source of 1 kBq ^{137}Cs and 1 kBq ^{137m}Ba. The value for the conversion factor calculated using VARSKIN3 is about 1.4 mSv/h/kBq/cm^2, for a thin source with no self absorption. The effect of self absorption was subsequently included by assuming an average thickness of material removed from stones in the leaching process of about 80 µm and an average density of

2.4 g cm^{-3}. Assuming a ^{137}Cs surface layer with these characteristics, the VARSKIN3 calculations predicted a reduction in skin dose rate by a factor of 2.2, to give a conversion factor of about 0.64 mGy/h/kBq/cm^2. This is in reasonable agreement with the value derived from TLD measurements, and gives confidence that the TLD measurements were interpreted correctly (see Section 9.1.2.2).

Table 82: Smartion and TLD measurements of (1 cm^2, 70 µm) skin dose rates for stones. Modified version of SERCO Table 38 (Cowper, 2009).

NPL Source number	Source volume/cm^3	Source area/cm^2	SmartIon skin dose rate/mSv h^{-1}	TLD skin equivalent dose rate/mSv h^{-1}	TLD/SmartIon ratio	Cs-137 (/kBq)[(a)]	Cs-137/Area kBq/cm^2
IM08010005	4.7	13.2	8.77	2.35	0.25	29.5	2.23
IM08010007	17	32	19.5	2.98	0.15	102	3.19
IM08010008	5.5	15	4.32	0.82	0.19	25.9	1.73
IM08010011	0.6	3.4	3.17	1.59	0.50	15.9	4.68
IM08010012	5.0	14	3.10	0.31	0.10	7.75	0.55
IM08010013	12	25	3.82	0.18	0.05	12.2	0.49
IM08010016	0.89	4.47	0.41	0.08	0.20	2.69	0.60
IM08010017	0.13	1.24	9.96	19.8	1.99	86.3	69.6
IM08010021	0.30	2.2	0.73	3.27	4.46	44.5	20.2
IM08010022	20	36	8.77	1.48	0.17	71.5	1.99
IM08010028	0.21	1.7	3.02	3.67	1.22	15.7	9.2
IM08010031	29	46	0.58	0.07	0.12	1.95	0.04

(a) Cs-137 activity is taken from SERCO report, Table 42 (Cowper, 2009)

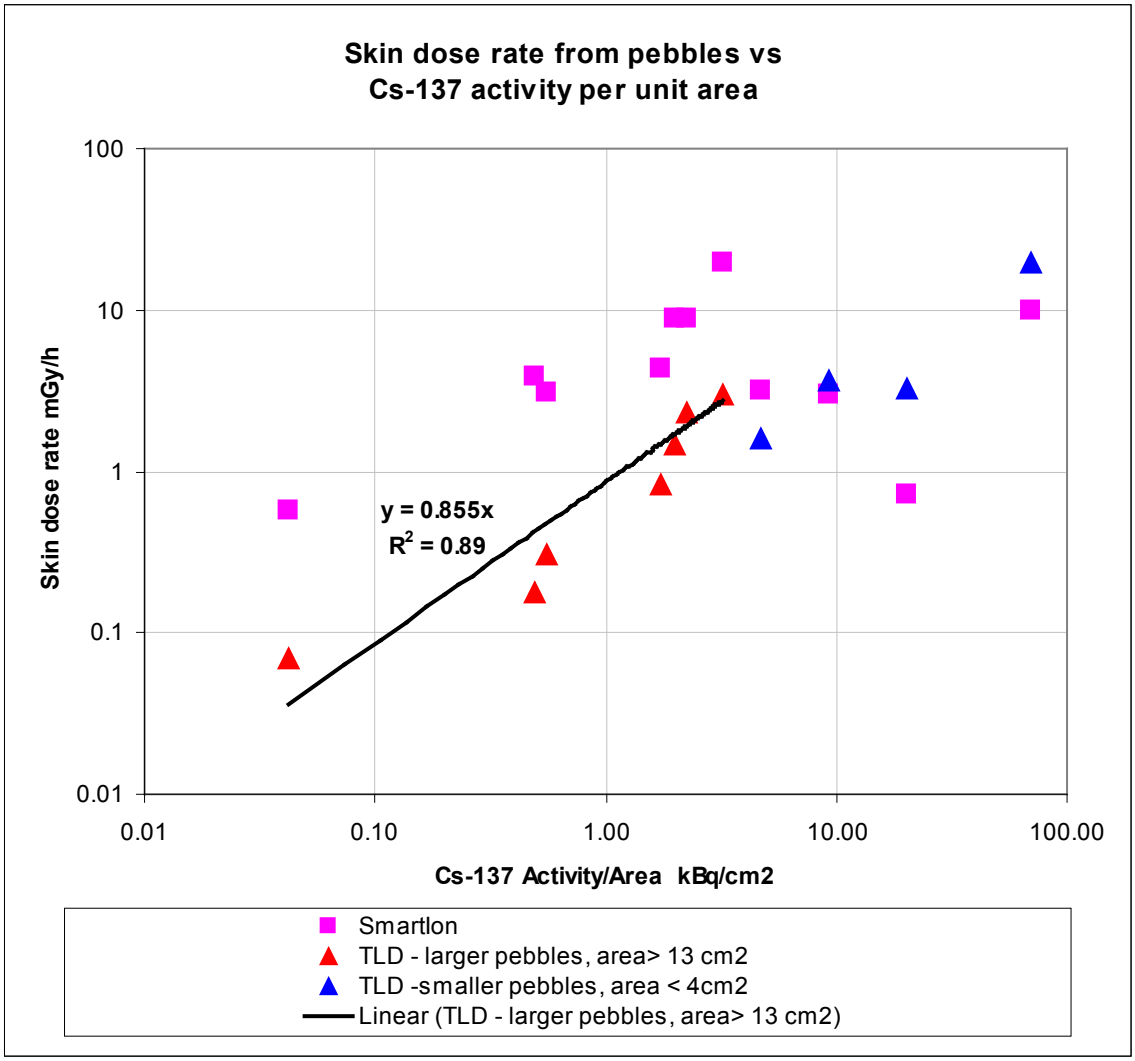

Figure 18: Measured (1 cm^2, 70 µm) skin dose rates for stones vs. ^{137}Cs activity per unit area of the stone surface. A regression analysis using only stones with surface areas greater than 13 cm^2 gives a regression coefficient of 0.86 mSv/h/kBq/cm^2.

9.1.2 Limitations of the measurements and calculations of skin dose rates

The University of Birmingham study identified a number of shortcomings in the results reported in the SERCO and AMEC reports (Cowper, 2009; Delaney et al, 2009) which should be taken into account.

9.1.2.1 Beta-rich particles

TLD dose rate measurements are likely to be under-estimates because of the difficulty of aligning the small TLD dosemeters centrally on the beta-rich particles, the majority of which have effective diameters < 1-2 mm. Corrected SmartIon measurements may also be underestimates because the correction factor of 95 used by SERCO for Sellafield

particles is lower than the correction factor of about 250 found to be appropriate for Dounreay fuel fragments (Aydarous et al, 2008), and the reason for this difference is unclear. Dounreay fuel fragments are similar to many of the Sellafield beta-rich particles, being composed primarily of ^{137}Cs (Dounreay Fast Reactor (DFR) samples) or a mixture with approximately equally amounts of $^{90}Sr/^{90}Y$ (Materials Testing Reactor (MTR) samples), with a density of ~ 3.1 g cm^{-3}. If a correction factor of 250 is used, the skin dose rates estimated would be proportionally higher and the discrepancy with the TLD data would therefore be increased. Given the lack of definitive information on the measurement protocol used, the University of Birmingham study also queried whether the correct protocol was followed with respect to the separation between the particle and the SmartIon ion chamber window.

With respect to the calculations of dose rate made by AMEC, deviations from particle sphericity, and preferential distribution of activity on or towards the surface, both increase the calculated skin dose rate by factors of up to about 2 for sources with the dimensions, shapes and densities of the beta-rich particles. This difference between measured and calculated skin dose rates is therefore partly explicable since calculated dose rates are based on spherical particles and uniformly distributed radioactivity through the whole of the particle volume. Better agreement between measured and calculated values would probably be achieved if more specific calculations were based on actual sizes, shapes and densities of the individual particles. However, the University of Birmingham study reported significant differences in estimates of particle size reported by AMEC and SERCO (Cowper, 2009), with the SERCO : AMEC ratio of particle volumes reported extending over a wide range (0.1-30). At present, this discrepancy precludes more realistic calculations. Calculated dose rates might provide a more powerful confirmation of measured dose rates if the discrepancies between the evaluations of particle size (and particle density) could be reconciled.

9.1.2.2 Beta-rich stones

It is unclear what SmartIon and TLD correction factors were applied to SERCO's dose rate measurements on stones, if any. It would be expected that the SmartIon correction factor would be less than the value of 95 used for beta-rich particles, since the stones are much larger than the particles and larger sources would irradiate a larger proportion of the ion chamber volume. The larger the stone, the smaller the correction factor should be.

If the contamination on the stones is uniformly distributed over the stone surface then the TLD measurements should not require correcting for the area of 0.18 cm^2 to obtain the (1 cm^2, 70 μm) dose rate, as is required for beta-rich particles.

9.1.3 Comparison with results for Dounreay Fuel Fragments

It is instructive to compare and contrast the skin dose rates from Sellafield particles with those from Dounreay fuel fragments (DFFs) (Harrison et al, 2005; Charles, 2009; DPAG, 2008). Figure 19 shows a comparison of measured and calculated skin dose

rates per unit ^{137}Cs activity for DFFs (MTR and DFR)[5] and Sellafield beta-rich particles. The data shown encompass the full range of ^{137}Cs:^{90}Sr ratios found in Sellafield particles. The Dounreay DFR fuel fragments all have low ^{90}Sr content whereas the MTR fuel fragments have approximately equal amounts of ^{137}Cs and ^{90}Sr. In contrast to the Sellafield particles, the DFFs are reasonably uniform in terms of particle density (3.2 g cm^{-3}) and activity per unit mass (about 2 GBq g^{-1}). The uniformity of DFF characteristics are related to their common origin from single reactor operations (MTR or DFR). This uniformity facilitates extrapolation of dose estimates based on ^{137}Cs content and fragment type. The relatively high skin dose rate from the higher activity DFFs also enables skin doses and depth doses to be conveniently measured using radiochromic dye film (RDF). Although RDF provides more direct and accurate skin dose measurements than either TLD or SmartIon measurements, its low sensitivity requires long term exposures.

All DFFs with ^{137}Cs activities below ~10^5 Bq had masses below 1 mg whereas almost half of the Sellafield beta-rich particles that were subjected to detailed analysis (all with < 10^5 Bq ^{137}Cs) have masses considerably in excess of this (average about 40 mg). For DFFs in this size/activity region, self absorption is negligible, whereas it is significant for the Sellafield particles with higher masses. As a result Figure 19 shows good agreement between the measured skin dose rates for the smaller Sellafield beta-rich particles with relatively high levels of ^{90}Sr/^{90}Y (solid red and open red triangles) and the extrapolated measured and calculated dose rates for Dounreay fuel fragments. The larger beta-rich Sellafield particles with high ^{137}Cs/^{90}Sr ratios (solid black and open black triangles) exhibit dose rates much lower than the extrapolated DFF values. These general conclusions appear to be robust even given the uncertainties and inconsistencies in the dose rate measurements for the Sellafield particles.

[5] DFFs (MTR and DFR) is short for Dounreay Fuel Fragments (Materials Testing Reactor and Dounreay Fast Reactor)

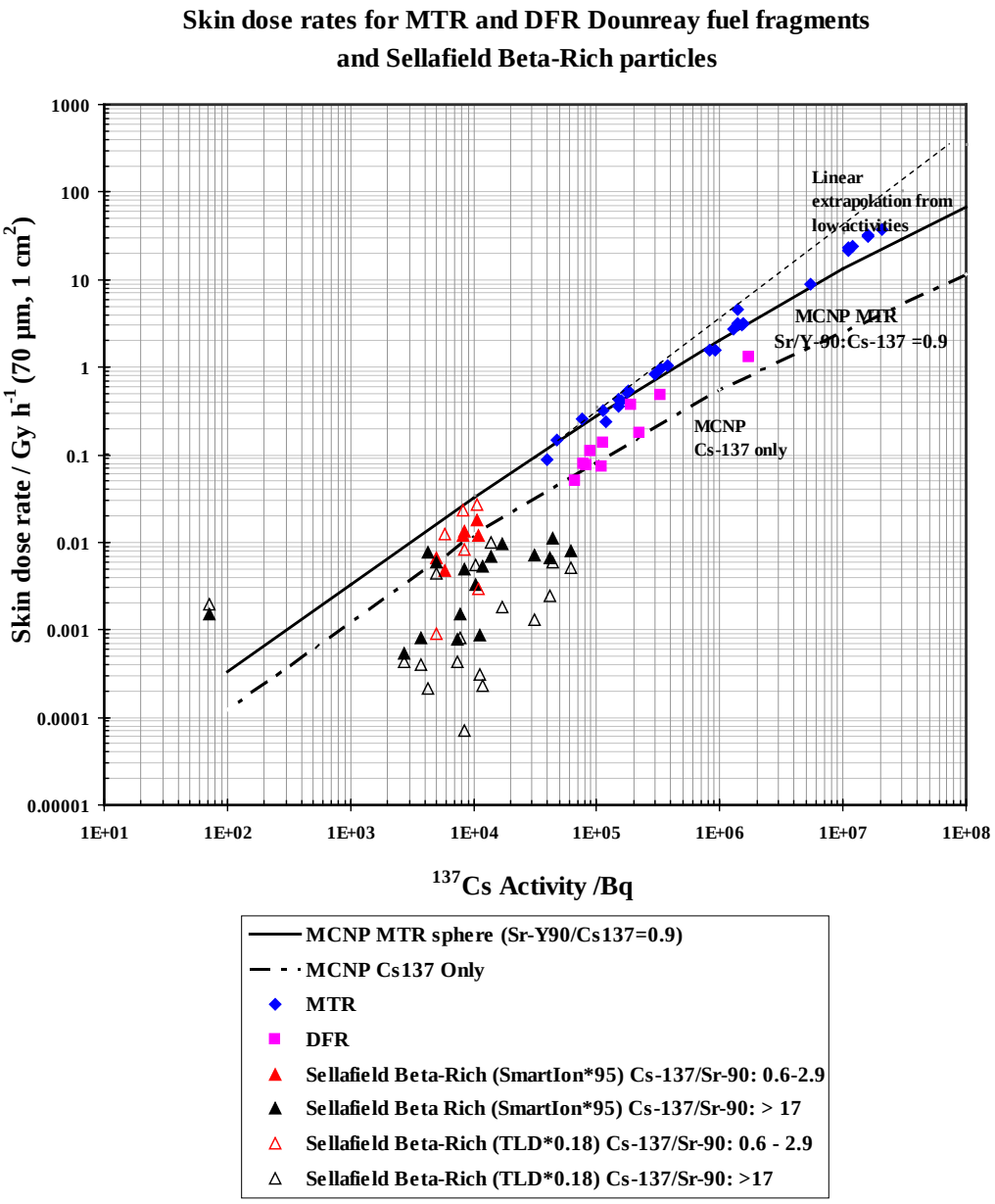

Figure 19: Skin dose rates from Dounreay fuel fragments and Sellafield beta-rich particles. Dose rates for Dounreay fuel fragments were measured using radiochromic dye film. For the Sellafield particles TLD and SmartIon (corrected) measurements are shown. Dose rates are indicated for 'Sr/Y-90-rich' (Cs-137/Sr90: 0.6-2.9) and 'Sr/Y-90 poor' (Cs-137/Sr90 >17) Sellafield particles, which correspond to Dounreay MTR and DFR samples, respectively.

9.1.4 Potential health effects of beta-rich Sellafield particles on skin

9.1.4.1 Health effects of beta-rich particles

The most appropriate way to assess the likelihood that deterministic effects could occur is to determine whether the threshold for the effect could be exceeded. The threshold is usually set at the level of dose corresponding to a risk of 1% that the effect would occur. Typically, thresholds are between 20% and 50% of the level of dose corresponding to a

risk of 50% that the effect would occur (NRPB, 1996). The (1 cm^2, 70 μm) threshold dose for localised skin ulceration from small radioactive particles is about 2 Gy. This threshold dose only applies for particles in *stationary* contact; if the particle moves by a distance much greater than its own size, then the threshold value would be significantly higher. For the particle with the highest dose rate found in the SERCO and AMEC studies (29.7 mGy h^{-1}), the exposure time required to exceed this dose level is about 67 hours. Referring to the dose rate values calculated by AMEC, Delaney et al (2009) notes that the required exposure time for the next most active particle is approximately 3 times greater, and for the least active particle exposure times longer than 16,000 hours are required to exceed 2 Gy, It is extremely unlikely that particles could remain in contact with the skin for times as long as 67 hours. The topic of realistic upper bounds on likely exposure times is discussed in detail in 5.4.

For the highest activity beta-rich particle found up until August 2009 (110 kBq ^{137}Cs, but with an unknown ^{90}Sr content), it is estimated that the (1 cm^2, 70 μm) dose rate would be approximately 100 mGy h^{-1}. This value was determined by assuming that the dose rate for the particle with the highest dose rate calculated by AMEC can be scaled by its ^{137}Cs content. By applying this scaling, it is implicitly and conservatively assumed that the ^{137}Cs:^{90}Sr ratio of the 110 kBq particle is 0.66:1, the ratio found for the particle with the highest calculated dose rate. For this hypothetical 110 kBq particle, the exposure time required to reach the threshold for localised skin ulceration would be approximately 20 hours. It is very unlikely that particles could remain in stationary contact with the skin for times as long this. It should be noted that if the threshold value was reached, there would still only be about a 1% risk that the effect would occur in the exposed individual, and the severity of the effect would be relatively low. As skin dose rates increase above the threshold, the risk of the effect and its severity would both increase.

It is apparent from Section 9.1.3 that the Sellafield beta-rich particles studied to date are similar in a number of respects to the Dounreay fuel fragments (DFFs) that have been studied extensively in a number of reports (Harrison et al, 2005; Charles, 2009; DPAG, 2006; DPAG, 2008; Darley et al, 2003; Charles et al, 2005). It is therefore useful to consider the extent to which the analysis of health risks from Dounreay particles can be applied or adapted for an analysis of the health risks of beta-rich particles at Sellafield. The Sellafield beta-rich particles studied to date fall into two groups: those with a significant proportion of $^{90}Sr/^{90}Y$ (^{137}Cs:^{90}Sr = 0.6-2.9) and those containing predominantly ^{137}Cs. DFFs may also be categorised into two groups: MTR fuel fragments (^{137}Cs:^{90}Sr about 1.1) and DFR fuel fragments (predominantly containing ^{137}Cs). DFFs have densities about 3.1 g cm^{-3} while the majority of Sellafield beta-rich particles have densities in the range 1.5 – 4.5 g cm^{-3}. The majority of Sellafield beta-rich particles, like DFFs with the same range of activities, have dimensions less than about 2mm. In consequence, they produce spatially non-uniform dose distributions over an area of less than about 1 cm^2. Some of the larger Sellafield beta-rich particles have higher self absorption and more uniform spatial distributions of dose than do the smaller DFFs. Sellafield beta-rich particles, like DFFs, have only small amounts of actinides, including ^{241}Am and various plutonium radionuclides. None of the Sellafield beta-rich particles found up till August 2009 has ^{137}Cs activities significantly in excess of 10^5 Bq. In comparison, DFFs have activities up to about 10^8 Bq (although activities are no greater than about 10^6 Bq on public access areas).

On the basis of the results of the characterisation of the limited number of particles studied to date by SERCO (Cowper, 2009), it appears that the biological effects of the majority of Sellafield beta-rich particles can be linked to ^{137}Cs activity in the same way as has been done for DFFs. Specifically, because the majority of the Sellafield beta-rich particles have low ^{90}Sr/^{90}Y levels, they may be considered in the same way as DFR DFFs. For some of the larger Sellafield beta-rich particles, the skin dose rates per unit ^{137}Cs activity will be even less than for DFR DFFs (Figure 19). Treating Sellafield beta-rich particles in the same way as MTR DFFs will thus in general provide over-estimates of skin dose rates and predicted health effects compared to those predicted for DFFs but may be useful to put the radiological significance of the beta-rich particles into context.

It is informative to reproduce below the general discussion section (Section 2.7) of the HPA report (Harrison et al, 2005) which considered the health implications of DFFs:

> *The available animal data on the effects of hot particle irradiation of skin, mainly from studies using pigs but supported by human data, allow the estimation of an ED_{50} value (1 cm^2, 70 µm) for acute ulceration of about 10 Gy and a threshold of about 2 Gy. It is clear from these data, together with data for larger area skin exposures, that toleration of radiation will be increased when a particle moves during skin contact, by even a few mm, and when dose rates are low. Taking no account of this amelioration of their possible effect, … (the table below) … provides a summary of time taken for MTR particles to deliver doses of 0.5 Gy, 2 Gy and 10 Gy, corresponding to the ICRP dose limit (see below), the estimated threshold and the ED_{50} value, respectively. The short times required for 10^8 Bq ^{137}Cs MTR particles to cause ulceration illustrate the high probability of such damage in the event of such contact. For 10^5 Bq ^{137}Cs MTR particles, typical of the most active particles found at Sandside Bay, stationary contact for more than 7 hours is required before ulceration is expected to occur. It can be concluded that contact with such particles is unlikely to cause ulceration, although a particle trapped against the skin for longer periods of a day or two may cause a small ulceration.*
>
> *(The table below) … includes estimates of time taken for particles to deliver a dose of 0.5 Gy, corresponding to the ICRP dose limit (0.5 Gy). This is the limit for localised skin exposure of workers and can be regarded as conservative when applied to hot particle exposures since the threshold for effects is around 2 Gy (NRPB, 1997).*

Estimates of time taken for MTR particles* to deliver doses corresponding to the ICRP dose limit, threshold and ED50 for acute ulceration

Activity	*Dose rate†*	*Time to:*		
Bq ^{137}Cs	*Gy h^{-1}*	*ICRP limit: 0.5 Gy*	*Threshold: 2 Gy*	*ED_{50}: 10 Gy*
10^4	*0.03*	*17 hours*	*3 days*	*2 weeks*
10^5	*0.3*	*<2 hours*	*7 hours*	*33 hours*
10^6	*2 – 4*	*8 – 15 minutes*	*0.5 – 1 hours*	*2 – 5 hours*
10^7	*15 – 30*	*1 – 2 minutes*	*4 – 8 minutes*	*20 - 40minutes*
10^8	*70 -140*	*<30 seconds*	*1 – 1.5 minutes*	*<10 minutes*

**Applying standard assumptions used in this report including a specific activity of 2 GBq ^{137}Cs g^{-1} and an activity ratio of 0.9 for ^{90}Sr/^{90}Y:^{137}Cs.*

†Dose rate ranges take account of possible differences in shape and hence energy self-absorption within larger particles (see text).

On the basis of radiobiological data reviewed by the HPA (Harrison et al, 2005), and in accord with ICRP (ICRP, 1991a) & NCRP (NCRP, 1999) reviews, the Dounreay Particle Advisory Group (DPAG, 2006) placed Dounreay fuel fragments into three categories, depending on their hazard. The categories were expressed in terms of ^{137}Cs activity and skin dose rate (1 cm^2, 70 μm) for MTR DFFs, and are shown in Table 83.

This categorisation was maintained in the DPAG Fourth Report (DPAG, 2008). For the Sellafield beta-rich particles, the same values of skin dose (column 3 in Table 83) should be appropriate for defining similar categories of biological effect (significant, relevant & minor). It could be argued that the related ^{137}Cs levels (column 2) should be increased for Sellafield beta-rich particles in view of their generally lower measured skin doses compared to DFR DFFs of the same ^{137}Cs activity. However, the uncertainties and lack of coherence of the measured skin dose rates for the Sellafield particles argues against such a relaxation.

Table 83: DPAG hazard categories for Dounreay fuel fragments

DPAG Category	Cs-137/ Bq	Skin dose rate/Gy/h (1 cm^2, 70 μm)	Effects on health
Significant	> 10^6	> 3	Visible effects within a few hours if kept in stationary contact with skin; serious ulceration after 1-2 weeks
Relevant	10^5 - 10^6	0.3 - 3	Discernible effects after seven hours if kept in stationary contact with skin; reddening after 1-2 days
Minor	< 10^5	< 0.3	No discernible health effects even if kept in stationary contact with skin. No requirement for monitoring or removal.

Since only one of the particles found up until August 2009 in the vicinity of Sellafield has an activity in excess of 10^5 Bq and that activity is only marginally greater, ie, 110 kBq (Dalton, 2010), and since the skin dose rates per unit ^{137}Cs activity assessed for Dounreay are conservative for Sellafield particles, it is reasonable to assign all of these particles to the DPAG "Minor" category. It may be concluded that …"*There would be no discernible health effects even if the particle was kept in stationary contact with skin.* … for any time of exposure that could reasonably be expected.

9.1.4.2 Health effects of beta-rich stones

In contrast to the Sellafield beta-rich particles, the Sellafield stones have no analogue in the study of health effects due to radioactive contamination at Dounreay (Harrison et al, 2005). In comparison with the small beta-rich particles, the stones are extended sources which give rise to relatively uniform exposure of areas of the skin with which they may make contact. The stones investigated to date are contaminated predominantly with ^{137}Cs, with the contamination confined to the surface layers with depths up to 80-160 μm. Americium-241 is present at low levels (Cowper, 2009) and makes a minor contribution to skin dose. For the larger stones the skin dose rate (1 cm^2, 70 μm) will be related to the ^{137}Cs activity per unit surface area of the stone rather than the total activity. Figure 18 indicates an appropriate conversion factor based on TLD measurements of 0.86 mGy/h/kBq/cm^2. For these extended sources the highly-localised ulceration seen at doses above 2 Gy for classical hot particles will not be observed although at higher doses > 10-20 Gy there will be classical moist-desquamation and ulceration over areas approximately equal to the projected area of the stone on the skin surface. For the stone with the highest dose rate (19.8 mGy h^{-1}) measured in the SERCO characterisation study (Cowper, 2009), the exposure time required to exceed this dose level is about 500 hours. It is extremely unlikely that stones could remain in contact with the skin for times more than a few hours and this would only be the case for stones with diameters less than a few mm. Even if contact were to be maintained, the dose would be received over an extended period (~20 days) rather than as an acute exposure and the threshold would be significantly higher than 10-20 Gy as a result.

This stone had a total ^{137}Cs activity of 86 kBq and a surface concentration of 70 kBq cm^{-2}. It is worthy of note that this places this object well within the DPAG “minor” category, since the threshold dose rate of 0.3 Gy/h that could give rise to minor effects would require a ^{137}Cs surface concentration of about 350 kBq/cm^2 (using the conversion factor of 0.86 mGy/h/kBq/cm^2). This value has not been exceeded to date for those stones where measured data allow the surface concentration to be evaluated. For objects in the DPAG minor category, it may be concluded that … “*There would be no discernible health effects even if the (object) was kept in stationary contact with skin*” … for any time of exposure that could reasonably be expected.

For the highest activity beta-rich stone found up until August 2009, recorded in Sellafield Ltd’s Beach Monitoring Summary spreadsheet as having an activity of 875 kBq ^{137}Cs, the (1 cm^2, 70 μm) dose rate would be no greater than 200 mGy h^{-1}, and the exposure time required to reach the threshold would be approximately 50 hours. It is extremely unlikely that stones could remain in contact with the skin for times as long as this.

9.1.4.3 Health effects of ^{60}Co

The highest ^{60}Co activities recorded in Sellafield Ltd.’s Beach Monitoring Summary spreadsheet (Dalton, 2010) are 19.7 kBq for a particle and 23.5 kBq for a stone. The highest ^{60}Co activity of the objects investigated in the SERCO study (Cowper, 2009) is 6.35 kBq, for a 2 mm length of metal wire. VARSKIN3 (Durham, 2006) calculations predict a (1 cm^2, 70 μm) skin dose rate of about 2.4 mGy h^{-1} for this object, 20-50% higher than the measured value by SERCO. The calculation assumed a slab geometry

with dimensions 2 mm x 70 μm x 70 μm and a density of 7.5 g cm^{-3} appropriate for steel. The skin dose rate (1 cm^2, 70 μm) for ^{60}Co-bearing objects is an indicator of biological effect just as for other sources. The measured skin dose rate for this object is several times less than that for an MTR or DFR DFF with a ^{137}Cs/^{137m}Ba activity equal to the ^{60}Co activity. None of the ^{60}Co objects found up till August 2009 have activities in excess of 10^5 Bq, and so may be placed well within the DPAG "minor" category. For objects in the DPAG minor category, it may be concluded that … "*There would be no discernible health effects even if the particle was kept in stationary contact with skin*" … for any time of exposure that could reasonably be expected.

9.1.5 Health effects on the skin as a surrogate for other organs/tissues

9.1.5.1 Auditory canal, anterior nasal compartment, ear drum and cornea of eye

As noted in Section 8.6.3.1, the most comprehensive consideration of the possibility of hot particle damage to skin and other organs is that included in NCRP Report No 130 (NCRP, 1999). While concentrating on the most likely types of hot particle exposures of the skin, the NCRP review also considered possible effects of particle entry into the ear or eye. This has been summarised extensively in the context of the health effects of Dounreay fuel fragments (Harrison et al, 2005). In summary, NCRP concluded that the same limits should apply to the skin lining the auditory canal, the anterior nasal compartment and the ear drum as to other skin regions. They also concluded that the same limit should prevent damage to the cornea of the eye, the site at greatest risk if a particle were to lodge in the eye.

On this basis, the considerations described above for particles and stones in contact with the skin can be taken to apply to objects in contact with the cornea of the eye and the skin lining the auditory canal and the anterior nasal compartment. It can therefore be stated that it is very unlikely that objects could remain in contact for times long enough to reach deterministic thresholds.

9.2 Skin doses and stochastic effects

As discussed in Section 8.7, ICRP (1991a) relates the risk of skin cancer to the average dose to the total area of skin, 1.9 m^2 in adult man and 0.48 m^2 for a one year old child (ICRP, 2002). No value is presented for a 3 month old infant, so the value for a new-born infant (0.24 m^2) is taken to apply. Charles et al (2005) have shown that the use of mean dose to predict carcinogenic risks, as advocated by the ICRP, is appropriate for hot particle exposures.

The (1 cm^2, 70 μm) threshold dose for observable skin ulceration from small radioactive particles is approximately 2 Gy for particles in stationary contact (Section 9.1.4). A dose of 2 Gy delivered to 1 cm^2 of skin corresponds to an equivalent dose to the skin of 0.1 mSv in adults, 0.4 mSv in one year old children and 0.8 mSv in 3 month old infants. The effective dose is then the equivalent dose to skin multiplied by the tissue weighting factor, w_T, for the skin of 0.01: that is, 1 μSv for adults 4 μSv for one year old children and 8 μSv in 3 month old infants. There will be a larger contribution to the effective dose from objects located at the body surface due to a small whole body exposure from the

gamma emissions of ^{137}Cs. Walters et al (1999) evaluated this to be between 0.2 – 3.8 μSv h^{-1} MBq^{-1}, depending on the location of the radioactive source on the body. This dose from ^{137}Cs will increase estimated effective doses corresponding to 2 Gy to 1 cm^2 of skin to maximum values of about 4 μSv in adults, about 25 μSv in one year old children and no greater than 100 μSv in 3 month old infants. These dose estimates assume that the dose from a particle deposited on the skin would be delivered to an area of skin no greater than 1 cm^2. If the area of skin receiving a signficant absorbed dose was greater than 1 cm^2 (which could occur as a result of irradiation by more than one particle, for instance), then the estimated equivalent and effective doses would increase in proportion to the irradiated area.

As discussed in Section 9.1, none of the objects found up until August 2009 result in skin doses that approach the threshold for localised skin ulceration, and so it is clear that stochastic risks for resulting from beta-rich particles in contact with the skin are negligible.

9.3 Doses and deterministic effects resulting from ingestion

Harrison et al (2005) described the methods used to compute absorbed doses to the rectosigmoid colon from ingestion of Dounreay fuel fragments using ICRP's Human Alimentary Tract Model (HATM) (ICRP, 2006b). These authors summarised the main features of the HATM model, outlined the differences in approach to biokinetic and dosimetric modelling compared with that of the ICRP Publication 30 model (ICRP, 1979), and discussed acute radiation effects within the GI tract.

The rectosigmoid colon is the region of the GI tract that receives the greatest doses from ingested beta-rich objects because it has the narrowest diameter of the three segments into which the colon is divided in the HATM. Furthermore, at some ages, the transit time is longest in the rectosigmoid.

A similar approach has been adopted for Sellafield beta-rich objects as was used for Dounreay fuel fragments (DFF). The calculations for DFFs were performed for spherical uranium/aluminium particles of different diameters containing homogenously distributed ^{137}Cs and ^{90}Sr/^{90}Y. The mass fraction of uranium in the objects was taken to be 15% and the density was assumed to be 3.1 g cm^{-3}. In contrast to the precisely-defined Dounreay particles, the beta-rich objects found near Sellafield are more diverse. Particle composition 'indications' from SEM/EDAX analyses include various permutations of 'Fe, Fe oxide, rusted, silicate, quartz, steel, feldspar, salt coated', etc (Cowper, 2009).

It is possible that self-absorption may be less important for Sellafield beta-rich objects because, as the Dounreay particles were fuel fragments, the radionuclide activity was assumed to be homogeneously distributed through the particle volume. The Sellafield objects do not appear to be fuel fragments, so unless they are particularly porous, it may be that the activity is deposited on or near the surface. This detail can only be clarified when the objects are better characterised. However, even if the activity on Sellafield objects is surface-distributed, they will still not irradiate a target as efficiently as a point source. Assuming a relatively convex surface, about half the radioactive

emissions would be expected to escape the object unimpeded. The remaining half emitted into the object interior could be variously scattered, absorbed, attenuated and/or eventually escape, with the outcome depending on the object's size and composition, as well as the radionuclide.

In order to apply the Dounreay methodology to Sellafield objects, the dose rates to the rectosigmoid colon computed as a function of object diameter for DFFs were extrapolated to zero diameter in order to eliminate the influence of the specific chemical composition, effectively modelling the object as a point source. As a result, self-absorption by the object is neglected, and so the corresponding dose-rates must be regarded as upper bounds. This conservative approach is adequate provided the computed doses are well below thresholds for deterministic effects. If this were to be shown not to be the case then more accurate calculations taking into account the composition and size of Sellafield beta-rich objects would be required.

Two kinds of absorbed doses were computed for Dounreay objects, depending on the assumed object path while transiting the colon. As objects are unlikely to maintain a fixed radial position as they descend the colon, 'expectation' doses average the absorbed dose from objects at different radial positions within the lumen, taking into account the probability of the object being situated at a particular position. 'Maximum' doses assume the worst case where the object is in contact with the mucosal lining of the rectosigmoid during transit. Figure 20 shows the variation of expectation dose-rates with object diameter for a Dounreay fragment randomly transiting the rectosigmoid of a 1 year old child. Penetrating (photon) and non-penetrating (beta) components of ^{137}Cs emissions are designated p and np, respectively. With the exception of the photon component, the effect of self-absorption becomes apparent for object diameters greater than about 30 μm for the relatively low energy ^{90}Sr beta spectrum (mean and maximum energies of about 0.2 and 0.55 MeV) and greater than about 100 μm for the more energetic ^{90}Y spectrum (mean and maximum energies of about 0.9 and 2.3 MeV). When the dose-rates are extrapolated to zero diameter it is found in all cases that they are less than 1% higher than dose-rates computed for the smallest object diameter considered of 3 μm. It is therefore assumed that the dose-rates for the point source are the same as those from the 3 μm diameter particle.

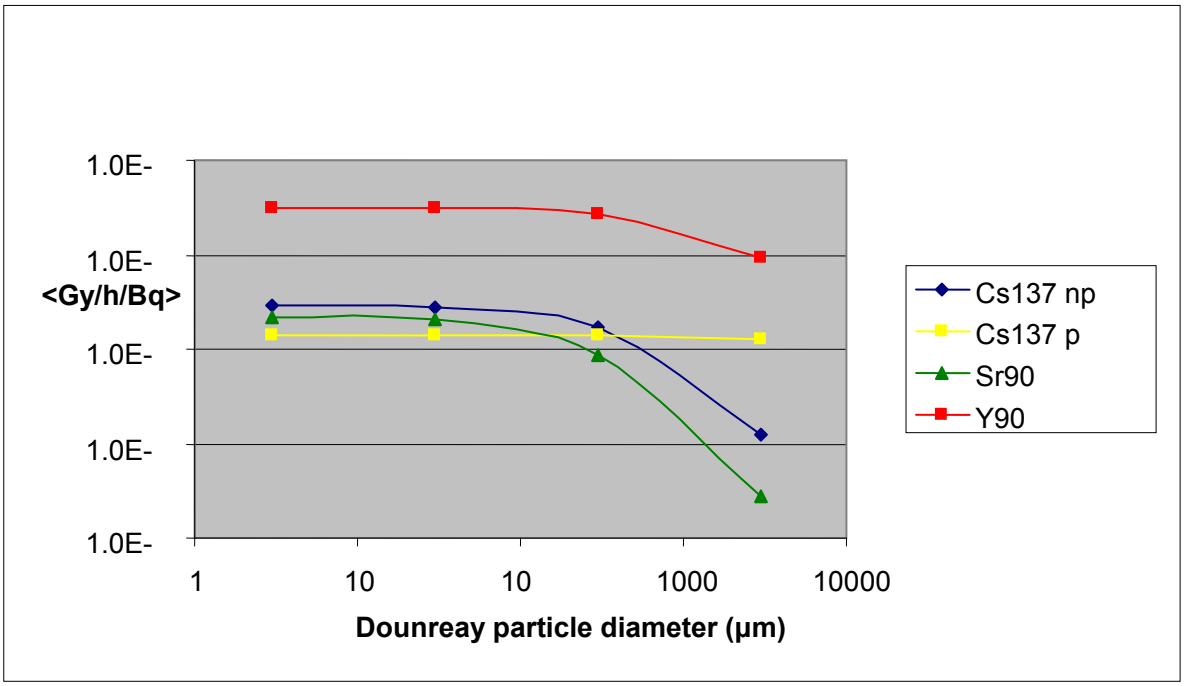

Figure 20: Expectation dose rates to the rectosigmoid of a 1 year old child (280-300 µm target cell depth). Penetrating (photon) and non-penetrating (beta) components of ^{137}Cs emissions are designated p and np, respectively.

The expectation and maximum dose-rates presented in Table 84 and Table 85 are for 3 µm particles descending the rectosigmoid of an adult and a 1 year old child, calculated using the HATM reference rectosigmoid diameters of 3 cm and 2 cm, respectively. The quoted doses are upper bounds, as explained earlier.

Table 84: Expectation and maximum absorbed dose rates to the rectosigmoid colon of an adult

Expectation[(a)] dose rates from point sources, Gy/h/Bq			Maximum[(b)] dose rates from point sources, Gy/h/Bq		
Cs-137	Sr-90	Y-90	Cs-137	Sr-90	Y-90
$1.2\ 10^{-10}$	$5.5\ 10^{-11}$	$7.9\ 10^{-10}$	$1.6\ 10^{-9}$	$1.7\ 10^{-9}$	$4.4\ 10^{-9}$

(a) Object performing random walk through lumen

(b) Object in contact with mucosal layer during transit

Table 85: Expectation and maximum absorbed dose rates to the rectosigmoid colon of a 1 year old child

1y old expectation[(a)] dose rates from point sources, Gy/h/Bq			1y old maximum[(b)] dose rates from point sources, Gy/h/Bq		
Cs-137	Sr-90	Y-90	Cs-137	Sr-90	Y-90
$4.4\ 10^{-10}$	$2.2\ 10^{-10}$	$3.1\ 10^{-9}$	$4.4\ 10^{-9}$	$4.6\ 10^{-9}$	$1.2\ 10^{-8}$

(a) Object performing random walk through lumen

(b) Object in contact with mucosal layer during transit

It was not possible to compute dose rates for a 3 month old infant because values for the length, radius and mass of the rectosigmoid colon are not available (ICRP, 2006b). From a consideration of the values of these parameters for a newborn infant, a best estimate for the dose rates for a 3 month old infant is that they would be approximately four times higher than those for a 1 year old child, with an upper limit of 10 on this factor.

The computed dose-rates are expressed as Gy/h/Bq, and can be easily scaled by reference rectosigmoid transit time (h). Absorbed doses to the recto-sigmoid colon were assessed for both adult males and adult females because doses for the female are slightly larger than for the male which is mainly due to the default transit time being 16 h for the female but only 12 h for the male. Absorbed doses to the recto-sigmoid colon for adults given in the report are those calculated for females as shown in Table 86, which presents absorbed doses per Bq intake for an adult (16 h transit) and a 1y old (12 h transit).

Table 86: Expectation and maximum absorbed doses to the rectosigmoid colon per Bq intake

	Expectation[(a)] rectosigmoid dose (Gy)			Maximum[(b)] rectosigmoid dose (Gy)		
	Cs-137	Sr-90	Y-90	Cs-137	Sr-90	Y-90
Adult	$2.0\ 10^{-9}$	$8.8\ 10^{-10}$	$1.3\ 10^{-8}$	$2.6\ 10^{-8}$	$2.7\ 10^{-8}$	$7.1\ 10^{-8}$
1-y old child	$5.2\ 10^{-9}$	$2.7\ 10^{-9}$	$3.7\ 10^{-8}$	$5.3\ 10^{-8}$	$5.5\ 10^{-8}$	$1.4\ 10^{-7}$

(a) Object performing random walk through lumen

(b) Object in contact with mucosal layer during transit

(c) Default transit times are 16 h for an adult (based on an adult female) and 12 h for a 1y old child

(d) Target cell depth = 280-300 μm

These doses become less realistic as the activity increases because the point source assumption implies an infinite specific activity, whereas the objects have to be a finite size to contain or retain any activity. As an illustration, the effect of object size on self-absorption for dose-rates per Bq from the pure beta emitters ^{90}Sr and ^{90}Y is shown in Table 87. The expectation dose-rates per Bq for ingestion by adults of fuel fragments with diameters in the 3 μm to 3 mm range have been normalised to the corresponding 3 μm diameter value. The Table shows that, assuming a diameter of 3 μm when the true object size is greater, results in conservative dose estimates.

Table 87: Effect of object size on self-absorption for ^{90}Sr and ^{90}Y

Diameter (μm)	Expectation dose rates (Gy/h/Bq) normalised to 3 μm diameter value, for adults	
	Sr-90	Y-90
3	1.00	1.00
30	0.92	0.99
300	0.39	0.87
3000	0.01	0.28

For ^{90}Sr, the dose-rate per Bq is two orders of magnitude less for a 3 mm object relative to a 3 μm particle. For the more energetic ^{90}Y spectrum the dose-rate per Bq is reduced by a factor of about 4 for a 3 mm particle compared with a 3 μm particle.

The beta-rich particle with the highest ^{137}Cs activity is recorded in Sellafield Ltd's Beach Monitoring Summary spreadsheet (Dalton, 2010), as containing about 1.1 10^5 Bq. From the tables above, upper bounds for rectosigmoid expectation doses after ingestion of such a particle are 0.15 mGy, 0.2 mGy and 0.52 mGy for the adult male, adult female and 1y old respectively. Corresponding upper bounds for the maximum doses (particle in contact with wall during transit) are roughly ten times the expectation doses, ie, 2 mGy, 2.6 mGy and 5.3 mGy, respectively.

The highest activity object listed by Dalton (2010) is a stone with an activity of 8.75 10^5 Bq, about 10 times that of the particle above. Since it has an average diameter of 35 mm, inadvertent ingestion is not possible although adults and older children could deliberately ingest such an object. A conservative estimate of dose may be obtained by scaling the values obtained for the 1.1 10^5 Bq particle. The upper bounds for the maximum doses resulting from deliberate ingestion of this stone are 21 mGy and 42 mGy for an adult a a 1 year old, respectively. These estimates neglect self absorption by the stone, and must therefore be overestimates. No allowance is made here for any possible ^{90}Sr content of the stone, since the evidence from the SERCO study (Cowper, 2009), indicates that the ^{137}Cs:^{90}Sr ratios for stones are very high.

SERCO's analysis of the ^{90}Sr content of 19 beta-rich particles (Cowper, 2009) found the greatest ^{90}Sr activity to be 4.9 10^4 Bq. Assuming the ^{90}Y daughter to be in equilibrium, the combined expectation rectosigmoid doses for an adult and a 1 year old are 0.7 mGy and 2 mGy, respectively. The corresponding upper bounds for maximum doses are 4.8 mGy and 9.8 mGy.

Since none of the beta-rich particles was detected by measurement of ^{90}Sr/^{90}Y, Sellafield Ltd.'s Beach Monitoring Summary spreadsheet (Dalton, 2010) does not list any ^{90}Sr or ^{90}Y particle activities. As a result, information on the highest ^{90}Sr/^{90}Y activity in the particles found to date is not available. The highest ^{137}Cs particle activity is approximately 1.1 10^5 Bq, and making the conservative assumption that the ^{137}Cs:^{90}Sr ratio is the lowest found in the SERCO study, 0.61:1 (Cowper, 2009) indicates that this particle might contain 1.8 10^5 Bq ^{90}Sr and 1.8 10^5 Bq ^{90}Y. For this hypothetical particle, the upper bounds for rectosigmoid expectation doses calculated using the stated assumptions are 2.8 mGy and 7.9 mGy for an adult and a 1 y old, respectively. Corresponding upper bounds for the maximum doses (particle in contact with wall during transit) are 20 mGy and 41 mGy, respectively. All the upper bounds scale with activity.

All of the dose calculations presented here assume the default transit time through the colon. In the event that a particle became trapped, perhaps as a result of constipation, then doses would be larger and would be scale linearly with the ratio of the residence time and the default transit time. Harrison et al (2005) estimated that in extreme cases absorbed doses to the colon may be increased by factors of up to ten in consequence.

NRPB (1996) quotes a threshold dose of 23 Gy for acute effects in the colon. Generally the risk of acute effects for doses below the threshold is taken to be zero. Noting 'the highly judgemental nature of the threshold' the authors have related their threshold to a 1% risk of effects occurring.

In conclusion, the ^{137}Cs and ^{90}Sr object activities reported to date are orders of magnitude less than those that could give rise to deterministic effects on the rectosigmoid colon following ingestion. The highest ^{137}Cs particle activity found up to August 2009 (1.1 10^5 Bq) would result in an absorbed dose to the rectosigmoid colon no greater than about 40 mGy (1 year old child, upper bound dose, maximum value, ie, particle in contact with colon wall during transit), assuming a ^{137}Cs:^{90}Sr ratio of 0.61:1. It is estimated that the absorbed dose to the rectosigmoid colon for a 3 month old infant would be about four times this value. The highest ^{137}Cs activity found in a stone (8.75 10^5 Bq) would result in an absorbed dose to the rectosigmoid colon no greater than 42 mGy (1 year old child, upper bound dose, maximum value, ie, object in contact with colon wall during transit, with the default transit time). These doses are about 1000 times less than the threshold for deterministic effects. Even if a particle became trapped in the colon, it is very unlikely that it would remain long enough to cause deterministic effects.

It should be noted that this stone could not be ingested inadvertently as it has an average diameter of 35 mm. For an object containing the highest ^{90}Sr activity reported to date (4.9 x 10^5 Bq), the absorbed dose would be no greater than 10 mGy (1 year old child, upper bound dose, maximum value, ie, object in contact with colon wall during transit, ^{90}Y assumed to be in equilibrium with ^{90}Sr). This dose is about 2000 times less than the threshold for deterministic effects. The doses for point sources tabulated in this report should be used cautiously and considered as upper bounds for rectosigmoid colon doses from Sellafield beta-rich objects. Overestimates in dose are likely to increase with increasing object activity because self-absorption has been neglected.

9.4 Doses and stochastic risks resulting from ingestion

Stochastic risks arising from ingestion of Sellafield beta-rich objects have also been considered. Harrison et al (2005) briefly reviewed ICRP's dosimetric system for the evaluation of stochastic risk, which involves the use of radiation and tissue weighting factors to evaluate equivalent doses to organs and effective dose. These authors also summarised the systemic biokinetic models for caesium, strontium, yttrium and cobalt.

Table 88 summarises the results of dose calculations for beta-rich objects for each of the beta-emitting radionuclides listed in the table, for the maximum activities found for each radionuclide. The table lists 3 month old, 1-year old and adult ingestion dose coefficients and the corresponding effective doses for ingestion, making the pessimistic assumption that the ICRP default gut uptake fractions (f_1) apply to all the activity in the object and not just the mass fraction of the object that is soluble. Table 88 shows that the radionuclides that make the greatest contribution to effective dose are ^{90}Sr and ^{137}Cs. For the object which contains 49 kBq ^{90}Sr, that radionuclide gives rise to effective doses of 1.4 mSv, 3.6 mSv and 11.2 mSv for an adult, a 1 year old child and a 3 month old infant respectively. The ^{137}Cs content of that object (31 kBq) also makes a contribution to the effective dose: 0.3 mSv, 0.4 mSv and 0.7 mSv for an adult, a 1-year old child and a 3 month old infant respectively. For the object which contains the highest activity of ^{137}Cs, 1.1 10^5 Bq, that radionuclide gives rise to effective doses of 1.3 mSv, 1.2 mSv and 2.3 mSv, respectively.

The object which contains the highest ^{137}Cs, ^{106}Ru and ^{125}Sb activities is in fact a stone with an 'average' size of 35 mm. Such an object could not be inadvertently ingested, but it could be deliberately ingested by adults and older children (see Section 6.1). Contributions to the effective dose from radionuclides other than ^{137}Cs are negligible; the ^{137}Cs activity is 8.75 10^5 Bq and ingestion of this stone would result in an effective dose of 11 mSv for both an adult and a 1 year old child.

Committed effective doses from ingestion are strongly dependent on the gut uptake fraction (f_1) assumed in the calculation. As noted above, ICRP's default values were pessimistically assumed to apply to all of the activity in the object rather than just the soluble fraction. In the SERCO object characterisation study (Cowper, 2009), the ^{137}Cs and ^{90}Sr soluble fractions were determined for the beta-rich objects investigated by making measurements of three components: activity leached from the object by seawater; activity leached from the object by gut fluid simulant, and the activity resulting from total dissolution of the remaining object in a strong acid. For the seven particles with the highest ^{90}Sr activities (> 500 Bq), the activity in the saltwater and gut fluid leachates was very low, implying that uptake from the gastro-intestinal tract is expected to be much lower than that predicted by assuming that the f_1 value applies to all of the activity in the object. The true effective doses for ingestion of ^{90}Sr must therefore be much less than those listed in Table 88. For some of the smaller activity ^{90}Sr particles, a significant fraction of the total activity is present in the gut fluid leachate, but effective doses for these lower activity particles assuming the default f_1 value are typically only a few μSv.

For ^{137}Cs, the evidence from the SERCO particle leaching measurements is that particle solubilities are also relatively low, so the effective doses listed in Table 88 must again be overestimates.

The population of beta-rich objects and the corresponding probabilities of encounter were estimated within specified ^{137}Cs activity bands (Table 17). To obtain an upper estimate of the overall risk to a beach user for each activity band, estimates of committed effective dose have been made for the most active object within each band. The most active beta-rich particle found up until August 2009 contains 110 kBq ^{137}Cs and so is allocated to the 30 – 300 kBq range, while the particle with the highest ^{137}Cs content in the 3 – 30 kBq band has an activity of 30 kBq.

Table 89 summarises the committed effective doses that would result from the ingestion of these particles by a 3-month old infant, a 1-y old child and an adult, using the values of e(50) given in Table 88. The conservative assumptions are made that the ^{137}Cs:^{90}Sr ratio is the lowest found in the SERCO study (Cowper, 2009), ie, 0.61:1, and that the ICRP default gut uptake fractions (f_1) apply to all the activity in the particle and not just the mass fraction of the particle that is soluble. Making these assumptions, ingestion of the most active beta-rich particle would result in committed effective doses of 6.5 mSv, 15 mSv and 44 mSv for an adult, a 1-year old child and a 3 month old infant, respectively.

As discussed in Section 6.1, people with the medical condition called pica can deliberately ingest non-food materials such as sand and possibly large objects. In order to address this, committed effective doses that would result from the ingestion of beta-

rich stones have been calculated. The most active beta-rich stone found up untill August 2009 contained 875 kBq ^{137}Cs and so is allocated to the 300 – 3000 kBq band, while the stones with the highest ^{137}Cs contents in the 30 – 300 kBq and 3 – 30 kBq band contain 259 kBq ^{137}Cs and 30 kBq ^{137}Cs, respectively.

Table 88: Committed effective doses (E(50 or E(70)) for the highest activity found of each radionuclide in a beta-rich object

Nuclide	Maximum activity found (Bq)	Object ID	3 month old			1 year old child			Adult		
			f_1	e (ingestion) (Sv/Bq)	E(70) from max activity found (mSv)	f_1	e (ingestion) (Sv/Bq)	E(70) from max activity found (mSv)	f_1	e (ingestion) Sv/Bq	E(50) from max activity found (mSv)
^{60}Co	$2.35\ 10^{4}$	2007/11/12/06	0.6	$5.40\ 10^{-8}$	1.27	0.3	$2.7\ 10^{-8}$	$6.35\ 10^{-1}$	0.1	$3.4\ 10^{-9}$	$7.99\ 10^{-2}$
^{90}Sr	$4.88\ 10^{4}$	IM08010051 LSN 1129215	0.6	$2.30\ 10^{-7}$	$1.12\ 10^{1}$	0.4	$7.3\ 10^{-8}$	$3.56\ 10^{0}$	0.3	$2.8\ 10^{-8}$	$1.37\ 10^{0}$
^{99}Tc	$7.80\ 10^{1}$	IM08010009 LSN 1102165	1.0	$1.00\ 10^{-8}$	$7.80\ 10^{-4}$	0.5	$4.8\ 10^{-9}$	$3.74\ 10^{-4}$	0.5	$6.4\ 10^{-10}$	$4.99\ 10^{-5}$
^{106}Ru	$3.39\ 10^{3}$	2008/01/31/01[(a)]	-	-	$2.85\ 10^{-1}$	0.05	$4.9\ 10^{-8}$	$1.66\ 10^{-1}$	0.05	$7.0\ 10^{-9}$	$2.37\ 10^{-2}$
^{126}Sn	$1.69\ 10^{2}$	2008/02/05/02	0.04	$5.00\ 10^{-8}$	$8.45\ 10^{-3}$	0.02	$3.0\ 10^{-8}$	$5.07\ 10^{-3}$	0.02	$4.7\ 10^{-9}$	$7.94\ 10^{-4}$
^{125}Sb	$2.04\ 10^{3}$	2008/01/31/01[(a)]	-	-	$2.24\ 10^{-2}$	0.1	$6.1\ 10^{-9}$	$1.24\ 10^{-2}$	0.1	$1.1\ 10^{-9}$	$2.24\ 10^{-3}$
^{134}Cs	$1.93\ 10^{3}$	2009/01/21/01/SEL	1.0	$2.60\ 10^{-8}$	$5.02\ 10^{-2}$	1.0	$1.6\ 10^{-8}$	$3.09\ 10^{-2}$	1.0	$1.9\ 10^{-8}$	$3.67\ 10^{-2}$
^{137}Cs	$8.75\ 10^{5}$	2008/01/31/01[(a)]	-	-	$1.84\ 10^{1}$	1.0	$1.2\ 10^{-8}$	$1.05\ 10^{1}$	1.0	$1.3\ 10^{-8}$	$1.14\ 10^{1}$
^{137}Cs	$1.1\ 10^{5}$	2008/01/22/01	1.0	$2.10\ 10^{-8}$	2.31	1.0	$1.2\ 10^{-8}$	1.2	1.0	$1.3\ 10^{-8}$	1.3
^{154}Eu	$2.97\ 10^{2}$	2008/01/11/01	0.005	$2.50\ 10^{-8}$	$7.43\ 10^{-3}$	0.0005	$1.2\ 10^{-8}$	$3.56\ 10^{-3}$	0.0005	$2.0\ 10^{-9}$	$5.94\ 10^{-4}$

(a) Object ID 2008/01/31/01 is a stone that is too large to be inadvertently ingested, although it could be deliberately ingested by adults and older children

.

Table 89: Activities and committed effective doses for the beta-rich particles with the highest ^{137}Cs content in each activity band

^{137}Cs activity band (kBq)	Particle activity (kBq)		Committed effective dose (Sv)		
	^{137}Cs	^{90}Sr [a]	3-m old	1-y old	Adult
30 – 300	110 [b]	180	4.38×10^{-2}	1.45×10^{-2}	6.48×10^{-3}
3 – 30	30 [c]	49	1.19×10^{-2}	3.95×10^{-3}	1.77×10^{-3}

(a) ^{137}Cs:^{90}Sr ratio assumed to be the lowest found in the SERCO study (Cowper, 2009), ie, 0.61:1.

(b) Particle LSN 1146151

(c) Particle LSN 1135557

Table 90 summarises the committed effective doses that would result from the ingestion of stones with these activities by a 1 year old child and an adult, using the values of e(50) given in Table 88. No allowance is made for any possible ^{90}Sr content of the stone, since the evidence from the SERCO study indicates that the ^{137}Cs:^{90}Sr ratios for stones are very high. The conservative assumption is made that the ICRP default gut uptake fractions (f_1) apply to all the activity in the stone and not just the mass fraction of the stone that is soluble. Ingestion of the most active stone would result in doses of 11 mSv for both an adult and a 1 year old child.

Table 90: Activities and committed effective doses for the beta-rich stones with the highest ^{137}Cs content in each activity band

^{137}Cs activity band (kBq)	Object activity (kBq)		Committed effective dose (Sv)	
	^{137}Cs	^{90}Sr	1-y old	Adult
300 - 3000	875 [a]	0	1.05×10^{-2}	1.14×10^{-2}
30 – 300	259 [b]	0	3.11×10^{-3}	3.37×10^{-3}
3 – 30	30 [c]	0	3.59×10^{-4}	3.89×10^{-4}

(a) LSN 1147709

(b) LSN 1189583

(c) LSN 1148824

The risks of fatal cancer following ingestion of the most active beta-rich particle in each activity band are shown in Table 91, and for the most active beta-rich stone in each activity band in Table 92. The risks are for all cancers, calculated using the ICRP Publication 103 excess relative and additive risk models for all solid cancers and the UNSCEAR 2006 relative and additive risk models for leukaemia (Haylock, 2010). For simplicity, the same risk factors that were calculated for ingestion of ^{239}Pu (Section 8.4) have been taken to apply to ingestion of the radionuclides in beta-rich objects. For these radionuclides, doses are protracted over shorter periods than for plutonium, but this could result in increases in the risk factors of only 20-30%, well within the uncertainties in the risk factors themselves. It should be noted that uncertainties on these risk factors are likely to be large, particularly for infants and children.

Table 91: Lifetime risk of death from all cancers after ingestion of the most active beta-rich particle in each activity band (Table 89)

Age group	Age at time of intake	^{137}Cs activity band (kBq)	Committed effective dose (Sv)	Lifetime risk (%)
3-month old infant	100 days	300 - 3000	-	-
		30 – 300	4.38×10^{-2}	0.6%
		3 – 30	1.19×10^{-2}	0.2%
1-year old child	1 year	300 - 3000	-	-
		30 – 300	1.45×10^{-2}	0.2%
		3 – 30	3.95×10^{-3}	0.06%
Adult	20 years	300 - 3000	-	-
		30 – 300	6.48×10^{-3}	0.06%
		3 – 30	1.77×10^{-3}	0.02%

^{137}Cs:^{90}Sr ratio assumed to be the lowest found in the SERCO study (Cowper, 2009), ie, 0.61:1

Table 92: Lifetime risk of death from all cancers after ingestion of the most active beta-rich stone in each activity band (Table 90)

Age group	Age at time of intake	^{137}Cs activity band (kBq)	Committed effective dose (Sv)	Lifetime risk (%)
1-year old child	1 year	300 - 3000	1.05×10^{-2}	0.2%
		30 – 300	3.11×10^{-3}	0.05%
		3 – 30	3.59×10^{-4}	0.006%
Adult	20 years	300 - 3000	1.14×10^{-2}	0.1%
		30 – 300	3.37×10^{-3}	0.03%
		3 – 30	3.89×10^{-4}	0.004%

^{90}Sr content of the stones assumed to be negligible

9.5 Inhalation of beta-rich particles

The highest activity particle found in the SERCO study (Cowper, 2009) that could deposit in the lungs if inhaled has an aerodynamic diameter of 29 μm and a ^{137}Cs activity of 8.4 kBq. If the ^{137}Cs:^{90}Sr ratio is pessimistically assumed to be 0.61:1, then a dose calculation for a one year old child performed using default ICRP parameter values (in particular an activity median aerodynamic diameter of 1 μm, which is associated with the highest dose per unit intake values) indicates an effective dose of about 6 mSv. Values for older children and adults would be lower. A more realistic calculation would result in dose estimates significantly less than 6 mSv.

Since effective doses arising from inhalation of beta-rich particles are low, the probability of deterministic effects arising from inhalation is essentially zero.

9.6 Summary of results for doses and risks to health from beta-rich objects

9.6.1 Skin doses from beta-rich objects: deterministic effects

SERCO's particle characterisation study investigated 26 beta-rich particles, and AMEC carried out radiological assessments for 19 of these particles, using data provided by SERCO. The highest (1 cm^2, 70 μm) dose rate for a particle was 29.7 mGy h^{-1}, calculated by AMEC. The ^{137}Cs activity of this particle was 32.4 kBq and the ^{137}Cs:^{90}Sr ratio was approximately 0.66:1. The highest measured (1 cm^2, 70 μm) dose rate was 26.5 mGy h^{-1}, measured by TLD (thermo-luminescence dosimetry). The higher dose rate particles generally have higher ^{90}Sr contents, because the dose rate per unit activity for a hypothetical particle containing only ^{90}Sr is typically about six times higher than for a similar particle containing only ^{137}Cs. The highest dose rate for a particle whose content was dominated by ^{137}Cs was about 12 mGy h^{-1}, measured by TLD.

The exposure time required for a particle giving a dose rate of 29.7 mGy h^{-1} to reach the 2 Gy threshold for localised skin ulceration is 67 hours. The ^{90}Sr content of the highest activity beta-rich particle found up till August 2009 (110 kBq ^{137}Cs) was not measured, but making the conservative assumption that the ^{137}Cs:^{90}Sr ratio for this particle is equal to that for the particle with the highest calculated dose rate (ie, 0.66:1), the (1 cm^2, 70 μm) dose rate from this hypothetical particle would be approximately 100 mGy h^{-1}. For this particle, the exposure time required to reach the threshold would be approximately 20 hours. It is very unlikely that particles could remain in stationary contact with the skin for such lengths of time.

If it is assumed that the maximum feasible exposure time is 8 hours, and the conservative assumption of a ^{137}Cs:^{90}Sr ratio of 0.66:1 is also made, then a particle would have to have an activity of at least 270 kBq ^{137}Cs in order for the 2 Gy threshhold to be reached. For a hypothetical particle containing only ^{90}Sr, the activity required to reach the 2 Gy threshhold would be approximately 400 kBq.

For stones (defined as an object of diameter equal to or greater than 2 mm), the highest (1 cm^2, 70 μm) dose rate was 19.8 mGy h^{-1}, measured by TLD. The threshold for ulceration / moist desquamation resulting from contact with extended radioactive sources is 10 – 20 Gy. The exposure time required to reach the 10 Gy threshold for a pebble/stone giving a dose rate of 19.8 mGy h^{-1} is 500 hours. For a stone with a ^{137}Cs activity equal to that of the highest activity beta-rich stone found up until August 2009 (875 kBq ^{137}Cs), the (1 cm^2, 70 μm) dose rate would be approximately 200 mGy h^{-1}, and the exposure time required to reach the 10 Gy threshold would be approximately 50 hours. It is extremely unlikely that pebbles or stones could remain in contact with the skin for times as long this.

9.6.2 Skin doses from beta-rich objects: stochastic risk

An object containing ^{137}Cs giving an absorbed dose of 2 Gy to 1 cm^2 of skin would give an effective dose of about 4 μSv in adults about 25 μSv in 1 year old children and no greater than 100 μSv in 3 month old infants. None of the objects found to date result in

skin doses that approach the threshold for skin ulceration, so it is clear that stochastic risks resulting from beta-rich objects in contact with the skin are negligible.

9.6.3 Ingestion of beta-rich objects: deterministic effects

The highest ^{137}Cs particle activity found up until August 2009 is 110 kBq. The ^{90}Sr content was not measured, but if ^{137}Cs is the only radionuclide present in this particle, then the upper bounds for the maximum absorbed doses to the rectosigmoid colon resulting from ingestion of this particle are 2.6 mGy and 5.3 mGy for an adult and a 1 year old child, respectively. It is assumed that the particle remains in contact with the gut wall during transit, and that the default transit time applies. If a ^{137}Cs:^{90}Sr ratio is conservatively assumed to be 0.61:1, the corresponding upper bounds for maximum absorbed doses would be 19 mGy and 40 mGy for an adult and a 1 year old child, respectively. It is estimated that the absorbed dose to the rectosigmoid colon for a 3 month old infant would be about four times the value for a 1 year old child.

The highest activity beta-rich object is a stone with an activity of 8.75 10^5 Bq. Since it has an average diameter of 35 mm, inadvertent ingestion is not possible although adults and older children could deliberately ingest such an object. Conservative estimates of the upper bounds for the maximum doses resulting from ingestion of this stone are 21 mGy and 42 mGy for an adult and a 1 year old child, respectively. These estimates neglect self absorption by the stone, and must therefore be overestimates. No allowance is made for any possible ^{90}Sr content of the stone, since the evidence from the SERCO study indicates that the ^{137}Cs:^{90}Sr ratios for stones are very high.

Predicted absorbed doses are orders of magnitude less than the threshold value for acute effects in the colon, which is estimated to be 23 Gy.

9.6.4 Ingestion of beta-rich objects: stochastic risk

For a particle containing 110 kBq ^{137}Cs, and assuming ^{137}Cs is the only radionuclide present, committed effective doses resulting from ingestion would be 1.3 mSv, 1.2 mSv and 2.3 mSv, for an adult, a 1 year old child and a 3 month old infant, respectively. Assuming a ^{137}Cs:^{90}Sr ratio equal to the lowest value found in the SERCO particle characterisation study (ie, 0.61:1), committed effective doses would be 6.5 mSv, 15 mSv and 44 mSv for an adult, a 1 year old child and a 3 month old infant, respectively. It is conservatively assumed that the ICRP default gut uptake fractions (f_1) apply to all the activity in the particle and not just the mass fraction of the particle that is soluble.

The corresponding lifetime risk of exposure-induced death from all cancers is estimated to be 0.06% for an adult, 0.2% for a 1 year old child and 0.6% for a 3 month old infant. Uncertainties on these risk estimates are likely to be large, particularly for children.

Deliberate ingestion of the stone with a ^{137}Cs activity of 8.75 10^5 Bq would result in an effective dose of 11 mSv for both an adult and a 1-year old child. The corresponding lifetime risk of exposure-induced death from all cancers is estimated to be 0.1% for an adult and 0.2% for a 1 year old child. Uncertainties on these risk estimates are likely to be large, particularly for children.

9.6.5 Inhalation of beta-rich particles: stochastic risk

The highest activity particle found in the SERCO study (Cowper, 2009) that could deposit in the lungs if inhaled has an aerodynamic diameter of 29 μm and a ^{137}Cs activity of 8.4 kBq. If the ^{137}Cs:^{90}Sr ratio is pessimistically assumed to be 0.61:1, then a dose calculation for a one year old child performed using default ICRP parameter values (in particular an activity median aerodynamic diameter of 1 μm, which is associated with the highest dose per unit intake values) indicates an effective dose of about 6 mSv. Values for older children and adults would be lower. A more realistic calculation would result in dose estimates significantly less than 6 mSv. Effective doses for all age groups arising from inhalation of a beta-rich particle are estimated to be no more than 6 mSv, and are likely to be significantly less than that value. Corresponding lifetime risks for all age groups would be no more than 0.1% and again are likely to be significantly less than that value.

9.6.6 Inhalation of beta-rich particles: deterministic effects

Since effective doses arising from inhalation of beta-rich particles are low, the probability of deterministic effects arising from inhalation is essentially zero.

10 OVERALL RISKS TO HEALTH

The annual probability of coming into contact with an object while spending time on a beach has been estimated for both alpha-rich and beta-rich objects (Section 7). When evaluating the overall risks to the health of a beach user in the unlikely event that contact with an object does occur, effects on health arising from both deterministic effects and stochastic effects must be considered:

Deterministic effects. If absorbed doses are well below thresholds, then deterministic effects will not occur whatever the probability of encounter (Sections 8.6 and 9.1).

Stochastic effects. The overall risk to the beach user may be determined by multiplying the annual probability of coming into contact with an object by the risk that that person would contract a fatal cancer during his or her lifetime if contact with the object did occur (Sections 8.2 and 9.4). It is justified to multiply the two factors together since they are independent of each other (ICRP, 2007). The result of this calculation is the probability that the person would contract a fatal cancer at some point during his or her lifetime as a result of using a beach for a period of 1 year.

The overall risks from alpha-rich and beta-rich objects on the five beaches considered are discussed below in Sections 10.1 (stochastic risks) and 10.2 (deterministic effects). Some general conclusions on the health risk to people using other beaches along the Cumbrian coastline are presented in Section 10.4.

The overall risks discussed are derived using cautious assumptions about the probability of encountering an object and the activity content of these objects. In most cases, risks are evaluated assuming that the objects contain the highest activity content of all objects retrieved from the beaches in each activity range considered up until August 2009 and that the highest probabilities of encountering an object apply (using the 97.5th percentile

of the distribution across all beach users). Beach users with higher than average beach occupancy are covered within these conservative estimates.

10.1 Overall risks of fatal cancer for a beach user from exposure to particles

The overall risk to a beach user of fatal cancer must take into account both the probability that a particle may be encountered by the person and the risk of fatal cancer in the unlikely event that the person does encounter such a particle. The probability of encounter depends on the activity of the particle, (with lower activity particles being associated with higher probabilities of encounter), and so the overall risk to the beach user has been determined separately for each of the activity bands defined in Table 5.

As noted in Section 8, the greatest potential for stochastic effects on health is from the ingestion of alpha-rich and beta-rich particles. Table 93 shows the highest estimated lifetime risk of fatal cancer for an adult resulting from one year's potential exposure by ingestion. The estimated probability of ingesting a particle (corresponding to the 97.5th percentile of the distribution) and the resulting overall risk to the beach user is shown for the highest activity particle in each activity band. Table 94 shows the same information for young children (1 year old).

Table 93 Highest overall risks of fatal cancer for an adult beach user associated with possible ingestion of alpha-rich and beta-rich particles as a result of using a beach for a period of 1 year

Activity band, kBq	Highest activity particle in activity band, kBq[a]	Effective dose[b], mSv	Lifetime risk of cancer if particle ingested, % [c]	Highest annual probability of ingesting a particle[d]	Overall risk of fatal cancer
Alpha-rich					
1000 (>300)	634	20	0.2	$4\ 10^{-12}$	$8\ 10^{-15}$
100 (30 – 300)	200	6	0.06	$2\ 10^{-10}$	$1\ 10^{-13}$
10 (3 – 30)	30	0.8	0.007	$1\ 10^{-8}$	$7\ 10^{-13}$
Total					$8\ 10^{-13}$
Beta-rich					
1000 (>300)[e]	-	-	-	-	-
100 (30 – 300)	100	6.5	0.06	$2\ 10^{-11}$	$1\ 10^{-14}$
10 (3 – 30)	30	1.8	0.02	$4\ 10^{-10}$	$8\ 10^{-14}$
Total					$9\ 10^{-14}$
Total overall risk					$9\ 10^{-13}$

a) Activity of radionuclide detected: ^{241}Am for alpha-rich particles; ^{137}Cs for beta-rich particles.

b) Calculated doses take account of other radionuclides measured in the particles that will contribute significantly to the dose. For alpha-rich particles, the dose is from ^{241}Am, ^{238}Pu and ^{239}Pu. For beta-rich particles, the dose is calculated for ^{137}Cs and ^{90}Sr and a conservative ratio of 1.0: 1.6 ^{137}Cs : ^{90}Sr has been assumed.

c) Lifetime risk is calculated for the highest activity particle in each activity band

d) Value is the 97.5th percentile of the distribution for all beach users.

e) No beta-rich particles have been found in this activity band.

Ingestion of alpha-rich particles gives rise to overall risks that are about an order of magnitude higher than those for the ingestion of beta-rich particles for adult beach users and about two orders of magnitude higher for young children. Nevertheless, the highest overall risks are estimated to be extremely small, with the chance of dying from cancer as a result of one year's potential exposure being less than 1 in 100,000 million (for ingestion of an alpha-rich particle by a 1 year old child). The highest overall risks are from the lower activity particles because the probability of encountering these is several orders of magnitude higher than for the highest activity particles, as shown in Table 93 and Table 94. The probability of ingesting an alpha-rich particle with the highest activity found (containing 634 kBq ^{241}Am) on the beaches around the Sellafield site is extremely low, a factor of 10,000 times less than the values for the 3 – 30 kBq ^{241}Am band.

Table 93 and Table 94 present the overall risk that a fatal cancer could occur during the lifetime of a beach user arising from use of the beach over a period of one year. Making the pessimistic assumption that the population of objects on the beaches remains at current levels over the lifetime of a beach user, the overall risk from a lifetime's potential exposure is still extremely low, being less than 1 in 1000 million.

It is possible that individuals who regularly use the beaches are also high consumers of locally caught seafood. No direct monitoring of offshore sediments has been carried out that can be used to clarify the quantity and nature of radioactive particles that could become incorporated in seafood along the west Cumbrian coastline, although this is being considered for the future. In the meantime, the likelihood of members of the public ingesting a radioactive particle from the consumption of seafood and the associated health risks has been estimated using a conservative scoping approach as described in Section 6.6 and Appendix I. Currently available information has been used and the assumption made that an individual is a high-rate consumer of all species of shellfish identified during the latest habit survey in 2008 (Cefas, 2009). The overall health risk to an individual with high beach occupancy as well as a high consumption of seafood is still very small and lower than 1 in 100 million (10^{-8}) per year. It should be noted that an investigation of the Cefas monitoring database for incidences of high activities in mollusc samples (Cefas, 2008b) did not identify any samples where the activity levels recorded approached those in analyses of particles found on the beaches.

Table 94: Highest overall risks of fatal cancer for a young child beach user associated with possible ingestion of alpha-rich and beta-rich particles as a result of using a beach for a period of 1 year

Activity band (central value), kBq	Highest activity particle in activity band, kBq[a]	Effective dose[b], mSv	Lifetime risk if particle ingested, % [c]	Highest annual probability of ingesting a particle[d]	Overall risk of fatal cancer
Alpha-rich					
1000 (>300)	634	55	1	-[e]	-
100 (30 – 300)	200	14	0.3	$6\ 10^{-10}$	$2\ 10^{-12}$
10 (3 – 30)	30	2	0.04	$3\ 10^{-8}$	$1\ 10^{-11}$
Total					$1\ 10^{-11}$
Beta-rich					
1000 (>300)[e]	-	-	-	-	-
100 (30 – 300)	100	15	0.2	$7\ 10^{-11}$	$1\ 10^{-13}$
10 (3 – 30)	30	4	0.06	$3\ 10^{-10}$	$2\ 10^{-13}$
Total					$3\ 10^{-13}$
Total overall risk					$1\ 10^{-11}$

a) Activity of radionuclide detected: ^{241}Am for alpha-rich particles; ^{137}Cs for beta-rich particles.

b) Calculated doses take account of other radionuclides measured in the particles that will contribute significantly to the dose. For alpha-rich particles, the dose is from ^{241}Am, ^{238}Pu and ^{239}Pu. For beta-rich particles, the dose is calculated for ^{137}Cs and ^{90}Sr and a conservative ratio of 1.0: 1.6 ^{137}Cs : ^{90}Sr has been assumed.

c) Lifetime risk is calculated for the highest activity article in each activity band

d) Value is the 97.5th percentile of the distribution for all beach users.

e) Particles of the activity only found on Sellafield beach and there is no evidence that young children spend time on this beach.

f) No beta-rich particles have been found in this activity band.

10.2 Likelihood of deterministic effects from exposure to particles

The most important factor to address when considering the likelihood of deterministic effects is whether the threshold for the effect could be exceeded. As noted in Sections 8.8 and 9.5, the exposure routes with the greatest potential for deterministic effects on health are direct beta-gamma irradiation of the skin resulting from stationary contact of beta-rich and alpha-rich objects with the skin, and ingestion of beta-rich objects.

For an object to deliver a radiation dose to the skin such that there is a likelihood of it giving rise to very localised ulceration of the skin, it has to remain in stationary contact with the same small area of skin. This is very unlikely in an environment where people are on a beach undertaking a range of activities.

The threshold dose for localised skin ulceration is approximately 2 Gy, and for beta-rich particles the predicted skin dose rate from the highest ^{137}Cs activity particle found up untill August 2009 would be approximately 100 mGy h^{-1} (making a conservative assumption about the ^{90}Sr content of the particle). The exposure time required to reach this threshold is 20 hours. The skin dose rate from the alpha-rich particle with the highest ^{241}Am activity found up untill August 2009 is approximately 8 mGy h^{-1} and the exposure time to reach the same threshold is about 250 hours. It is very unlikely that particles could remain in

stationary contact with the skin for times as long this, and it can reasonably be concluded that skin dose thresholds could not be exceeded by objects with these activities.

The threshold dose for deterministic effects to the gastro-intestinal tract is 23 Gy, and the highest assessed absorbed dose to the rectosigmoid colon from ingestion of beta-rich particles is 42 mGy, a factor of 500 less than the threshold. Clearly, the threshold dose could not be exceeded.

Given these reassuring findings, the probability of encountering such objects is of secondary importance. However, it may be noted that the annual probability of encountering a beta-rich object on the skin, either directly or from an object trapped in clothing or shoes, will be less that 10^{-5} (chance of 1 in 100,000 per year) based on the 97.5^{th} percentile of the distribution of beach users. For a typical beach user, the likelihood of getting an object on the skin is at least a factor of ten lower.

10.3 Objects with low activity levels

It is not possible to conclude from the monitoring data whether there are very few objects on the beaches containing less than a few kBq or whether they mostly cannot be detected with the available detection systems. The risk of fatal cancer from ingestion of alpha-rich particles with this activity content is estimated to be much less than 1 in a million, the level of risk that HSE considers to be the upper limit for an acceptable level of risk (2001). Even if probabilities of encounter approach unity, the overall risk to a beach user would not exceed this. For beta-rich particles, it is estimated that tens of particles would have to remain in stationary contact with a small area of skin for several days before any localised skin ulceration would occur: this is not a realistic scenario. It should also be noted that if a lot of very small, low activity objects are present on the beaches they will become part of the ambient levels of contamination on the beach which are routinely monitored (see RIFE reports, eg, Cefas, 2009a).

10.4 Risks for other beaches

The evidence from the beach monitoring programme and habit surveys suggests that users of other beaches along the West Cumbrian coastline are no more likely to come into contact with a radioactive object than they are on the 5 beaches considered in detail in this study. The monitoring on some of the beaches has been limited both in extent and frequency and so it cannot be ruled out that some high activity objects may be present. However, given that the highest activity objects which have been found on beaches close to the Sellafield site do not give rise to health risks of concern, it is highly unlikely that health risks would be of concern for the beaches further away.

10.5 Overall risks from exposures to stones

As noted in Section 6, there may be beach users with the rare medical condition known as pica, one aspect of which can be the deliberate ingestion of large non-nutritional

objects. In the unlikely event that an adult with pica spends time on the beaches, the overall risk associated with ingesting an alpha-rich stone is estimated to be at least an order of magnitude lower than the probability of ingesting a particle. For beta-rich stones, the overall risk is about the same as that for beta-rich particles. As discussed in Section 2.3, the majority of beta-rich stones have been found on Sellafield beach, which it should be noted is used by very few individuals; the risks to users of other beaches from the ingestion of beta-rich stones would be extremely low and about two orders of magnitude lower than that from ingestion of beta-rich particles.

The threshold dose for skin ulceration as a result of contact with a stone, at 10 Gy, is higher than that for a particle because a stone is a distributed source rather than a point source. The skin dose rate from the beta-rich stone with the highest ^{137}Cs activity found up until August 2009 would be approximately 200 mGy h^{-1} and the exposure time to reach the threshold is about 50 hours. It is extremely unlikely that an object could remain in stationary contact with the skin as long as this and it can reasonably be concluded that skin dose thresholds could not be exceeded by objects with these activities.

10.6 Overall health risks for three month old infants

For completeness, the health risks to 3 month old infants have also been assessed and are discussed in Sections 8 and 9. The main difference between the health risks for 3 month old infants and other children is for the ingestion of objects. If a 3 month old infant ingested an object, the committed effective doses received would be higher than those for a 1 year old child. In the unlikely event that an alpha-rich particle with the activity given in Section 8.4 was ingested, the estimated dose would be in the region of 300 mSv with the corresponding lifetime risk of death from all radiation-induced cancers estimated to be about 4%. For a beta-rich particle with the activity given in Section 9.6.4, the estimated committed effective dose would be in the region of 40 mSv if it is conservatively assumed that the ICRP default gut uptake fractions (f_1) apply. The corresponding lifetime risk of death from all radiation-induced cancers is estimated to be about 0.6% (see Section 9.4). Ingestion of stones has not been considered because this is not a realistic exposure pathway for infants.

As 3 month old infants are not mobile, the probability of encountering an object on the beach will be significantly lower than the values estimated for a 1 year old child given in Table 94 Even if it is very cautiously assumed that the probability of a 3 month old infant encountering an object is the same as that of a 1 year old child, the lifetime risk of death from all radiation-induced cancers is very low and less that 10^{-10} per year. In reality, the risks will be lower than those for young children who are mobile on the beach.

Considering deterministic health effects from ingestion of a particle, the calculated absorbed dose for a 3 month old infant from ingestion of a beta-rich particle with the activity given in Section 9.4 would be approximately 100 times less than the threshold value for acute effects in the colon (23 Gy) (Supporting Scientific Report, Section 9.3).

The probability of encountering an object on the beach for a 3 month old infant will be significantly lower than the values estimated for a 1 year old child given in Table 94 because they are not active. Even if it is very cautiously assumed that the probability of a

3 month old infant encountering an object is the same as that of a 1 year old child, the overall health risk are very low and less that 10^{-10} per year. In reality, the overall health risks will be lower than those for young children who are active on the beach.

10.7 Overall risks arising from uptake from a contaminated wound

Appendix E presents the results of a scoping calculation of the overall risk associated with alpha-rich particles embedded in a wound. Stochastic risk arising from uptake of radionuclides from the wound site is the most important factor to consider. Overall risks of fatal cancer were estimated to be of the order of 10^{-12} – 10^{-13}. Given the uncertainties involved in this scoping calculation, it is concluded that overall risks from ingestion and from uptake via a wound for alpha-rich particles are broadly similar.

10.8 Public perception of risk

The main purpose of this study is to quantify the levels of risk to health for people who may encounter radioactive objects on beaches in the vicinity of the Sellafield nuclear site. Risks of cancer, or risks of death, are often expressed as a percentage (eg, a 0.001% risk of fatality), or as an odds ratio (eg, a chance of 1 in 10,000 of contracting cancer). However, perception of risk is not based simply on numerical estimates of the probability of occurrence of particular effects on health. The risks to health arising from exposure to materials that cannot be seen, and exposures over which the person has little or no control, are usually perceived by people to be elevated above those indicated by an objective, quantitative assessment. It may thereore be helpful for people to compare the overall risks estimated from radioactive objects on the beaches with other every day health risks that are relevant to beach users. To aid this discussion, reference has been made to a Health and Safety Executive publication, Reducing Risks, Protecting People (HSE, 2001).

10.8.1 'Acceptable', 'tolerable' and 'unacceptable' levels of risk

HSE has defined levels of risk of death that correspond to what they consider as "acceptable", "tolerable" and "unacceptable" (HSE, 2001). Unacceptable risks are those that the HSE would aim to prevent occurring regardless of the benefits that incurring such a risk may bring. At the other end of the scale are those risks which the HSE regard as acceptable, that is, they do not pose a significant problem and excessive regulation to reduce the risk further is not warranted. This level of risk corresponds to what the HSE believes members of the public would view as insignificant or trivial in their daily lives. In between these two regions of risk lie those risks described as tolerable where the HSE expects measures to be employed to reduce risks further, if it is not prohibitively expensive to do so, by means of an optimisation process.

HSE believes that an individual risk of death of one in a million per annum for both workers and the public corresponds to a very low level of risk and should be used as a guideline for the boundary between broadly acceptable and tolerable levels of risk (HSE, 2001). For the boundary between the tolerable and unacceptable risk of death, HSE

suggest a value of 1 in 10,000 per annum for members of the public who have a risk imposed on them.

To put these values into perspective, activities that many people undertake regularly have a risk associated with them that lies in the "tolerable" range of the risk spectrum. An example of such a risk is the risk of death in a transport related accident (approximately 10^{-5} per year or 1 in 100,000). Indeed many activities which people are prepared to accept in their daily lives for the benefits they bring, for example using gas and electricity, entail or exceed levels of risk that the HSE views as acceptable.

10.8.2 Representative every day health risks

Information was collected on risks for the general population of the UK that can be associated with beach use; Table 95 presents some of the data. These risks are mainly based on information from the 2005 UK mortality statistics database (ONS, 2005). It is not expected that such statistics will vary significantly from year to year. In order to provide some robustness against small changes that may occur year on year, the risks in Table 95 are presented only within order of magnitude bands.

Table 95: Representative every day risks

Probability	Risk
10^{-5} - 10^{-4}	Annual risk of death from malignant melanoma of the skin
10^{-6} - 10^{-5}	Annual risk of death from all leisure activities in UK coastal waters
	Maximum annual probability of encountering a radioactive particle on Sandside beach from contaminated fuel fragments from the Dounreay nuclear site (Smith and Bedwell, 2005)
	Risk of blindness from toxocara parasite
10^{-7} - 10^{-6}	Annual risk of death when angling in UK coastal waters
	Annual risk of death when swimming in UK coastal waters
	Annual risk of death in UK marine waters reported to the MCA for the summer months (start May – end September)
10^{-8} - 10^{-7}	Annual risk of death from a dog bite
	Annual risk of death when canoeing in UK coastal waters
	Annual risk of death in UK marine waters reported to the MCA for the winter months (start October – end April)
	Annual risk of death from insect stings

10.8.3 Information specific to the Cumbrian coast

An attempt was also made to collect information on health risks associated specifically with activities carried out on the Cumbria coast, but the available data was sparse. Nevertheless, it is worthy of note that the Maritime and Coastguard Agency (MCA) (MCA, 2009) have reported that, between 2005 and 2009, six deaths were reported around St Bees and three deaths were reported at Ravenglass, with ten injuries also reported at St Bees.

11 RELIABILITY OF THE ASSESSMENT OF OVERALL RISK TO BEACH USERS

11.1 Robustness of the approach

The approach adopted made use of all the information available at the time of the study and is considered to be adequate for its intended purpose, ie, to determine whether risks to the health of beach users could be significant. Estimates of the population of objects on beaches were based on data on object finds from the beach monitoring programme and on information on the sensitivity of the detection system. All monitoring data collected from the Groundhog Evolution2^{TM} detection system which was in use up to August 2009 has been taken into account; the adequacy of beach monitoring for the assessment of risks to health is discussed in Section 11.2. It is considered that detection sensitivity is well characterised for detection of objects containing ^{241}Am, ^{137}Cs and ^{60}Co; the characterisation of capabilities for direct detection of ^{90}Sr in objects is discussed in Section 12.1.2.

A comprehensive investigation of activities engaged in by beach users was carried out, making use of detailed habit surveys. Distributions rather than single values were defined for the time spent on beaches by each of the beach use groups and age groups identified, and specific consideration was given to “high occupancy” beach users (ie, people for whom time spent on the beaches is at the upper end of these distributions). These distributions allowed full account to be taken of the range of beach occupancy times and beach activities in determining probabilities than a radioactive object could be encountered.

Radiation doses and risks to health have been assessed for all significant pathways by which a person could encounter a radioactive object and incur a radiation dose. Specific assessments have been made of the radiation doses that would result from encountering the highest activity objects that have been found by the beach monitoring programme. Dose assessments used the most up-to-date information, data and models, and are considered to provide reliable assessments of risks to health. There are inevitably uncertainties associated with the estimation of the likelihood that beach users encounter an object while using the beaches. All potential exposure pathways that could lead to beach users coming into contact with an object have been considered. The use of distributions on the parameter values that describe the exposure pathways encompasses both the variability across the population and the uncertainty in the parameter value. The uncertainty in the calculated probabilities of encountering an object is not of significance in relation to the low levels of overall health risks that have been determined.

11.2 Adequacy of beach monitoring

The detection capability of the beach monitoring systems in use is such that any beta-rich object that would give rise to skin ulceration could easily be detected with 100% detection probability to a depth of 30 cm through measurement of their ^{137}Cs content, provided it can be assumed that objects do not have Cs:Sr ratios significantly less than the lowest

value found to date (ie, 0.61:1). Only if such objects had Cs:Sr ratios below about 0.25:1 would it be possible for some of them to remain undetected.

Capabilities of the beach monitoring systems for detection of alpha-rich objects are more limited because of the fundamental physical nature of the detection process, specifically because of the absorption within the beach material of the low energy photons resulting from radioactive decay of ^{241}Am. The ingestion of alpha-rich particles is the only exposure pathway that could give rise to significant health risks if a particle is encountered and then only if the particle activity approaches or exceeds that of the most active particles found. An alpha-rich particle containing 100 kBq ^{241}Am can be detected by Groundhog Evolution2™ with a probability greater than about 5% only to a depth of 5cm and an alpha-rich particle containing 1000 kBq ^{241}Am can be detected with a probability greater than about 5% only to a depth of 10 cm. Thus, the capabilities of beach monitoring systems for detection of alpha-rich objects at depth may not meet the requirements needed to ensure the detection of particles that could give rise to a significant risk to health in the event that ingestion occurs. The performance of the recently-introduced Synergy system should offer improved sensitivity, but it is extremely unlikely that it will be capable of detecting 1000 kBq ^{241}Am particles with 100% efficiency at depths of 10 – 15 cm.

12 MAJOR UNCERTAINTIES AND RECOMMENDATIONS FOR FUTURE WORK

The sources of major uncertainty in this assessment of risks to health and recommendations for future work are discussed below. Those recommendations that would help to confirm that protection is adequate are distinguished from those that would improve the assessment of risks to health.

12.1 Confirmation that protection of the public is adequate

12.1.1 Beach monitoring programme

HPA has previously advised the EA that the detection of alpha-rich objects with activities of greater than 10^7 Bq of alpha-emitting radionuclides should prompt an urgent review of the risks to public health (Appendix A). No such objects have been detected to date, but continued regular monitoring of Sellafield beach and monitoring at one or two other beaches with high public occupancy will provide regulators and the public with continued reassurance that risks associated with radioactive objects in the environment remain very low.

12.1.2 Detection of objects containing ^{90}Sr

To date, objects containing ^{90}Sr have not been detected through direct measurement of their ^{90}Sr content, but rather as a result of detection of their ^{137}Cs content. Whether there may be significant numbers of objects on the beaches that contain only ^{90}Sr, or have very low ^{137}Cs:^{90}Sr ratios, is therefore an open question. As noted in Section 4.1.5, there is some doubt as to whether the Groundhog Evolution2™ system achieved the expected

performance for detection of ^{90}Sr particles. Therefore, it is recommended that further work should be carried out to determine the reasons for this discrepancy, with the aim of improving detection capabilities for objects that contain predominantly ^{90}Sr, if practicable. If objects with very low ^{137}Cs:^{90}Sr ratios are present, the aim should be to improve detection of objects with ^{90}Sr activities in excess of 400 kBq with the objective of detecting particles that could result in skin doses equal to the 2 Gy threshold for ulceration over an exposure period of 8 hours.

12.1.3 Inhalation of small alpha-rich particles

The size and the activity of alpha-rich particles appear to be linked; the larger the particle, the higher its activity (see Section 8.5). The minimum detectable activity of the Groundhog Evolution2™ system corresponds to an aerodynamic diameter of about 300 µm, and this raises the question whether smaller particles with lower activities are present but remain undetected by beach monitoring. For particle sizes that are likely to be inhaled (that is, entering the nose or mouth), the effective dose resulting from inhalation of a *single* particle would be no greater than a few mSv. The possibility remains that larger numbers of particles at the smaller particle sizes, perhaps formed by the sequential break-up of larger particles, could be inhaled and then penetrate to and deposit in the lungs. It is recommended that environmental monitoring data should be reviewed to determine whether this potential pathway of exposure needs further evaluation. Results of the existing high-volume air sampling programme should be reviewed to determine whether the alpha-contamination component of the aerosol at or near the beaches being monitored is of any radiological concern. An analysis should be performed to determine whether the sequential break-up of larger particles could give rise to a component of contamination on the beaches or in the local atmospheric environment that is distinguishable from the ubiquitous contamination present in the beach environment. If so, environmental monitoring data including the routine monitoring of ambient contamination levels in beach sediments (see RIFE report, eg, Cefas, 2009) should be reviewed to determine if the available data indicate whether this component is present. Consideration should also be given as to what monitoring and measurements could be performed to identify and characterise the component.

12.2 Improvements in the assessment of health risks

12.2.1 Beach monitoring

In some circumstances, uncertainties in the estimate of the number of objects present can be quite large. If only a few objects have been found and particularly where they are present at depths where the probability of detection is low, the uncertainty in the estimate of the actual number of objects in a given monitored area can be large.

This is particularly noticeable for Drigg beach, where only a small number of alpha-rich objects have been found, but the estimated population of particles is higher than for any of the other beaches considered (see Section 4.2, Table 22). Only 30% of Drigg beach has been monitored, whereas for Braystones, Seascale, Sellafield and St Bees beaches, the total areas monitored exceed the area of each beach because of repeated monitoring.

Uncertainties in the estimates for Drigg beach can only be reduced as more monitoring data becomes available.

The accuracy of the assessment of the population of objects (Section 4.2) would be improved if more accurate data were available on the depths of particles detected and retrieved as a result of the beach monitoring programme. Current procedures could be reviewed to determine whether more accurate and reliable measurements of depth could be made.

12.2.2 Performance of the Groundhog Synergy system

In August 2009 a new system, Groundhog Synergy, was brought into operation as a replacement for the Groundhog Evolution2™ system (see Section 4.4). The new system is more sensitive to particles containing ^{241}Am and as expected the number of alpha-rich objects being found has increased. This increased find rate does not necessarily mean that there is an increase in the number of objects actually present on the beaches, since the increase could be completely attributable to improvements in sensitivity. Further work is needed to resolve the issue. Firstly, a comparison should be made of the numbers of objects found and their activities, before and after the introduction of Synergy. The comparison should be made for measurements made over the same areas of beach. Since detection probability for ^{241}Am decreases rapidly with increasing object depth, the comparison is best made for objects detected on or very close to the surface, although comparisons at greater depths will also be useful. Secondly, the detection probabilities for Synergy should be quantified by carrying out an investigation analogous to that carried out for Groundhog Evolution (Scientific Basis Report, Section 4.1). A decision should then be made as to whether there is a need to review the assessment of overall risk to beach users taking into account data on the increased number of objects detected by Synergy.

12.2.3 Detection of alpha-rich objects at depth

Capabilities of the beach monitoring systems for detection of alpha-rich objects at depth are limited by the physical nature of the detection process and also by currently available technology. These capabilities may not meet the detection requirements needed to ensure that particles that would give rise to high doses are found in the event that ingestion of an object occurs. If technical advances are made that would allow reliable detection of alpha-rich objects at greater depths than is currently achievable either with the Evolution2™ or the Synergy systems, consideration should be given to their implementation for monitoring of the beaches in the vicinity of the Sellafield site.

12.2.4 Further *in vivo* studies of intestinal absorption

The *in vivo* experiments indicated a relatively wide range of uptake fractions for the particles studied. While most of the *in vivo* measurements for Pu and Am uptake fractions lay in the range 1×10^{-7} to 1×10^{-6}, the highest value found was 2.4×10^{-5}. A value of 3×10^{-5} has been recommended as being suitable conservative for assessments of ingestion dose for all alpha-rich particles. If higher activity alpha-rich particles are found, there may be a need to refine this recommendation in order to provide more realistic dose assessments that take account of the physical and chemical characteristics of the particle

(see Section 12.2.6). At the present time, however, there does not appear to be a compelling reason to carry out further *in vivo* studies.

12.2.5 Skin dosimetry: Recommendations of the University of Birmingham study

A number of shortcoming were founds in the measurements of skin dose rates reported by SERCO (Cowper, 2009) and the calculations of skin dose rates reported by AMEC (Delaney et al, 2009). These shortcomings are discussed in Section 9.1.2.1. In future studies, particularly if higher activity particles are found, the use of stacks of radiochromic dye film (RDF) to provide definitive skin dose measurements at various depths over 1 cm^2 is recommended. Due to the low sensitivity of RDF this would be time consuming since the threshold dose is about 10 Gy. Exposure times of 6-12 weeks could well be required for the higher dose rate particles examined in studies to date. Use of RDF would however avoid the limitations of small TLD dosemeters, and provide a definitive correction factor to aid the use of more rapid measurements using the SmartIon dose rate meter.

12.2.6 Further classification of radioactive objects

One objective of this work was to decide whether a more detailed classification system for objects is needed so that an assessment of potential hazard can be based on factors such as an improved knowledge of particle size, distribution of activity, data on solubility in seawater and in the gut and better estimates of gut uptake factors. Where possible, a methodology would be developed for the assessment of potential doses for each classification of object based on established non-destructive measurements such as a characteristic photon emission. This requires an investigation of potential correlations between information on particle characterisation and dose estimates derived from consideration of the various exposure pathways described in this study.

This could be a particularly useful approach for the evaluation of stochastic risks arising from ingestion of alpha-rich particles. Ingestion doses are strongly dependent on particle uptake fractions, and as has been noted in Section 8.2.7 and shown in Figure 10, these fractions are highly variable, ranging from about 10^{-8} to 10^{-5} with a maximum value of 2.4 10^{-5}. If it were to be possible to infer the particle uptake fraction from easily accessible information of chemical composition, for example, then more realistic dose and risk assessments would be possible for individual particle finds. In the absence of such a method, it is necessary to make a conservative assumption regarding particle uptake fraction. As noted in Section 8.4, a value of 3 10^{-5} has been recommended in this report.

As can be seen in Figure 10, two particles have uptake fractions that are about an order of magnitude higher than the upper value for the remainder of the particles studied. Information from Cowper (2009) was reviewed to determine whether there are any common features in the physical properties of these two particles that distinguish them from the remaining eight particles. However, none of the data on these two particles indicated they were clearly similar in any respect or clearly different from the other eight particles. One shortcoming of the available data is that chemical composition is determined from the results of scanning electron microscopy (SEM) and energy-dispersive X-ray analysis (EDAX). These techniques provide information on the chemical

composition of small areas of the surface of particles, and it is unclear whether the information obtained is representative of the bulk of the particle.

With the currently available information, it appears that a more detailed classification scheme is not yet feasible. If a judgement is made that such a classification scheme might be useful for the assessment of health risks, then it is recommended that consideration should be given to obtaining more comprehensive information on the chemical composition of both the volume and the surface layer of alpha-rich objects. However, given that the overall health risks to beach users are very low, the justification for developing such a classification scheme is doubtful.

13 CONCLUSIONS

The conclusion of this study, based on the current information available, is that the overall health risks to beach users are very low and significantly lower than other risks that people accept when using beaches. Based on the inforamtion available at the time of the study, the highest calculated lifetime risks of radiation-induced fatal cancer are of the order of one hundred thousand times smaller than the level of risk that the Health and Safety Executive considers to be the upper limit for an acceptable level of risk (HSE, 2001). It is also very unlikely that deterministic effects such as skin ulceration could occur from encountering an object.

The ingestion of alpha-rich particles has the greatest potential to give rise to significant health risks. However, the very low likelihood of ingestion occurring means that the overall health risk remains very low and less than one in ten thousand million (10^{-10}) per year.

Continued regular monitoring of Sellafield beach and monitoring at one or two other beaches with high public occupancy will provide regulators and the public with continued reassurance that risks associated with radioactive objects in the environment remain very low.

Individuals who regularly use the beaches may also be high consumers of locally caught seafood. The overall health risk to an individual with high beach occupancy as well as a high consumption of seafood is also estimated to be very small.

A number of recommendations have been made with the objective of providing further confirmation that protection of the public is adequate and improving the assessment of health risks. In particular, a recommendation is made that an investigation should be carried out of the increases in the number of alpha-rich objects being found by the recently-introduced Groundhog Synergy beach monitoring system. This increased find rate does not necessarily mean that there is an increase in the number of objects actually present on the beaches, since the increase could be completely attributable to improvements in sensitivity for particles containing ^{241}Am that are expected from the Synergy system. A possible approach for such an investigation has been proposed. Following this investigation, a decision should be made as to whether there is a need to

review the assessment of overall risk to beach users taking into account data on the increased number of objects detected by Synergy.

Capabilities of the beach monitoring systems for detection of alpha-rich objects at depth are limited by the physical nature of the detection process and also by currently available technology. These capabilities may not meet the requirements arising from a consideration of the health effects in the event that ingestion of an object occurs. If technical advances are made that would allow reliable detection of alpha-rich objects at greater depths than is currently achievable either with the Evolution2™ or the Synergy systems, consideration should be given to their implementation for monitoring of the beaches in the vicinity of the Sellafield site.

14 ACKNOWLEDGEMENTS

The authors acknowledge the contributions to this work made by Richard Haylock at HPA. They also acknowledge the valuable contribution made by Monty Charles from the University of Birmingham who carried out the assessment of potential radiation doses to the skin that could arise from contact with the radioactive objects found on the beaches.

15 REFERENCES

Aydarous AS, Charles MW and Darley PJ (2008). Dose distribution measurements and calculations for Dounreay hot particles. *Radiat Prot Dosim*, **128** (2), 146-158.

Beals JAJ, Funk LM, Fountain R and Sedman R (1994). Quantifying the distribution of inhalation exposure in human populations: distributions of minute volumes in adults and children. *Environmental Health Perspectives*, **104**, 9.

Brown J and Etherington G (2011). Health risks from radioactive objects on beaches in the vicinity of the Sellafield site. Chilton, HPA-CRCE-018.

Cefas (2008a). Radiological habits survey: Sellafield beach occupancy, 2007. Environment Report RL 02/08.

Cefas (2008b). A report on the investigation of the Cefas monitoring database for incidence of high activities in mollusc samples. Cefas contract report C2706 available at www.cefas.co.uk/publications/environment/Cefas-database-report.pdf.

Cefas (2009a). Radioactivity in Food and the Environment, RIFE-14, Environment Agency, Food Standards Agency, Northern Ireland Environment Agency and Scottish Environment Protection Agency

Cefas (2009b). Radiological habits survey: Sellafield 2008. Cefas contract report C2848 available at www.cefas.co.uk/publications/environment/Sellafield-2008-final-report.pdf.

Cefas (2010). Radiological habits survey: Sellafield beach occupancy, 2010. Environment Report RL 01/10.

Charles M, Harrison J, Darley P, Fell T, Aydarous AS, Phipps A and Smith T (2005). Health implications of Dounreay fuel fragments: Estimates of doses and risks. In Proceedings of the Seventh

International Symposium of the Society for Radiological Protection, Cardiff, pp 23-29 (Society for Radiological Protection, 2005)

Charles MW (2009). Health Effects of Dounreay Hot Particles: A Benchmark for the Evaluation of Doses and Risks. Invited paper. In NATO Advanced Research Workshop: Hot Particles Released From Different Nuclear Sources, May 2007 (NATO, Yalta, 2009)

Cowper M [Editor] (2009). Analysis of Beach Monitoring Finds – Final Report Issue 2, December 2009. Report to Sellafield Ltd. Serco Technical & Assurance Services (an operating division of Serco Ltd) SERCO/TAS/002037/1. [Sellafield Ltd, Reference: ESR 11 9030/4510192548.]

Currie LA (1968). Limits for Qualitative Detection and Quantitative Determination: Application to Radiochemistry. *Anal Chem*, **40**, 586-593.

Dalton AP (2010). Personal communication. Sellafield beach monitoring spreadsheet dated 18th January 2010.

Darley PJ, Charles MW, Fell TP and Harrison JD (2003). Doses and risks from the ingestion of Dounreay fuel fragments. *Radiat Prot Dosim*, **105** (1-4), 49-54.

Davies M (2009). Personal communication.

Delaney L, Major RO and Charles M W (2009). Beach Monitoring Dose Assessment Support, Task 3. AMEC Report 14738/TR/0003, Issue 2, June 2009.

DPAG (2006). Dounreay Particles Advisory Group, Third Report. Scottish Environmental Protection Agency (SEPA) September 2006. ISBN: 1-901322-64-5.

DPAG (2008). Dounreay Particles Advisory Group, Fourth Report. Scottish Environmental Protection Agency (SEPA) November 2008. ISBN: 1-901322-69-6.

Durham J S (2006). VARSKIN 3: Computer code for assessing skin dose from skin contamination. Developed for the Nuclear Regulatory Commission (NRC) contract number NRC-DR-04-05-086 by Dr James Durham, Center for Nuclear Waste Regulatory Analyses, Southwest Research Institute, San Antonio, TX 78238. NUREG/CR-6918.

Environment Agency (2009). Sellafield Radioactive Particles in the Environment. Environment Agency Strategy for Responding to Particle Finds. http://www.environment-agency.gov.uk/static/documents/Business/EA_Strategy_for_Responding_to_Particle_Finds.pdf

Fell TP, Phipps AW and Smith TJ (2007). The internal dosimetry code PLEIADES. *Radiat Prot Dosim*, **124,** 327-338.

Gilvin PJ, Luo LZ, Baker ST, Hill CE and Rotunda JE (2007). Type testing of an extremity finger stall dosemeter based on Harshaw TLD EXTRADTM technology. *Radiat Prot Dosim*, **123** (3), 329-336.

Harrison JD (2011). Personal communication, Health Protection Agency, UK.

Harrison JD, Fell TP, Phipps AW, Smith TJ, Ellender M, Ham GJ, Hodgson A and Wilkins BT (2005). Health Implications of Dounreay Fuel Fragments: Estimates of Doses and Risks. Chilton, RPD-RE-11-2005.

Haylock R (2010). Personal communication.

HPA (2006). Dose criteria for the designation of radioactively contaminated land. Chilton, RCE-2.

HSE (2001). Reducing risks, protecting people. HSE's decision-making process. HSE Books. HMSO, Norwich, UK. ISBN 0 7176 2151.

ICRP (1979). Limits on intakes of radionuclides for workers. ICRP Publication 30. Pt 1. *Ann ICRP*, **2** (3/4). Pergamon Press, Oxford.

ICRP (1991a). The biological basis for skin dose limitation. ICRP Publication 59. *Ann ICRP*, **22** (2). Pergamon Press, Oxford.

ICRP (1991b). 1990 Recommendations of the ICRP. ICRP Publication 60. *Ann ICRP*, ***21*** (1-3). Pergamon Press, Oxford.

ICRP (1993). Age-dependent doses to members of the public from intake of radionuclides. Pt 2, Ingestion dose coefficients. ICRP Publication 67. *Ann ICRP*, **23** (3-4). Pergamon Press, Oxford.

ICRP (1994). Human respiratory tract model for radiological protection. ICRP Publication 66. *Ann ICRP*, **24** (1-3). Pergamon Press, Oxford.

ICRP (1996). Age-dependent doses to members of the public from intake of radionuclides. Pt.5: Compilation of ingestion and inhalation dose coefficients. ICRP Publication 72. *Ann ICRP*, **26** (1). Pergamon Press, Oxford.

ICRP (1997). Individual monitoring for internal exposure of workers – Replacement of ICRP Publication 54. ICRP Publication 78. *Ann ICRP*, **27** (3-4). Pergamon Press, Oxford.

ICRP (2002). Basic anatomical and physiological data for use in radiological protection: Reference values. ICRP Publication 89. *Ann ICRP*, **32** (3-4). Pergamon Press, Oxford.

ICRP (2006a). Assessing dose of the representative person for the purpose of radiation protection of the public and the optimisation of radiological protection: broadening the process. ICRP Publication 101. *Ann ICRP*, **36** (3). Elsevier Science Ltd, Oxford.

ICRP (2006b). Human alimentary tract model for radiological protection. ICRP Publication 100. *Ann ICRP*, **36** (1-2). Elsevier Science Ltd, Oxford.

ICRP (2007). Recommendations of the ICRP. ICRP Publication 103. *Ann ICRP,* **37** (2-4). Elsevier Science Ltd., Oxford.

ICRU (1997). Dosimetry of external beta rays for radiation protection. ICRU Report 56. Bethesda, MD, USA.

Kowe R, Carey AD, Jones JA and Mobbs SF (2007). GRANIS: A model for the assessment of external photon irradiation from contaminated media of infinite lateral extent. Chilton, HPA-RPD-032.

MCA (2009). Marine Coastguard Agency, private communication.

NCRP (1999). Biological effects and exposure limits for 'hot particles'. NCRP Report No 130. NCRP Report No 130. National Council on Radiation Protection and Measurements, Bethesda, Washington DC.

NRPB (1996). Risks from deterministic effects of ionising radiation. *Doc NRPB*, **7** (3).

NRPB (1997). Assessment of skin doses. *Doc NRPB*, **8 (**3).

Nuvia (2008). Groundhog Evolution2™ Limits of Detection for Particles of ^{241}Am, ^{90}Sr, ^{6O}Co and ^{137}Cs. Nuvia Report 87204/TR/013, Issue A (April 2008).

Nuvia (2010a). Large scale beach trials to evaluate the operational performance of Groundhog Evolution2™. Nuvia Report 87257/TR/003 (Draft) (January 2010).

Nuvia (2010b). Sellafield Beach Trials: Large scale beach trials to evaluate the operational performance of Groundhog Synergy system. COMARE 10-SWG-02

ONS (2005). Review of the registrar general on deaths by cause, sex and age, in England and Wales, 2005. Office for National Statistics, London, Series DH2 No 32.

Parker T (2010). Personal communication, Sellafield Ltd, UK.

Pellow PGD, Hodgson A, Ellender M, Etherington G, Ham G, Fell TP and Harrison JD (2009). The intestinal absorption of plutonium and americium from particles recovered on Cumbrian beaches. Contract Report. Chilton, RPD-DA-09-2009. [Sellafield Ltd Reference: ESR 11 9030/4510192548]; SERCO reference: SERCO/TAS/002037/4].

Pellow PGD, Hodgson A, Etherington G, Ham G, Fell TP and Harrison JD (2010). The intestinal absorption of plutonium and americium from a further five particles recovered on Cumbrian beaches. Contract Report. Chilton, CRCE-DA-13-2010-Revision 1. [Sellafield Ltd Reference: ESR 11 9030/4510192548, SERCO/TCS/002037/1, Issue 2].

Rohloff F and Heinzelmann M (1996). Dose rate by photon radiation to the basal layer of the epidermis in the case of skin contamination. *Radiat Prot Dosim*, **63** (1), 15-28.

Smith KR and Bedwell P (2005). Public Health Implications of Fragments of Irradiated Fuel: Module 3: The likelihood of encountering a fuel fragment on Sandside beach. Chilton, RPD-EA-9-2005.

Smith KR, Bedwell P, Etherington G and Youngman M (2006). Public health implications of fragments of irradiated fuel. Module 4: esternal dose rates on Sandside beach and other miscellaneous information. Chilton, RPD-EA-1-2006.

Tandy S (2007). Sellafield Radioactive Particles in the Environment. Note for the record of a workshop held at the Environment Agency, Penrith on 28 June 2007. Final published form 24/9/07.

Turner JE and Huston TE (1991). ALDOSE: A computer code to calculate absorbed dose rate, dose equivalent rate, and dose-weighted LET as functions of depth in water irradiated by an alpha particle disc source. *Health Phys*, **60** (4), 584-589.

UNSCEAR (1996). Sources and effects of ionizing radiation. Report to the General Assembly, with Scientific Annex.

UNSCEAR (2006). Sources and effects of ionizing radiation. Report to the General Assembly, with Scientific Annexes.

Walters MD, Miller WH, Casey SL and Graham C (1999). Effective dose equivalent due to gamma-ray emissions from hot particles. *Health Phys*, **76,** 564-566.

Wilkins BT, Fry FA, Burgess PH, Fayers CA, Haywood SM, Bexon AP and Tournette C (1998). Radiological implications of the presence of fragments of irradiated fuel in the sub-tidal zone at Dounreay. Chilton, NRPB-M1005.

Youngman MJ and Etherington G (2003). Review of the procedures currently used for the monitoring of Sandside Bay. NRPB Contract Report, NRPB-DA/3/2003. Available online at http://www.sepa.org.uk/pdf/publications/technical/Sandside_April_2003.pdf

APPENDIX A Additional information on detection of objects on the beaches

A1 INTRODUCTION

As part of the work carried out by HPA at the request of EA, a study was carried out to provide an independent evaluation of the performance of the Groundhog Evolution2™ system, as well as to provide input data for estimating object populations as described in Section 4.1. Secondary aims were to compare the results of this evaluation with the results of recent *in situ* beach trials, and to discuss the performance of the Synergy system to the extent that this is currently possible.

This appendix contains additional information to that presented in Section 4.1.

A1.1 Information reviewed

Nuvia provided HPA with a document that describes the Groundhog Evolution2™ system, the object detection methodology, the criteria for detection of an object and the system's performance for detecting objects containing ^{241}Am, ^{90}Sr, ^{60}Co and ^{137}Cs (Nuvia, 2008). Calibration data have also been provided by Nuvia (Davies, 2009). For each of the four radionuclides (^{137}Cs, ^{60}Co, ^{90}Sr and ^{241}Am), a matrix of calibration factors was provided for:

(a) the object depths listed in Table A1;

(b) positions along the detector axis at distances of 0, 0.1 and 0.2 m from the end of the detector; and

(c) positions in the direction of travel at distances in the range 0 – 1.0 m (interval 0.1 m) (except for ^{90}Sr, where the range was 0 – 0.4 m).

Calibration factors were generally expressed in units of counts s^{-1} kBq^{-1}. This calibration factor array allows the response of the system to be calculated as it approaches and traverses the object at different speeds, for different object depths and at different object positions along the vector perpendicular to the direction of travel.

At the request of Nuvia, calibration data have not been reproduced in this report, for reasons of commercial confidentiality (Davies, 2009).

Table A1: Depths for which calibration factors were provided by Nuvia

	Cs-137	Co-60	Sr-90/Y-90	Am-241
Depths (m)	0 [a]	0 [a]	0	0 [a]
	0.05	0.05	0.01	0.05
	0.10	0.10	0.02	0.1
	0.15	0.15	0.04	0.15
	0.20	0.20	0.06	-
	0.30	0.30	0.11	-
	0.40	0.40	0.13	-

a) In Nuvia (2008), these values are actually given at an elevation of 0.0001 m above the surface.

Nuvia also supplied data files containing background data, recorded by Groundhog Evolution2™, as listed in Table A2. Data were provided for the 3rd detector in the five detector array (see Section A2.1), and these were taken to be representative of measurements made with the other four detectors. Data corresponding to object finds were removed from the data set by Nuvia. Each record in the data set contained nine fields, as listed in Table A3.

Table A2: Background data sets provided by Nuvia (Davies, 2009)

Location	Description of beach	Date of measurements	No of records
Barnscar, Drigg	sand	Oct 2007	27898
Barnscar, Drigg	shingle	Oct 2007	19264
Braystones	sand	Sept 2008	144754
Braystones	shingle	Sept 2008	12195
Drigg	sand	Oct 2007	44749
Seascale	sand	Oct 2007	74618
Seascale	shingle	Oct 2007	15080
Sellafield	low sand	June 2008	29765
Sellafield	high sand	June 2008	33634
St Bees	sand	April 2008	123756

Table A3: Background data set records

Record No	Field description
1	Identifier for each survey session
2	Date & time of measurement
3	OS grid reference (easting)
4	OS grid reference (northing)
5	Total gamma count (0 – approx 3000 keV) (counts s^{-1})
6	Counts in ^{137}Cs window (approx 580 – 740 keV) (counts s^{-1})
7	Counts in ^{137}Cs window (> 740 keV) (counts s^{-1})
8	Counts in ^{60}Co window (approx 1090 – 1400 keV) (counts s^{-1})
9	Counts in ^{137}Cs window (> 1400 keV) (counts s^{-1})

A2 DESCRIPTION OF THE GROUNDHOG EVOLUTION2™ BEACH MONITORING SYSTEM

A2.1 Survey Equipment

Information presented here is taken from the Nuvia report (2008). The vehicle-based system uses an array of sodium iodide (NaI(Tl)) gamma-ray detectors mounted on the front of a low ground-pressure vehicle. The detectors installed on the system are 76 mm in diameter and 400 mm long. Five detectors are arranged in a slightly staggered configuration (because of the photo-multiplier vacuum tubes attached to the detectors), as shown in Figure A1.

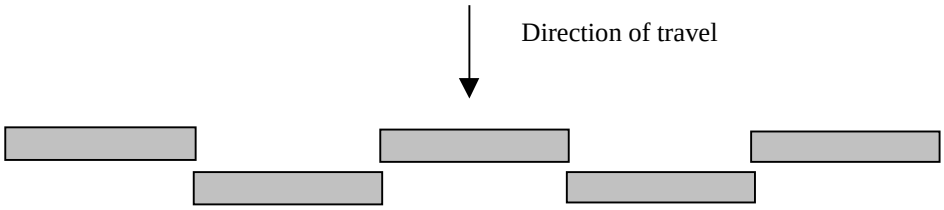

Figure A1: Detector array

The combination of five 400 mm long detectors provides a continuous monitoring width of 2.0 m. The axial centre of each detector is horizontal and less than 0.25 m above the ground surface on level ground. Each detector is installed in a weatherproof instrument case, which also includes the counting system and a gamma spectrometer. The spectrometer provides the ability to analyse “regions of interest” (ROI) of the gamma-ray spectrum as detailed in Table A3. The spectrometer over-samples by taking a one-second measurement five times per second. This avoids the reduction in sensitivity that arises when a one-second count terminates while the detectors are close to their point of closest approach to an object. Counts are analysed using the object detection criteria specified in Section A3.4.

A2.2 Surveying methodology

The vehicle is driven over the survey area at a speed of approximately 1.0 ms^{-1}, with a GPS system providing information for a 'moving map' of the area surveyed, and using an alarm facility to warn the operator if a maximum speed of 1.2 ms^{-1} is exceeded. Measurements recorded at a speed of 1.2 ms^{-1} or greater are later rejected during analysis.

Each pass across the beach surveys a width of 2.0 m. Successive passes are overlapped by some 0.3 m to try to ensure that all areas are adequately covered. If, during the course of a survey, an object alarm occurs, the vehicle is stopped and reversed slowly for up to 5 m, and then advanced slowly (at about 0.5 ms^{-1}) up to the original stopping point. If the object alarm is repeated during this process, the vehicle is stopped and a manual object search and recovery process is initiated.

A3 STATISTICAL ANALYSIS OF OBJECT DETECTION BY THE GROUNDHOG EVOLUTION2™ SYSTEM

A3.1 Simulation method

The method described below was originally developed for the evaluation of the performance of the Groundhog Evolution™ system for detection of objects containing ^{137}Cs at Dounreay (Youngman and Etherington, 2003). The main modifications made were to:

(a) include the calibration factor matrices for the other three radionuclides of interest;

(b) update the object detection algorithms; and

(c) allow input of background data in the format used for Sellafield measurements.

Counts measured by an array of detectors moving at a speed of 1 ms^{-1} over sand containing objects of ^{137}Cs, ^{60}Co, $^{90}Sr/^{90}Y$ or ^{241}Am were simulated using a Monte Carlo method. Speeds in the range 0.5 - 1.6 ms^{-1} can be simulated, if required. Separate simulation runs were carried out to determine the response of the detection system to objects of different activities and depths relative to the detector array. In each simulation run, computations were carried out to determine the counts measured by each of the detectors in the array as an object containing a specified activity passed through its field of view (Section A3.2). To simplify calculations, the position of the detector array was held fixed, while the object position in the direction of travel was increased in increments from its starting position at a rate determined by the scan speed. Each simulation run consisted of a large number of simulations of these object transits. The number of simulations was typically around 15000, but varied in the range 2000 - 60000, depending on the number of records contained in the background data file. The object activity, depth and the starting position relative to the detector array in the direction of travel were fixed for each simulation run, whereas the starting position normal to the direction of travel was chosen randomly.

Net counts measured in each second in defined regions of the gamma-ray spectrum (specified in Table A3) were determined using the calibration factor matrices provided by Nuvia. The net count is subject to measurement error due to the effect of counting statistics, and this was taken into account in the simulation. One difference between Groundhog Evolution™ and Groundhog Evolution2™ is the use of oversampling, as described in Section A2.1. This was not explicitly included in the Monte Carlo simulation, but its effect was allowed for by choosing a starting position and detector start time such that the count period was at its mid-point as the object passed directly below the detector array.

Gross counts were determined by adding net counts to the real background measurements obtained using the Groundhog Evolution2™ system. The object detection criteria specified by Nuvia (Section A3.4) were then applied to each 1-second measurement. Generally, only a fraction of the simulated objects are detected as they

pass through the field of view of the detector array. This fraction represents the detection probability for objects of the specified activity and depth.

A3.2 Simulation geometry

For ^{137}Cs, ^{60}Co and ^{241}Am, the field of view of the detector array is a rectangle 2 m long in its direction of travel and 2 m wide in the direction along its axis (ie, the rectangle ABFE in Figure A2). For ^{90}Sr, the rectangle is 0.8 m long. These dimensions are defined by the area for which calibration factors are available (Section A3.3). The length of the field of view is smaller for ^{90}Sr because calibration factors decrease more rapidly with distance for this radionuclide. The depth range over which calibration factors for ^{90}Sr are give (Table A1) is smaller for the same reason.

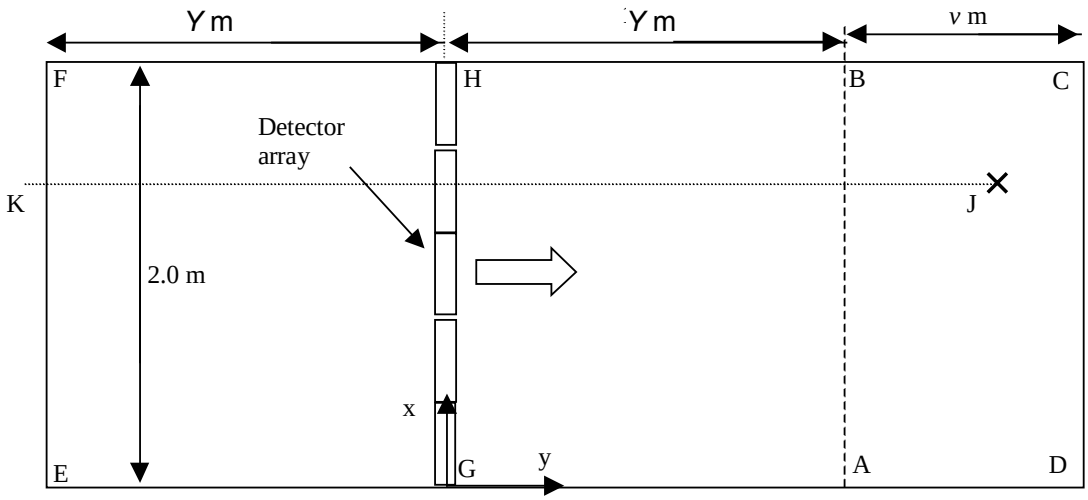

Note: For ^{137}Cs, ^{60}Co and ^{241}Am, Y = 1 m; for ^{90}Sr, Y = 0.4 m.

Figure A2 Simulation geometry for the five-detector Groundhog Evolution2™ system.

To simplify calculations, detectors are assumed to be in-line rather than staggered as in Figure A1. The effect of this assumption is discussed in Section A5. The starting position of the object is always in front of the field of view of the detector array, so that detectors start counting before the object enters the field of view. The starting position lies within the rectangle (ABCD), with the length (B-C) determined by the speed of the array, v, and can be pre-set or chosen pseudo-randomly. Detector start times can each be pre-set or chosen randomly. For the simulations reported here, starting positions and detector start times were chosen so that the count period was at its mid-point as the object passed directly below the detector array, to reproduce the effect of oversampling.

The simulation proceeds by incrementing the position of the object along the y-axis, with a typical step size of 0.05 m. Detector counts are accumulated as the object moves along the path (J → K). Each detector accumulates counts for a pre-set count time of 1 second. Counts are then recorded and the counter reset. After each count, the object detection criteria described in Section A3.4 are applied.

If an object passes directly below the two ends of adjacent detectors, then the counts from both detectors are taken into account. Otherwise, the count from only one detector is considered. This arises because calibration factors were only provided for objects passing directly below, and between the ends of, each detector (Nuvia, 2008). The detector or detectors for which counts are recorded are the "active" detector(s).

Response is somewhat poorer for object positions at the edge of the detector array, ie, along the paths (B-F) and (A-E). In practice, consecutive scans made with the detector array normally overlap in the x-direction by 0.3 m (Nuvia, 2008). This means that, if the object x-position is within 0.3 m of the end of the array (G or H in Figure A2), then a second pass is performed over this object, increasing the probability that it could be detected. Simulations can be performed with or without this overlap, but for the simulations reported here the overlap scan was always included.

A3.3 Calibration factors

Calibration factors, $CF(x,y)$, relating measured count rate to object activity were provided by Nuvia (Davies, 2009). These calibration factors are for a single detector at a height of 0.25 m above the surface. The x-axis is the vector described by the axis of the detector cylinder, with x=0 at the end of the detector and x=0.20 m at the position mid-way along the length of the detector. The y-axis is perpendicular to the x-axis, and lies in the horizontal direction of travel of the detector, with y=0 vertically below the detector. Calibration factors for x=0.30 m and x=0.40 m, and for y-values in the range $-Y$ m → -0.10 m, are generated by symmetry, that is, $CF(x,y) = CF((0.4-x),y)$ and $CF(x,y) = CF(x,-y)$.

For ^{137}Cs and ^{60}Co, calibration factors were provided for the gamma-ray spectrum regions of interest (windows) specified in Table A3. For ^{90}Sr/^{90}Y and ^{241}Am, calibration factors were provided for the total gamma count, also specified in Table A3.

A3.4 Object detection criteria

This description of the object detection criteria used by the Groundhog Evolution2™ system is taken from the Nuvia report (Nuvia, 2008).

^{137}Cs and ^{60}Co

Two criteria must be met simultaneously for an object alarm to occur:

A. The "Gross Gamma" Criterion

This criterion is set on the gross gamma (GG) count for the latest 1 second measurement. The criterion is:

$$GG_I \geq GG_M + C_{GG} \times GG_{Msd} \qquad (1)$$

where

≥ means "greater than or equal to"

GG_I is the latest Gross Gamma (GG) measurement

GG_M is the mean of the last 10 measurements of GG

GG_{Msd} is the "uncertainty on the mean" of the last 10 measurements of GG, or more precisely the Standard Error on the mean

C_{GG} is a defined "coverage factor".

The coverage factor C_{GG} is a constant that is chosen to optimise minimum detectable activities (MDA) and false alarm rates. Increasing C_{GG} decreases the frequency of false alarms associated with Gross Gamma measurements, but also increases the MDA. Nuvia chose a value of 9.0 for this factor (Davies, 2009).

B. The Region-of-Interest "ROI" criterion

This criterion is set on the count in the In-window (IW) ROI for the latest 1 second measurement. The criterion is:

$$IW_I \geq IW_P + C_{IW} \times IW_{Psd} \quad (2)$$

$$IW_P = AW_I \times (IW_M / AW_M)$$

where

IW_I is the latest "In-window" measurement

IW_P is the predicted IW measurement, assuming an object is not present

C_{IW} is a defined "coverage factor"

IW_{Psd} is the compound uncertainty in IW_P

AW_I is the latest "Above-window" measurement

IW_M is the mean of the last 10 IW measurements, calculated as a rolling average

AW_M is the mean of the last 10 AW measurements, calculated as a rolling average

The coverage factor C_{IW} is a constant that is similar in use to C_{GG}, as described above. Nuvia chose a value of 3.5 for this factor (Davies, 2009).

The compound uncertainty IW_{Psd} is defined as:

$$IW_{p_{sd}} = IW_p \sqrt{\left(\frac{\sqrt{AW_I}}{AW_I}\right)^2 + \left(\frac{IW_{sd}}{IW_m}\right)^2 + \left(\frac{AW_{sd}}{AW_m}\right)^2}$$

where

IW_{sd} is the standard deviation of the last 10 IW measurements, calculated as a rolling average

AW_{sd} is the standard deviation of the last 10 AW measurements, calculated as a rolling average

If an object is detected, the measurement is excluded from the rolling averages.

$^{90}Sr/^{90}Y$ and ^{241}Am

For these radionuclides, only the Gross Gamma criterion is applied. For these radionuclides, Nuvia chose a value of 18.0 for C_{GG} (Davies, 2009).

Application of the criteria

Both object detection criteria require information on rolling averages of the previous 10 background counts. To allow realistic simulations to be carried out, large data sets of real background measurements were used for the beaches considered, taken from actual scans made using the Groundhog Evolution2™ system (Section A1).

A4 SOFTWARE

A Visual Basic 6.0 program was originally written to implement the methodology for detection of ^{137}Cs particles at Dounreay (Youngman and Etherington, 2003). This code has been adapted (as described in section A3.1) so that it can be applied for evaluating object detection probabilities at Sellafield for other radionuclides. The code performs the Monte Carlo simulations and determines the object detection probabilities that result from application of the detection criteria described in Section A3.4. The assumptions made in implementing this simulation are described in Section A5.

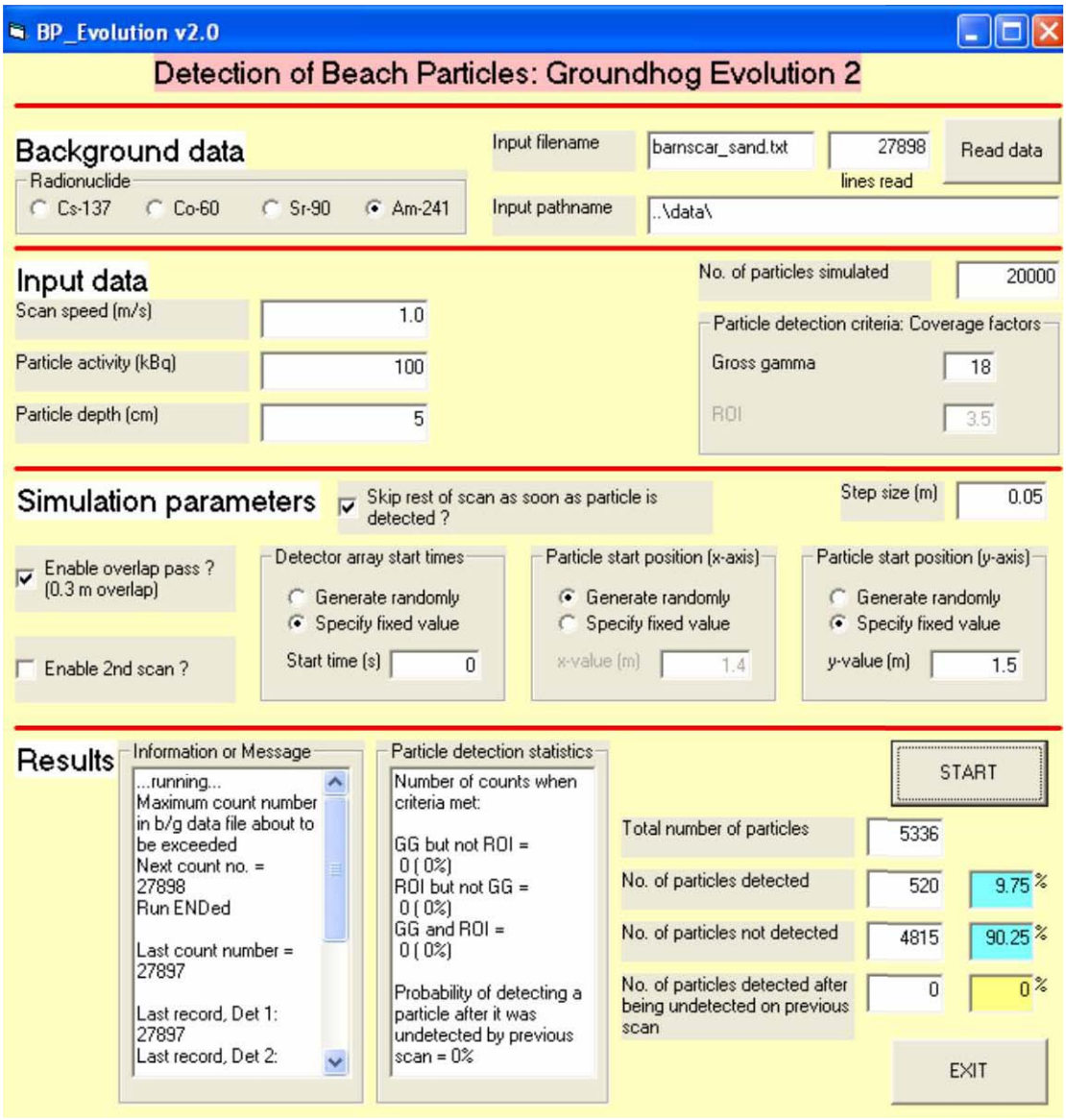

Figure A3: Input/output screen for Visual Basic program

The operation of the program is best described with reference to a specific example. Figure A3 shows the input/output screen at the end of a simulation run carried out to determine the detection probability for objects at a depth of 0.05 m containing 100 kBq of ^{241}Am, when the detector array is travelling at a speed of 1.0 ms^{-1}. As noted in Section A3.4, application of the detection criteria to each simulated count requires a calculation of the mean and standard deviation of counts for the ten previous background measurements. Therefore, the first step in a simulation run is to read in a background data set, in this case from the file *..\data\barnscar_sand.txt*, which contained 27898 records of measurements made on the sandy areas of Barnscar beach (part of Drigg beach).

Next, the scan speed, object activity and object depth for the simulation run are chosen. All of the calculations presented in this report were made for a scan speed of 1 m s^{-1}. Any value for object activity may be specified; for this study, object activities of, 1, 10, 100 and 1000 kBq have been chosen. The choice of object depth is limited to those given in Table B1 because calibration factors are available only for these depths.

In the example shown in Figure A3, 20000 object transits were requested, although only 5336 object transits could be carried out because of the limited size of the background dataset. The run time was 2.0 seconds (using a 2 GHz Intel Core2 Duo processor running Windows XP version 2002 SP3). For ^{241}Am, only the Gross Gamma criterion is applied and the value for the coverage factor C_{GG} used in the object detection criteria formulae was set at 18 (Section A3.4), although other values could be specified.

After specification of the input data, various options and parameter values can be set that determine how the simulation proceeds. The option of terminating an object transit simulation as soon as the object is detected was selected; this does not affect the results of the run, but does result in slightly shorter run times. A simulation step size of 0.05 m was chosen. Detector start times and object starting positions were both chosen as described in Section A3.2. All of the calculations were carried out using the 0.3 m overlap scans described in Section A3.2. The "2nd scan" option was not enabled; this would have allowed the determination of the probability that an object could be undetected on a first scan and then detected on a second scan, but this was not a requirement for this investigation.

A5 ASSUMPTIONS

A number of assumptions were made in implementing the Monte Carlo simulation for the Groundhog Evolution2™ beach monitoring system. These are described below.

- Detectors are in-line as shown in Figure A2, rather than staggered as is used in practice and shown in Figure A1. This assumption has an effect only when a simulated object passes directly below the two ends of adjacent detectors. The detector separation along the direction of travel is approximately 0.1 m, and since counts are accumulated over a 1 second period while the array moves a distance of 1 m, the effect of this simplifying assumption on the simulated count is negligible.
- The count time for each detector is always 1 second, and there is no time delay between counts.
- The position of objects along the direction of the axis of the detector array (ie, perpendicular to the direction of travel) is quantised, taking on one of the following values: x = 0, 0.1, 0.2, 0.3, 0.4, 0.5, 0.6, 0.7, 0.8, 0.9, 1.0, 1.1, 1.2, 1.3, 1.4, 1.5, 1.6, 1.7, 1.8, 1.9 or 2.0 m. (Calibration factors are only available at these intervals.)
- Conversely, the position of objects along the direction of travel can take on any value along the vector J-K in Figure A2.

- Calibration factors for positions along the direction of travel, intermediate between those for which calibration factors are provided, can be determined by linear interpolation.
- The response of the detector array to an object which does not pass through the field of view (ABFE in Figure A2) can be neglected.
- The response of a detector to an object whose horizontal position along the detector axis does not lie between the ends of the detector (ie, outside of its field of view as defined by the calibration factor matrix) can be neglected.
- Any overlap of adjacent scans is always equal to 0.3 m.
- Background data provided by Nuvia for the 3rd detector in the five detector array were taken to be representative of background measurements made with the other four detectors.
- The probability distribution of the real sample count is assumed to be a normal distribution with a standard deviation equal to $(N)^{1/2}$, where N is the true (ie, expectation value) of the sample count. This is a good approximation for N>10.
- For detection of ^{137}Cs and ^{60}Co objects, the number of In-window (IW) and Above-window (AW) measurements used in the rolling averages that are used in the calculation of the predicted IW measurement, IW_P, and the compound uncertainty, IW_{Psd}, is 10.
- GG_{Msd} (defined as the uncertainty on the mean for the “Gross Gamma” criterion) is the Standard Error on the mean.
- For detection of ^{137}Cs and ^{60}Co objects, the coverage factors C_{GG} and C_{IW} are equal to 9.0 and 3.5, respectively. For detection of ^{90}Sr and ^{241}Am objects, C_{GG} is equal to 18.

A6 RESULTS

A6.1 Object detection probabilities for the Groundhog Evolution2™ system

Object detection probabilities for ^{137}Cs, ^{60}Co, ^{90}Sr and ^{241}Am were determined for each of the ten beach areas listed in Table 12 in the main text, and are presented in Table A4 to Table A7. Each table presents the detection probabilities for object activities of 1 kBq (where calculated), 10 kBq, 100 kBq and 1000 kBq, respectively. Calculations were performed for 1 kBq objects only for Barnscar, Drigg (sand) and Braystones (sand) beaches, because for objects of this activity differences between beaches are insignificant given the low detection probabilities and consequent lack of precision. The object depths for which detection probabilities were calculated are listed in the Tables.

The maximum possible number of simulations was carried out for each simulation run, but this number was variable because it depends on the size of the background data set. For the calculations presented here, the number of simulations ranged from 2000 to 60000. The number of simulations is one of the main factors determining the precision

of the detection probability; the rounding adopted in Table A4 to Table A7 broadly reflects the level of precision for each reported value.

Table A4: Object detection probability for Groundhog Evolution2™, object activity = 1 kBq

Depth (m)		Scan speed (ms^{-1})	Probability (%)			
Cs,Co,Am	Sr		Cs-137	Co-60	Sr-90	Am-241
Barnscar beach, sandy areas (5100 – 5500)[a]						
0.0001	0	1.0	0.2	2	0.2	0.3
0.05	0.01	1.0	0	0.4	0.2	0.3
0.1	0.02	1.0	0	0.1	0.2	0.3
0.15	0.04	1.0	0	0	0.2	0.3
0.2	0.06	1.0	0	0	0.2	-
0.3	0.11	1.0	0	0	0.2	-
0.4	0.13	1.0	0	-	0.2	-
Braystones beach, sandy areas (27000 – 28000)[a]						
0.0001	0	1.0	0.1	1	0.2	0.3
0.05	0.01	1.0	0	0.4	0.2	0.2
0.1	0.02	1.0	0	0.2	0.2	0.2
0.15	0.04	1.0	0	0.1	0.2	0.2
0.2	0.06	1.0	0	0.1	0.2	-
0.3	0.11	1.0	0	0.1	0.2	-
0.4	0.13	1.0	0	-	0.2	-

a. No of object simulations, corresponding to a single pass through the background data file.
Notes:
1. 0.3 m overlap pass included.
2. 0.05 m simulation step size.
3. Simulated count rate measured over 1 s.
4. Simulated object x-coordinates chosen randomly in the 0 – 2 m range (x-axis is the detector axis).
5. Object starting y-coordinates (y-axis is the direction of travel) chosen to maximise detection probability (simulating the outcome of 10 times oversampling).

Table A5: Object detection probability for Groundhog Evolution2™, object activity = 10 kBq

Depth (m)		Scan speed (ms^{-1})	Probability (%)			
Cs,Co,Am	Sr		Cs-137	Co-60	Sr-90	Am-241
Barnscar beach, sandy areas (5100 – 9000)[a]						
0.0001	0	1.0	98	100	0.5	7
0.05	0.01	1.0	43	95	0.4	0.3
0.1	0.02	1.0	4	51	0.3	0.3
0.15	0.04	1.0	0.4	15	0.3	0.3
0.2	0.06	1.0	0	4	0.3	-
0.3	0.11	1.0	0	0.1	0.2	-
0.4	0.13	1.0	0	-	0.2	-
Barnscar beach, shingle areas (3500 – 6400)[a]						
0.0001	0	1.0	86	100	0.4	2
0.05	0.01	1.0	17	87	0.4	0.3
0.1	0.02	1.0	1	28	0.4	0.3
0.15	0.04	1.0	0.2	5	0.3	0.2
0.2	0.06	1.0	0	1	0.3	-
0.3	0.11	1.0	0	0.1	0.3	-
0.4	0.13	1.0	0	-	0.2	-
Braystones beach, sandy areas (27000 to 45000)[a]						
0.0001	0	1.0	94	100	0.4	5
0.05	0.01	1.0	25	95	0.3	0.3
0.1	0.02	1.0	2	52	0.3	0.2
0.15	0.04	1.0	0.2	15	0.3	0.2
0.2	0.06	1.0	0.1	3	0.3	-
0.3	0.11	1.0	0	0.2	0.2	-
0.4	0.13	1.0	0	-	0.2	-
Braystones beach, shingle areas (2200 – 3300)[a]						
0.0001	0	1.0	78	100	0.3	2
0.05	0.01	1.0	9	82	0.3	0.3
0.1	0.02	1.0	0.4	21	0.3	0.3
0.15	0.04	1.0	0	3	0.3	0.3
0.2	0.06	1.0	0	0.4	0.3	-
0.3	0.11	1.0	0	0	0.3	-
0.4	0.13	1.0	0	-	0.3	-
Drigg beach, sandy areas (8300 – 15000)[a]						
0.0001	0	1.0	98	100	0.4	9
0.05	0.01	1.0	46	97	0.4	0.2
0.1	0.02	1.0	5	60	0.3	0.1
0.15	0.04	1.0	0.5	21	0.3	0.1
0.2	0.06	1.0	0.1	5	0.2	-
0.3	0.11	1.0	0	0.3	0.2	-
0.4	0.13	1.0	0	-	0.1	-

Depth (m)		Scan speed (ms^{-1})	Probability (%)			
Cs,Co,Am	Sr		Cs-137	Co-60	Sr-90	Am-241
Seascale beach, sandy areas (14000 – 25000)[a]						
0.0001	0	1.0	98	100	0.4	6
0.05	0.01	1.0	41	93	0.3	0.2
0.1	0.02	1.0	4	47	0.3	0.1
0.15	0.04	1.0	0.4	14	0.2	0.1
0.2	0.06	1.0	0.1	3	0.2	-
0.3	0.11	1.0	0	0.2	0.1	-
0.4	0.13	1.0	0	-	0.1	-
Seascale beach, shingle areas (2800 – 5000)a						
0.0001	0	1.0	79	100	0.2	2
0.05	0.01	1.0	11	79	0.1	0.1
0.1	0.02	1.0	0.6	20	0.2	0.1
0.15	0.04	1.0	0.1	3	0.1	0.1
0.2	0.06	1.0	0.1	0.4	0.1	-
0.3	0.11	1.0	0	0	0.1	-
0.4	0.13	1.0	0	-	0.1	-
Sellafield beach, "low sand" areas (5500 – 10000)[a]						
0.0001	0	1.0	96	100	0.4	5
0.05	0.01	1.0	31	91	0.3	0.3
0.1	0.02	1.0	2	42	0.3	0.2
0.15	0.04	1.0	0.4	12	0.3	0.2
0.2	0.06	1.0	0.1	3	0.2	-
0.3	0.11	1.0	0	0.1	0.2	-
0.4	0.13	1.0	0	-	0.2	-
Sellafield beach, "high sand" areas (6200 – 9700)[a]						
0.0001	0	1.0	86	99	0.6	4
0.05	0.01	1.0	17	88	0.5	0.4
0.1	0.02	1.0	1	39	0.5	0.3
0.15	0.04	1.0	0.2	10	0.4	0.3
0.2	0.06	1.0	0.1	2	0.4	-
0.3	0.11	1.0	0.1	0.2	0.4	-
0.4	0.13	1.0	0.1	-	0.4	-
St Bees beach, sandy areas (23000 – 42000)[a]						
0.0001	0	1.0	92	100	0.4	5
0.05	0.01	1.0	22	94	0.3	0.2
0.1	0.02	1.0	2	50	0.3	0.2
0.15	0.04	1.0	0.2	15	0.2	0.2
0.2	0.06	1.0	0	3	0.2	-
0.3	0.11	1.0	0	0.2	0.2	-
0.4	0.13	1.0	0	-	0.2	-

Depth (m)		Scan speed (ms^{-1})	Probability (%)			
Cs,Co,Am	Sr		Cs-137	Co-60	Sr-90	Am-241

a. No of object simulations, corresponding to a single pass through the background data file.

Notes:

1. 0.3 m overlap pass included.
2. 0.05 m simulation step size.
3. Simulated count rate measured over 1 s.
4. Simulated object x-coordinates chosen randomly in the 0 – 2 m range (x-axis is the detector axis).
5. Object starting y-coordinates (y-axis is the direction of travel) chosen to maximise detection probability (simulating the outcome of 10 times oversampling).

Table A6: Object detection probability for Groundhog Evolution2™, object activity = 100 kBq

Depth (m)		Scan speed (ms^{-1})	Probability (%)			
Cs,Co,Am	Sr		Cs-137	Co-60	Sr-90	Am-241
Barnscar beach, sandy areas (5100 – 14000)[a]						
0.0001	0	1.0	100	100	91	100
0.05	0.01	1.0	100	100	76	10
0.1	0.02	1.0	100	100	65	0.3
0.15	0.04	1.0	93	100	32	0.2
0.2	0.06	1.0	37	100	13	-
0.3	0.11	1.0	1	38	3	-
0.4	0.13	1.0	0	-	1	-
Barnscar beach, shingle areas (3500 – 9600)[a]						
0.0001	0	1.0	100	100	61	100
0.05	0.01	1.0	100	100	37	3
0.1	0.02	1.0	100	100	27	0.3
0.15	0.04	1.0	79	100	10	0.2
0.2	0.06	1.0	16	98	4	-
0.3	0.11	1.0	0.2	21	1	-
0.4	0.13	1.0	0	-	0.7	-
Braystones beach, sandy areas (27000 – 72000)[a]						
0.0001	0	1.0	100	100	87	100
0.05	0.01	1.0	100	100	65	6
0.1	0.02	1.0	100	100	52	0.3
0.15	0.04	1.0	83	100	22	0.2
0.2	0.06	1.0	20	100	8	-
0.3	0.11	1.0	0.4	39	2	-
0.4	0.13	1.0	0	-	1	-
Braystones beach, shingle areas (2300 – 6100)[a]						
0.0001	0	1.0	100	100	46	100
0.05	0.01	1.0	100	100	23	2
0.1	0.02	1.0	100	100	17	0.3
0.15	0.04	1.0	67	100	6	0.3
0.2	0.06	1.0	11	98	2	-
0.3	0.11	1.0	0	16	0.9	-
0.4	0.13	1.0	0	-	0.6	-
Drigg beach, sandy areas (8300 – 22000)[a]						
0.0001	0	1.0	100	100	95	100
0.05	0.01	1.0	100	100	85	12
0.1	0.02	1.0	100	100	75	0.2
0.15	0.04	1.0	94	100	39	0.1
0.2	0.06	1.0	38	100	16	-
0.3	0.11	1.0	1	48	4	-
0.4	0.13	1.0	0.1	-	1	-

Depth (m)		Scan speed (ms^{-1})	Probability (%)			
Cs,Co,Am	Sr		Cs-137	Co-60	Sr-90	Am-241
Seascale beach, sandy areas (14000 – 37000)[a]						
0.0001	0	1.0	100	100	93	100
0.05	0.01	1.0	100	100	77	9
0.1	0.02	1.0	100	100	65	0.1
0.15	0.04	1.0	93	100	31	0.1
0.2	0.06	1.0	35	99	12	-
0.3	0.11	1.0	0.8	35	3	-
0.4	0.13	1.0	0.1	-	1	-
Seascale beach, shingle areas (2700 – 7500)[a]						
0.0001	0	1.0	100	100	57	100
0.05	0.01	1.0	100	100	31	2
0.1	0.02	1.0	100	100	23	0.1
0.15	0.04	1.0	67	100	8	0.1
0.2	0.06	1.0	11	97	3	-
0.3	0.11	1.0	0.1	15	1	-
0.4	0.13	1.0	0	-	0.5	-
Sellafield beach, "low sand" areas (5500 – 15000)[a]						
0.0001	0	1.0	100	100	89	100
0.05	0.01	1.0	100	100	68	7
0.1	0.02	1.0	100	100	56	0.2
0.15	0.04	1.0	88	100	23	0.2
0.2	0.06	1.0	26	99	9	-
0.3	0.11	1.0	0.6	32	2	-
0.4	0.13	1.0	0.1	-	0.8	-
Sellafield beach, "high sand" areas (6200 – 17000)[a]						
0.0001	0	1.0	100	100	79	99
0.05	0.01	1.0	100	100	55	5
0.1	0.02	1.0	99	100	43	0.4
0.15	0.04	1.0	71	100	16	0.3
0.2	0.06	1.0	14	98	7	-
0.3	0.11	1.0	0.4	29	2	-
0.4	0.13	1.0	0.1	-	1	-
St Bees beach, sandy areas (23000 – 62000)[a]						
0.0001	0	1.0	100	100	90	100
0.05	0.01	1.0	100	100	70	6
0.1	0.02	1.0	100	100	57	0.2
0.15	0.04	1.0	79	100	24	0.2
0.2	0.06	1.0	18	99	9	-
0.3	0.11	1.0	0.5	38	2	-
0.4	0.13	1.0	0	-	1	-

Depth (m)		Scan speed (ms^{-1})	Probability (%)			
Cs,Co,Am	Sr		Cs-137	Co-60	Sr-90	Am-241

a. No of object simulations, corresponding to a single pass through the background data file.

Notes:

1. 0.3 m overlap pass included.
2. 0.05 m simulation step size.
3. Simulated count rate measured over 1 s.
4. Simulated object x-coordinates chosen randomly in the 0 – 2 m range (x-axis is the detector axis).
5. Object starting y-coordinates (y-axis is the direction of travel) chosen to maximise detection probability (simulating the outcome of 10 times oversampling).

Table A7: Object detection probability for Groundhog Evolution2™, object activity = 1000 kBq

Depth (m)		Scan speed (ms^{-1})	Probability (%)			
Cs,Co,Am	Sr		Cs-137	Co-60	Sr-90	Am-241
Barnscar beach, sandy areas (5200 – 14000)[a]						
0.0001	0	1.0	100	100	100	100
0.05	0.01	1.0	100	100	100	100
0.1	0.02	1.0	100	100	100	11
0.15	0.04	1.0	100	100	100	0.3
0.2	0.06	1.0	100	100	100	-
0.3	0.11	1.0	95	100	100	-
0.4	0.13	1.0	8	-	100	-
Barnscar beach, shingle areas (3500 – 9600)[a]						
0.0001	0	1.0	100	100	100	100
0.05	0.01	1.0	100	100	100	100
0.1	0.02	1.0	100	100	100	3
0.15	0.04	1.0	100	100	100	0.3
0.2	0.06	1.0	100	100	100	-
0.3	0.11	1.0	82	100	100	-
0.4	0.13	1.0	3	-	96	-
Braystones beach, sandy areas (27000 – 72000)[a]						
0.0001	0	1.0	100	100	100	100
0.05	0.01	1.0	100	100	100	100
0.1	0.02	1.0	100	100	100	7
0.15	0.04	1.0	100	100	100	0.3
0.2	0.06	1.0	100	100	100	-
0.3	0.11	1.0	85	100	100	-
0.4	0.13	1.0	5	-	99	-
Braystones beach, shingle areas (2300 – 6100)[a]						
0.0001	0	1.0	100	100	100	100
0.05	0.01	1.0	100	100	100	100
0.1	0.02	1.0	100	100	100	2
0.15	0.04	1.0	100	100	100	0.3
0.2	0.06	1.0	100	100	100	-
0.3	0.11	1.0	71	100	99	-
0.4	0.13	1.0	2	-	94	-
Drigg beach, sandy areas (8300 – 22000)[a]						
0.0001	0	1.0	100	100	100	100
0.05	0.01	1.0	100	100	100	100
0.1	0.02	1.0	100	100	100	13
0.15	0.04	1.0	100	100	100	0.2
0.2	0.06	1.0	100	100	100	-
0.3	0.11	1.0	95	100	100	-
0.4	0.13	1.0	8	-	100	-

Depth (m)		Scan speed (ms^{-1})	Probability (%)			
Cs,Co,Am	Sr		Cs-137	Co-60	Sr-90	Am-241
Seascale beach, sandy areas (14000 – 37000)[a]						
0.0001	0	1.0	100	100	100	100
0.05	0.01	1.0	100	100	100	100
0.1	0.02	1.0	100	100	100	10
0.15	0.04	1.0	100	100	100	0.2
0.2	0.06	1.0	100	100	100	-
0.3	0.11	1.0	94	100	100	-
0.4	0.13	1.0	8	-	100	-
Seascale beach, shingle areas (2800 – 7500)[a]						
0.0001	0	1.0	100	100	100	100
0.05	0.01	1.0	100	100	100	100
0.1	0.02	1.0	100	100	100	3
0.15	0.04	1.0	100	100	100	0.1
0.2	0.06	1.0	100	100	100	-
0.3	0.11	1.0	71	100	99	-
0.4	0.13	1.0	2	-	95	-
Sellafield beach, "low sand" areas (5500 – 15000)[a]						
0.0001	0	1.0	100	100	100	100
0.05	0.01	1.0	100	100	100	100
0.1	0.02	1.0	100	100	100	8
0.15	0.04	1.0	100	100	100	0.2
0.2	0.06	1.0	100	100	100	-
0.3	0.11	1.0	89	100	100	-
0.4	0.13	1.0	6	-	100	-
Sellafield beach, "high sand" areas (6200 – 17000)[a]						
0.0001	0	1.0	100	100	100	100
0.05	0.01	1.0	100	100	100	99
0.1	0.02	1.0	100	100	100	5
0.15	0.04	1.0	100	100	100	0.4
0.2	0.06	1.0	100	100	100	-
0.3	0.11	1.0	75	100	99	-
0.4	0.13	1.0	3	-	98	-
St Bees beach, sandy areas (23000 – 62000)[a]						
0.0001	0	1.0	100	100	100	100
0.05	0.01	1.0	100	100	100	100
0.1	0.02	1.0	100	100	100	7
0.15	0.04	1.0	100	100	100	0.2
0.2	0.06	1.0	100	100	100	-
0.3	0.11	1.0	82	100	100	-
0.4	0.13	1.0	4	-	100	-

Depth (m)		Scan speed (ms^{-1})	Probability (%)			
Cs,Co,Am	Sr		Cs-137	Co-60	Sr-90	Am-241

a. No of object simulations, corresponding to a single pass through the background data file.
Notes:
1. 0.3 m overlap pass included.
2. 0.05 m simulation step size.
3. Simulated count rate measured over 1 s.
4. Simulated object x-coordinates chosen randomly in the 0 – 2 m range (x-axis is the detector axis).
5. Object starting y-coordinates (y-axis is the direction of travel) chosen to maximise detection probability (simulating the outcome of 10 times oversampling).

A6.2 MDAs determined by Nuvia and HPA

Nuvia (2008) have presented minimum detectable activities (MDAs) for what they label "typical case" and "worst case" measurements. These are derived from experimental measurements of calibration factors made in the laboratory using sources embedded in large containers of sand, and background data taken from one of the beaches monitored. The "typical case" corresponds to a measurement made over sandy areas of St Bees beach, with an "average detector geometry" and a scan speed of 1 m s^{-1}, while the "worst case" corresponds to a measurement made over shingle areas of Barnscar beach, with the object trajectory coinciding with the end of the detector and a scan speed of 1.2 m s^{-1}. Nuvia's MDAs for the typical case are compared with HPA's predictions for St Bees beach in Table A8. In order to determine MDAs at the 95% confidence level, calculations were performed iteratively to determine the object activity that would give an object detection probability of 95%. Comparisons have not been made for Barnscar beach, because the scan speed and position of the object with respect to the detector used by Nuvia (chosen to represent the "worst case") were different to those used in the HPA calculations.

Table A8: Comparisons of minimum detectable activity (MDA) (95% confidence level) for St Bees beach, as determined by Nuvia (Nuvia, 2008) and HPA

Depth (m)			Minimum detectable activity (95% detection level) (Bq)							
Cs,Co, Am	Sr	Scan speed (ms^{-1})	Cs-137		Co-60		Sr-90		Am-241	
			Nuvia	HPA	Nuvia	HPA	Nuvia	HPA	Nuvia	HPA
0.0001	0	1.0	9.0e3	1.1e4	4.0e3	5.2e3	1.5e5	1.1e5	4.0e4	3.7e4
0.05	0.01	1.0	1.5e4	2.6e4	8.0e3	1.0e4	1.9e5	1.4e5	3.8e5	3.6e5
0.1	0.02	1.0	3.7e4	6.3e4	1.6e4	2.1e4	2.1e5	1.6e5	3.7e6	3.5e6
0.15	0.04	1.0	-	-	-	-	2.8e5	2.2e5	3.3e7	3.1e7
0.2	0.06	1.0	1.7e5	2.9e5	5.0e4	7.0e4	3.9e5	2.9e5	-	-
0.3	0.11	1.0	8.3e5	1.3e6	1.8e5	2.5e5	5.9e5	4.5e5	-	-
-	0.13	1.0	-	-	-	-	8.1e5	6.2e5	-	-

Notes on HPA calculations:
1. 0.3 m overlap pass included
2. 0.05 m simulation step size
3. Simulated count rate measured over 1 s
4. Simulated object x-coordinates chosen randomly in the 0 – 2 m range (x-axis is the detector axis)
5. Object starting y-coordinates (y-axis is the direction of travel) chosen to maximise detection probability (simulating the outcome of 10 times oversampling)

A7 DISCUSSION AND CONCLUSIONS

A7.1 Performance of the Groundhog Evolution2™ system

For objects on the surface of the beach, HPA's calculations indicate MDAs of 11 kBq for ^{137}Cs, 5 kBq for ^{60}Co, 110 kBq for ^{90}Sr and 37 kBq for ^{241}Am. At greater depths (given in brackets), HPA's calculations indicate MDAs of 1.3 MBq for ^{137}Cs (0.3 m), 250 kBq for ^{60}Co (0.3 m), 620 kBq for ^{90}Sr (0.13 m) and 31 MBq for ^{241}Am (0.15 m).

A number of features may be observed in the data presented in Table A4 to Table A7:

1. For buried objects within 10 cm of the surface, the Groundhog Evolution2™ system is predicted to be most sensitive for objects containing ^{60}Co, followed in order of decreasing sensitivity by objects containing ^{137}Cs, ^{90}Sr and ^{241}Am.
2. However, for objects on the surface, the system is more sensitive to objects containing ^{241}Am than objects containing ^{90}Sr.
3. For all four radionuclides, an approximately exponential decrease in detection probability is found with increasing depth for those object activities where the detection probability varies over a significant part of the 0 – 100% range within the depth range investigated.

A7.2 Comparisons of MDA determined by Nuvia and HPA

Generally, agreement between the calculated MDAs is reasonable, although there are some differences. Best agreement is found for ^{241}Am measurements where HPA's values are about 95% of Nuvia's. For ^{90}Sr and ^{60}Co, HPA's values are about 75% and 130% of Nuvia's respectively. Poorest agreement is found for ^{137}Cs measurements, where HPA's values are about 170% of Nuvia's.

Possible reasons for differences between modelling and experimentally derived calibration factors include uncertainties in sand density, sand composition and water content of the sand. Nuvia compared their experimentally-derived calibration factor values with their own Monte Carlo modelling results and also found differences (Nuvia 2008). However, from the data presented in the Nuvia report, it is not possible to make a direct comparison between Nuvia's and HPA's MDAs derived from modelling. Nuvia's results do indicate that, for ^{241}Am, modelling predicts slightly lower MDAs than those predicted by the experimental measurements; while the reverse is true for ^{60}Co measurements. HPA's comparisons of MDAs derived from modelling and Nuvia's experimentally derived MDAs indicate similar findings for both radionuclides.

A8 ACKNOWLEDGEMENTS

The authors are grateful to Mike Davies of Nuvia for providing data and information relating to the Groundhog Evolution2™ beach monitoring system.

A9 REFERENCES

Currie LA (1968). Limits for Qualitative Detection and Quantitative Determination: Application to Radiochemistry. *Anal Chem*, **40**, 586-593.

Davies M (2009). Personal communication, Nuvia, UK.

Nuvia (2008). Groundhog Evolution2™ Limits of Detection for Particles of ^{241}Am, ^{90}Sr, ^{6O}Co and ^{137}Cs. Nuvia Report 87204/TR/013, Issue A (April 2008).

Youngman MJ and Etherington G (2003). Review of the procedures currently used for the monitoring of Sandside Bay. NRPB Contract Report, NRPB-DA/3/2003. Available online at http://www.sepa.org.uk/pdf/publications/technical/Sandside_April_2003.pdf.

APPENDIX B Worked example to estimate the population of objects on a beach using method 1

B1 INTRODUCTION

This Appendix provides a worked example of the use of method 1 to estimate populations of objects, as described in Section 4.2.1. Artificial monitoring data of objects found and detection probability were created for the purpose of demonstrating different aspects of the algorithm; they should not be taken as examples of real data.

B2 INPUT DATA

Table B1 presents hypothetical data on the activities and depths of objects found on a beach over the whole of the monitoring programme and B2 shows the corresponding detection probabilities for these objects. Note that the objects are banded by activity and detection depth, and detection probabilities are specified for a specific object activity at a specific depth.

Table B1: Example values for the cumulative number of objects found in each activity and depth band $N_{C,a,d}$

Activity	Sand depth				
	<= 2.5 cm	<= 7.5 cm	<=12.5 cm	<=17.5 cm	<=25 cm
<= 3 kBq					
<= 30 kBq	6	8	2	2	
<= 300 kBq		4	2		
> 300 kBq					

In this example, the number of objects expected to be found by a single, complete scan of the beach, $N_{S,a,d}$. is equal to half of these values

Table B2: Example detection probability data

Activity	Sand depth				
	0.0001 m	0.05 m	0.1 m	0.15 m	0.2 m
1 kBq	0.1	0	0	0	0
10 kBq	92	22	8	2	0
100 kBq	100	100	100	79	18
1000 kBq	100	100	100	100	100

B3 CORRECTION FOR REPEATED MONITORING

The cumulative number of objects found in each activity and depth band from all scans of a particular beach may be denoted by $N_{C,a,d}$, where *a* and *d* are indices indicating the

activity and depth band. The corresponding number of objects expected to be found by a single, complete scan of the beach may be denoted by $N_{S,a,d}$. $N_{S,a,d}$ may be determined from $N_{C,a,d}$ and the ratio of the area of the beach to the area monitored, as follows:

$$N_{S,a,d} = N_{C,a,d} \times A_{beach}/A_{monitored} \quad (1)$$

In this example, it is assumed that the total area monitored during the monitoring programme is equal to twice the area of the beach.

B4 INITIAL ESTIMATE OF THE POPULATION OF OBJECTS

In order to calculate the initial estimate, the detection efficiency is applied to the number of objects expected to be found in a complete, single scan in each activity and depth band:

$$P_{E1,a,d} = N_{S,a,d} \times 100/E_{a,d} \quad (2)$$

where *a* and *d* are indices indicating the activity and depth band, $P_{E1,a,d}$ is the initial estimate of the population of objects in each activity and depth band and $E_{a,d}$ is the detection probability for each activity and depth band.

The results for the initial estimate derived from the data in Table B1 and Table B2 are shown in Table B3.

Table B3: Initial estimate of the population of objects on the beach

Activity	Sand depth				
	<= 2.5 cm	<= 7.5 cm	<=12.5 cm	<=17.5 cm	<=25 cm
<= 3 kBq	0	0	0	0	0
<= 30 kBq	3.26	18.18	12.5	50	0
<= 300 kBq	0	2	1	0	0
> 300 kBq	0	0	0	0	0

B5 SECOND ESTIMATE OF THE POPULATION OF OBJECTS

A number of steps are performed to calculate the second estimate.

Step 1

For all non-zero first estimates where the relevant detection probability is greater than 10%, this result is accepted as the second estimate. Table B4 shows the numbers that are accepted as second estimates using this assumption. Note that blank cells represent as yet unaccepted numbers.

Table B4: First estimates that are accepted as second estimates of the population of objects on the beach

Activity	Sand depth				
	<= 2.5 cm	<= 7.5 cm	<=12.5 cm	<=17.5 cm	<=25 cm
<= 3 kBq					
<= 30 kBq	3.26	18.18			
<= 300 kBq		2	1		
> 300 kBq					

Step 2

This step applies when a first estimate of zero has been made, but objects have been found at greater depths. In this case, the population of objects in the next lower layer where at least one object has been found is substituted, making allowance for the difference in layer depths. Table B4 shows a zero first estimate for objects with activity greater than 30 kBq and less than or equal to 300 kBq in the topmost layer. Two objects are expected to be found from a single, complete scan of the beach in the next layer down (Table B1), but that layer is double the depth of the topmost layer; so the second estimate in the topmost layer is therefore 1. This is shown in Table B5 with earlier accepted estimates in grey.

Table B5: First estimates accepted as second estimates of the population of objects on the beach

Activity	Sand depth				
	<= 2.5 cm	<= 7.5 cm	<=12.5 cm	<=17.5 cm	<=25 cm
<= 3 kBq					
<= 30 kBq	3.26	18.18			
<= 300 kBq	1	2	1		
> 300 kBq					

Step 3

This step applies when a non-zero first estimate is made and when the detection efficiency is less than 10%. This estimate is compared with the mean plus two standard deviations of the first estimates for that activity band. The mean and standard deviation are calculated from the first estimates for all depths where the detection efficiency is more than 10%, with allowance being made for differences in layers depths. In Table B4, only objects with activity greater than 3 kBq and less than or equal to 30 kBq are affected. From the topmost two depths, where detection efficiency is greater than 10%, the mean of the first estimate is 2.47 cm^{-1} and the standard deviation is 1.65 cm^{-1}. The algorithm compares the first estimate with the mean plus 2 standard deviations, in this case 5.77 cm^{-1} or 28.9 objects in a 5 cm layer. The first estimate in the third layer is less than this and is therefore accepted; the first estimate in the fourth layer is greater than this and is therefore rejected, and the mean substituted as the second estimate. Table B6 shows the result of this step.

Table B6: First estimates accepted as second estimates of the population of objects on the beach

Activity	Sand depth				
	<= 2.5 cm	<= 7.5 cm	<=12.5 cm	<=17.5 cm	<=25 cm
<= 3 kBq					
<= 30 kBq	3.26	18.18	12.5	12.35	
<= 300 kBq	1	2	1		
> 300 kBq					

Step 4

Finally, all other results are assumed to be zero. The final set of second estimates is shown in Table B7.

Table B7: Second estimate of the population of objects on the beach

Activity	Sand depth				
	<= 2.5 cm	<= 7.5 cm	<=12.5 cm	<=17.5 cm	<=25 cm
<= 3 kBq	0	0	0	0	0
<= 30 kBq	3.26	18.18	12.5	12.35	0
<= 300 kBq	1	2	1	0	0
> 300 kBq	0	0	0	0	0

B6 ESTIMATE OF THE POPULATION OF OBJECTS PER HECTARE

To determine the population of objects per unit area of beach from the population of objects, the population of objects in each activity and depth band is divided by the area of the beach in hectares. Table B8 gives the population of objects assuming that the beach has an area of 100 hectares.

Table B8: Estimate of the population of objects per hectare

Activity	Sand depth				
	<= 2.5 cm	<= 7.5 cm	<=12.5 cm	<=17.5 cm	<=25 cm
<= 3 kBq	0	0	0	0	0
<= 30 kBq	$3.3\ 10^{-2}$	0.18	0.13	0.12	0
<= 300 kBq	$1\ 10^{-2}$	$2\ 10^{-2}$	$1\ 10^{-2}$	0	0
> 300 kBq	0	0	0	0	0
1 hectare = 10^4 m^2					

APPENDIX C External gamma dose rates from beta-rich objects on the beaches

Beta-rich and cobalt-rich objects on the beaches will give emit gamma-rays that could externally irradiate people using the beaches. This Appendix discusses the external gamma doses that people using the beach could receive from these objects and their likely significance in terms of health risks.

Although an assessment of the external irradiation from both cobalt-60 (^{60}Co) and caesium-137 (^{137}Cs) could be made it was decided to concentrate on ^{60}Co beacuse the external dose rate per unit activity of ^{60}Co is greater than that from ^{137}Cs and would therefore represent the more cautious radionuclide to include in this discussion. However, from Table 3 of the main text, the maximum activity of ^{137}Cs within objects removed from beaches (that is beta-rich objects) is greater than that for ^{60}Co, with the difference between the maximum activities being greater than the difference in the dose rate. Therefore, in this Appendix, the dose rate from ^{137}Cs is used in order to scope the highest dose rates that could result from coming into close proximity to an object on a beach, based on the objects found up to August 2009.

C1 MODELLING APPROACH

Using the potential number of objects (Table 20 and Table 21 of the main text) and the beach area (Table 19 of the main text), the area of each beach that could, on average, contain a single object can be estimated. These estimated areas are shown in Table C1. The smallest area on any beach that is likely to contain a radioactive object above 10 kBq is around 1200 m^2. This is approximately equal to a square area of 35 m by 35 m. The typical range of gamma-rays in air is of the order of a few tens of metres. This implies that, on average, a beach user will not be exposed to gamma-rays from more than one object at any time. It was assumed in the following evaluation of this exposure pathway that external gamma exposure to a radioactive object is equivalent to an exposure from a point source and that exposure to a beach user could occur whilst either standing or lying on the beach. Although there may be some small differences in the dose rate from radiation emitted from a particle when compared to that from a stone due to more self absorption within stones, for this discussion it is assumed that this is insignificant and that radionuclides associated with particles and stones will give essentially the same dose rate per unit activity.

Table C1: Beach area (m^2) potentially containing a single object with a radioactivity of 10 kBq or above

	Braystones beach	Drigg beach	Seascale beach	Sellafield beach	St Bees beach
Alpha-rich particle	$9.2\ 10^3$	$1.2\ 10^3$	$9.0\ 10^4$	$1.4\ 10^4$	$7.7\ 10^3$
Beta-rich particle	$2.3\ 10^4$	$1.3\ 10^5$	$6.9\ 10^4$	$1.5\ 10^4$	$1.2\ 10^5$
Cobalt-rich particle	$6.8\ 10^5$	$1.9\ 10^5$	$2.7\ 10^6$	$2.1\ 10^6$	$2.6\ 10^6$
Alpha-rich stone	-	-	-	$1.7\ 10^4$	-
Beta-rich stone	$9.3\ 10^5$	-	$3.5\ 10^5$	$7.6\ 10^3$	-
Cobalt-rich stone	-	-	-	$2.9\ 10^6$	-

(a) Only objects above 10 kBq are considered here as that is the object population for which a reasonably good estimate can be made of the actual object population taking into account the probability of detection. See Section 4.3.

For these calculations an object was assumed to have 1000 kBq of ^{137}Cs (and its decay product, ^{137m}Ba). It is noted from Table 3 of the main text that the maximum radioactivity of any beta-rich object found using the Groundhog Evolution2™ system is approximately 900 kBq (a stone) and that the mean radioactivity of all the beta-rich objects is approximately 30 kBq (Dalton, 2010). In addition to using a high activity for the object it was also assumed that this object was located on the surface of the beach in order to maximise the dose rate from it to a person using the beach. The dose rates estimated within this Appendix can therefore be considered to be cautious and representative of the maximum dose rates from any objects found using the Groundhog Evolution2™ system.

The MicroShield program (Negin, 1986) was used to calculate the external gamma dose rate from the object described above. MicroShield calculates dose rates using the point-kernel method, allowing for attenuation and build-up (accounting for the contribution to dose from multiple scattering of gamma rays) in air and any shielding present between the source and the point where the dose rate is calculated. It is an extensively used code that is simple to operate, but, as noted below, does have some limitations regarding the definition of spatial geometry. Preliminary calculations indicated that the external doses would be low and thus it was considered that the use of more complex and computing intensive calculational methods, such as Monte Carlo codes, was not appropriate in these circumstances.

Microshield calculates dose rate at a point. For an individual at a significant distance from a point source the radiation field incident on the individual will be relatively uniform and it would be appropriate to use the radiation field at any point to estimate the effective dose to the individual. However, at shorter distances the radiation field incident on an individual will be significantly non-uniform. For example, assuming an individual of height 2 m is standing 1 m from a point source, the dose received by the head will be lower by a factor of 2.5 than that to the torso. Under such circumstances it is necessary to choose a point at which the dose is determined and assume that this dose is representative of that to the whole body. For a standing individual, the dose to the torso, which is assumed to be 1 m above the ground, was chosen to represent the dose to the whole body. This is an assumption that has been used in other studies and is consistent with the relative radiosensitivity of organs within the torso compared with the

extremities. For an individual lying on the beach it was assumed that their torso was directly above an object and the doses at 0.1 m (that is to the centre of the torso), with an additional distance accounting for a suitable air gap, were representative of exposure of the whole body.

A further limitation of MicroShield is the assumption that all radiation is incident normal to the surface of the human body. This is a good approximation when there exists a significant (of the order of metres) distance between the source and the point at which the dose is received. As this distance diminishes the approximation breaks down. This is because photons are attenuated within the body before irradiating the organs and tissues of concern, and the attenuation depends on the amount of body tissue through which the photons have to pass. Radiation from point sources close to a body typically arrives at an angle to that body and therefore incurs a greater amount of attenuation. Hence, with regard to 'short' (of the order of centimetres) distances between the source and the exposed individual, the doses generated by MicroShield are likely to be conservative.

Dose rates to individuals standing on the beach, directly above an object, and at a series of horizontal distances (0.1, 0.2, 0.5, 1, 2, 5, 10, 20, 50 and 100 m) away from that point were determined. Dose rates to individuals lying on the beach were calculated assuming 10 mm and 50 mm air gaps between an object and skin, thus implying total distances of 110 mm and 150 mm (to the centre of the torso), respectively.

The largest dose rates received will occur when there is no shielding, that is when an object resides on the surface of the beach. However, for comparative purposes objects buried at depths of 50, 100 and 200 mm were also considered for an individual standing on a beach. A bulk density of sand on a beach of $2\ 10^{6}$ g m^{-3} was used to characterise the shielding.

C2 RESULTS AND CONCLUSIONS

Estimated external gamma dose rates are presented in Table C2 for an object of 1000 kBq of ^{137}Cs on the surface of the sand, ie, only air exists between the object and the person. The dose rates calculated are very small.

Table C2: External gamma dose rate from a point source of ^{137}Cs with a radioactivity content of 1000 kBq

Horizontal Distance from object (m)	Vertical Distancefrom object (m)	Effective Dose Rate (µGy h^{-1})[(a)]
Individual lying on the beach		
0	0.11	$4.9\ 10^{0}$
0	0.15	$2.6\ 10^{0}$
Individual standing on the beach		
0	1	$5.9\ 10^{-2}$
0.1	1	$5.8\ 10^{-2}$
0.2	1	$5.7\ 10^{-2}$
0.5	1	$4.7\ 10^{-2}$
1	1	$3.0\ 10^{-2}$
2	1	$1.2\ 10^{-2}$
5	1	$2.2\ 10^{-3}$
10	1	$5.8\ 10^{-4}$
20	1	$1.4\ 10^{-4}$
50	1	$2.8\ 10^{-5}$
100	1	$5.0\ 10^{-6}$

(a) Using an effective dose per unit air kerma free-in-air conversion factor of 0.8. This is the value for rotationary geometry for 1 MeV photons and is also used to represent an approximate value for other geometries which were assumed to be possible when the body is lying down (anterior-posterior; posterior-anterior; left or right lateral) (ICRP, 1996)

It is unlikely that an individual would spend a significant time in close proximity to an object, but even if this did occur the doses would be small. For example, assuming an individual lies directly above an object containing 1000 kBq of ^{137}Cs for 4 hours they would receive an exposure of approximately 20 µGy.

C3 REFERENCES

Dalton AP (2010). Personal communication, Sellafiedl Ltd, UK.

ICRP (1996). International Commission on Radiological Protection. Age-dependent Doses to members of the Public from Intake of Radionuclides. Pt.5: Compilation of Ingestion and Inhalation Dose Coefficients. ICRP Publication 72. *Ann ICRP*, **26** (1). Pergamon Press, Oxford.

Negin CA (1986). MICROSHIELD – A microcomputer program for analyzing dose rate and gamma shielding. CONF-861102, ISSN 0003-018x CODEN TANSA. *Trans Am Nucl Soc*, **53**, 421-422.

APPENDIX D The probability of a particle becoming trapped in the eye or ear

Exposure pathways by which an individual could come into contact with a radioactive object include inhalation, ingestion and skin contact. Estimates of the probability of individuals encountering an object by these exposure pathways have been estimated within this study. However, it was also considered important to investigate the likelihood of a particle becoming trapped in other parts of the body, particularly the ear, due to the potentially long time such a particle could be present before it was detected and removed. This Appendix considers the probability of a particle becoming trapped in the eye and in the ear following a visit to the beach. It should be noted that stones were considered to be too large to be trapped in the ear or eye without being removed quickly and so they are not considered further in this Appendix.

The approach adopted has been to estimate the likelihood of an individual getting a grain of sand in the eye or ear and subsequently the likelihood of this being a radioactive particle. From Table C1 the minimum beach area that could contain a radioactive particle is around 1200 m^2 for an alpha-rich particle. The depth of sand that this particle could reside in was assumed to be 0.15 m. The mass of sand within this volume, assuming a bulk sand density of 2 10^6 g m^{-3}, is 3.6 10^8 g.

The mass of a single grain of sand can be estimated using the following equation.

$$mg = (4/3) * \pi * (rg)^3 * \rho_{grain}$$

where

mg = Mass of a sand grain, g

rg = Radius of sand grain, assumed to be 1 10^{-4} m, see below

ρ_{bulk} = Bulk density of sand, 2 10^6 g m^{-3}

The radius of a grain of sand can vary considerably but was assumed to be 1 mm, consistent with the upper size of particles as defined in this study. Using the above equation, the mass of a single grain of sand is approximately 8 10^{-6} g. Within 3.6 10^8 g of sand there are therefore approximately 4.5 10^{13} grains of sand. As there is, on average, one particle within the volume containing this many grains of sand, the probability of a grain of sand being a radioactive particle is 2.2 10^{-14}.

It is not unrealistic to assume that when an individual is on a beach there could be grains of sand in the ear. The amount of sand that could be in the ear at any time cannot be known for certain as it would depend on many factors including the size of the individual, what they were doing, how often the head comes into contact with sand, how much sand is either placed in the ear or removed from it by the action of fingers, etc. For this scoping calculation it was assumed that the sand loading on the skin of the ear would be the same as the sand loading on other parts of the body, ie, between 0.5

and 50 mg cm^2 (see Table H1 in Appendix H) and that the surface area of skin in each ear is of the order of a few cm^2. Using these values, the mass of sand in the ears at any time could be approximately 1 10^{-3} and 1 10^{-1} g. Using the mass of a grain of sand estimated previously, the number of grains of sand that could be in the ear at any time can be estimated to be between 125 and 12500. The probability that there is a radioactive particle in the ear is therefore between approximately 3 10^{-12} and 3 10^{-10}.

No dependence on time has been taken into account in the above estimation and so, as a cautious assumption, the above probability could be related to the probability of a particle getting into the ears over a period of an hour. Taking a conservative value of annual beach occupancy of a thousand hours, the annual probability of a radioactive particle getting into the ear is around 10^{-9} to 10^{-7}.

For the eye it is expected that an object approaching the size of a grain of sand would cause some irritation and would be removed quickly, limiting the length of time that an object would be present in the eye. For this scoping calculation, it was conservatively assumed that a new grain of sand would get into for eye once per hour whilst an individual is on the beach. Taking a conservative value of annual beach occupancy of a thousand hours, 1000 grains of sand could get into the eyes per year. Assuming that a radioactive particle has an equal probability of getting into the eye as a grain of sand, which is extremely conservative, the annual probability of a particle getting into the eye is approximately 10^{-11}.

The probabilities of getting a radioactive object in the eye or the ear that have been calculated above are for a high occupancy beach user. For a beach user with occupancy around the median value of the distribution of all beach users, the probability would be approximately an order of magnitude lower.

APPENDIX E Overall risk associated with a particle embedded in a wound

With respect to overall health risks to a beach user resulting from an object embedded in a wound, the highest risks are associated with alpha-rich particles, and stochastic risk arising from uptake of radionuclides from the wound site is the most important factor to consider. As has been demonstrated for the ingestion pathway (Section 8.8.2), absorbed doses to organs resulting from uptake would be orders of magnitude lower than the thresholds for deterministic effects. With respect to localized absorbed doses to tissues at the wound site, these are likely to be delivered to subcutaneous tisses for which specific risk estimates are not available. Significant uncertainties are associated with both the estimation of the probability that a particle could become embedded in a wound, and the estimation of doses and risks to health should a particle become embedded. These uncertainties arise mainly from lack of data with which to characterise this pathway, and because dosimetry relating to contamination of wounds for the specific case of individuals using a beach requires further development. This Appendix presents the results of a scoping calculation that is intended to give an indication of the importance of this pathway for overall risks to health in comparison to the pathways that have been considered in greater detail in the main part of this report.

E1 PROBABILITY THAT A PARTICLE COULD BECOME EMBEDDED IN A WOUND

The annual probability that a particle could become embedded in a wound may be determined by multiplying together three subsidiary probabilities: (a) the annual probability that a particle could come into contact with the skin of a beach user; (b) the probability that the beach user could have a wound in which a particle could become embedded; and (c) the probability that a particle on the skin could be embedded in a wound.

The annual probability that a particle could come into contact with the skin

The annual probability of an alpha-rich particle coming into contact with intact skin is approximately 5 10^{-6}, for a typical high occupancy beach user.

The probability that the beach user could have a wound

A high occupancy beach user spends approximately 1000 h on the beach. It is postulated that the maximum time that such a person could have a wound in which a particle could become embedded is 10 h (ie,1% of the time spent on the beach), so the probability that an individual beach user would have such a wound at any time is 0.01. The condition of the wound would need to be such that a particle could become

embedded at a depth sufficient to allow uptake of a radionuclide to occur. This would exclude wounds covered with dressings, and wounds for which healing is well-advanced.

The probability that a particle on the skin could be embedded in a wound

It is cautiously assumed that the area of skin occupied by a wound is 1 cm^2, and that any particle within this area could become embedded in the wound at a depth sufficient to allow uptake of a radionuclide to occur. The mean value for the area of exposed skin while on a beach is typically in the range 1000 - 3000 cm^2, for an adult, and 300 – 700 cm^2 for a 1 year old child. The wound would therefore occupy about 0.05% of the exposed skin of an adult, and so the probability that a particle on the skin could be embedded in a wound is 5 10^{-4}.

Combining these probabilities indicates that the annual probability for an adult beach user that a particle could become embedded in a wound is no greater than 2.5 10^{-11}. The annual probability for a young child could be a factor of 4 - 5 higher.

E2 ESTIMATION OF EFFECTIVE DOSE RESULTING FROM UPTAKE FROM AN ALPHA-RICH PARTICLE

The main factor determining effective dose resulting from uptake from a wound site is the fractional transfer factor, f_W, which is the fraction of the activity contained in the particle that is dissolved into body fluids and is available for uptake by the organs of the body. No specific information on this factor is available for particles found in the vicinity of the Sellafield site. Two approaches have been used to estimate effective doses that may arise as a result of uptake from an alpha rich particle, as described below.

E2.1 Experimental determination of uptake for particles found at Maralinga

Studies have been carried out to determine f_W in laboratory rats for contaminated particles from the former nuclear weapons test site at Maralinga in South Australia (Harrison et al, 1990). A number of particles were investigated, but the Maralinga material that is likely to be most similar to alpha-rich particles found in the vicinity of the Sellafield site is the that designated “Oxide 8/1”, which is an oxide containing ^{239}Pu and ^{241}Am. Uptake of ^{239}Pu was measured at 1, 6 and 12 months, while uptake of ^{241}Am was measured at 1 and 6 months. Values ranged from 6 10^{-5} to 1 10^{-4}, and it was concluded that there was no clear evidence of continued uptake after 1 month. Dose coefficients (effective doses per Bq uptake) are similar for ^{238}Pu, $^{239/240}$Pu and ^{241}Am, with those for $^{239/240}$Pu being the highest. Values for $^{239/240}$Pu for a 1-year old child and an adult are 7.3 10^{-4} Sv/Bq and 4.5 10^{-4} Sv/Bq, respectively.

The most active alpha-rich particle that could be encountered by an adult has a total activity of 1.03 MBq, while for children the corresponding activity is 323 kBq (Section 10.1). Using the dose coefficients for $^{239/240}$Pu and assuming a value for f_W of 1 10^{-4} for

adults and children results in effective doses of 30 mSv and 50 mSv for a 1-year old child and an adult, respectively.

E2.2 Theoretical prediction of uptake made using the NCRP wound model

The model of wound biokinetics and dosimetry developed by the US National Council on Radiation Protection and Measurements (NCRP, 2006) can be used to predict uptake from the wound site, and the resulting effective dose for adults. The model was implemented for a fragment[1] containing ^{239}Pu in an insoluble form. The rate of uptake is predicted to be very low for the first 2-3 days after introduction of the fragment at the wound site, reaches a maximum at about 70 days, and then reaches a constant value of about 10% of the peak uptake rate after about 1000 days. This rate of uptake then continues for the lifetime of the person.

This prediction of long term uptake appears to be unrealistic for the case of a beach user. Long term uptake is only possible if the fragment becomes permanently embedded, and this would only occur in the event of a serious lesion. Beach users engaging in leisure activities would only have superficial pre-existing wounds (minor cuts or grazes), and if a beach user incurred a serious injury while on the beach, then they would remove themselves (or be removed) from the beach immediately to seek medical attention. Since any wound in which a fragment could become embedded would be superficial, it is reasonable to suppose that the fragment would be removed by normal mechanisms (washing, mechanical action ("wear and tear"), removal of a scab, etc) within a few days. If the most active alpha-rich particle (containing a total of 1.03 MBq ^{238}Pu, $^{239/240}$Pu and ^{241}Am) remained embedded for a period of 10 days, the effective dose resulting from uptake over this period would be approximately 20 mSv.

E2.3 Estimates of risks of fatal cancer

Although the results of the Maralinga study and the predictions of the NCRP wound model are in disagreement regarding the time pattern of uptake, they predict similar effective doses in the event that the most active alpha-rich particle found to date became embedded in a wound, ie, a few 10s of mSv.

The lifetime risks of fatal cancer that would result from an uptake giving rise to a committed effective dose of 1 Sv are estimated to be 16% and 9% for a 1 year old child and a 20 year old adult, respectively (Section 8.4). Using the effective doses estimated in Section 0, the estimated risks of fatal cancer in the unlikely event that the most active alpha-rich particle that could be encountered was embedded in the skin are 0.4% and 0.5% for these age groups.

[1] "Fragment" is NCRP's terminology for an object with a size greater than 20 um.

E2.4 Estimates of overall risks to health

As explained in Section 10, where stochastic risk is the dominant factor, overall risk to the beach user may be determined by multiplying the annual probability of coming into contact with an object by the risk that that person would contract a fatal cancer during his or her lifetime if contact with the object did occur. Multiplying the annual probability that a particle could become embedded in a wound (Section E2.1) by the risk of fatal cancer if a particle did become embedded (Section E2.3) gives values for overall risks of fatal cancer of the order of 10^{-12} – 10^{-13}. Given the uncertainties involved in this scoping calculation, it is concluded that overall risks from ingestion and from uptake via a wound for alpha-rich particles are similar.

E3 REFERENCES

Harrison JD, Hodgson A, Haines JW and Stather JW (1990). Biokinetics of plutonium-239 and americium-241 in the rat after subcutaneous deposition of contaminated particles from the former nuclear weapons test site at Maralinga: Implications for human exposure. Chilton, NRPB-M198.

NCRP (2006). Development of a Biokinetic Model for Radionuclide-Contaminated Wounds and Procedures for Their Assessment, Dosimetry and Treatment. NCRP Report No 156.

APPENDIX F Supplementary information on the ingestion of objects

This Appendix discusses the size range of objects that could be ingested, both inadvertently and deliberately, and possible ingestion rates. The information on soil ingestion rates has largely been taken from Smith and Bedwell, 2005.

F1 INGESTION

Inadvertent ingestion of discrete objects might occur through the consumption of contaminated food or through normal hand-to-mouth actions. In either scenario, common sense suggests that there is no lower limit to the size of object that might become attached to food, such as a sandwich, or the eater's hand and therefore transferred to the mouth. However, the upper end of what could be ingested is dependent on the age of the individual and, to some extent, on the individual as each person is likely to have slightly different tolerances to the size of an object they are capable of swallowing. This is discussed in the following sections.

F2 INADVERTENT INGESTION

For objects on food common sense suggests that there might be an upper size of object above which someone might find food gritty and unpalatable. In this case, the person is likely to spit out the mouthful taken and not eat any further food, reducing the opportunity to ingest a discrete object. For hard, irregularly shaped objects, the lower limit of detection in the mouth is around 10 μm (Engelen et al, 2005) above which food has a gritty texture. For objects which are softer and without hard edges, such as the particles found naturally in chocolate, the size for detection can be larger and may be undetectable in the mouth up to around 25 μm. The ability to detect an increase in grittiness (or conversely, a decrease in smoothness) appears to level off at around 80 μm for hard objects (Engelen et al, 2005) and so a conservative, order-of-magnitude upper size limit for inadvertent ingestion of undetected discrete objects could be taken as 100 μm.

It should also be noted that the concentration of particulate matter has a significant effect on palatability (Imai et al, 1995). It is reasonable to assume that a person might tolerate a certain amount of grittiness in food and may willingly consume objects larger than 100 μm provided there were few of them, for example a speck of eggshell in an egg sandwich. The same could be said for objects transferred to the mouth without food. It can be concluded that, provided the number of objects is small, and dependent upon the individual concerned, a person might consume the objects rather than spit them out. A conservative upper size limit for detecting discrete objects that may be present in the mouth by accident but which could be ingested would be an order of magnitude higher than that for consciously detecting the object in the mouth, ie 1 mm.

For comparison, the International System defines sand as having grain sizes between 20 µm and 2 mm (The Open University, 2002).

F2.1 Review of inadvertent soil ingestion data

Review by Simon (1998)

In 1998 a review of the literature covering both inadvertent ingestion of soil and geophagia was produced by Simon (1998). It indicated that the most reliable estimates of inadvertent soil intake were from studies that had inferred their findings from the quantity of soil trace elements measured in faeces, and, in this context, he listed the following 6 papers: Binder et al (1986), Linsalata and Eisenbud (1986), Clausing et al (1987), Calabrese et al (1989), Davis et al (1990) and van Wijnen et al (1990). Simon noted that - "there is a paucity of studies which have been specifically designed to determine soil ingestion rates …. Only four rigorously conducted empirical studies to quantify soil ingestion are noted in the English literature", these are listed as Binder et al (1986); Calabrese et al (1989); van Wijnen et al (1990) and Davis et al (1990). Simon noted that the findings of these studies provide ingestion rates that are expected to be suitable for typical US or European populations.

A summary of the data from these four studies (and two papers analysing data from two of these studies) is provided in Table F1, the text for which was taken from Table 3 in Simon (1998).

Simon noted that the majority of the available data were for children, with very few data for adults. He did state, however, that, "There appears to be a general consensus that among adults in western society who do not routinely contact the soil by occupation or hobby, intake of soil is very low – probably in the order of a few milligrams to a few tens of milligrams per day".

Simon briefly discussed the use of variability ranges and uncertainties on soil ingestion rates in dose assessments, but concluded that "Despite the rather adequate body of literature that documents the occurrence of soil ingestion, at present there is not sufficient information to adequately assess the true variability within any single group or uncertainty of mean intake values". A few publications were noted that have attempted to model the variability of intakes within a population, for example, Thompson and Burmaster (1991. Finley et al (1994) fitted the intake data from Stanek and Calabrese (1995) to a population distribution. For children they gave the 5^{th}, 10^{th}, 25^{th}, 50^{th}, 75^{th}, 90^{th}, and 95^{th} percentiles as 0, 0, 0, 16, 45, 67 and 110 mg d^{-1}.

Simon (1998) also provided a compilation of possible uncertainty distributions on inadvertent intake rates based on his judgment after reviewing the literature cited in the paper. He noted that "the central estimates are consistent with the consensus of numerous authors that 100 mg d^{-1} represents a reasonable value of intake for children" and that the ranges "may be assumed to represent a subjective 95% confidence interval for a representative individual". Simon's suggested distributions relevant to this study are given in Table F2.

Table F1: Review of inadvertent soil ingestion rates (data taken from Simon (1998))

Author(s)	Study description	Ingestion rate estimate
Binder et al (1986)	59 children in Montana (urban area) were studied in summer using fecal analysis for soil trace elements	181 mg d^{-1} (Al) 184 mg d^{-1} (Si) 1834 mg d^{-1} (Ti)
Calabrese et al (1989)	65 children, 1-4 years of age in greater Amherst, MA area (urban), fecal analysis for soil trace elements during 8 day period, one soil pica child identified	9 to 40 mg d^{-1} for non-pica, 5 to 8 g d^{-1} for pica
Davis et al (1990)	104 school children randomly selected, 2–7 years of age in SE Washington State (urban and rural areas) fecal analysis for soil trace elements	39 mg d^{-1} (Al) 82 mg d^{-1} (Si) 245 mg d^{-1} (Ti)
Van Wijnen et al (1990)	Two different groups in summer in the Netherlands were studied and compared to hospitalised children, using fecal analysis for titanium: Day care groups: Camping groups	 0 to 90 mg d^{-1} (geometric mean) 30 to 200 mg d^{-1}
Thompson and Burmaster (1991)	Reanalysed data of Binder et al (1986) using actual stool weights, fitted parametric (lognormal) distributions	59 mg d^{-1} (geometric mean) 91 mg d^{-1} (arithmetic mean) 126 mg d^{-1} (standard deviation)
Stanek and Calabrese (1995)	Revision of estimates presented in Calabrese et al (1989)	Range of median daily soil ingestion of 64 subjects over 365 days: 1 – 103 mg d^{-1} Range of average daily soil ingestion of 63 subjects over 365 days: 1 – 2268 mg d^{-1} Median of the daily average soil ingestion for 64 subjects: 75 mg d^{-1} Range of upper 95% soil ingestion estimates: 1 – 5263 mg d^{-1} Median upper 95% soil ingestion estimate of 64 subjects over 365 days: 252 mg d^{-1}

Table F2: Suggested values of soil ingestion model parameters for inadvertent ingestion, from Simon (1998)

Lifestyle	Distributions on ingestion rates (g d^{-1}) [(a)]	
	Adult	Child [(b)]
Rural lifestyles – heavily vegetated, forest and fields	LN(0.1, 3.2)	LN(0.1, 4.2)
Rural lifestyles – sparsely vegetated	LN(0.2, 3.2)	LN(0.2, 4.2)
Suburban lifestyles – including lawns, parks, recreational areas, some gardens	LN(0.1, 3.2)	LN(0.1, 4.2)

(a) LN. Lognormal distribution (geometric mean, geometric standard deviation)

(b) Child approximately 1-6 years

Review of literature produced following Simon (1998)

A literature review of papers on soil ingestion produced since 1985 was undertaken. The majority of the papers identified had been considered, or were related to, those

reviewed by Simon. Those studies not considered by Simon, or which have been published after the report by Simon, are discussed briefly below.

Stanek et al (1997) reported the results of a study on adult ingestion rates. This gave a median of 1 mg d^{-1}, an average of 10 mg d^{-1}, a standard deviation of 94 mg d^{-1}, a 75th percentile of 49 mg d^{-1} and a 95th percentile of 331 mg d^{-1}.

Calabrese et al (1997) provided an analysis of 64 children residing on a contaminated site in Montana. This gave a median of < 1 mg d^{-1} and a 95th percentile of 160 mg d^{-1}. However, it was noted that the method has a residual negative error suggesting estimates were below the actual values. The magnitude could not be quantified but it was stated that it was likely not to affect the mean by more than 40 mg d^{-1}. The impact on the upper end was less clear.

Stanek (2000) provided daily estimates for 64 children (age 1 – 4 years). This gave a mean of 31 mg d^{-1}, a median of 17 mg d^{-1}, a 95th percentile over 7 days of 133 mg d^{-1}, over 30 days of 112 mg d^{-1}, over 90 days of 108 mg d^{-1} and over 365 days of 106 mg d^{-1}. It was stated that these provide basic distributions that could serve as a starting point for Monte Carlo risk assessments.

EPA recommendations

Using the results of studies carried out up until 1997 the US EPA (1999) recommended for children the use of 100 mg d^{-1} as a mean value and 400 mg d^{-1} as an upper estimate of the mean. A value of 50 mg d^{-1} was recommended for adults.

Assumptions used in the CLEA contaminated land model

In modelling soil ingestion by children from birth to six years the Contaminated Land Exposure Assessment (CLEA) model (Defra and EA, 2002) treats the daily ingestion rate as a lognormal distribution with a specified range that uses the EPA recommendations as a basis. The distribution has an approximate mean rate of 100 mg d^{-1} and a 97.5th percentile rate of about 400 mg d^{-1} (50th percentile – 64 mg d^{-1} and 95th percentile - 303 mg d^{-1}). It was noted that no tracer studies had been undertaken on older children and only two on adults. The soil ingestion rates for older children and adults in the CLEA model were treated deterministically (ie, single point value). For older children the value was set at 100 mg d^{-1} and for adults at 50 mg d^{-1}.

F2.2 Recommended inadvertent ingestion rates of sand for this study

For this study inadvertent ingestion rates of sand on beaches were required for various age groups. None of the papers mentioned above specifically relate to sand, although some of the children in the study by van Wijnen et al (1990) were camping by a beach. It was assumed, however, that inadvertent ingestion rates for sand would be similar to those for soil and thus sand ingestion rates could be determined by considering the data on soil ingestion rates. This approach is consistent with that adopted for the

assessment of contaminated beaches around the Dounreay site (Smith and Bedwell, 2005).

Young children - Daily ingestion rates

On the basis of the data summarised in the above sections, drawing in particular on the results for children in camp sites from van Wijnen et al (1990), the EPA guidance (based on experimental data up to 1997), and the approach taken in CLEA, it seemed reasonable for children below the age of around 6 to adopt the distribution on daily intakes used in CLEA. This was defined as follows: mean 100 mg d^{-1}, 50th percentile 64 mg d^{-1}, 95th percentile 303 mg d^{-1} and 97.5th percentile 400 mg d^{-1}. The distribution is given in Table F3.

Table F3: Distributions on soil intake rates for infants (<3 years)

Distribution parameters	Daily intake rate mg d^{-1}	Hourly intake rate, mg h^{-1} (assuming daily exposure of 2 hours)	Hourly intake rate, mg h^{-1} (assuming distribution on daily exposure – see text)
Mean	100	50	47
50th percentile	64	32	32
95th percentile	303	151	134
97.5th percentile	400	200	176

Young children - Hourly ingestion rates

All the experimental studies reviewed focussed on the daily ingestion rate. As the exposures considered in this study are short term and episodic inadvertent ingestion rates were required in terms of mg h^{-1}. It was therefore necessary to derive a distribution on hourly rates from the distribution on daily intakes mentioned above. The average hourly intake rate for any given exposure was given by the following:

$HI = DI / ED$

where

HI = hourly intake, mg h^{-1}

DI = daily intake, mg d^{-1}

ED = exposure duration, h d^{-1}

The daily intake clearly depends both on the amount of time spent outdoors that day and the activities undertaken whilst outside. It is likely that younger children in this age range (ie, under around 3 years old) would have a higher average hourly ingestion rate but would be outside for less time than the upper end of the age range. Thus the daily intakes for both may be similar, but the actual hourly rates would be higher for the younger children. Unfortunately, the data available do not make hourly rates simple to derive as none of the studies give detailed information on the time spent with access to soil.

One study investigating the outdoor play behaviour of children (under 18 years old, no further age breakdown was given) (Wong et al, 2000) indicated that the median reported play frequency was 7 days per week in warm weather and 3 days per week in cold weather. The median play duration was 3 hours per day in warm weather (5^{th} percentile – 1 hour per day, 50^{th} percentile – 3 hours per day, and 95^{th} percentile - 8 hours per day) and 1 hour per day in cold weather (5^{th} percentile – 1 hour per day, 50^{th} percentile – 1 hour per day, and 95^{th} percentile - 4 hours per day). Considering the results from this study and other factors such as sleep requirements and the types of activities undertaken in the experimental studies discussed above, it was considered that typical daily exposure would be around 2 hours per day.

Assuming a daily exposure of 2 hours and the distribution on daily intake rates given above, a distribution on the hourly intake rate was derived. This is presented in Table F3. However, assuming a single exposure duration is rather simplistic. A distribution on hourly intake rate was therefore also derived assuming a distribution on daily exposure duration. A lognormal distribution was assumed with 50^{th} percentile equal to 2 hours and 95^{th} percentile equal to 6 hours.

The distribution on hourly intake rate was determined using a Crystal Ball spreadsheet. For the correlation between daily exposure duration and daily intake rates a correlation factor of 0.5 was used*. The resulting distribution is presented in Table F3. This is very similar to that generated using a defined 2 hourly exposure duration but is a slightly 'narrower' distribution. Clearly the distribution on exposure durations is highly uncertain. Other possible distributions were therefore also examined, including a triangular distribution with min - 1 h d^{-1}, most likely - 2 h d^{-1} and max - 5 h d^{-1} and another lognormal distribution with 0.1^{th} percentile 1 h d^{-1} and 99.9^{th} percentile of 6 h d^{-1}. Various correlation values were also considered. In all cases the 50^{th} percentile was in the region of 30 mg h^{-1}, the mean around 40 mg h^{-1}, and the 97.5^{th} percentile ranged from 110 to 190 mg h^{-1}.

On the basis of this analysis and consideration of the basic data reviewed it was decided that for this study the following distribution on hourly intake rate be used for young children: 50^{th} percentile 30 mg h^{-1} and 97.5^{th} percentile 175 mg h^{-1} (mean - 45 mg h^{-1}).

Children

In the absence of specific data for this age group a distribution on hourly intake rate between that for younger children and adults was used: 50^{th} percentile 6 mg h^{-1} and 97.5^{th} percentile 35 mg h^{-1} (mean – 9 mg h^{-1}).

* Assuming no correlation generated a mean hourly intake of 60 mg h^{-1} and a 97.5^{th} percentile of 306 mg h^{-1}, which seemed inconsistent with the distribution on daily intake rate. Using a correlation of 0.75 reduced the mean to around 40 mg h^{-1} and the 97.5^{th} percentile to 115 mg h^{-1}.

Adults

Developing a range for older children and adults was more difficult given the lack of basic data. For adults the formula proposed by Sedman and Mahmood (1994) for modelling the change in consumption rate with age suggests dividing the rates for young children by a factor of 10. This distribution is generally consistent with the conclusion of Simon (1998) in that "there appears to be a general consensus that among adults in western society who do not routinely contact the soil by occupation or hobby, intake of soil is very low – probably of the order of a few milligrams to a few tens of milligrams per day*".* Although adults on a beach come into contact with sand and thus potentially may be considered to have a higher intake, the size of sand grains is such that they are relatively easily detected in food and on hands and therefore there is less likelihood of inadvertent ingestion.

Only one of the studies reviewed related to adult intake rates (Stanek et al, 1997), which gave a median of 1 mg d^{-1}, an average of 10 mg d^{-1}, a standard deviation of 94 mg d^{-1}, a 75^{th} percentile of 49 mg d^{-1} and a 95^{th} percentile of 331 mg d^{-1}. Whilst the median and average values are broadly consistent with those proposed here the high percentiles are almost at the level of young children which did not seem generally appropriate.

On this basis the following distribution on hourly sand intake rate was used for adults: 50^{th} percentile 3 mg h^{-1} and 97.5^{th} percentile 17.5 mg h^{-1} (mean – 4.5 mg h^{-1}).

F3 DELIBERATE INGESTION

For the purposes of this study, deliberate ingestion is taken to be the deliberate consumption of non-food items but without the knowledge that the item may be contaminated. One such group are young children described as having the rare medical condition known as pica who persistently ingest non-nutritive substances for a period of time. As this is a rare condition, there is insufficient evidence to model ingestion of sand for children with pica and inadvertent ingestion separately (Smith and Bedwell, 2005). Smith and Bedwell (2005) also stated that the experimental studies on ingestion rates for soil and sand (see above) include some element of this behaviour. They therefore considered that the recommended distribution of inadvertent ingestion rates for young children also include those for children with pica.

The mouthing of a wide variety of non-food substances which can also be ingested can also occur. This is most common in people with developmental disabilities, including autism and mental retardation, and in children between the ages of 2 and 3 (Cheng and Tam, 1999; Ashworth et al, 2009).

F3.1 Object sizes that are deliberately ingested

Evidence suggests that, as with inadvertent ingestion, there is no lower limit on the size of the objects ingested; the upper size limit is constrained only by what the consumer can place in their mouth. The ICRP's Human Alimentary Tract Model (HATM) (ICRP, 2006) models the lower part of the adult human head as a right circular cylinder containing the oral cavity, tongue, teeth and associated salivary glands. The teeth are

represented by a semicircular arc with an internal radius of 36 mm. Teeth provide a rigid limit to what can be put in the mouth and therefore swallowed, and a rounded upper limit of 70 mm is suggested. Shahverdian et al (to be published) present a case study of an adult who deliberately ingested stones ranging in size from 1 cm to 5.5 cm; this supports the choice of 70 mm as an upper limit in size.

The HATM model of the mouth only applies to adults as there is insufficient data to extend the model to children. Studies on the ingestion of foreign bodies by children (Cheng and Tam, 1999) have found that the average age of children swallowing a 28 mm coin (US $2 coin) is 7-8 years, whilst the average age of children swallowing a 15 mm coin (US 5¢ coin) is around 2 years. Based on this, conservative upper limits of 40 mm for an 10 year old child and 20 mm for a 1 year old child have been chosen. There is anecdotal evidence of objects that are deliberately ingested by children that supports the choice of these conservative upper limits (Steigler, 2005).

F4 REFERENCES

Ashworth M, Hirdes JP and Martin L (2009). The social and recreational characteristics of adults with intellectual disability and pica living in institutions. *Research in Developmental Disabilities*, **30**, 512-520

Binder S, Sokal D and Maughan D (1986). Estimating soil ingestion: the use of tracer elements in estimating the amount of soil ingested by young children. *Archives of Environmental Health*, **41**, 341-345.

Calabrese EJ, Barnes R, Stanek 3rd EJ, Pastides H, Gilbert CE, Veneman P, Wang X, Lastity A and Kostecki PT (1989). How much soil do young children ingest: an epidemiologic study. *Reg Toxicol Pharmacol*, **10**, 123-137.

Calabrese EJ, Stanek EJ 3rd, Pekow P and Barnes RM (1997). Soil ingestion estimates for children residing on a superfund site. *Ecotoxicol Environ Saf*, **36** (3), 258-268.

Cheng W and Tam PKH (1999). Foreign-body ingestion in children: Experience with 1,265 cases. *J Pediatric Surgery*, **34** (10), 1472-1476.

Clausing B, Brunekreef B, and van Wijnen JH (1987). A method for estimating soil ingestion in children. *Int Arch Occup Environ Med*, **59**, 73-82.

Davis S, Waller P, Buschbom MA, Ballou J and White P (1990). Quantitative estimates of soil ingestion in normal children between the ages of 2 and 7 years: population-based estimates using aluminium, silicon and titanium as soil tracer elements. *Archives of Environmental Health*, **45**, 112-122.

Defra and EA (2002). The Contaminated Land Exposure Assessment Model (CLEA): Technical basis and algorithms. R&D Publication, CLR10.

Engelen L, de Wijk RA, van der Bilt A, Prinz JF, Janssen AM, Bosman F (2005). Relating particles and texture perception. Physiology & Behavior 86[1-2], 111-117, 2005/9/15.

Finley B, Proctor D, Scott P, Harrington N, Paustenbach D and Price P (1994). Recommended distributions for exposure factors frequently encountered in health risk assessment. *Risk Analysis*, **14**, 533-553.

ICRP (2006). Human Alimentary Tract Model for Radiological Protection. ICRP Publication 100. *Ann ICRP*, **36** (1-2).

Imai E, Hatae K and Shimada A (1995). Oral perception of grittiness: effect of particle size and concentration of the dispersed particles and the dispersion medium. *J Texture Studies*, **26** (5), 561-576.

Linsalata P and Eisenbud M (1986). Ingestion estimates of Th and the light rare earth elements based on measurements of human feces. *Health Phys*, **50**, 163-167.

Sedman RM and Mahmood RJ (1994). Soil ingested by children and adults reconsidered using the results of recent tracer studies. *J Air and Waste Manag Assoc*, **4**, 141-144.

Shahverdian DE, Mariyappa A, Wisinger D et al (To be published). Successful removal of cecal stones by using a colonoscope in an individual with repeated lithophagia. *Gastrointestinal Endoscopy.* In Press, Corrected Proof.

Simon SL (1998). Soil ingestion by humans: a review of history, data, and etiology with application to risk assessment of radioactively contaminated soil. *Health Phys*, **74** (6), 647-672.

Smith KR and Bedwell P (2005). Public Health Implications of Fragments of Irradiated Fuel: Module 3: The likelihood of encountering a fuel fragment on Sandside beach. Chilton, RPD-EA-9-2005.

Stanek EJ and Calabrese EJ (1995). Daily estimates of soil ingestion in children. *Environ Health Perspectives*, **103**, 277-285.

Stanek EJ 3rd, Calabrese EJ, Barnes R and Pekow P (1997). Soil ingestion in adults – results of a second pilot study. *Ecotoxicol Environ Saf*, **36** (3), 249-257.

Stanek EJ 3rd and Calabrese EJ (2000). Daily soil ingestion estimates for children at a Superfund site. *Risk Anal*, **20** (5), 627-635.

Stiegler LN (2005). [Web page] Understanding pica behaviour: a review for clinical and education professionals. Available at http://www.accessmylibrary.com/coms2/summary_0286-9076504_ITM [accessed 11-02-2009]. (The Gale Group).

The Open University (2002). *Environmental Science: Water and Life*. Milton Keynes: The Open University. p 55.

Thompson KM and Burmaster DE (1991). Parametric distributions for soil ingestion by children. *Risk Analysis*. **11**, 339-342.

US EPA (1999). Exposure factors handbook, EPA 600-C-99-01. US EPA, Washington, DC.

Van Wijnen JG, Clausing P and Brunekreef B (1990). Estimated soil ingestion by children. *Env Res*, **51**, 147-162.

Wong EY, Shirai JH, Garlock TJ and Kissel JC (2000). Adult proxy responses to a survey of children's dermal soil contact activities. *J Expo Anal Environ Epidemiol*, **10** (6 pt1), 509-517.

APPENDIX G Supplementary information on object inhalation

This Appendix contains a discussion on the effect that object size has on its inhalability and how this is likely to affect where such an object will deposit in the respiratory system. Also discussed is the derivation of sand loading in air and the inhalation rates which are used in the assessment of the probability of encountering an object via inhalation.

G1 PARTICLE INHALABILITY

Not all particles in the environment are inhalable. When a volume of air is inhaled, particles approaching the entry to the extrathoracic (ET) region [which comprises the anterior nose (ET_1) and the posterior nasal passages, larynx, pharynx and mouth (ET_2)] may escape due to their inertia or their settling velocity. Although inhalation has long been recognised as an important route of internal exposure, it was not until the late 1970s that it was proposed that, for health protection purposes, only particles capable of entering the nose and/or mouth during breathing posed a potential health risk and that not all particles had the same probability of being inhaled (Vincent, 1995; 2007). Historically, the sampling of coarse particles had been based on the 'total aerosol', which referred to all airborne particulate matter and most sampling instruments that purported to measure total aerosol were developed without regard to the dependence of sampling efficiency on particle size.

The first part of the process of aerosol exposure is the entry of the aerosol from the ambient air into the respiratory tract via the mouth and/or nose. The physics governing the entry of airborne particles into the nose and mouth are strongly dependent on a complex combination of many factors, including;

- Particle aerodynamic diameter[1] (d_{ae});
- wind speed;
- orientation of the subject with respect to the wind;
- breathing rate and pattern.

Similar factors are influential in how airborne particles enter aerosol sampling devices and from this emerged the idea of considering the human head as an aerosol sampler (Ogden and Birkett, 1977). This was an important conceptual step toward a new rationale and established the scientific link between actual human aerosol exposure and the technical sampling devices that are used to assess exposure - it was recognised that aerosol sampling should reflect that of the human exposure. From this developed the concept of aerosol inhalability (Vincent, 2007; Schmees et al, 2008).

[1] The aerodynamic diameter of a particle is the diameter of the unit density spherical particle that has the same settling velocity in air.

Particle inhalability is defined as that fraction of particles in an aerosol that can enter the ET region upon inhalation (Ménache et al, 1995) and is a function of particle size, breathing conditions, and ambient air velocity and direction (Hinds et al, 1998). Inhalability is also referred to as the intake or aspiration efficiency.

Studies have been conducted investigating the inhalability of particles as a function of their aerodynamic size. These studies involved sampling ambient aerosols, with aerodynamic particles up to 100 µm, through the nose and mouth orifices of life-sized adult mannequins placed in large wind tunnels at various angles to the direction of the flow. The results suggested that at low wind speed (up to 4 m s^{-1}) inhalability tends to decrease with increasing aerodynamic particle size, reaching a value of approximately 0.5 for particles larger than about 30 µm aerodynamic diameter (Ogden and Birkett, 1977; Vincent and Mark, 1982; Armbruster and Breuer, 1982; 1984). Vincent et al (1990) reviewed and summarised the available inhalability data and concluded that that 'effects associated with differences in wind speed and breathing patterns are relatively weak over quite wide ranges. So too are effects associated with nose-versus-mouth breathing and facial structural features'. In the recommendations of the American Conference of Governmental Industrial Hygienists (ACGIH, 1985), a curve was included as a convention for defining the inhalable (known at the time as 'inspirable') fraction according to the following relationship;

Inhalability $=0.50\ [1+\exp(-0.06.d_{ae})]$

where d_{ae} is the aerodynamic particle diameter (µm).

The curve of inhalability versus aerodynamic diameter at low wind speeds is shown in Figure G1. Understandably, the inhalability curve was not recommended for use with particles greater than 100 µm aerodynamic diameter.

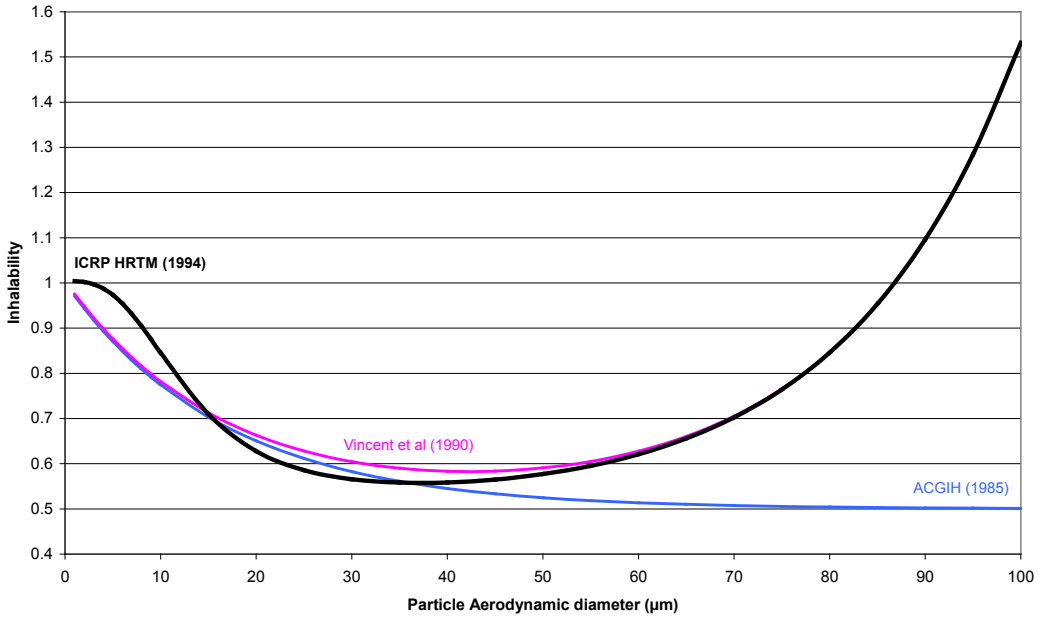

Figure G1: Inhalability versus aerodynamic diameter

The main purpose of the studies described above was the practical need to derive occupational health criteria, although it was also recognised that aerosol exposure in the outdoor environment is also important. Here an extended range of environmental conditions apply and wind speeds can reach well in excess of 10 m s^{-1} at ground level. For reference a wind speed of 10 m s^{-1} is classified as 5 on the Beaufort scale (fresh breeze, ~20 knot winds). Winds of this speed over land will cause tree branches of a moderate size to move and small trees to sway. Vincent et al (1990) showed that at wind speeds up to 9 m s^{-1} there was a clear tendency for the inhalability not only to increase with aerodynamic particle sizes above 50 µm, but even to exceed unity. This phenomena occurs because, as wind speeds increase, a greater fraction of larger particles impact – by virtue of their inertia – onto the mouth of the mannequin when it is oriented in forwards-facing directions than would occur in still or slowly moving air. It should be noted that this scenario assumes that particle inertia is the dominant mechanism governing inhalability and that gravity has a negligible effect, which may not be the case for very large particles or very low wind speeds. The authors proposed modifying the above equation by the addition of a term containing the wind speed, *U*, as shown below;

$$\text{Inhalability} = 0.50\,[1+\exp(-0.06\,d_{ae})] + 1 \times 10^{-5}\,U^{2.75}\exp(0.055\,d_{ae})$$

The resultant curve of inhalability versus aerodynamic diameter adjusted for high wind speeds is also shown in Figure G1 above. Again this function is only applicable for particles up to 100 µm aerodynamic diameter. In 1994 the International Commission for Radiological Protection (ICRP) adopted the following function for use in the Human Respiratory Tract Model (HRTM) as this better represented the inhalability of particles less than 10 µm aerodynamic diameter (ICRP, 1994).

$$\text{Inhalability} = 1 - 0.5*[1-(7.6*10^{-4}*d_{(ae)}^{2.8}+1)^{-1}]+1*10^{-5}*U^{2.75}*\exp(0.055*d_{(ae)})$$

It is important to note however that, as before, this function is limited to wind speeds from 1 to 9 m s^{-1} and is only applicable for particles less than 100 µm aerodynamic diameter.

There is a paucity of data for particles larger than 100 µm because of the difficulty associated with working with such large particles. Particle losses are high due to settling and impaction (see Figure G2). However recent studies have investigated the inhalability of larger particles, up to 140 µm, although only in very low wind speed conditions (Hsu and Swift, 1999; Kennedy and Hinds, 2002; Dai et al, 2005). The findings from these studies are consistent and show that inhalability drops off above about 120 µm aerodynamic diameter and above this size the intake will tend to be over-estimated if derived from air sampler measurements. It was further proposed that a cut-off occurs at about 135 µm aerodynamic diameter and that particles above this size are not inhaled. The reduction in inhalability is related to the aerodynamic behaviour of the particles, possibly a complicated interaction between particle physics and air motion in the region of the mouth or as a result of the competition between horizontal velocity and settling velocity. Unfortunately comparable data does not exist for higher wind speeds.

It is worth noting that particle inhalability for children may be different from that in adults due to differences in ET geometry and physical activity. Although several studies have been conducted on adults and adult sized mannequins, virtually no studies have investigated particle inhalability in children.

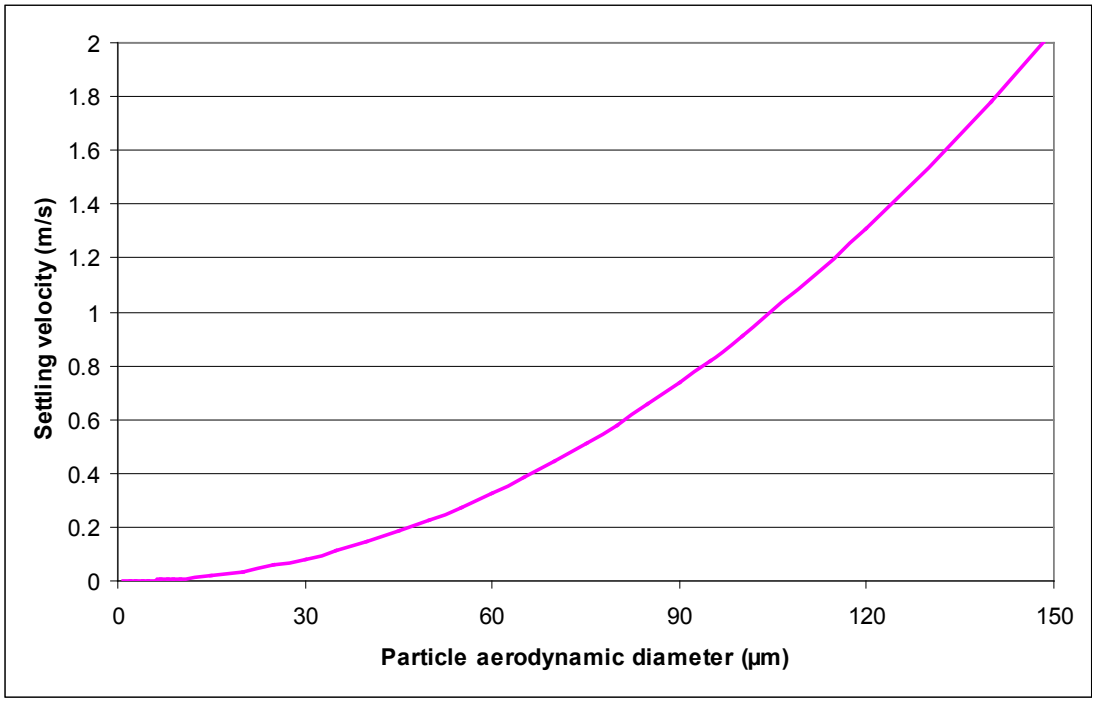

Figure G2: Settling velocities in air for particles up to 150 µm aerodynamic diameter

Inhaled particles may be exhaled immediately, deposited in the extrathoracic (ET) airways, or may penetrate to, and be deposited in, the lungs. Particles deposited in the ET airways are cleared extrinsically (eg, by nose blowing) or are cleared rapidly to the gastro-intestinal tract where intestinal absorption may take place. Some uptake of material deposited in the ET airways may also take place, although the rapid clearance of particles from the ET airways means that there is little time for dissolution and absorption to blood and intestinal absorption will dominate. Particles deposited in the ET airways will irradiate the local tissues; for the purposes of dose assessment the epithelial lining can be regarded as similar to skin (Harrison et al, 2005). Where deposition in the lungs is of most concern (either because of the resulting dose to the lungs or because of uptake of material from the lungs), then it is the fraction of particles available for inhalation that penetrate to the lungs that is of interest. This is referred to as the respirable fraction (Walsh, 2002). The longest retention times in the lungs occur for particles that deposit in the alveolar-interstitial region.

G2 SUSPENSION AND SETTLING OF LARGE PARTICLES

Particle size is important both for the amount of material inhaled and the amount suspended. Particle suspension is an extremely difficult process to quantify. Extensive reviews of the subject have provided an appreciation of the uncertainties associated with this process (Sehmel, 1980; Nicholoson, 1988). Suspension is a form of large-scale erosion describing the continual movement of particles as a function of surface stresses. The stresses are surface creep and suspension while the transport means depends on the particle diameter, wind speed and turbulence. Particles in the size range 1000-2000 μm diameter may roll or slide along the surface as a result of natural wind action (surface creep) while smaller particles (50 – 1000 μm diameter) may be lifted vertically in the air under the action of wind then quickly returned to earth due to gravitational settling (saltation). Particles less than 50 μm diameter may be suspended in response to wind action or disturbance and remain suspended for significant periods of time. Very small particles (0.1 μm or less) are unlikely to be suspended alone (Walsh, 2002). Once suspended the time the particles will remain airborne can be estimated from their settling velocity (Figure G2). As can be seen, other than in extremely violent wind conditions, large particles can only remain airborne for seconds at most.

However, where the requirement is to estimate radiation doses from the inhalation of suspended material then it is respirable particles, those capable of penetrating to the gas-exchange region of the lungs, that are of major concern (Walsh, 2002) as larger particles will deposit in the ET regions (Figure G3) and clearance from these regions is rapid, allowing little time for dissolution and absorption to blood. Under these conditions it would seem reasonable to assume that intestinal absorption will dominate uptake to blood. For the purposes of assessment of possible effects of local irradiation within the extrathoracic airways, the epithelial lining can be regarded as similar to skin (Harrison et al, 2005).

G2.1 Sand loading in air

It is widely recognized that sand, when disturbed by the action of wind, can, under certain conditions, be lifted off the residing surface (eg, a beach) and become airborne. Horikawa (1988) explained that on beaches where a strong seasonal wind blows, sand transport by wind is an important mechanism. If the wind speed reaches a critical value, sand grains on a loose sand surface begin to move. Winds of the same or higher speed have the potential to elevate the sand grains. The bulk of sand movement takes place close to the ground and the moving sand particles do not rise to a high elevation. Furthermore, the relatively large mass of the sand grains means that levels of suspension are quite small. However it is recognized that sand can be blown to heights of 1-2 metres. However, it is important to consider individuals' habits when considering whether they are likely to be on the beach during periods of windy conditions where sand is likely to be present above the surface. Persons frequenting a beach for seasonal leisure activities, eg, sunbathing or playing are less likely to visit the beach under inclement weather than those who have a commitment to a hobby, eg, angling or assigned to a routine activity, eg, dog walking. The sand loadings used in this study reflect the tendency for individuals, notably children and infants, to spend less time at the beach under windier conditions. It was also recognized that the loadings of sand in

air would generally be lower than for soil and dust because of the higher grain size. A literature survey identified only one study giving values of sand loadings in air above beaches (Haslam et al, 1994). This provided the results of a number of measurements of atmospheric dust loadings above a range of beach types in Cumbria. On the basis of the experimental data described by Haslam a sand loading for children and infants of 10^{-4} g m^{-3} was used here, with an associated range of 10^{-3} g m^{-3} to 10^{-5} g m^{-3}. It was thought that adults may tolerate higher loadings and would be more likely to use the beach throughout the year under a wider range of weather conditions. Thus a best estimate sand loading, applicable to adults, of 5 10^{-4} g m^{-3} was considered applicable, with an associated range of 5 10^{-3} g m^{-3} to 10^{-5} g m^{-3}.

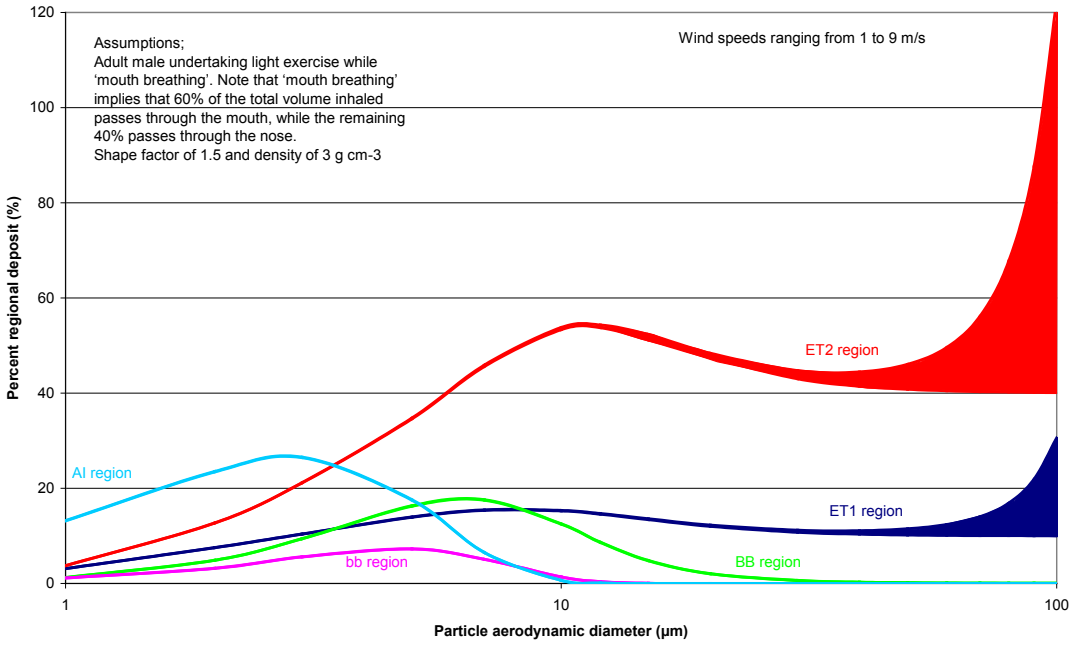

Figure G3: Probability of deposition in each HRTM region for particles ranging in size from 1 to 100 µm aerodynamic diameter (note log scale) in a wind speeds from 1 m s^{-1} up to 9 m s^{-1}.

G3 RESPIRATORY TRACT DOSES

The ICRP HRTM considers the deposition and subsequent behaviour of inhaled aerosols of different particle sizes. Deposition in the different regions of the respiratory tract depends on particle aerodynamic diameter, breathing rate and tidal volume of the lungs. This report is concerned with the inhalation of single particles and thus percent regional deposition is not meaningful. However, estimates of regional distribution can be interpreted in this application in terms of the probability of a particle depositing in the different regions.

Using a computer program implementation of the HRTM, LUDEP (Jarvis et al, 1996), the probabilities of deposition were determined for particles ranging in size from 1 to 100 μm aerodynamic diameter in wind speeds from 1 to 9 m s^{-1}. The results are shown in Figure G3. In obtaining these data it was assumed that the subject was an adult male undertaking light exercise while 'mouth breathing' and that the inhaled particle was deposited and not exhaled. It was also assumed that the particle had the ICRP defaults for shape factor (1.5) and density (3.0 g cm^{-3}). Note that 'mouth breathing' implies that 60% of the total volume inhaled passes through the mouth, while the remaining 40% passes through the nose and that percent regional deposition in excess of 100% is an artefact resulting from the use of the ICRP HRTM expression to describe inhalability of large particles at higher wind speeds (explained in detail above).

The figures shows that the larger particles (>30 μm) will be deposited almost exclusively in the extrathoracic airways before reaching the lungs. It is only for particles smaller than about 10 μm aerodynamic diameter that there is a significant probability of the particle reaching the alveolar-interstitial region of the lungs.

G4 CONCLUSIONS

There are no data to support a recommendation of an upper limit on the particle size that can be inhaled on the beaches around the Sellafield site, particularly if wind speeds exceed 4 m s^{-1}. However, the ICRP HRTM suggests that particles larger than about 30 μm aerodynamic diameter will deposit almost exclusively in the extrathoracic region (a cut-off of 100 μm aerodynamic diameter is suggested as an upper limit) and that only particles smaller than 10 μm aerodynamic diameter are likely to reach the alveolar-interstitial region of the lungs.

G5 REFERENCES

ACGIH (American Conference of Government Industrial Hygienists) (1985). Air Sampling Procedures: Particle Size-Selective Sampling in the Workplace. Cincinnati, Ohio.

Armbruster L and Breuer H (1982). Investigations into defining inhalable dust. In WH Walton (Ed), Inhaled Particles V, pp 21-32. Pergamon, Oxford.

Dai Y-T, Juanga Y-R,Wub Y-y, Breyssec PN, Hsub D-J (2005). In vivo measurements of inhalability of ultra large aerosol particles in calm air by humans.

Harrison JD, Fell TP, Phipps AW, Smith TJ, Ellender M, Ham GJ, Hodgson A and Wilkins BT (2005). Health Implications of Dounreay Fuel Fragments: Estimates of Doses and Risks. Chilton, RPD-RE-11-2005.

Hinds WC, Kennedy NJ, and Tatyan K (1998). Inhalability of Large Particles for Mouth and Nose Breathing. *J Aerosol Sci*, **29**, Suppl S277-S278.

Hsu D-J and Swift DL (1999). The Measurements of Human Inhalability of Ultralarge Aerosol in Calm Air Using Mannikins. *J Aerosol Sci*, **30** (10), 1331-1343.

ICRP (1994) Human Respiratory Tract Model for Radiological Protection. ICRP Publication 66. *Ann ICRP*, **24** (1-3). Oxford, Pergamon Press.

Jarvis NS, Birchall A, James AC, Bailey MR and Dorrian M-D (1996). LUDEP 2.0, personal computer program program for calculating internal doses using ICRP Publication 66 respiratory tract model. Chilton, NRPB-SR287.

Kennedy NJ, Hinds WC (2002). Inhalability of large solid particles. *J Aerosol Sci*, **33**, 237–255.

Ménache MG, Miller FJ and Raabe OG (1995). Particle Inhalability Curves For Humans And Small Laboratory Animals. *Ann Occup Hyg*, **39** (3), 317-328.

Nicholoson KW (1988). A Review of Particle Resuspension. *Atmos Environ*, **22** (12), 2639-2651.

Ogden TL and Birkett JL (1977). The human head as a dust sampler. In: Inhaled Particles IV (Ed WH Walton), pp 93-105. Pergamon Press Oxford.

Schmees DK, Wu Y-H and Vincent JH (2008). Experimental methods to determine inhalability and personal sampler performance for aerosols in the ultra-low windspeed environments. *J Environ Monit*, **10**, 1426-1436.

Sehmel GA (1980). Particle resuspension: a review. *Environ Int*, **4**, 107-127.

Vincent JH (1995). Aerosol Science for Industrial Hygenists. Pergamon Press

Vincent JH and Mark D (1982). Application of blunt sampler theory to the definition and measurement of inhalable dust. In WH Walton (Ed), Inhaled Particles V, pp 3-19. Pergamon, Oxford.

Vincent JH, Mark D, Miller BG, Armbruster L and Ogden TL (1990). Aerosol inhalability at higher wind speeds. *J Aerosol Sci*, **21** (4), 577-586.

Vincent JH (2007). Aerosol Sampling. Wiley and Sons, Chichester, UK.

Walsh (2002). Calculation of Resuspension Doses for Emergency Response. Chilton, NRPB-W1.

APPENDIX H Supplementary information on material on the skin

There are few data on the size of particles that are likely to stick to skin. One study on a variety of soils (including sandy-type soils) found that particles above 0.1 mm are unlikely to stick to skin, and that dry particles above 50 µm did not adhere to dry skin (Sheppard and Evenden, 1994). Experience suggests, however, that it is entirely possible for sand grains to adhere to the skin. Therefore, a conservative upper limit to object size for a beach location, where neither object or skin are likely to be entirely dry, has been assumed to be 1 mm (approximately the upper size of a grain of sand).

H1 LITERATURE REVIEW OF SOIL ADHERENCE TO SKIN

A literature survey was undertaken to identify information relating to the loading of sand on skin and clothing. The literature survey found no specific references to sand and no references to the adherence of soil on clothes. It did, however, identify a small number of papers on dermal soil loading. It is clear from the literature that the amount of soil that comes into contact with the skin depends upon a number of factors, including:

- exposed skin area;
- type of activity involved;
- duration of initial contact; and
- texture and wetness of the soil.

The US EPA (US EPA, 1992) suggested that an average value for soil loading may be 0.2 mg of soil per cm^2 of skin and that a reasonable worst case might be 1 mg cm^{-2}. In the CLEA contaminated land exposure assessment model (Defra and EA, 2002) a soil loading of 1 mg cm^{-2}, the EPA reasonable worst case, was assumed.

In Sedman (1989) data from a few studies were averaged to produce a skin soil loading of 0.5 mg cm^{-2}, for children aged 1 to 3, with lower values for older children and adults. The purpose of the suggested values was for the derivation of action levels.

A number of the papers reviewed presented detailed measurements of dermal soil loadings for a number of activities. Of particular interest in this context was Holmes et al (1999). This paper also contains the data presented in Kissel et al (1996), which was an earlier publication by the same project team. In this paper pre and post activity soil loadings from hands, forearms, lower legs, faces and feet were reported for volunteers engaged in various occupational and recreational activities. This data provides a useful perspective on the types of behaviour likely to lead to soil contact falling within general classes of activity such as background and low, moderate, or high contact. A number of conclusions were drawn from the experimental data including the following:

- post-activity loadings are typically higher than pre-activity levels, demonstrating that exposure is episodic;

- hand loadings are dependent upon the class of activity;
- hand loadings generally provide conservative estimates of loadings on non-hand body parts within activity classes; and
- hand loadings do not provide conservative estimates of non-hand loadings across activity classes.

In all, measurements from 200 individuals were made. It was suggested on the basis of the data that it might be useful to distinguish background, low, moderate and high contact categories using the following ranges of soil loading on the hands:

Background	< 0.01 mg cm^{-2}
Low contact activity	0.01 – 0.1 mg cm^{-2}
Moderate contact activity	0.1 – 1.0 mg cm^{-2}
High contact activity	>1.0 mg cm^{-2}

Groups having hand loadings falling within the moderate contact category included irrigation system installers, gardeners, archeologists, construction workers, farmers, water utility crews, heavy equipment operators, and reed gatherers. The EPA default range (0.2 – 1.0 mg cm^{-2}) largely overlaps what are defined as moderate contact activities (US EPA, 1992).

Only one type of activity produced geometric mean hand loadings above 1.0 mg cm^{-2} (in the high contact activity band). These were children transported to a muddy river bank to play. Their mean hand loadings were above 10 mg cm^{-2}.

The results support the view that hand loadings usually provide conservative estimates of nonhand loadings within activities. The only caveat is that loadings on bare feet are likely to be roughly equivalent to loadings on hands. Loadings on faces, forearms and lower legs were found to be roughly 20 to 60% of hand loadings.

Finley et al (1994) reviewed the literature on soil adherence and proposed the use of a standard probability density function (PDF) of soil adherence. This standard PDF is lognormally distributed; the arithmetic mean and standard deviation are 0.52 ± 0.9 mg of soil per cm^2 of skin. They considered that their review indicated that soil adherence under environmental conditions would be minimally influenced by age, sex, soil type, or particle size and thus their proposed PDF should be considered applicable to all settings. The 50^{th} and 95^{th} percentile values of the PDF (0.25 and 1.7 mg of soil per cm^2 of skin, respectively) are very similar to the EPA estimates of average and upper bound soil adherence (0.2 and 1.0 mg of soil per cm^2 of skin) (US EPA, 1992).

H2 THE EFFECT OF PARTICLE SIZE ON DERMAL LOADING OF SOIL

The experimental data discussed above was based on soils rather than sand. Soils in general consist of particles smaller in size than sand. It was considered important

therefore to explore the relationship between particle size and dermal adherence to provide an input to the derivation of appropriate dermal adherence values to use in this study.

Sheppard and Evenden (1994) examined the impact on adhesion of particle size. They studied the dermal adhesion properties of 11 different soils including a number of sandy soils. They found that adhering skin surfaces preferentially selected particles with diameters smaller than 0.1 mm. For soils that originally had few particles smaller than 0.1 mm, the particle size distribution of the adhering soil was markedly different from that of the original soil. They found that dry particles above 50 μm did not adhere to dry skin. However, this effect was less marked when the soil moisture was higher.

An earlier study (Que Hee et al, 1985) looked at the adherence of house dust and hand dust. They considered the impact of particle size on adherence. The results are difficult to interpret but seem to indicate that adherence does not change significantly with particle size.

Driver et al (1989) (as reported in Finley et al 1994b) found a two fold adherence difference between unsieved and very fine (150 μm) soil particles.

The US EPA concluded in 1992 (EPA, 1992) that while particle size may influence adherence, there were insufficient data to develop quantitative relationships between particle size and skin adherence.

H3 RECOMMENDED DERMAL LOADING OF SAND ON SKIN FOR USE IN THIS STUDY

In the absence of any specific data on the loading of sand on skin it was necessary to use the above information on the adherence of soil to skin to estimate sand adherence. From the information above on the effects of particle size, and, importantly, general practical experience, it was assumed that dry sand will adhere to skin less well than soil. This is because soil contains particles smaller in size than sand and smaller particles more readily adhere to skin. On the basis of the information above, particularly that from Holmes et al (1999), for activities involving contact with dry sand a best estimate assumption of dermal loading on hands and, if applicable, feet of 0.1 mg cm^{-2} (1 g m^{-2}) was used. This is slightly below the EPA average value of 0.2 mg cm^{-2} (US EPA, 1992) to reflect the lower adherence properties of sand, and is the lower point of the moderate contact range as defined by Holmes (1999). For probabilistic calculations a triangular distribution was adopted covering the Holmes (1999) low and moderate contact activity ranges, that is 0.01 mg cm^{-2} to 1.0 mg cm^{-2} (0.1 to 10 g m^{-2}), with the peak at 0.1 mg cm^{-2} (1 g m^{-2}). The dermal loading on skin other than on hands and feet was assumed to be a factor of 0.5 lower than that on hands and feet on the basis of a conservative assessment of the results in Holmes et al (1999). The data used for dermal loading of dry sand are summarised in Table H21.

Table H1 : Dermal loading of sand (g m^{-2})

	Age group	2.5%	Mean	97.5%	Best estimate[(b)]	Distribution type
Dermal loading wet sand [(a)]	All	5	50	500	5	Triangular
Dermal loading dry sand [(a)]	All	0.1	1	10	1	Triangular
Dermal loading of sand on other parts of the body compared with hands and feet					5	-

(a) Values from Smith and Bedwell (2005).

(b) Value used for high occupancy beach users.

It was assumed that dermal loading of wet sand would be greater than that of dry sand. When on a beach it is not unusual, following paddling etc, to have feet completely covered in a fine layer of wet sand. Dermal loadings of soil of a few tens of milligrams per square centimetre were only encountered by Holmes et al (1999) for children playing in mud by a river where these children had dermal loadings of soil on hands of between approximately 30 and 60 mg cm^{-2}. This was considered to be above that which would normally be present on the skin regarding sand and given the ability of the larger sand grains to adhere to the skin. On the basis of the above data, for activities involving contact with wet sand, such as bait digging, winkle picking, paddling and digging in the sand close to the sea, a best estimate assumption of dermal loading on hands and, if applicable, feet of 5 mg cm^{-2} (50 g m^{-2}) was used. For probabilistic calculations a triangular distribution covering the range 0.5 mg cm^{-2} to 50 mg cm^{-2} (5 to 500 g m^{-2}) with the peak at 5 mg cm^{-2} (50 g m^{-2}) was used. The dermal loading on skin other than hands and feet was, as above, assumed to be a factor of 0.5 lower than that on hands and feet.

H4 AREA OF SKIN COVERED WITH SAND

The skin areas for various parts of the body were required in order to determine the quantities of sand that may adhere to skin. Distributions on skin areas were not required because the overall probabilities being determined are for individuals assumed to have ‘standard’ physical characteristics. Therefore only best estimate values were required. The areas of the body identified as key for this assessment (following consideration primarily of habits and clothing) were: palms of hand and outstretched fingers, whole hands, lower arms, lower legs, soles of feet, total feet and total body area. The skin areas used are presented in Table H2. The total body areas are those from ICRP Publication 32 (ICRP, 2002). The areas of individual body parts were determined by multiplying these total skin areas by the mean ratios of area of body part to total skin area published in US EPA (1997). The only exceptions are for the soles of the feet and palms and outstretched fingers, which are assumed to be 50% of the areas of the feet and hands, respectively.

Table H2: Skin surface areas of various parts of the body (m^2)

	Lower Arms	Lower Legs	Hands	Palms & outstretched fingers	Feet	Soles of feet	Total Body
Adult	0.11	0.24	0.099	0.050	0.13	0.065	1.90
Child (10 y)	0.059	0.13	0.059	0.030	0.085	0.043	1.12
Infant (2 y)	0.026	0.049	0.028	0.014	0.037	0.019	0.53

H4.1 Skin areas covered in sand

Table H3 gives the body area covered by sand for activities taking place within time spent at leisure or walking during visits to the beach in warm weather. For leisure, the skin areas were those used by Smith and Bedwell (2005) for the assessment of fuel fragments on beaches around the Dounreay site. For walking activities, the areas were derived for this study based on the areas of the body that were likely to come into contact with sand when walking whilst mostly clothed.

In order to provide clarity on what the skin areas within Table H3 means in terms of the mass of sand on the skin an example is given below. For this example, consider the sand covered areas shown in Table H3 for a young child spending leisure time on the beach. From Table H1 and Table H3 the minimum amount of sand present on the body is given by:

$$= 0.028\ m^2 * 0.1\ g\ m^{-2} + (0.026\ m^2 * 0.1\ g\ m^{-2}) / 2$$

$$= 0.004\ g \text{ of sand}$$

The mean mass of sand present on a young child spending leisure time on the beach is given by:

$$= 0.065\ m^2 * 50\ g\ m^{-2} + (0.075\ m^2 * 1\ g\ m^{-2}) / 2$$

$$= 3\ g \text{ of sand}$$

The maximum mass of sand present on a young child spending leisure time on the beach is given by:

$$= 0.065\ m^2 * 500\ g\ m^{-2} + (0.0675\ m^2 * 500\ g\ m^{-2}) / 2$$

$$= 49\ g \text{ of sand}$$

Table H3: Total skin areas for exposure in warm conditions (m^2) [(a)]

Activity	Age group	Body area	Minimum	Mean	Maximum	Best estimate	Distribution type
Leisure (wet sand)	Young child [(b)]	Hand/feet	0	0.065	0.065	0.065	Triangular
		Body	0	0	0.0675	0	
Leisure (dry sand)	Young child [(c)]	Hand/feet	0.028	0	0	0	Triangular
		Body	0.026	0.075	0	0.075	
Leisure (wet sand)	Child [(b)]	Hand/feet	0	0.144	0.144	0.144	Triangular
		Body	0	0	0.136	0	
Leisure (dry sand)	Child [(c)]	Hand/feet	0.059	0	0	0	Triangular
		Body	0.059	0.189	0	0.189	
Leisure (wet sand)	Adult [(b)]	Hand/feet	0	0.229	0.229	0.229	Triangular
		Body	0	0	0.246	0	
Leisure (dry sand)	Adult [(c)]	Hand/feet	0.099	0	0	0	Triangular
		Body	0.11	0.35	0	0.35	
Walking (wet sand)	Young child [(d)]	Hand/feet	0	0.028	0.065	0.028	Triangular
		Body	0	0	0	0	
Walking (dry sand)	Young child [(e)]	Hand/feet	0.028	0	0	0	Triangular
		Body	0	0.026	0.075	0.026	
Walking (wet sand)	Child [(d)]	Hand/feet	0	0.059	0.144	0.059	Triangular
		Body	0	0	0	0	
Walking (dry sand)	Child [(e)]	Hand/feet	0.059	0	0	0	Triangular
		Body	0	0.059	0.189	0.059	
Walking (wet sand)	Adult [(d)]	Hand/feet	0	0.099	0.229	0.099	Triangular
		Body	0	0	0	0	
Walking (dry sand)	Adult [(e)]	Hand/feet	0.099	0	0	0	Triangular
		Body	0	0.11	0.35	0.11	

(a) It is the combined wet and dry sand areas that will be used in this assessment and these areas should be viewed together, see the worked example in the text on how these areas are used to determine the mass of sand present on the skin

(b) Minimum has no exposure to wet sand; mean equals hands and feet exposed to wet sand; maximum equals 25% of total body exposed to wet sand, including both hands and feet. From Smith and Bedwell (2005)

(c) Minimum equals lower arms and hands exposed to dry sand; mean equals lower arms and legs exposed to dry sand; maximum equals no exposure to dry sand. From Smith and Bedwell (2005)

(d) Minimum has no exposure to wet sand; mean equals hands exposed to wet sand; maximum equals hands and feet exposed to wet sand. Assumed for this assessment

(e) Minimum equals hands exposed to dry sand; mean equals lower arms exposed to dry sand; maximum equals lower arms and lower legs exposed to dry sand. Assumed for this assessment

H5 ASSESSING THE PROBABILITY OF ENCOUNTERING AN OBJECT ON THE SKIN

The probability of encountering an object on the skin is directly related to the mass of sand on the skin, assuming that an object has an equal probability of coming into contact with the skin as a grain of sand. The amount of sand on the skin depends on whether the sand is wet or dry, see Table H1. In addition, Table H1 shows that the amount of sand per unit area of skin depends on where on the body it is, with the hands and feet assumed to have twice as much sand per unit area of skin compared to other

parts of the body. Due to these relastionships between the condition of the sand and where it is on the body, the mass of sand on the skin can be expressed in terms of the wet sand loading on hands and feet. These relationships are given below.

Mass of dry sand on hands * 0.02 = Mass of wet sand on the hands

Mass of wet sand on the body * 0.5 = Mass of wet sand on the hands

Mass of dry sand on the body * 0.01 = Mass of wet sand on the hands

The mass of sand on the body in periods of warm weather is a sum of the mass of wet and dry sand on all parts of the body. Therefore the mass of sand on the skin during warm weather is given by the following.

$M_{sand,w} = DL_{hf,ws} * [(A_{h,ws} + (A_{rest,ws} * 0.5) + (A_{h,ds} * 0.02) + (A_{rest,ds} * 0.01)]$

Where

$M_{sand,w}$ = Mass of sand on the skin during warm weather, g

$DL_{hf,ws}$ = Dermal loading of wet sand, g m^{-2}, see Table H1

$A_{h,ws}$ = Dermally exposed area of the hands to wet sand, m^{-2}, see Table H3

$A_{rest,ws}$ = Dermally exposed area of the body to wet sand, m^{-2}, see Table H3

$A_{h,ds}$ = Dermally exposed area of the hands to dry sand, m^{-2}, see Table H3

$A_{rest,ds}$ = Dermally exposed area of the body to wet sand, m^{-2}, see Table H3

In cold weather only the skin of the hands was only assumed to be exposed to wet sand. For cold weather, therefore, the mass of sand on the skin is given by the following equation.

$M_{sand,c} = DL_{hf,ws} * A_{h,ws}$

where

$M_{sand,c}$ = Mass of sand on the skin during cold weather, g

$DL_{hf,ws}$ = Dermal loading of wet sand, g m^{-2}, see Table H1

$A_{h,ws}$ = Dermally exposed area of the hands to wet sand, m^{-2}, see Table H3

The mass of sand on the skin during the year is a sum of the mass of sand on the skin in both warm and cold conditions. The annual mass of sand on the skin is given by the following equation.

$M_{sand,t} = M_{sand,w} + M_{sand,c}$

However, to estimate the annual probability of encountering an object hat is associated with sand on the skin, the fraction of the year spent on the beach in either warm or cold conditions needs to be accounted for. The probability of encountering an object within the sand on the skin during trips to the beach is estimated using the following equation.

$P_{skin} = T * N * (F_w * M_{sand,w} + F_c * M_{sand,c})$

Where

P_{skin} = Probability of encountering a radioactive object on the skin

T = Duration of time spent on the beach (hours).

N = Number of radioactive objects per gram of sand, g^{-1}

F_w = Fraction of time spent on the beach in warm weather conditions, dimensionless

$M_{sand,w}$ = Average mass of sand adhering to the skin per hour spent on the beach during warm weather, g h^{-1}

F_c = Fraction of time spent on the beach in cold weather conditions, dimensionless

$M_{sand,c}$ = Average mass of sand adhering to the skin per hour spent on the beach during cold weather, g h^{-1}

H5.1 Sand covered skin areas

The above equations present the probability of encountering an object in terms of the parameters $M_{sand,w}$ and $M_{sand,c}$. In order to allow the exposed skin areas to be included within the statistical calculations, the area component of these parameters require sfurther defining. Within $M_{sand,w}$ the part of the equation given by

$[(A_{h,ws} + (A_{rest,ws} * 0.5) + (A_{h,ds} * 0.02) + (A_{rest,ds} * 0.01)]$

represents the skin area that is exposed to wet sand during trips to the beach in warm weather. For visits to the beach in cold weather, the equivalent skin area is given by $A_{h,ws}$. These skin areas are given in Table H4 and Table H5, respectively, with information for use within the statistical calculation.

Table H4: Skin areas that could be exposed to wet sand in warm weather conditions (m^2)[(a)]

Activity	Age group	2.5%	Mean	97.5%	Best estimate[(b)]	Distribution type
Leisure	Young child	0.00082	0.06575	0.09875	0.06575	Triangular
Leisure	Child	0.00177	0.14589	0.212	0.14589	Triangular
Leisure	Adult	0.00308	0.2325	0.352	0.2325	Triangular
Walking	Young child	0.00056	0.02826	0.06575	0.02826	Triangular
Walking	Child	0.00118	0.05959	0.14589	0.05959	Triangular
Walking	Adult	0.00198	0.1001	0.2325	0.1001	Triangular

(a) The number of decimal places does not represent a correspondingly high degree of accuracy in these values; these are the values calculated using the method described in Appendix H as input to the assessment.

(b) Value used for the high occupancy beach users.

Table H5: Skin areas that could be exposed to wet sand in cold weather conditions (m^2)

Activity	Age group	2.5%	Mean	97.5%	Best estimate[a]	Distribution type
Leisure (wet sand)	Young child [b]	0	0.00175	0.007	0.00175	Triangular
Leisure (wet sand)	Child [c]	0	0.03	0.059	0.03	Triangular
Leisure (wet sand)	Adult [c]	0	0.05	0.099	0.05	Triangular
Walking (wet sand)	Young child [b]	0	0.00175	0.007	0.00175	Triangular
Walking (wet sand)	Child [c]	0	0.03	0.059	0.03	Triangular
Walking (wet sand)	Adult [c	0	0.05	0.099	0.05	Triangular

(a) Value used for the high occupancy beach users.

(b) 2.5% value assumes no exposure to wet sand, the mean value assumes 25% of one palm is exposed to wet sand and the 97.5% value assumes one palm is exposed to wet sand.

(c) 2.5% values assumes no exposure to wet sand, the mean value assumes palms of both hands are exposed to wet sand and the 97.5% value assumes both hands are exposed to wet sand.

H6 FRACTION OF TIME SPENT ON THE BEACH IN WARM AND COLD WEATHER CONDITIONS

The activities undertaken on the beach and the clothing worn, and thus the amount of skin exposed, depend to a significant extent on the weather. In order to give some indication of the range on the likelihood of encountering an object in sand on a visit to the beach, probabilities were determined for each exposed group for trips to the beach in 'cold' and 'warm' conditions. Cold conditions reflect time spent on the beach in winter and most of spring and autumn, when the weather is cool and individuals are generally warmly dressed against the elements and their activities generally limited to walking on the beach or playing ball games, for example. Warm conditions reflect days when the weather is warm enough for sunbathing, perhaps swimming and for infants to dig and play in wet sand.

H6.1 Leisure and walking activities

Young children were assumed to typically spend all of their time on the beach in warm conditions, with an assumed distribution on the time spent in warm conditions being between 0.75 and 1 of the time spent on the beach. This takes into account the fact that adults are unlikely to often expose young children to cold weather.

At the other end of the scale adult walkers are likely to brave more inclement weather and dog walkers, for example, use the beach every day regardless of what the weather is like. Given the assumption that "cold" conditions occur throughout most of autumn and spring as well as winter (overall taken to be 75% of the year), and that for most adult walkers the time spent on the beach was equally divided during the year, the best estimate of the fraction of the time spent on the beach during periods of warm weather is equal to 0.25. This value was assumed to have a range of between 0.25 and 0.5 which accounts for the marginal favouritism to "warm" conditions as well as accounting for those walkers who are only present in the summer months.

The fraction of visits undertaken by children in warm conditions was placed between those of young children and adult walker groups, bearing in mind that their tolerance of cold conditions is likely to be between these respective groups. The time that adults spend on leaisure activiries on the beach was assumed to be the same as that for children.

H7 REFERENCES

Defra and EA (2002). The Contaminated Land Exposure Assessment Model (CLEA): Technical basis and algorithms. R&D Publication CLR10.

Driver JH, Konz JJ and Whitmyre (1989). Soil adherence to human skin. *Bull Environ Contam Toxicol*, **43**, 814-820.

Finley BL, Scott PK and Mayhal DA (1994). Development of a Standard Soil-to-Skin Adherence Probability Density Function for Use in Monte Carlo Analyses of Dermal Exposure. *Risk Analysis*, **14** (4), 555-569.

Holmes Jr KK, Shirai JH, Richter KY and Kissel JC (1999). Field Measurement of Dermal Soil Loadings in Occupational and Recreational Activities. *Environ Research Section A*, **80**, 148-157.

ICRP (2002). Basic Anatomical and Physiological Data for Use in Radiological Protection: Reference Values. ICRP Publication 89. *Ann ICRP*, **32** (3-4).

Kissel JC, Richter KY and Fenske RA (1996). Field Measurement of Dermal Soil Loading Attributable to Various Activities: Implications for Exposure Assessment. *Risk Analysis*, **16** (1), 115-125.

Que Hee SS, Peace B, Clark CS, Boyle JR, Bornschein RL and Hammond PB (1985). Evolution of Efficient Methods to Sample Lead Sources, Such as House Dust and hand Dust, in the Homes of Children. *Env Res*, **38,** 77-95.

Sedman RM (1989). The development of applied action levels for soil contact: A scenario for the exposure of humans to soil in a residential setting. *Environ Health Perspectives*, **79**, 291-313.

Sheppard SC and Evenden WG (1994). Contaminant Enrichment and Properties of Soil Adhering to Skin. *J Environ Qual*, **23** (3), 604-613.

Smith KR and Bedwell P (2005). Public health implications of fragments of irradiated fuel. Module 3: The likelihood of encountering a fuel fragment on Sandside beach. Chilton, RPD-EA-9-2005.

US EPA (1992). Dermal exposure assessment: Principles and Applications. EPA 600-8-91-011B, US EPA, Washington.

US EPA (1997). Exposure Factors Handbook: Volume 1, General Factors. EPA/600/P-95/002Fa.

APPENDIX I Screening assessment to estimate health risks to seafood consumers from radioactive particles

No direct monitoring of offshore sediments has been carried out that can be used to clarify the likelihood and nature of radioactive particles that could become incorporated in seafood along the west Cumbrian coastline, although this is being considered for the future. In the meantime, it is important to scope the likelihood of members of the public ingesting a radioactive particle from the consumption of seafood and the associated health risks.

The Food Standards Agency (FSA), with support from HPA, EA and Sellafield Ltd via the Sellafied Sea-bed Monitoring Working Group, has undertaken a scoping assessment of the risks to seafood consumers from ingestion of radioactive particles. The methodology adopted is that developed for the assessment of the risks to seafood consumers from radioactive fuel fragments in the vicinity of the Dounreay nuclear site (Smith and Bedwell, 2005; and Wilkins et al, 1998). The FSA assessment is included within this report on the HPA study on health risks from radioactive objects on beaches in the vicinity of the Sellafield site so that the health risks can be considered along side those for people using the beaches.

The most recent habit survey undertaken in the Sellafield area (Cefas, 2009) identified local consumption of fish, crustacea and molluscs which had been caught locally. Any mature fish that are caught and consumed would be gutted and so the chance that a local person might consume a radioactive particle is very small. Individuals who consume fish caught on a recreational basis have been included in the population groups considered in the main assessment (see Section 5.2). The consumption of fish has, therefore, not been considered further.

The 2008 habit survey (Cefas, 2009) identified consumption of a range of local shellfish with the main species identified as brown crabs, common lobsters, winkles and mussels. The feeding habits of lobsters and crabs could lead to sediment being inadvertently ingested. Small particles of less than 1um are passed into a digestive gland with larger particles passing directly into the hind gut and voided (Wilkins et al, 1998). For both lobsters and crabs, the digestive gland may be consumed but all other parts of the alimentary canal would normally be discarded. The implications for this assessment are therefore that, unless a radioactive particle is inadvertently transferred into the edible parts during preparation, the direct ingestion of a particle is most unlikely. However, for completeness, in order to scope the probability of consumers of crabs and lobsters ingesting a radioactive particle, these species have been included. As a result of their grazing habits, the gut of molluscs may contain substantial amounts of sediment and since the flesh is cooked and consumed whole, the consumption of these animals presents a possible means by which particles could be ingested (Wilkins et al, 1998).

The following general assumptions have been made in the scoping assessment:

a monitoring data from Sellafield Ltd have been used to determine the 95th percentile of the distribution of the number of objects found per hectare of beach sediment based on the data from all the beaches monitored (Parker, 2010). The numbers of particles in the inter-tidal zone along the west Cumbrian coastline is assumed to be the same as that on the beaches in the absence of any other data at the current time;

b the particles detected on the beaches (< 1 mm diameter) can be ingested by molluscs and crustaceans;

c the distribution of particles with depth is uniform;

d the highest radioactivity content from all particles detected and retrieved from the beaches monitored has been used (Dalton 2010). For alpha-rich particles values of ^{241}Am, ^{238}Pu and $^{239/240}$Pu activity content have been taken into account. For beta-rich particles the value for ^{137}Cs activity content has been used. Many beta-rich particles contain some ^{90}Sr which would also contribute to any dose from ingestion of a particle. To be consistent with the HPA assessment, a conservative ratio of 1:1.6 ^{137}Cs:^{90}Sr has been used to estimate the ^{90}Sr activity content. The activity content for each radionuclide used is given in Table I1;

e all particles in the beach sediment and subsequently in the guts of seafood contain the activity content given in Table I1. This is a very conservative assumption as the majority of particles will have significantly lower levels of activity;

f a value for the 95th percentile value of the detection depth associated with the activity content of particles used in the scoping assessment was determined by Sellafield Ltd (Parker, 2010). The depths used were 0.04 m for alpha-rich particles based on the ^{241}Am content and 0.08 m for beta-rich particles based on their ^{137}Cs content;

g only adult seafood consumers have been considered as their consumption is much higher than for children, typically by a factor of 10 – 30 (Cefas, 2009). Annual consumption rates from the 2008 habit survey have been used; the 97.5th percentiles of the distribution of intake rates for each species considered (molluscs, crabs and lobsters). The consumption rates used are given in Table I2.

I1 PROBABILITY OF ENCOUNTERING A PARTICLE FROM CONSUMING SEAFOOD

The probability of ingesting a radioactive particle incorporated into shellfish gathered from inter-tidal areas along the west Cumbrian coastline has been determined using the following approach.

The number of objects in each animal is given by the following equation,

$Fw = Fd \times Sw$

Where:

Fw = number of particles in an individual animal

F_d = number of particles per gramme of sediment

Sw = typical mass of sand/sediment in gut of animal, g, see Table I3

Note that it has been assumed that the number of objects per gramme of sand in the digestive tract of each species of animal is the same as on a beach.

F_d was calculated by the following equation,

$F_d = Fm / (D \times R \times S_d)$

Where:

F_m = number of particles per m^2, see Table I1

D = depth of sediment, m, see text

R = packing ratio of sediment, see Table I1

S_d = density of sediment, g m^{-3}, see Table I1

Shellfish consumption rates are given in terms of kg per year. For use in this study, these were converted to the number of individual animals of each species consumed per person per year using the following equation,

$Cw = Wir / (Mw \times Ef \times Gf)$

Where:

Cw = number of each species ingested per person per year, y^{-1}

WIr = consumption rate of each species, kg y^{-1}, see Table I2

Mw = mass of individual species, kg, see Table I3

Ef = edible fraction of species expressed as a fraction of the whole mass of the animal, see Table I3

Gf = fraction of gut of each species consumed, see Table I3

The annual probability of an individual consuming a fuel fragment in shellfish is then determined as follows,

$P_{ing,a} = Fw \times Cw$

Where:

$P_{ing,a}$ = annual probability of a shellfish consumer ingesting a radioactive particle, y^{-1}

Table I1 Information on radioactive particles and beach characteristics

Parameter	Value[a]
Density of sediment/sand, g m^{-3}	2.6 10^{6}
Packing density of sediment	0.56
Number of alpha-rich particles per m^2	2.62 10^{-4}
Number of beta-rich particles per m^2	3.05 10^{-4}
Activity content of alpha-rich particles[b], Bq:	
^{241}Am	6.34 10^{5}
^{238}Pu	8.4 10^{4}
$^{239/240}Pu$	3.09 10^{5}
Activity content of beta-rich particles[b], Bq:	
^{137}Cs	4.60 10^{4}
^{90}Sr[c]	7.54 10^{4}

a) Precision of values used reflects precision of input data provided and to be consistent with Smith and Bedwell (2005)

b) Taken from Sellafield monitoring data spreadsheet dated 18 January 2010 and precision of data reflects that presented.

c) Calculated assuming a ratio of Sr:Cs of 1.6:1

Table I2 Summary of consumption rates (kg y^{-1}) in the Sellafield area from the 2008 habits survey report (Cefas, 2009)

Food Group	97.5 %ile consumption rate, kg y^{-1}
Molluscs	36.2
Crabs	30.7
Lobster	3.85

Table I3 Characteristics of seafood species (Wilkins et al, 1998)

Parameter[a]	Molluscs[b]	Crabs	Lobster
Sediment in digestive tract (g)	0.6	5.0	6.0
Mass of animal (kg)	0.015	0.6	0.6
Edible fraction	0.25	0.48	0.36
Fraction of gut consumed	0.2	0.7	0.02

a) Maximum values taken from Wilkins et al, 1998.

b) Values for winkles are assumed for all molluscs.

c) Value for brown crabs used as species identified as that consumed in habit survey (Cefas, 2009).

The estimated annual probabilities of encounter for an adult consuming shellfish are given in Table I4. The consumption of molluscs gives rise to the highest probability of

encountering a particle. The findings of a study in which the Cefas monitoring database for mollusc samples sourced from the Sellafield area was investigated to identify if there were incidences of high activities that could be due to contaminated particles are helpful to put the estimated probabilities of encounter into perspective (Cefas, 2008). The study concluded that, under the search criteria adopted, Cefas' monitoring and analysis database was not found to contain any samples that would conclusively indicate the ingestion of a contaminated particle. Although a number of samples did contain activity concentrations that exceeded the arbitrary secondary screening level set, they did not approach the activity levels recorded in analyses of particles found on the beaches (Cefas, 2008). It is likely, therefore, that given this finding and the conservative approach taken in estimating the probability of a seafood consumer ingesting a particle, that the values given in Table I4 are very conservative.

Table I4: Probability of an adult encountering a radioactive particle from the consumption of shellfish

Particle type	Probability per year			
	Crabs	Lobsters	Molluscs	Total[a]
Alpha-rich	$1.7\ 10^{-6}$	$9.6\ 10^{-9}$	$5.2\ 10^{-6}$	$6.9\ 10^{-6}$
Beta-rich	$9.8\ 10^{-7}$	$5.6\ 10^{-9}$	$3.0\ 10^{-6}$	$4.0\ 10^{-6}$

a) The total value is only applicable if it is assumed that an individual is a high-rate consumer of all species of shellfish.

I2 HEALTH RISKS TO SHELLFISH CONSUMERS

The probability of coming into contact with a particle from consuming shellfish has been estimated for both alpha-rich and beta-rich objects as described in Section I1. The overall risk to a seafood consumer must take into account both the probability that a particle may be ingested by a consumer and the risk of fatal cancer in the unlikely event that the person does ingest such a particle. This overall risk may be determined simply by multiplying the probability of encounter by the risk of fatal cancer, since the two factors are independent.

Overall health risks have been calculated assuming the particles contain the 95th percentile of the distribution of activity contents of all particles retrieved from the beaches to date and using the conservative probabilities of encountering a particle that have been calculated and presented in Table I4. Individuals with higher than average shellfish consumption are covered within these conservative estimates. The dose coefficients used are the same as those used in the main study (see Sections 8 and 9). The values are reproduced here for completeness and are given in Table I5.

Table I5: Ingestion dose coefficients for adults

Radionuclide	Dose coefficient, Sv Bq^{-1}
^{241}Am	$1.9\ 10^{-8}$
^{238}Pu	$1.9\ 10^{-8}$
$^{239/240}Pu$	$1.9\ 10^{-8}$
^{137}Cs	$1.3\ 10^{-8}$
^{90}Sr	$7.3\ 10^{-8}$

Table I6 shows the lifetime risk of fatal cancer for an adult if a particle is ingested. Table I7 shows the overall risks to a seafood consumer taking into account the estimated probability of ingesting a particle via seafood.

Table I6: Ingestion doses to a seafood consumer associated with ingestion of alpha-rich and beta-rich particles

Particle type	highest activity, kBq	Effective dose[a], mSv	Lifetime risk of fatal cancer if particle ingested
Alpha-rich			
^{241}Am	634	12	
^{238}Pu	84	1.6	
$^{239/240}Pu$	309	5.9	
Total	1027	19.5	$9.8\ 10^{-4}$
Beta-rich			
^{137}Cs	46	1.4	
^{90}Sr	75.4	13.2	
Total	121.4	14.6	$7.3\ 10^{-4}$

a) Calculated doses take account of other radionuclides measured in the particles that will contribute significantly to the dose. For alpha-rich particles, the dose is from ^{241}Am, ^{238}Pu and ^{239}Pu. For beta-rich particles, the dose is calculated for ^{137}Cs and ^{90}Sr. A conservative ratio of 1.0: 1.6 ^{137}Cs : ^{90}Sr has been assumed.

b) The same dose coefficients have been used as in the main study. Values are given in Table J5.

The overall health risks estimated for adult shellfish consumers from ingesting alpha-rich or beta-rich particles are very small and lower than 1 in 100 million. It should be noted that the total overall risk is based on the assumption that an individual is a high-rate consumer of all species of shellfish using the ingestion rates identified during the latest habit survey in 2008.

Table I7: Highest overall health risks to an adult seafood consumer associated with possible ingestion of alpha-rich and beta-rich particles

Particle type	Lifetime risk if particle ingested	Annual probability of ingesting a particle from shellfish consumption	Overall risk
Alpha-rich	$9.8\ 10^{-4}$		
Molluscs		$5.2\ 10^{-6}$	$5.1\ 10^{-9}$
Crabs		$1.7\ 10^{-6}$	$1.6\ 10^{-9}$
Lobster		$9.6\ 10^{-9}$	$9.4\ 10^{-12}$
Total		$6.9\ 10^{-6}$	**$6.7\ 10^{-9}$**
Beta-rich	$7.3\ 10^{-4}$		
Molluscs		$3.0\ 10^{-6}$	$2.2\ 10^{-9}$
Crabs		$9.8\ 10^{-7}$	$7.1\ 10^{-10}$
Lobster		$5.6\ 10^{-9}$	$4.1\ 10^{-12}$
Total		$4.0\ 10^{-6}$	**$2.9\ 10^{-9}$**

I3 REFERENCES

Cefas (2008). A report on the investigation of the Cefas monitoring database for incidences of high activities in mollusc samples. Cefas contract report C2706 available at www.**cefas**.co.uk/publications/environment/**Cefas**-database-**report**.pdf

Cefas (2009). Radilogical habits survey: Selalfield, 2008. Cefas contact report C2848 available at **www.cefas.co.uk/publications/environment/Sellafield-2008-final-report.pdf**

Dalton A (2010). Personal communication, Sellafield Ltd. Provision of Sellafield monitoring spreadsheet dated 18th January 2010.

Parker T (2010). Personal communication, Sellafield Ltd, January 2010.

Smith KR and Bedwell P (2005). Public health implications of fragments of irradiated fule. Module 3: The likelihood of encountering a fuel fragment on Sandside beach. Available at **www.sepa.org.uk/radioactive_substances/rs_publications**

Wilkins BT et al (1998). Radiological implications of the presence of fragments of irradiated fuel in the sub-tidal zone at Dounreay. Chilton, NRPB-M1005.

APPENDIX J Hourly probability of encountering an object on a beach

This Appendix provides additional information on the probability of encountering a radioactive object during a visit of one hour to any of the beaches considered. This information can be used to estimate the probability of encounter using new data on beach occupancy as it becomes available. Although the probabilities per hour could be used to compare the probabilities of encounter during an hourly visit for the different beaches, this should not be used to suggest that it is preferable to use any one beach over another. The data presented should be used within the context that, for all beaches, the probability of encounter is very low and the health risks are very small.

Table J1 presents the activity band ranges used in this Appendix. This is a reproduction of Table 17 of the main text and is included here for ease of reference for use with the tables presented within this Appendix.

Table J1: Activity bands used for estimating object populations

Representative activity (kBq)[(a)]	Range of activity levels in each band (kBq)	
	Minimum	Maximum
10	3	30
100	30	300
1000	300	3000

(a) Object populations have not been estimated for objects with activities less than 3 kBq, as discussed in Section 4.3.

J1 RELATIVE SIGNIFICANCE OF BEACH USER AND PATHWAY

The highest hourly probability of encountering an object whilst using a beach is for adult anglers. Table J2 shows the relative probabilities of encountering an object on a beach for each of the assessed age groups and beach uses in relation to the group with the highest hourly probability of encounter (adult anglers). These relative values are independent of the population of objects and hence they are applicable for each of the object radionuclide classes (alpha-rich, beta-rich and cobalt-rich), activity content of the objects, and for all beaches. The table shows, for example, that for adults using the beaches for walking or leisure, the overall probability of encountering an object is about 65% to 85% of that for an adult who uses the beach to fish or dig bait.

The relative importance of the individual exposure pathways are shown in Table J3. This is a copy of Table 47 of the main text, being reproduced here for ease of reference.

Reference should be made to Section 7 of the main text for a detailed explanation of how to use the information within Table J2 and Table J3 with the beach specific hourly probabilities presented in later Sections of this Appendix.

Table J2: Relative probabilities of encountering an object on a beach for each age group and beach use for a generic beach beach user[(a)]

Adult			Child			Young child		
Angling	Leisure	Walking	Angling	Leisure	Walking	Angling	Leisure	Walking
1.00	0.84	0.63	0.97	0.64	0.55	0.36	0.50	0.45

(a) Adult angler was the age group and beach activity that was calculated to have the highest probability of encounter

(b) The relative probabilities of encounter are subject to variation as they are based on statistical results. The values in this table are for the 50% (median) results

Table J3: Percentage contribution of each exposure pathway to the median probability of encountering a radioactive particle on a beach for a generic beach user[(a)]

	Particle inadvertently ingested	Particle inhaled	Particle trapped under a nail	Particle trapped in shoes	Particle on the skin	Particle trapped in clothes
Adult - leisure	0.007	0.0014	1.0	41	51	6.5
Adult - fishing	0.0059	0.0016	0.64	33	58	8.2
Adult - walking	0.0093	0.0018	1.2	54	31	13
Child - leisure	0.018	0.00028	0.81	52	42	4.9
Child - fishing	0.012	0.00017	0.4	34	60	5.2
Child - walking	0.021	0.00031	0.95	61	29	9.0
Young child - leisure	0.12	0.00019	0.57	68	28	3.0
Young child - walking	0.13	0.00021	0.63	76	18	5.3

(a) Due to the use of statistics in the derivation of these values there will be some variation in the contribution when other percentiles of the distribution are considered.

J2 MAXIMUM HOURLY PROBABILITY OF ENCOUNTERING RADIOACTIVE OBJECTS ON THE BEACHES

This Section contains results of the maximum hourly probability of encounter for each beach for both general beach users and beach users with high annual occupancy. Results are presented for each age group and beach activity group considered. The hourly probability is given for each of the particle types and for a range of activity content for both particles and stones. The probabilities of encounter for each activity band take account of the number of particles estimated in each activity band, as described in Section 4.2. The total probability of encounter for each particle type can be obtained by summing the probabilities across the different activity bands represented by the midpoints of 10 kBq, 100 kBq and 1000 kBq.

Table J4 to Table J8 present the probability of encountering a radioactive particle per hour spent on each of the beaches considered and for each age group who may use the beach. Children and young children were not observed using Sellafield beach during the habit surveys. However, these age groups are included here for completeness.

Table J9 to Table J11 give the probability of encountering radioactive stones per hour spent on each of the beaches considered and for each age group who may use the

beach. For stones, probabilities of encounter have only been calculated for those beaches where monitoring has found radioactive stones.

The hourly probabilities in the tables can be scaled directly by the hours spent on a beach over any given period. Where necessary, the total probability of encountering a particle and a stone can be obtained by summing the separate probabilities together, noting the cautious nature of such a total as discussed in Section 7 of the main text. It should be remembered that the estimated object populations are based on the total objects found during monitoring and are based on an average over time. This means that the object populations may not be applicable when assessing the probability of encounter over short periods of time, for example a period of a few hours or days.

Table J4: Highest hourly probability of encountering a radioactive particle on Braystones beach[a]

		Alpha-rich particle		Beta-rich particle		Cobalt-rich particle
		10 kBq	100 kBq	10 kBq	100 kBq	10 kBq
Adult[b]	2.5%	$3.5\ 10^{-9}$	$4.3\ 10^{-10}$	$1.2\ 10^{-9}$	$1.7\ 10^{-11}$	$2.6\ 10^{-11}$
	50%	$1.8\ 10^{-8}$	$2.2\ 10^{-9}$	$6.0\ 10^{-9}$	$8.3\ 10^{-11}$	$1.3\ 10^{-10}$
	97.5%	$5.8\ 10^{-8}$	$7.1\ 10^{-9}$	$2.0\ 10^{-8}$	$2.7\ 10^{-10}$	$4.4\ 10^{-10}$
Child[c]	2.5%	$3.5\ 10^{-9}$	$4.2\ 10^{-10}$	$1.2\ 10^{-9}$	$1.6\ 10^{-11}$	$2.6\ 10^{-11}$
	50%	$1.7\ 10^{-8}$	$2.1\ 10^{-9}$	$5.9\ 10^{-9}$	$7.9\ 10^{-11}$	$1.3\ 10^{-10}$
	97.5%	$5.6\ 10^{-8}$	$6.8\ 10^{-9}$	$1.9\ 10^{-8}$	$2.6\ 10^{-10}$	$4.2\ 10^{-10}$
Young child[d]	2.5%	1.7E-09	2.1E-10	6.1E-10	7.8E-12	1.3E-11
	50%	8.8E-09	1.1E-09	3.0E-09	4.0E-11	6.5E-11
	97.5%	2.3E-08	2.8E-09	8.1E-09	1.1E-10	1.7E-10

(a) The estimated particle population does not contain any particles with a radioactivity content of 1000 kBq.

(b) Highest probabilities of encounter are for the adult angler.

(c) Highest probabilities of encounter are for child angler.

(d) Highest probabilities of encounter are for young child leisure.

Table J5: Highest hourly probability of encountering a radioactive particle on Drigg beach[a]

		Alpha-rich particles		Beta-rich particles		Cobalt-rich particles
		10 kBq	100 kBq	10 kBq	100 kBq	10 kBq
Adult[b]	2.5%	$3.0\ 10^{-8}$	$5.8\ 10^{-10}$	$6.9\ 10^{-11}$	$6.9\ 10^{-11}$	$9.6\ 10^{-11}$
	50%	$1.5\ 10^{-7}$	$2.9\ 10^{-9}$	$3.4\ 10^{-10}$	$3.4\ 10^{-10}$	$4.9\ 10^{-10}$
	97.5%	$5.1\ 10^{-7}$	$9.5\ 10^{-9}$	$1.1\ 10^{-9}$	$1.1\ 10^{-9}$	$1.6\ 10^{-9}$
Child[c]	2.5%	$3.0\ 10^{-8}$	$5.6\ 10^{-10}$	$6.6\ 10^{-11}$	$6.6\ 10^{-11}$	$9.4\ 10^{-11}$
	50%	$1.5\ 10^{-7}$	$2.8\ 10^{-9}$	$3.3\ 10^{-10}$	$3.3\ 10^{-10}$	$4.6\ 10^{-10}$
	97.5%	$4.9\ 10^{-7}$	$9.1\ 10^{-9}$	$1.1\ 10^{-9}$	$1.1\ 10^{-9}$	$1.5\ 10^{-9}$
Young child[d]	2.5%	1.5E-08	2.8E-10	3.5E-11	3.2E-11	4.7E-11
	50%	7.7E-08	1.4E-09	1.7E-10	1.7E-10	2.4E-10
	97.5%	2.1E-07	3.8E-09	4.6E-10	4.5E-10	6.4E-10

(a) The estimated particle population does not contain any particles with a radioactivity content of 1000 kBq.

(b) Highest probabilities of encounter are for the adult angler.

(c) Highest probabilities of encounter are for child angler.

(d) Highest probabilities of encounter are for young child leisure.

Table J6: Highest hourly probability of encountering a radioactive particle on Seascale beach[a]

		Alpha-rich particles		Beta-rich particles		Cobalt-rich particles
		10 kBq	100 kBq	10 kBq	100 kBq	10 kBq
Adult[b]	2.5%	$2.3\ 10^{-10}$	$1.8\ 10^{-10}$	$3.6\ 10^{-10}$	$2.4\ 10^{-11}$	$6.8\ 10^{-12}$
	50%	$1.2\ 10^{-9}$	$8.9\ 10^{-10}$	$1.8\ 10^{-9}$	$1.2\ 10^{-10}$	$3.4\ 10^{-11}$
	97.5%	$3.8\ 10^{-9}$	$2.9\ 10^{-9}$	$5.8\ 10^{-9}$	$4.0\ 10^{-10}$	$1.1\ 10^{-10}$
Child[c]	2.5%	$2.3\ 10^{-10}$	$1.7\ 10^{-10}$	$3.4\ 10^{-10}$	$2.3\ 10^{-11}$	$6.6\ 10^{-12}$
	50%	$1.1\ 10^{-9}$	$8.5\ 10^{-10}$	$1.7\ 10^{-9}$	$1.2\ 10^{-10}$	$3.3\ 10^{-11}$
	97.5%	$3.7\ 10^{-9}$	$2.8\ 10^{-9}$	$5.6\ 10^{-9}$	$3.8\ 10^{-10}$	$1.1\ 10^{-10}$
Young child[d]	2.5%	1.1E-10	8.7E-11	1.8E-10	1.1E-11	3.3E-12
	50%	5.8E-10	4.4E-10	8.7E-10	5.9E-11	1.7E-11
	97.5%	1.5E-09	1.2E-09	2.4E-09	1.6E-10	4.5E-11

(a) The estimated particle population does not contain any particles with a radioactivity content of 1000 kBq.

(b) Highest probabilities of encounter are for the adult angler.

(c) Highest probabilities of encounter are for child angler.

(d) Highest probabilities of encounter are for young child leisure.

Table J7: Highest hourly probability of encountering a radioactive particle on Sellafield beach

		Alpha-rich particles			Beta-rich particles		Cobalt-rich particles
		10 kBq	100 kBq	1000 kBq[a]	10 kBq	100 kBq	10 kBq
Adult[b]	2.5%	$1.6\ 10^{-9}$	$1.0\ 10^{-9}$	$9.9\ 10^{-12}$	$1.8\ 10^{-9}$	$5.6\ 10^{-11}$	$8.9\ 10^{-12}$
	50%	$8.2\ 10^{-9}$	$5.0\ 10^{-9}$	$5.0\ 10^{-11}$	$8.8\ 10^{-9}$	$2.8\ 10^{-10}$	$4.5\ 10^{-11}$
	97.5%	$2.7\ 10^{-8}$	$1.6\ 10^{-8}$	$1.6\ 10^{-10}$	$2.9\ 10^{-8}$	$9.2\ 10^{-10}$	$1.5\ 10^{-10}$
Child[c]	2.5%	$1.6\ 10^{-9}$	$9.8\ 10^{-10}$	$9.5\ 10^{-12}$	$1.7\ 10^{-9}$	$5.4\ 10^{-11}$	$8.6\ 10^{-12}$
	50%	$8.0\ 10^{-9}$	$4.8\ 10^{-9}$	$4.7\ 10^{-11}$	$8.5\ 10^{-9}$	$2.7\ 10^{-10}$	$4.3\ 10^{-11}$
	97.5%	$2.6\ 10^{-8}$	$1.6\ 10^{-8}$	$1.5\ 10^{-10}$	$2.8\ 10^{-8}$	$8.9\ 10^{-10}$	$1.4\ 10^{-10}$
Young child[d]	2.5%	8.1E-10	4.9E-10	4.9E-12	8.9E-10	2.7E-11	4.3E-12
	50%	4.1E-09	2.5E-09	2.4E-11	4.4E-09	1.4E-10	2.2E-11
	97.5%	1.1E-08	6.6E-09	6.5E-11	1.2E-08	3.7E-10	5.9E-11

(a) Maximum activity for an alpha-rich particle found on the beach is 634 kBq ^{241}Am.

(b) Highest probabilities of encounter are for the adult angler.

(c) Highest probabilities of encounter are for child angler.

(d) Highest probabilities of encounter are for young child leisure.

Table J8: Highest hourly probability of encountering a radioactive particle on St Bees beach[a]

		Alpha-rich particles		Beta-rich particles	Cobalt-rich particles
		10 kBq	100 kBq	10 kBq	10 kBq
Adult[b]	2.5%	$4.6\ 10^{-9}$	$1.6\ 10^{-10}$	$3.0\ 10^{-10}$	$6.9\ 10^{-12}$
	50%	$2.3\ 10^{-8}$	$7.8\ 10^{-10}$	$1.5\ 10^{-9}$	$3.5\ 10^{-11}$
	97.5%	$7.6\ 10^{-8}$	$2.6\ 10^{-9}$	$4.9\ 10^{-9}$	$1.2\ 10^{-10}$
Child[c]	2.5%	2.3E-09	7.7E-11	1.5E-10	3.3E-12
	50%	1.2E-08	3.9E-10	7.4E-10	1.7E-11
	97.5%	3.1E-08	1.0E-09	2.0E-09	4.6E-11
Young child[d]	2.5%	2.3E-09	7.7E-11	1.5E-10	3.3E-12
	50%	1.2E-08	3.9E-10	7.4E-10	1.7E-11
	97.5%	3.1E-08	1.0E-09	2.0E-09	4.6E-11

(a) The estimated particle population does not contain any particles with a radioactivity content of 1000 kBq.

(b) Highest probabilities of encounter are for the adult angler.

(c) Highest probabilities of encounter are for child angler.

(d) Highest probabilities of encounter are for young child leisure.

Table J9: Highest hourly probability of encountering a radioactive stone on Braystones beach[a)]

		Beta-rich stones
		100 kBq
Adult[b]	2.5%	$2.0\ 10^{-11}$
	50%	$9.9\ 10^{-11}$
	97.5%	$3.3\ 10^{-10}$
Child[c]	2.5%	$1.9\ 10^{-11}$
	50%	$9.5\ 10^{-11}$
	97.5%	$3.2\ 10^{-10}$
Young child[d]	2.5%	9.5E-12
	50%	4.9E-11
	97.5%	1.3E-10

(a) The estimated actual particle population does not contain any particles with a radioactivity content of 1000kBq.

(b) Highest probabilities of encounter are for the adult angler.

(c) Highest probabilities of encounter are for child angler.

(d) Highest probabilities of encounter are for young child leisure.

Table J10: Highest hourly probability of encountering a radioactive stone on Seascale beach[a]

		Beta-rich stones	
		10 kBq	100 kBq
Adult[b]	2.5%	$6.4\ 10^{-11}$	$7.9\ 10^{-12}$
	50%	$3.2\ 10^{-10}$	$3.8\ 10^{-11}$
	97.5%	$1.0\ 10^{-9}$	$1.3\ 10^{-10}$
Child[c]	2.5%	$6.4\ 10^{-11}$	$7.5\ 10^{-12}$
	50%	$3.0\ 10^{-10}$	$3.7\ 10^{-11}$
	97.5%	$9.9\ 10^{-10}$	$1.2\ 10^{-10}$
Young child[d]	2.5%	3.2E-11	3.7E-12
	50%	1.6E-10	1.9E-11
	97.5%	4.2E-10	5.1E-11

(a) The estimated actual particle population does not contain any particles with a radioactivity content of 1000kBq.

(b) Highest probabilities of encounter are for the adult angler.

(c) Highest probabilities of encounter are for child angler.

(d) Highest probabilities of encounter are for young child leisure.

Table J11: Highest hourly probability of encountering a radioactive stone on Sellafield beach[(a)]

		Alpha-rich stones		Beta-rich stones			Cobalt-rich stones
		10 kBq	100 kBq	10 kBq	100 kBq	1000 kBq[(b)]	10 kBq
Adult[c]	2.5%	$2.2\ 10^{-9}$	$3.3\ 10^{-12}$	$3.1\ 10^{-9}$	$2.7\ 10^{-10}$	$2.2\ 10^{-11}$	$6.3\ 10^{-12}$
	50%	$1.1\ 10^{-8}$	$1.7\ 10^{-11}$	$1.6\ 10^{-8}$	$1.3\ 10^{-9}$	$1.1\ 10^{-10}$	$3.2\ 10^{-11}$
	97.5%	$3.6\ 10^{-8}$	$5.4\ 10^{-11}$	$5.1\ 10^{-8}$	$4.4\ 10^{-9}$	$3.6\ 10^{-10}$	$1.0\ 10^{-10}$
Child[d]	2.5%	$2.1\ 10^{-9}$	$3.2\ 10^{-12}$	$3.1\ 10^{-9}$	$2.6\ 10^{-10}$	$2.1\ 10^{-11}$	$5.9\ 10^{-12}$
	50%	$1.1\ 10^{-8}$	$1.6\ 10^{-11}$	$1.5\ 10^{-8}$	$1.3\ 10^{-9}$	$1.1\ 10^{-10}$	$3.0\ 10^{-11}$
	97.5%	$3.5\ 10^{-8}$	$5.2\ 10^{-11}$	$4.9\ 10^{-8}$	$4.2\ 10^{-9}$	$3.5\ 10^{-10}$	$1.0\ 10^{-10}$
Young child[e]	2.5%	1.1E-09	1.6E-12	1.6E-09	1.3E-10	1.1E-11	3.0E-12
	50%	5.5E-09	8.3E-12	7.8E-09	6.6E-10	5.4E-11	1.5E-11
	97.5%	1.5E-08	2.2E-11	2.1E-08	1.8E-09	1.5E-10	4.2E-11

(a) These probabilities of encounter are for the adult angler. Table J2 shows how the relationship of other beach uses and age groups are related to these results

(b) Maximum activity for a beta-rich stone found on the beach is 875 kBq

(c) Highest probabilities of encounter are for the adult angler.

(d) Highest probabilities of encounter are for child angler.

(e) Highest probabilities of encounter are for young child leisure.

APPENDIX K Review of published data on the absorption of ingested plutonium and americium in adults

In the absence of human data, data from other mammalian species are considered the most important because the absorption processes are expected to operate in a similar way. Animal data on the absorption of Pu in species including rodents, pigs, dogs and primates was extensively reviewed in ICRP Publication 48 (ICRP, 1986) and by Harrison (1983; 1991). The chemical form ingested is an important factor affecting absorption. The lowest values obtained are for the oxide, ranging from about 2 10^{-4} in the rat (Sullivan, 1980) to about 3 10^{-8} in the pig (Smith, 1970). These large differences are probably a reflection of the solubility of the oxide preparation, which is low and is affected by the temperature of production (Mewhinney et al, 1976), the proportion of small particles present (Stather et al, 1975) and the specific activity of the isotope (Fleischer and Raabe, 1977). Mixed Pu-sodium oxides contain a higher proportion of very small particles (about 1 nm diameter) than the pure oxides (Stather et al, 1975) and suspensions of ^{238}Pu oxide are more prone to radiolytic breakdown to small particles than those of ^{239}Pu oxide (Fleischer and Raabe, 1977) and therefore Pu-sodium and ^{238}Pu oxides tend to be more soluble than ^{239}Pu oxide. Comparisons of the behaviour of inhaled Pu oxide and mixed U/Pu oxides in rats and baboons showed that although solubility in the lung was low in each case, transfer of Pu to liver and bone was about two to three times greater for the mixed oxide (Lataillade et al, 1995).

The range in values of uptake for Pu administered to animals as the nitrate, chloride or bicarbonate is not as large as for the oxide. In general, the results are between 10^{-4} and 10^{-5}. Fasting has been shown to increase absorption by up to an order of magnitude. Absorption in mice fasted for 8 hours before and 8 hours after the administration of ^{236}Pu bicarbonate was about 10^{-3} compared with 2 10^{-4} in fed animals (Larsen et al, 1981). Higher values of 10^{-3} to 2 10^{-3} have been reported for uptake of ^{237}Pu nitrate given as a single dose to rats and mice (Sullivan, 1981; Sullivan et al, 1982). These results were taken as evidence of increased absorption at low masses. However, in experiments to determine the effect of chronic ingestion at low concentrations, a value of 3 10^{-5} was obtained for the nitrate in rats (Weeks et al, 1956) and 10^{-5} for the bicarbonate in hamsters (Stather et al, 1981). It would appear that in general ingested mass and valence are not important factors in Pu absorption. However, for Pu(V), in baboons, absorption is approximately 1 10^{-2} for an ingested mass of 5 10^{4} μg kg^{-1} whereas it is approximately 1 10^{-4} for an ingested mass of 10 μg kg^{-1} (Métivier et al, 1985).

The absorption of Pu administered to animals as organic complexes or incorporated into food materials is generally greater than for inorganic forms (ICRP, 1986). For example, most of the reported values for Pu citrate are in the range 6 10^{-5} to 6 10^{-4} and those for Pu nitrate are in the range of 10^{-5} to 10^{-4}. In comparison, the absorption range of Pu-tributylphosphate, an organic form of importance in nuclear fuel reprocessing was measured by Métivier et al (1983) in rats as about 10^{-4} to 2 10^{-4}.

There are less data available on absorption of Pu in humans. Popplewell et al (1994) and Ham and Harrison (2000) measured the fractional absorption (f_1) of soluble ^{244}Pu

administered as a citrate solution with a mid-day meal to five volunteers. The values obtained were in the range of 10^{-4} to 10^{-3}, with a mean value of 6 10^{-4}. Hunt et al (1986; 1990) carried out two studies of the absorption of Pu by volunteers eating winkles collected on the Cumbrian coast near to the Sellafield plant. The overall f_1 value obtained for Pu was 2 10^{-4} with a range of 2 10^{-5} to 5 10^{-4}. Mussalo-Rauhamaa et al (1984) estimated the f_1 value for fallout Pu in humans eating contaminated reindeer meat by comparing the ratio of body content to dietary intake of $^{239/240}$Pu in people who had lived in Lapland or the urban areas of southern Finland. The f_1 was about 8 10^{-4} but there were large uncertainties associated with this estimate.

Data on the absorption of americium in animals was also reviewed in ICRP Publication 48 (ICRP, 1986) and by Harrison (1983; 1991). Absorption values for Am nitrate or chloride administered to rodents were in the range 2 10^{-4} to 10^{-3}. For Am oxide in fresh suspension, absorption was about 10^{-4} in rats (Sullivan, 1980) and 6 10^{-5} in hamsters (Stather et al, 1979). Results for rodents and primates suggest that the absorption of Am, unlike Pu, is not increased by binding to organic ligands.

The only human data available on absorption of Am are those of Hunt et al (1986; 1990) who carried out two studies of the absorption of Pu and Am by volunteers fed shellfish winkles collected on the Cumbrian coast near to the Sellafield plant. The average f_1 value obtained for Am was 1 10^{-4} with a range of 4 10^{-5} to 3 10^{-4}.

In ICRP Publication 67 (ICRP, 1993), human data for neptunium, plutonium, americium and curium were summarised and using this information in conjunction with human data for thorium and available animal data, it was concluded that these data provided a sufficient basis for the use of a value of 5 10^{-4} for unknown compounds of Pu and Am. Subsequently, in ICRP Publication 68 (ICRP, 1994) the f_1 values of 1 10^{-4} and 1 10^{-5} were adopted for the specific case of ingestion by workers of Pu nitrate and Pu oxide respectively.

K1.1 References

Fleischer RL and Raabe OG (1977). Fragmentation of respirable PuO_2 particles in water by alpha decay - a mode of dissolution. *Health Phys*, **32**, 253-257.

Ham GJ and Harrison JD (2000). The gastrointestinal absorption and urinary excretion of Pu in male volunteers. *Radiat Prot Dosim*, **87**, 267-272.

Harrison JD (1983). The gastrointestinal absorption of plutonium, americium and curium. *Radiat Prot Dosim*, **5**, 19-35.

Harrison JD (1991). The gastrointestinal absorption of the actinide elements. *Sci Tot Environ*, **100**, 43-60.

Hunt GJ, Leonard DRP and Lovett MB (1986). Transfer of environmental plutonium and americium across the human gut. *Sci Tot Environ*, **53**, 89-109.

Hunt GJ, Leonard DRP and Lovett MB (1990).Transfer of environmental plutonium and americium across the human gut: A second study. *Sci Tot Environ*, **90**, 273-282.

ICRP (1986). International Commission on Radiological Protection. The Metabolism of Plutonium and Related Elements. ICRP Publication 48. *Ann ICRP*, **16** (2/3). Pergamon Press, Oxford.

ICRP (1993). International Commission on Radiological Protection. Age-dependent Doses to Members of the Public from Intake of Radionuclides. Pt.2. ICRP Publication 67. *Ann ICRP*, **23** (3/4). Pergamon Press, Oxford.

ICRP (1994). International Commission on Radiological Protection. Dose Coefficients for Intakes of Radionuclides by Workers. ICRP Publication 68. *Ann ICRP*, **24** (4). Pergamon Press, Oxford.

Laitaillade G, Verry M, Rateau G, Métivier H and Masse R (1995). Plutonium solubility in rat and monkey lungs after inhalation of industrial plutonium oxide and mixed uranium and plutonium oxide. *Int J Radiat Biol*, **67**, 373-380.

Larsen RP, Bhattacharyya MH, Oldham RD, Moretti ES and Spaletto MI (1981). Continued studies of the gastrointestinal absorption of plutonium in rodents. In: Annual Report for Radiological and Environmental Research Division, Argonne National Laboratory, Illinois. ANL-81-85 (Pt II), pp 105-116.

Métivier H, Masse R and Lafuma J (1983). Metabolism of plutonium introduced as tri-N-butyl phosphate complex in the rat and removal attempts by DTPA. *Health Phys*, **44**, 623-634.

Métivier H, Madic C, Bourges J and Masse R (1985). Valency five, similarities between plutonium and neptunium in gastrointestinal uptake. In: Speciation of Fission and Activation Products in the Environment. (RA Bulman and JR Cooper, Eds.) Elsevier Applied Science Publishers, London, pp 175-178.

Mewhinney JA, Muggenburg BA, McClellan RO and Miglio JJ (1976). The effect of varying physical and chemical characteristics of inhaled plutonium aerosols on metabolism and excretion. In: Proc Int Seminar on Diagnosis and Treatment of Incorporated Radionuclides. Vienna, IAEA, pp 87-97.

Mussalo-Rauhamaa H, Jaakola T, Mietttinen JK and Laiho K (1984). Plutonium in Finish Lapps - An estimate of the gastrointestinal absorption of plutonium by man based on a comparison of the plutonium content of Lapps and southern Finns. *Health Phys*, **46**, 549-559.

Popplewell DS, Ham GJ, McCarthy W and Lands C (1994). Transfer of plutonium across the human gut and its urinary excretion. In: Proc Workshop on Intakes of Radionuclides: Detection, Assessment and Limitation of Occupational Exposure. *Radiat Prot Dosim*, **53**, 241-244.

Smith VH (1970). Fate of ingested $^{238}PuO_2$ in miniature swine. In: Pacific Northwest Laboratory Annual Report for 1969. Pt 1. Biomedical Sciences. Richland, Wash, BNWL-1306, pp 62-63.

Stather JW, Howden S and Carter RF (1975). A method for investigating the metabolism of the transportable fraction of plutonium aerosols. *Phys Med Biol*, **20**, 106-124.

Stather JW, Harrison JD, Rodwell P and David AJ (1979). The gastrointestinal absorption of plutonium and americium in the hamster. *Phys Med Biol*, **24**, 396-407.

Stather JW, Harrison JD, David AJ and Sumner SA (1981). The gastrointestinal absorption of plutonium in the hamster after ingestion at low concentrations in drinking water. *Health Phys*, **41**, 780-783.

Sullivan MF (1980). Absorption of actinide elements from the gastrointestinal tract of rats, guinea pigs and dogs. *Health Phys*, **38**, 159-171.

Sullivan MF (1981). Influence of plutonium mass on absorption from the gastrointestinal tract of adult and neonatal rodents. In: Pacific Northwest Laboratory Annual Report for 1980. Pt 1. Biomedical Sciences. Richland, Wash, PNL-3700, pp 185-186.

Sullivan MF, Miller BM and Ryan JL (1982). Gut-related radionuclide studies. In: Pacific Northwest Laboratory Annual Report for 1981. Pt 1, Biomedical Sciences. Richland, Wash, PNL-4100, pp 119-122.

Weeks MH, Katz J, Oakley WD, Ballou JE, George LA, Bustad LK, Thompson RC and Kornberg HA (1956). Further studies on the gastrointestinal absorption of plutonium. *Radiat Res*, **4**, 339-347.